THE PREDICTION OF STICKING IN DAIRY POWDERS

A thesis presented in partial fulfilment of the requirements for the degree of
Doctor of Philosophy in Bioprocess Engineering at Massey University

Kylie D. Foster

B. Tech (Hons)

2002

ABSTRACT

Sticking and caking of dairy powders during processing and storage is a serious problem in the dairy industry. The mechanisms for sticking and caking in dairy powders were identified. In high fat powders, fatty liquid bridges form between adjacent particles when the powder is exposed to temperatures where the milk fat is molten. If the powder is later exposed to temperatures where some of the milk fat can crystallise, then the bridges between the particles partially solidify, giving some strength to the powder. The mechanism was shown to be related to the amount of surface fat that solidifies during cooling, after the powder has been exposed to higher temperatures.

Amorphous sugars were also shown to be responsible for the sticking and caking of dairy powders. Stickiness occurs when the glass transition temperature of the powder is exceeded. Above the glass transition temperature, the viscosity of the amorphous glass reduces allowing flow of amorphous material and the formation of bridges between adjacent particles. This mechanism was shown to be viscosity related and the rate of sticking was found to be dependent on the amount that the glass transition temperature is exceeded by, not the temperature and humidity conditions required to achieve this. This mechanism was shown to hold for amorphous glucose, galactose, sucrose, maltose and fructose. Previous work has shown this to be the case for amorphous lactose.

A model was developed for predicting sticking conditions in dairy powders. This model required methods for predicting the isotherms and glass transition temperature profiles for multicomponent powders. It was found that the isotherm can be predicted from the weighted addition of the components isotherms. A new method for predicting the glass transition temperature was proposed and validated in this work. The new method predicts the glass transition temperature from the weighted addition of the glass transition temperatures of the amorphous components at a given water activity. This method gave better predictions than traditional methods used. The model for predicting sticking conditions was validated using a variety of dairy powders.

ACKNOWLEDGEMENTS

The completion of my PhD stands as a great reminder of the love, support and general good nature of many human beings. And these people I would like to thank:

My primary supervisor, Tony Paterson, thank you for your consistent support, in all aspects of what it is to be Kylie. Thanks also for the faith that you had in me and the lack of pressure applied (especially towards the end) was greatly appreciated. I am very grateful to have had the opportunity to do a PhD under your supervision. My secondary supervisor, John Bronlund, thank you for the guidance you gave me mainly at the start and end of my project. Your clear and logical thought is a gift. I would also like to thank Greg Brooks and Scott Billings who have done projects in related areas over the last three years. The general stickiness chit-chat and discussion of experimental problems was not only valuable but always incredibly thrilling. I notice that you have both had complete career changes!

Thanks to the New Zealand Dairy Board (now New Zealand Milk Powder Limited) for their sponsorship of this project and Fonterra Research Centre for their assistance with this project. In particular, thanks to Eileen Boyte, Kevin Couper, Richard Lloyd, Andrew Saunders, Steve Haylock and Jennifer Chamberlain. Many thanks also to various other people at NZMP, Fonterra Research Centre, Longburn, Hawera and Waitoa sites for their help.

This project could not have been done without the help of many people in the Institute of Technology and Engineering. Thank you Ann-Marie Jackson, Mike Sahayam, John Sykes, Bruce Collins and Don McLean for your technical support. Thanks also to Gary Radford and Steve Glasgow from the Institute of Food, Nutrition and Human Health, for the use of various pieces of equipment. Also, I would like to thank Lisa Valenzuela and Joan Brooks for their general helpfulness and kindness.

Many thanks to my fantastic friends, who have provided me with endless entertainment (on reflection, sometimes a little too much entertainment), love and support and who have helped keep me sane (almost) over the last three years. In particular, I would like to thank Kathryn and Mike L (no one else has equalled your appreciation for fine food and coffee), Jo, Jennie, Lisa, Stephen, Krisha, Jess, Maxine and cousin Anna for being truly wonderful. A special thanks to Mike C for finding endless humour in my "stickology" project. But mostly, thank you Mike for the selfless giving of your time and the support you gave me during the final (stressful and very late nights) stages of writing up.

My family, Mum, Dad, Robert, Michelle and Arnie, I simply couldn't have asked for better. I love and appreciate you all and thank you for guiding me to where I am today.

TABLE OF CONTENTS

CHAPTER 4 PREDICTION OF THE GLASS TRANSITION TEMPERATURE

CHAPTER 5 AMORPHOUS SUGAR STICKING MECHANISM

CHAPTER 6 FAT MELTING MECHANISM

CHAPTER 7 PREDICTION OF STICKING AND CAKING CONDITIONS IN DAIRY POWDERS

CHAPTER 8 CONCLUSIONS AND SUGGESTIONS FOR FUTURE WORK

LIST OF FIGURES

LIST OF TABLES

CHAPTER 1

PROJECT OVERVIEW

1.1 PROBLEM DEFINITION

The sticking and caking of dairy based powders has been a problem in the dairy industry for many years. These problems have generally been solved through experience and extensive trial and error experiments in order to identify the processing and product conditions required to avoid caking problems. As a result, sticking and caking problems in whole and skim milk powders are rarely encountered. Over the last decade, the dairy industry has begun developing specialty dairy powders for which the conditions required to avoid caking have not yet been identified.

At the present time, there is not an adequate understanding of the mechanisms for sticking and caking in dairy based powders, therefore, the processing and product conditions required to produce a caking free powder have to be determined by trial and error. This trial and error approach is time consuming, expensive and opens up the risk of damaging customer relations.

An alternative approach is to gain an understanding of the mechanisms involved in sticking and caking and how each component of the powder interacts and contributes to the sticking and caking phenomena. This is the approach that this project has taken. It was aimed at developing an understanding of the mechanisms involved in sticking and caking and being able to predict the conditions to be avoided to prevent these problems, based on the composition of the powder. This approach should allow sticking and caking problems, and conditions for their avoidance, to be identified during the formulation of new powders. It is also useful in eliminating complaints in existing powders.

1.2 PROPOSED STICKING AND CAKING MECHANISMS

Sticking, caking, crystallisation and collapse are time, temperature and moisture dependent phenomena that are often encountered during the production and storage of dry powders. These phenomena are particularly a problem during the drying and storage of sugar-rich foods [Levine and Slade 1986, Bhandari *et al.* 1997]. Before the sticking and caking mechanisms can be discussed, definitions for sticking and caking used in this work are required. Sticking has been defined as the stage when liquid bridges between particles have formed and the sticky stage exists while the bridges are in the liquid state. Liquid bridging occurs as a result of there being sufficient flow to build a bridge between two particles as they come into contact. The driving force for flow is surface tension [Downton *et al.* 1982, Wallack and King 1988]. These liquid bridges may be of molten fat, amorphous sugar or a concentrated sugar solution material. Stickiness refers to both particle-particle stickiness, as would occur during spray drying and storage, and particle-wall stickiness, as would occur during spray drying. With time these liquid bridges can crystallise. Crystallisation leads to the

irreversible consolidation of the liquid bridges [Aguilera *et al.* 1995]. Caking is defined as the stage where crystallisation is occurring and hence solid bridges are forming. Collapse occurs when there is a pronounced loss of product structure due to the thickening of interparticle bridges owing to viscous flow, reduction in interparticle spaces, and deformation of particle clumps due to gravity and surface tension. Collapse leads to a decrease in volume (shrinkage), as the matrix can no longer support its own weight [Bellows and King 1973, Tsourouflis *et al.* 1976].

The following mechanisms for sticking and caking have been identified and play important roles in the caking of dairy-based powders.

1.2.1 Amorphous Sugar Caking

Amorphous sugar caking is due to the powder being exposed to conditions where the amorphous sugar, which is initially present in an immobile glass state, is able to transform into a rubbery state [Tsourouflis *et al.* 1976, Downton *et al.* 1982, Wallack and King 1988, Peleg 1993a, Aguilera *et al.* 1995]. The temperature at which the amorphous material transforms from a glassy to a rubbery state is known as the glass transition temperature. In the rubber phase, the molecules in the amorphous sugar are capable of movement, flow and crystallisation. As a result, it is thought that flow of amorphous material causes the formation of rubber bridges between adjacent particles. If the powder remains above the glass transition temperature for long enough, crystallisation of the amorphous sugar will occur and a solid bridge will form. At this stage the powder has caked. Amorphous lactose caking has been identified as the probable cause of caking in a dairy powder with added sugar [Paterson and Bronlund 1997] and a dairy base powder [Foster and Paterson 2001] and to worsen caking in cream powders [Crofskey 2000] which also experience significant caking due to the high fat content.

1.2.2 Humidity Caking

Humidity caking occurs when the powder is put into conditions which allow moisture from the environment to adsorb onto the surface of the powder allowing liquid bridging between particles. This causes components of the powder surface to dissolve and form a saturated solution. If the powder is then put into a lower relative humidity environment or the temperature of the environment increases, the liquid bridges crystallise forming solid bridges. Humidity caking has been identified as the probable cause of caking in bulk α-lactose monohydrate [Bronlund 1997], crystalline sucrose [Bagster 1970, Ludlow and Aukland 1990, Billings 2002] onion powder [Peleg and Mannheim 1977] and fertilisers [Rutland 1991]

1.2.3 Fat Melting Mechanism

It is possible that the fat present on the surface of powder particles is capable of causing noticeable flowability problems. If the temperature is increased during storage or processing, some of the fat may melt forming liquid bridges of fatty composition. If the temperature later drops, the fatty liquid bridges can solidify resulting in a lumpy

product. Levels of free fat in a powder can increase as a result of amorphous lactose crystallisation. Milk powders consist of spherical particles of amorphous lactose containing embedded micellar casein and fat globules [Pearce 1992]. Amorphous lactose crystallisation causes the expulsion of protein, minerals and fat from the ordered structure of the crystals to the surface of the powder. These observations have also coincided with an increase in the degree of caking [Munns 1989]. In this case it is thought that the cause of caking is in fact due to the amorphous lactose caking and that the increase in free fat could compound the problem. Crofskey (2000) found that the high levels of fat in cream powders were enough to cause flow problems in these powders.

1.2.4 Protein Sticking

Proteins are extremely hygroscopic and have been shown to cause caking problems in fish products and soya sauce powders where hydrolysed proteins are present [Hamano and Sugimoto 1978, Aguilera *et al.* 1993, Netto *et al.* 1998]. Recent work [Burr 1999] on a whey protein isolate powder gave no indication of caking. Therefore the effect of proteins on caking is unclear. Protein aggregation reactions can result from water sorption during processing and storage. These reactions include thiol-disulphide interchanges, the formation of other covalent bonds mediated by lysine residues, and conformational (non-covalent) changes [Liu *et al.* 1991, Townsend and DeLuca 1991].

1.3 OVERALL PROJECT AIMS

The overall aims of this research were to:

1. Investigate the caking and sticking properties of the major and minor components of dairy powders
2. Formulate a mathematical model using the acquired knowledge to enable a prediction to be made about the caking and sticking properties of dairy powders
3. Test the validity of the model against the caking and sticking properties of various dairy powders
4. Have a method for recommending the final moisture contents that must be achieved for a particular dairy powder, given its composition, in order to avoid sticking and caking problems.

Amorphous lactose is one of the main components in dairy powders and a lot of work has recognised amorphous lactose as being the major contributing factor to sticking and caking of milk powders [White and Cakebread 1966, Chuy and Labuza 1994, Jouppila and Roos 1994a,b, Lloyd *et al.* 1996, Jouppila *et al.* 1997]. As a result, there is a lot of literature on the contribution of lactose to sticking and caking problems, as reviewed in the following chapter.

CHAPTER 2

STICKING AND CAKING PROPERTIES OF LACTOSE – A REVIEW

2.1 INTRODUCTION

Much work has been done on the contribution of lactose to the sticking and caking problems experienced with dairy powders. This work recognised lactose, in the amorphous form, as being the major contributing factor to caking of milk powders [White and Cakebread 1966, Chuy and Labuza 1994, Jouppila and Roos 1994a,b, Lloyd *et al.* 1996, Jouppila *et al.* 1997]. More recently, Brooks (2000) investigated the sticking properties of amorphous lactose and Bronlund (1997) investigated caking of crystalline lactose in bulk storage. The work by Bronlund (1997) and Brooks (2000) appears to be the most recent developments in this area and will be reviewed in this chapter. Subsequent chapters will review the contribution of other components, those found in milk and added sugars, on the sticking and caking problems found with dairy powders.

2.2 PROPERTIES OF LACTOSE RELATING TO STICKING AND CAKING PROBLEMS

Lactose is a reducing disaccharide and consists of the hexose sugars, glucose and galactose. The bond between the glucose molecule and galactose molecule develops between carbon atom four of glucose and carbon atom one of galactose [Pritzwald-Stegmann 1986] as shown in figure 2.1.

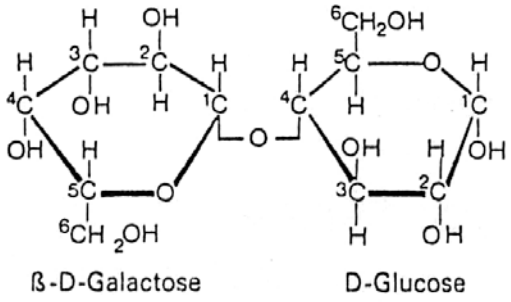

Figure 2.1: α-lactose chemical structure

Lactose is capable of existing in the following forms:

1. Lactose in solution in both α and β isomers
2. Crystalline lactose (both α and β anhydrous forms and as an α monohydrate)
3. Amorphous lactose
4. A mixture of both crystalline and amorphous lactose

Lactose contains a free aldehyde group, and is therefore capable of existing in two stereoisomeric forms, α and β. When either form is dissolved, a change from one form

into the other, through mutarotation, takes place until an equilibrium ratio between α and β lactose is reached [Roetman and Buma 1974]. The equilibrium ratio of β/α in solution at 20°C is 1.59 in pure water [Lowe 1993]. It is noted that Nickerson (1974) found this value to be 1.68. The equilibrium ratio in solution is slightly affected by differences in temperature but not by differences in pH [Nickerson 1974]. Buma (1970) showed that the β/α ratio in spray-dried lactose powders is dependent on the outlet temperature of the drier. There is a linear relationship for the β/α ratio and drying temperature minus 10°C for spray dried amorphous lactose powders. Buma (1970) concluded that the outlet drier temperature minus 10°C is probably the temperature at which the powder particles became solid.

Mutarotation involves a mechanism whereby the basic catalyst removes a proton from one part of the molecule and the acid supplies a proton to another part of the molecule, while at the same time the ring opens and then recyclises to give the isomeric form of the compound [Isbel and Pigman 1969]. In an aqueous solution containing only lactose and water, the basic catalyst is OH^- and the acid is H_3O^+ from the dissociation of water. Mutarotation is affected by temperature [Herrington 1934, Haase and Nickerson 1966, Holsinger 1988, Foster 1998], pH [Troy and Sharp 1930, Foster 1998] and salts [Herrington 1934, Haase and Nickerson 1966, Foster 1998].

Butler (1998) presented equations for predicting the equilibrium solubility of lactose (equations 2.1 and 2.2). Equation 2.1 describes the equilibrium solubility below 93.5°C, where α-lactose is the stable form. Equation 2.2 describes the equilibrium solubility above 93.5°C, where β-lactose is the stable form. The solubility of β-lactose is much greater than the solubility of α-lactose therefore, if α-lactose is added to water (at temperatures less than 93.5°C), the initial solubility limit of α-lactose is reached very quickly. Mutarotation then occurs to convert α-lactose to β-lactose in order to establish an equilibrium ratio between the two isomers. This in turn allows further dissolution of α-lactose into solution and this continues until the final solubility limit is reached [Bronlund 1997]. The α-lactose solubility of a saturated solution is given by equation 2.3 [Visser 1982 cited in Butler 1998]. The *F* factor gives the depression effect of various disaccharides on α-lactose solubility and can be found using equation 2.4 [Butler 1998]. K_L is the equilibrium constant and can be found using equation 2.5. The solubility of β-lactose can be found using equation 2.6.

$$C_s = \exp(2.389 + 0.028\mathrm{T}) \qquad (\mathrm{T} < 93.5°\mathrm{C}) \tag{2.1}$$

$$C_s = \exp(3.569 + 0.015\mathrm{T}) \qquad (\mathrm{T} > 93.5°\mathrm{C}) \tag{2.2}$$

$$C_{\alpha s} = \frac{C_s - FK_L(C_L - C_s)}{K_L + 1} \tag{2.3}$$

$$F = 0.0159 + 0.00023\mathrm{T}^{1.36} \qquad (\text{where T} = 25 - 60°\mathrm{C}) \tag{2.4}$$

$$K_L = \frac{k_1}{k_2} = \frac{C_{\beta s}}{C_{\alpha s}} \tag{2.5}$$

$$C_{\beta s} = C_s - C_{\alpha s} \tag{2.6}$$

where
C = lactose concentration (g anhydrous lactose/100g water)
$C_{\alpha s}$ = α-lactose solubility (g α-lactose/100g water)
C_s = lactose solubility (g lactose/100g water)
$C_{\beta s}$ = β-lactose solubility (g β-lactose/100g water)
F = factor accounting for depression effect of disaccharides
k_1 = rate constant of α- to β-lactose (min^{-1})
k_2 = rate constant of β- to α-lactose (min^{-1})
K_L = equilibrium constant
T = temperature (°C)

Since β-lactose is more soluble than α-lactose, when β-lactose is added to water an initially high solubility is reached. Herrera *et al.* (1999) stated that as mutarotation occurs the α-lactose molecules in solution become supersaturated and crystallise out of solution. At the equilibrium concentration, the β-lactose crystals will have converted, through solution, to α-lactose monohydrate crystals due to α-lactose's lower solubility limit. Bronlund (1997) further stated that above 93.5°C β-lactose becomes the lactose anomer which has the limiting solubility and the opposite of the above behaviour is observed.

The mechanisms and conditions for sticking and caking in crystalline lactose and amorphous lactose are different, therefore they will be reviewed separately.

2.2.1 Crystalline Lactose

Commonly, lactose exists in the crystalline form as α-lactose monohydrate ($C_{12}H_{22}O_{11}.H_2O$). α-lactose monohydrate is formed by crystallisation from a lactose solution below 93.5°C. Crystalline α-lactose adsorbs little moisture until it begins to dissolve at water activities greater than 0.8 [Linko *et al.* 1981]. β-lactose is crystallised from solution above 93.5°C. Crystalline β-lactose is anhydrous and has different properties to α-lactose monohydrate, including increased sweetness and solubility [Pancoast and Junk, 1980]. α- and β-lactose also differ in specific rotation, melting point and hygroscopicity [Aguilera *et al.* 1995]. Table 2.1 shows data taken from Buma (1965), Harper (1992) and Pritzwald-Stegmann (1986) and serves as a comparison of the properties of α-lactose monohydrate and β-lactose anhydride.

Table 2.1: General properties of α-lactose monohydrate and β-lactose anhydride.

Properties	α-Lactose monohydrate	β-Lactose anhydride
Molecular weight [g/mol]	360	342
Density [g/cm³]	1.545	1.59
Melting point [°C]	202	252
Boiling point [°C]	Disintegration not far above melting	
Heat of combustion [kJ/kg]	16106	15465
Specific rotation $[\alpha]_D^{20}$	+52.5°	+34°
Specific heat [kJ/kgK]	1.251	1.193
Heat of solution [kJ/kg]	-50.24	-9.62

2.2.1.1 Crystalline Lactose Isotherms

The isotherm for α-lactose monohydrate was measured by Bronlund (1997) for powders of different particle size and at temperatures of 12, 20, 30 and 40°C. No temperature or particle size effects were observed and the data was fitted with the three stage sorption (tss) isotherm model given below (eq 2.7, 2.8, 2.9) and discussed in section 3.2.2.3:

$$M = \frac{M_o cHfa_w H'}{(1-fa_w)[1+(cH-1)fa_w]} \tag{2.7}$$

$$H' = 1 + \frac{H-1}{H}\frac{1-fa_w}{1-a_w}[h+(1-h)a_w] \tag{2.8}$$

$$H = 1 + \frac{1-f}{f}\frac{(fa_w)^h}{1-a_w} \tag{2.9}$$

where M = moisture content including residual moisture (g water/g dry powder)
M_o = monolayer moisture content (g water/g dry powder)
c = constant related to the energy of bonding
f = constant which corrects the properties of the multilayer with respect to the bulk liquid
h = number of layers comprising the second sorption stage

The parameters M_o, f, c and h for the model are 0.025 g/100g dry lactose, 0.92, 8.8 and 30 respectively. The moisture adsorption isotherm predicted using this model is given in figure 2.2. An isotherm for β-lactose was not given by Bronlund (1997), due to β-lactose picking up moisture and converting to α-lactose during storage over saturated salts with a water activity of greater than 0.6.

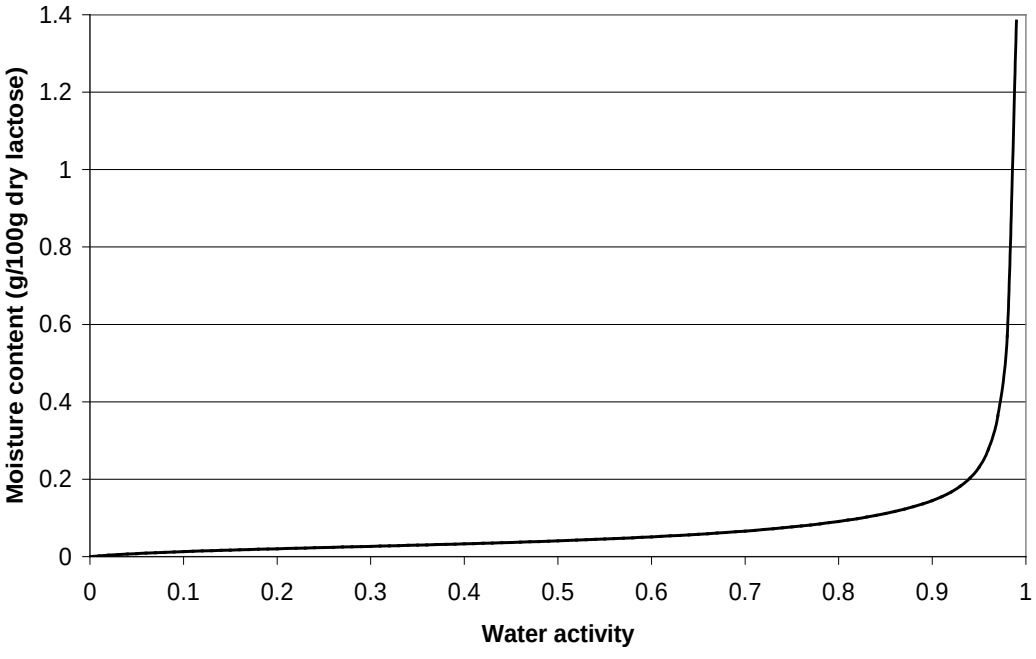

Figure 2.2: Moisture sorption isotherm of α-lactose monohydrate

2.2.1.2 Sticking and Caking of Crystalline Lactose

Bronlund (1997) termed the mechanism for caking in bulk lactose as humidity caking. This type of caking occurs when the sugar is exposed to high relative humidity conditions. Moisture collects in the contact points between adjacent lactose crystals due to capillary condensation effects. The moisture that is absorbed to the surface of these contact points allows the crystal surface to dissolve and form liquid bridges of the saturated sugar solution. This stage of liquid bridging was termed as lumping. If the lumped lactose powder is then exposed to lower relative humidity conditions, moisture will then desorb from the particle surface. The desorption of moisture results in the supersaturation of the dissolved lactose in the liquid bridge, allowing a driving force for crystallisation. This results in the formation of a solid bridge which has considerably more strength than the liquid bridges present when the lactose has lumped. The stage of solid bridging was termed caking. The humidity caking mechanism is illustrated in figure 2.3, as taken from Bronlund (1997).

Bronlund (1997) constructed a model to predict the conditions for caking in bulk lactose. This model also included the effect of amorphous lactose and the migration of moisture due to temperature gradients in the bulk powder. It was found that there was less than 5% amorphous lactose in bulk crystalline lactose. Therefore caking due to the amorphous lactose was insignificant. The amorphous lactose was important, as it acts as a moisture sink (holding much more moisture than crystalline lactose), which can be released to the crystalline lactose upon crystallisation. This in turn would increase the amount of moisture available to the crystalline lactose, which would contribute to

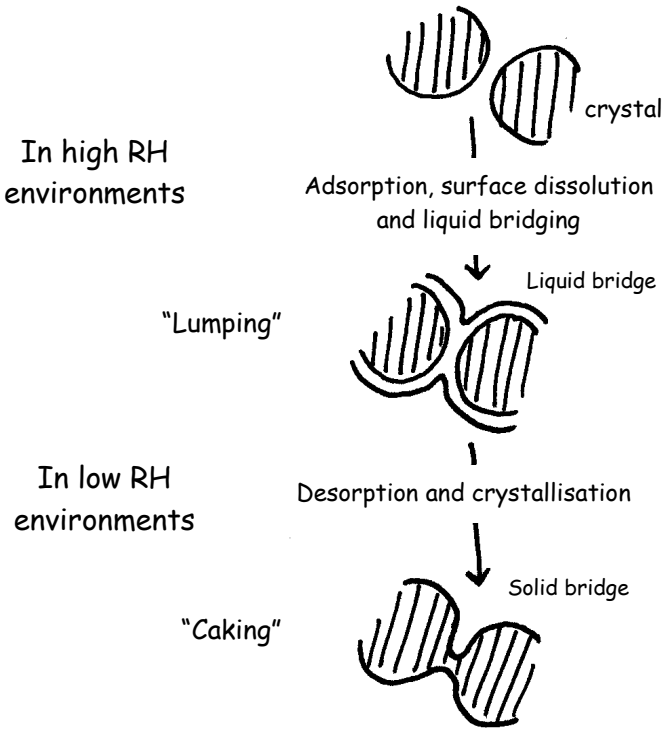

Figure 2.3: Humidity caking mechanism

caking. Using the model with expected storage conditions, the powder should be stored below $0.57a_w$ if no amorphous lactose is present. If amorphous lactose is present then the powder should be stored below $0.25a_w$.

2.2.2 Amorphous Lactose

Amorphous lactose is formed when lactose in solution is dried quickly, as is the case during spray drying. It can also be formed by freeze drying and quenching from a melt. The isotherm and glass transition temperature profile are the most important physical properties of amorphous lactose when dealing with sticking problems. These are discussed below.

2.2.2.1 Amorphous Lactose Isotherm

Brooks (2000) found that there was a lot of offset in some of the moisture sorption data for amorphous lactose given in the literature. It was found that in some cases the total moisture contents were used as opposed to the moisture content obtained gravimetrically, which does not measure residual moisture. The moisture content measured gravimetrically is with respect to a zero moisture content obtained by drying over phosphorous pentoxide. Drying amorphous lactose over phosphorous pentoxide (P_2O_5) is the standard method for giving a completely dry material. However, further drying of amorphous lactose samples in an oven found that there is still some residual moisture present in the sample [Brooks 2000]. The total moisture content was given in cases where the amount of moisture was measured using the Karl Fisher titration techniques. The discrepancy between the data was corrected for by applying a measured value of 1.0g/100g dry powder for the residual moisture. The corrected isotherm can be seen in figure 2.4.

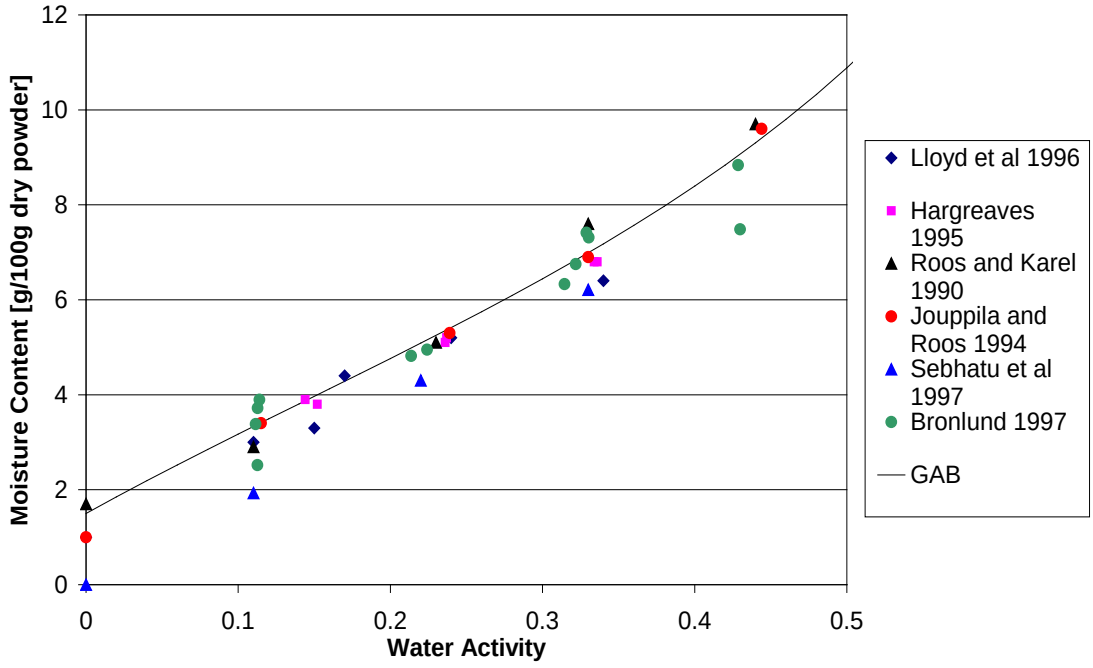

Figure 2.4: Amorphous lactose moisture sorption isotherm

The isotherm was fitted with the GAB model given in equation 2.10. This model was fitted to the isotherm data obtained gravimetrically i.e. the data whose moisture content stated does not include the residual moisture, as P_2O_5 was used to give zero moisture content. Referring to figure 2.4, the GAB model was fitted to the original data given by Roos and Karel (1990), Jouppila and Roos (1994a), Hargreaves (1995), Lloyd *et al.* (1996), Bronlund (1997) and Sebhatu *et al.* (1997). The data shown in figure 2.4 has had the residual moisture content added. The residual moisture can be included during prediction by adding 1.0g/100g dry powder to the amount predicted using the GAB model below (equations 2.10 and 2.11). Brooks (2000) found that a residual moisture content of 1.0g/100g dry powder is likely to remain after drying a powder over P_2O_5 for the typical equilibration time of three weeks.

$$M_f = \frac{M_o f c a_w}{(1 - f a_w)[1 + (c - 1) f a_w]} \tag{2.10}$$

$$M = M_f + 1.0 \tag{2.11}$$

where M = moisture content including residual moisture (g water/g dry powder)
M_f = moisture content not including residual moisture (g water/g powder)
M_o = monolayer moisture content (g water/g dry powder)
c = constant related to the energy of bonding
f = constant which corrects the properties of the multilayer with respect to the bulk liquid

The parameters for the model, M_o, f and c, were found to be 6.27g/100g dry powder, 1.01 and 2.81 respectively.

2.2.2.2 Amorphous Lactose Glass Transition Temperature Profile

Brooks (2000) also found that there was offset in some the published data on the glass transition temperature profile of amorphous lactose. It was found that much of this offset was due to the residual moisture in the amorphous lactose sample. The residual moisture present in a sample, which has been dried over phosphorous pentoxide, can have a plasticising effect on amorphous lactose. It is noted that pure amorphous lactose (i.e. with no α-lactose monohydrate) must be used, as oven drying will remove the water of crystallisation from α-lactose monohydrate as well as the free moisture. Only the free moisture effects the T_g of amorphous materials, therefore the free moisture content, as opposed to the total moisture content, should be stated. Brooks (2000) found that correcting the data for this residual moisture gave a much better agreement between the different authors. With these corrections made it was then possible to predict the T_g of amorphous lactose given the moisture content. This was done using the Gordon and Taylor equation, as given in section 4.2.2, with the variables T_{g1} and k equal to 115°C and 6.9 respectively. Using these parameters, it is then possible to use the total moisture content (including the residual moisture) to predict the T_g of amorphous lactose.

Brooks (2000) used the moisture sorption isotherm and Gordon and Taylor equation (equation 4.1) to predict the T_g of amorphous lactose from the water activity. This was

done by determining the moisture content at a given water activity and then calculating the T_g with respect to that moisture content. This approach was found to be only moderately successful. Brooks (2000) found that a better prediction was obtained by making predictions directly from the water activity. A third order equation (equation 2.12) gave the best fit to this data and can be used to predict the T_g of amorphous lactose given the water activity of the powder. A dry T_g of 101°C should be used at $0.0a_w$ as this is the commonly accepted value for amorphous lactose that has been dried over phosphorous pentoxide [Roos and Karel 1990, Brooks 2000].

$$T_g = -530.66(a_w)^3 + 652.06(a_w)^2 - 366.33a_w + 99.458 \qquad [0 < a_w < 0.575] \qquad (2.12)$$

2.2.2.3 Sticking and Caking of Amorphous Lactose

Amorphous lactose can exist as either a glass or a rubber. A glass is defined as a solid-like material that has a disordered liquid-like structure and is characterised by molecular immobility due to the high viscosity of around 10^{12} – 10^{13} Pa.s [Noel *et al.* 1991, White and Cakebread 1966]. A glass can undergo a second order phase change at a certain temperature giving a rubbery material due to its decreased viscosity (10^6-10^8 Pa.s [Peleg 1993a, Downton *et al.* 1982, Wallack and King 1988, Blanshard 1995]. The temperature at which this change occurs is called the glass transition temperature (T_g). It is the increased flow, due to the lower viscosity, of the material in the rubbery state that allows stickiness, caking, collapse and crystallisation to occur. The T_g is sensitive to plasticisers, such as moisture [Levine and Slade 1986, Levine and Slade 1988], therefore a glass material can enter the rubbery state in two ways. At a constant moisture content or water activity, the glass can enter the rubbery state by an increase in

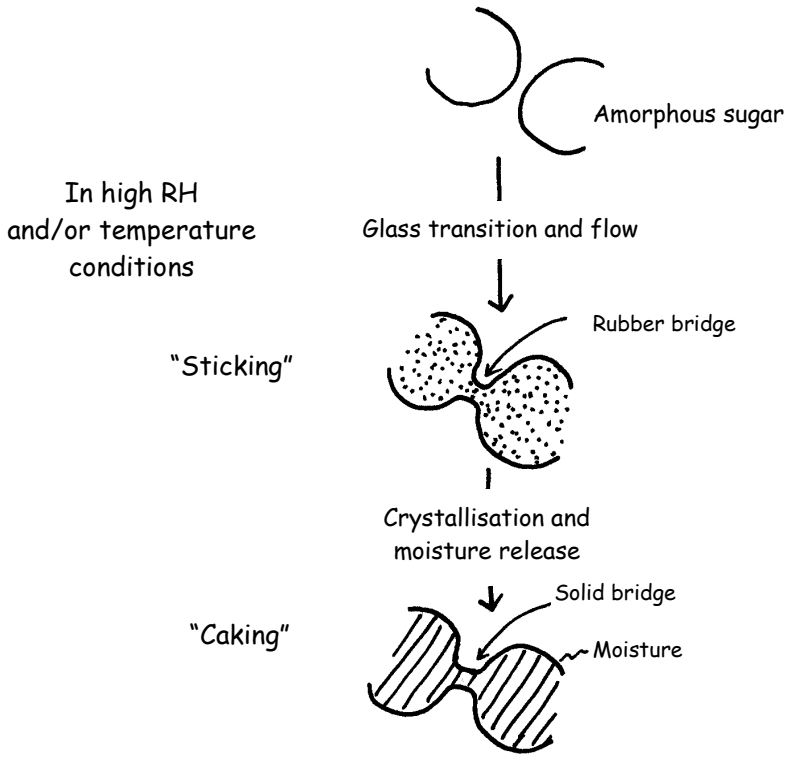

Figure 2.5: Amorphous lactose caking mechanism

the ambient temperature. At a constant temperature, a rubbery state can result from exposure to more humid environments which will reduce the T_g of the powder to below ambient temperatures. Amorphous lactose caking is initiated by either an increase in temperature to above T_g or an increase in moisture content and water activity reducing the T_g to below ambient temperatures. As the glass transition temperature is exceeded, flow can occur due to a reduced viscosity, which allows the formation of liquid bridges between contacting particles. This renders the powder sticky and if it remains above the glass transition temperature for a long enough period of time, crystallisation can occur. Crystallisation results in the formation of solid bridges rendering the sample caked. As crystallisation occurs, moisture is released which may then be taken up by the rest of the powder, thus, initiating sticking and subsequent caking in the rest of the powder. The mechanism for this type of caking is shown in figure 2.5.

Paterson *et al.* (2001) developed the blow test to measure the caking strength of milk powder. The test involved passing air through a small diameter tube held at a fixed height and angle above a powder bed. The flow rate of air through the tube was increased until a channel was blown into the powder bed. The flow rate is recorded and is a measure of the caking strength or stickiness of the powder. The blow test was developed to determine the cause of caking in a dairy powder, which was found to be due to the amorphous lactose [Paterson and Bronlund 1997]. Brooks (2000) modified this test for ease of use in situations with a larger powder bed where multiple readings were to be taken over a period of time under constant temperature and relative humidity conditions. The test involved bringing a testing chamber to the desired relative humidity and temperature conditions using a rig capable of doing this. The powder sample was then placed on a segmented distributor plate and the caking strength was measured with time.

Brooks (2000) demonstrated that the sticking behaviour of amorphous lactose is determined only by the amount that the glass transition temperature is exceeded by and not the conditions used to do this. Therefore, different combinations of temperature and water activity, giving the same $T\text{-}T_g$, would show the same relationship of caking strength with time. After investigating the sticking behaviour of amorphous lactose, Brooks (2000) recommended that to avoid sticking problems during storage, the powder should be dried to conditions below the glass transition temperature of the amorphous lactose. Using the maximum likely temperature that the powder is to experience during storage enables prediction of the water activity that the powder should be dried to. Drying to that water activity or lower will ensure that the powder is never exposed to conditions where the T_g is exceeded. Brooks (2000) also suggested that a $T\text{-}T_g$ of 10°C would be a good limit to remain below during processing. Under these conditions, amorphous lactose takes longer than 3 hours of contact time to reach a moderate level of stickiness. At a $T\text{-}T_g$ of greater than 25°C, amorphous lactose becomes sticky almost instantaneously. Therefore, these conditions should be avoided in all areas of processing.

Work done by Burr (1999) investigating the cause of caking in cheese powder found that the amorphous lactose caking mechanism was responsible for caking in such powders during storage. The powders were left in varying relative humidity conditions at room temperature for two weeks. The caking strength was then measured using the blow test and termed either free flowing, lumped (initial stages of caking) or caked. It

was found that lumping occurred significantly below the T_g of the powder as predicted using the T_g profile for amorphous lactose. Caking started at a $T-T_g$ of 10°C.

Further work was done by Keir (2001) with spray-dried milk powders containing varying levels of lactose, protein and fat. It was found that the T_g of the powder could be predicted by the cubic equation (2.12) given by Brooks (2000) using the measured water activity of the powder. The stickiness behaviour of milk powders did differ from that of pure amorphous lactose. A milk powder tested at a $T-T_g$ of 20°C did not show any tendency to become sticky over time (5 hours experimentation). Therefore a $T-T_g$ of 25°C is unlikely to cause instantaneous sticking in milk powders, as occurs in pure amorphous lactose powders. From Keir's (2001) work, it appears that the recommendations by Brooks (2000) for operating dryers at conditions to give a $T-T_g$ of 10°C are too conservative. A higher $T-T_g$ could be used and still provide safe operating conditions. From examination of plant operating curves and the T_g profile of amorphous lactose, Keir (2001) stated that the $T-T_g$ required for stickiness to occur may be 30°C or higher, especially considering the short residence time in the dryers. In the light of this work it is therefore probable that safe dryer operation could take place using temperature and humidity conditions giving a $T-T_g$ of greater than 10°C.

2.3 CLOSURE

A review of the current literature on lactose has found that the moisture sorption isotherms for amorphous lactose and α-lactose monohydrate are given by equations 2.10 and 2.7 respectively. The T_g profile for amorphous lactose is given by equation 2.12. The mechanism for sticking with amorphous lactose was found to be related to the $T-T_g$ of the powder, rather than the moisture content or temperature of the powder. The rate of sticking increases as the $T-T_g$ increases. At a $T-T_g$ greater than 25°C, sticking for pure amorphous lactose samples is almost instantaneous. However, the same was not found to be true with dairy powders which contain components other than lactose. The $T-T_g$ for instantaneous sticking appears to be significantly higher. Therefore, further work is required to determine the $T-T_g$ that should be used during drying to ensure that sticking does not occur. The suggested $T-T_g$ should not be too conservative as this would result in dryers being run at a slower rate of drying than is necessary. This is obviously not ideal, as it would decrease dryer throughput and therefore increase the drying costs associated with the powder.

Dairy powders consist of other components apart from lactose, therefore the properties of these other components need to be investigated. Sticking and caking properties are related to the moisture present in the powder through the glass transition temperature concept. Chapter 3 gives details of the isotherms for dairy powder components and a method for predicting the isotherms for dairy powders based on their compositions. Chapter 4 investigates the effect of moisture on the T_g of the different components of dairy powders and also the prediction of T_g profiles based on the composition of a powder.

CHAPTER 3

PREDICTION OF MOISTURE SORPTION ISOTHERMS FOR DAIRY POWDERS

3.1 INTRODUCTION

Water plays an important role with respect to the properties of food powders. In particular, water effects the glass transition temperature (T_g) and consequently the sticking and caking properties of powders during processing and storage. Moisture sorption isotherms for powders describe the equilibrium relationship between the moisture content of the powder and the relative humidity of the surrounding environment [Labuza 1968]. It is necessary to know or be able to predict isotherms for dairy powders, so that the moisture content that the final powder should be dried to, can be determined. The moisture content that the powder should be dried to will depend on the composition of the powder and in particular, the amount of amorphous sugars present. The final moisture content will be restricted by how much moisture can be associated with the amorphous sugar so that it remains stable during storage. Upon determining the allowable moisture content for the amorphous sugars, by using T_g profiles as discussed in chapter 4, the amount of moisture associated with the other components can be determined so that all components are in equilibrium, i.e. they have the same water activity.

If dairy companies dried powders to a specific water activity, determined by the T_g profile for the powder, then the isotherms would not be required. However, since it is common practice to dry to a specified moisture content and that the moisture content is often required by the customer, isotherms need to be either measured or reliably predicted. Since it is time consuming to measure isotherms for all powders, a method for predicting isotherms would be useful. This chapter investigates a method for predicting isotherms for dairy powders, based on the weighted addition of the powder components' isotherms. This method requires accurate isotherms for the dairy powder components, therefore the initial focus of this chapter is determining the components' isotherms.

3.2 MOISTURE SORPTION ISOTHERMS

The sorption isotherm is a plot of the amount of water sorbed as a function of the water activity or relative humidity of the vapour space surrounding the material. At equilibrium, the water activity is related to the relative humidity of the surrounding vapour by the relationship (equation 3.1):

$$a_w = \frac{p}{p_o} = \text{Equilibrium relative humidity} \qquad (3.1)$$

where a_w = water activity

p = water vapour exerted by the food material at T_e [Pa]
p_o = vapour pressure of pure water at temperature T_e [Pa]
T_e = equilibrium temperature of the system [°C]

It is important to note the temperature at which an isotherm is measured. For general food powders, the amount of water held at a certain a_w decreases as temperature increases [Labuza 1968] and has been shown to follow the Clausius-Clapeyron relationship (equation 3.2) [Bell and Labuza 2000]. With increasing temperature, an increase in water activity at a given moisture content occurs as the bond between the water molecule and the OH group of the food solid breaks. This allows the water to become free, which results in an increase in water activity [Jaya *et al.* 2002].

$$\frac{d\left(\ln a_w\right)}{d\left(\frac{1}{T}\right)} = -\frac{Q_s}{R} \tag{3.2}$$

where Q_s = net isosteric heat of sorption on homogenous sites (excess binding energy for removal of water) [kJ/mol]
R = ideal gas constant [kJ/mol K]
T = temperature [K]

This temperature effect has been seen with casein [Loncin *et al.* 1968], whey protein concentrate [Hermansson 1977], skim milk powder [Berlin *et al.* 1970], non-fat milk powder [Heldman *et al.* 1965], amorphous sucrose [Iglesias *et al.* 1975], amorphous glucose [Loncin *et al.* 1968] and sugar beet root [Iglesias *et al.* 1975]. This temperature effect however was not observed for amorphous lactose [Bronlund 1997], amorphous maltose [Audu *et al.* 1978] or α-lactose monohydrate [Audu *et al.* 1978, Bronlund 1997]. The reverse has been found to be true for some sugars and foods containing sugars, e.g. crystalline fructose [Audu *et al.* 1978]. With sugars, when the powder is exposed to higher temperatures, the sugar dissolves in the newly formed free water. This results in a decrease in the water activity with the increase in temperature (or an increase in the amount of water held at a given water activity) [Jaya *et al.* 2002].

Brunauer (1945) classified moisture sorption isotherms as being either type I, II or III. Type I is typical of anticaking agents, type II is sigmoidal shaped and is representative of most foods and type III represents the isotherm for pure crystalline substances. Labuza (1968) stated that isotherms can be divided into three regions depending on the state of the water present. The first region, which covers the water activity range of 0.00 to about 0.35, represents the adsorption of a monomolecular film of water. The second region (around 0.35 to 0.60 water activity) represents the adsorption of additional layers of water over the monolayer. The third region (above 0.60 water activity) represents water condensing into the pores of the material, followed by dissolution of the soluble material present [Lomauro *et al.* 1985]. Labuza (1968) stated that these regions cannot be defined by any specific water activity and may overlap. As a result of the isotherm being divided into regions, isotherm equations developed based on a particular water activity range are only good for that range.

3.2.1 Isotherm Measurement

Moisture sorption isotherms are typically obtained gravimetrically by exposing the sample to atmospheres of known relative humidity [Berlin *et al.* 1968, Iglesias *et al.* 1975, Iglesias *et al.* 1980, Linko *et al.* 1981, Jouppila and Roos 1994a]. Usually the isotherm is created by putting samples into controlled humidity chambers at a constant temperature and measuring the weight gain with time until equilibrium occurs. There are a number of ways for achieving a controlled relative humidity environment [Bell and Labuza 2000], however the use of saturated salt solutions is the most commonly used method. Saturated salt solutions are placed at the bottom of desiccators to give constant equilibrium relative humidity environments. The equilibrium relative humidity of different salt solutions [Richardson and Malthus 1955, Rockland 1960, Greenspan 1977] is given in table 3.1 for four temperatures. To measure a true adsorption isotherm, the powder should be dried to zero moisture without changing the properties of the powder prior to isotherm measurement. This can dramatically increase the experimentation time, therefore it is not uncommon to measure a working isotherm. A working isotherm does not require the powder to be completely dry first, but measures the initial moisture content for the powder which is then used to correct the moisture gains/losses for the powders exposed to relative humidities greater than zero. The powders should be left in the controlled relative humidity environments until equilibrium is reached, which is usually 3 weeks [Bell and Labuza 2000].

Table 3.1: Equilibrium relative humidities of saturated salt solutions at different temperatures

Salt	Relative Humidity			
	4°C	20°C	34°C	50°C
Lithium chloride	0.11	0.11	0.11	0.11
Potassium acetate	0.23	0.23		
Potassium fluoride			0.24	0.21
Magnesium chloride	0.34	0.33	0.32	0.30
Potassium carbonate	0.43	0.43	0.43	
Magnesium nitrate	0.59	0.54		0.45
Sodium bromide	0.64		0.54	0.51
Potassium iodide			0.67	0.64
Sodium chloride	0.76		0.75	0.74
Potassium chloride	0.88		0.83	0.81
Potassium nitrate	0.96		0.90	

The following method was used to measure the isotherms for the components and powders given in this chapter and chapter 7. Powders of a known weight were placed in the desiccators and left to equilibrate for 3 weeks (20 and 34°C), 5 months (4°C) and 6 weeks (50°C). The powder samples were then reweighed after this time and the moisture content determined. The initial moisture content of the powder was obtained by placing over P_2O_5 which gives a relative humidity environment of close to 0%. The moisture content of the powder at each relative humidity was calculated using equation 3.3.

$$M = \frac{W_i M_i + \Delta W(1 + M_i)}{W_i} \tag{3.3}$$

where W_i = initial mass of sample (g water + dry powder)
M_i = initial moisture content of sample (g water/g dry powder)
ΔW = final – initial mass of sample (g water)
M = moisture content of sample (g water/g dry powder)

3.2.2 Isotherm Models

Many models have been developed to describe isotherms or parts thereof, some with more success than others. The following is not intended to be a review of these models, rather a discussion on those models which have been successful and are used extensively (i.e. BET and GAB models) and models which are extensions or alternatives of the GAB model (i.e. three stage sorption model, Peleg's double powder model and Lewicki's 3 parameter model).

3.2.2.1 BET Model

The BET model, developed by Brunauer *et al.* (1938), is given by equation 3.4:

$$M = \frac{M_o a_w}{(1 - a_w)[1 + (c - 1)a_w]} \tag{3.4}$$

where M = moisture content (g water/g dry solid)
M_o = monolayer moisture content (g water/g dry solid)
c = constant related to the energy of bonding

Although this model is applicable over a limited range, water activities of 0.0 to 0.3-0.5, it is discussed as it is the foundation of other models including the GAB model. The BET model employs the monolayer concept in which the molecule is bound tightly on a homogeneous surface. Labuza (1975) stated that this may not be totally correct since the food surface interaction is heterogeneous.

The sorption process described by the BET model is regulated by two mechanisms. The first mechanism is with Langmuir kinetics where gas molecules are adsorbed on selected sites at the solid surface until the surface is covered by a layer of gas one molecule thick. The second mechanism concerns the condensation of subsequent layers onto the monolayer [van den Berg 1985]. The state of adsorbate molecules in the second and higher layers is the same as in the liquid-like state [Timmermann and Chirife 1991]. Traditionally the monolayer moisture content has been determined from the intercept and slope of an $a_w/[M(1-a_w)]$ vs a_w plot in the applicable water activity range [Karel 1975, Labuza 1984].

M_o is the moisture content at which a single layer of water molecules has been adsorbed on available sites on the solid surface. As a result, it is commonly used as a measure of the specific surface area of a sample. Bronlund (1997) stated that since no values for the adsorption of water to sugars have been given in literature, the average cross-sectional area (10 – 13 Angstom^2 per molecule) given in McClellan and Hansberger (1967) can be used as an estimate to allow the calculation of the specific surface area of

150,000 m^2/m^3. The constant *c* relates to the bonding energy of the adsorbate onto the solid surface. Brunauer *et al.* (1938) showed that equation 3.5 applies:

$$c \approx e^{\left(\frac{E_1 - E_L}{RT}\right)} \tag{3.5}$$

where E_1 = bonding energy of monolayer adsorbed molecules
E_L = bonding energy of molecules adsorbed on subsequent layers

3.2.2.2 GAB Model

The failure of the BET model at higher water activities led to the development of the GAB model [van den Berg 1985]. The three parameter GAB model was developed by Guggenheim (1966), De Boer (1953) and Anderson (1946) and is represented by equation 3.6:

$$M = \frac{M_o cfa_w}{(1 - fa_w)[1 + (c-1)fa_w]} \tag{3.6}$$

where *c* and M_o are the constants from the BET model and *f* is a constant which corrects the properties of the multilayer molecules with respect to the bulk liquid.

The state of the adsorbate molecules was postulated to be the same in the second and higher layers but different from that in the liquid-like state. This assumption led to the development of the GAB model with the introduction of a third parameter *f*. At *f*=1, the GAB model reduces to the BET model. If *f* is less than unity, a lower sorption than that demanded by the BET model is predicted and allows the GAB isotherm to be applicable up to high water activities ($a_w \cong 0.9$) [Boquet *et al.* 1979, van den Berg 1985]. The constant *f* is dependent on the energy of bonding of the multilayer molecules. Anderson (1946) showed that the energies of bonding of the second to ninth layers are equal and given by equation 3.7:

$$f \approx e^{\left(\frac{E_{2\to 9} - E_L}{RT}\right)} \tag{3.7}$$

Values of *f*>1 are not possible for two reasons, the first being physical and the second being purely mathematical. Referring to equation 3.7, $(E_{2\to 9} - E_L)$ is the energy necessary to adsorb a mole of liquid onto already existing adsorbed layers several molecules deep. Hence, the heat of adsorption in the second to ninth layers should be lower than the heat of liquefaction. Therefore $(E_{2\to 9} - E_L)$ must be negative. From equation 3.7 it can be seen that as $(E_{2\to 9} - E_L) \to -\infty$, $f \to 0$ and when $(E_{2\to 9} - E_L) \to 0$, *f*=1. Therefore *f* is in the range from 0 to 1 [Lewicki 1997]. Lewicki (1997) also stated that in terms of entropy, a negative value of $(E_{2\to 9} - E_L)$ indicates that the adsorbate in the second to ninth layer is more ordered than in the liquid phase. If $(E_{2\to 9} - E_L)$ was positive (giving *f*>1), this would indicate that the free energy change in adsorption is more negative than the free energy of liquefaction.

From a mathematical point of view Lewicki (1997) stated that values of $f>1$ are unfeasible. From equation 3.6, for $f>1$, $M<0$ above a certain value of water activity where the water activity is given by $a_w = 1/f$. At that water activity the GAB model becomes discontinuous and at $a_w>1/f$ acquires negative values. Lewicki (1997) concluded that for a relatively good description of the sigmoid-shaped isotherm and to fulfil the requirements of the BET model, the constants should be in the region:

$$0.24 < f \leq 1$$

$$5.67 \leq c \leq \infty$$

Within these ranges, the calculated monolayer values do not differ by more than ±15.5% from the true monolayer capacity.

Chirife *et al.* (1992) found that for proteins $f = 0.84 \pm 0.03$SD, for starchy materials $f = 0.74 \pm 0.03$SD and for whey protein concentrate (non-dialyzable fraction) $f = 0.82$ over the water activity range 0.05-0.95. Schar and Ruegg (1985) found f for casein (whole acid) and calcium caseinate to be 0.79 and 0.81 respectively over a_w 0.10-0.90.

The GAB equation can also be extended to take into consideration the effects of temperature (equation 3.8):

$$M = \frac{CF_T M_m a_w}{(1 - F_T a_w)[1 + (C-1)F_T a_w]} \qquad (3.8)$$

where $C = c_o \exp(\Delta H_1/RT)$
$F_T = f_o \exp(\Delta H_2/RT)$
$M_m = M_{mo} \exp(\Delta H/RT)$
$\Delta H_1 = H_m - H_n$ (J/mol)
$\Delta H_2 = H_1 - H_n$ (J/mol)
$\Delta H = R[T_1T_2/(T_2-T_1)]\ln(a_{w2}/a_{w1})$ with temperature in Kelvin

H_m and H_n are the heats of sorption of the monolayer and multilayer of water respectively. H_1 is the heat of condensation of water vapour at the given temperature (J/mol). c_o, f_o and M_{mo} are the adjusted constants for the temperature effect. The model was found to be satisfactory for temperatures as low as 4°C and as high as 140°C for concave, convex, sigmoid and almost straight isotherms [Singh and Singh 1996].

Modifications have been made to the GAB model in order to increase the range of applicability. Schuchmann *et al.* (1990) showed that the range could be extended to 0.98-0.99 by replacing a_w in the GAB model with the transform $-\ln(1-a_w)$.

3.2.2.3 T.S.S. Model

A three stage sorption process was assumed by Timmermann (1989) and Timmermann and Chirife (1991). Timmermann and Chirife (1991) suggested that the second sorption stage introduced by the GAB model may be limited to a certain number of layers. Thereafter, a third stage is available for the sorbate molecules which has true liquid like properties as postulated by the BET model. In summary, the three stage sorption model represents

I: the strongly sorbed monolayer
II: the following h-1 layers, much less strongly sorbed
III: the remaining layers, up to infinity, of 'pure liquid' characteristics

and is given by equation 3.9 to 3.11:

$$M = \frac{M_o cHfa_w H'}{(1 - fa_w)[1 + (cH - 1)fa_w]} \tag{3.9}$$

$$H' = 1 + \frac{H - 1}{H}\frac{1 - fa_w}{1 - a_w}[h + (1 - h)a_w] \tag{3.10}$$

$$H = 1 + \frac{1 - f}{f}\frac{(fa_w)^h}{1 - a_w} \tag{3.11}$$

where M = moisture content including residual moisture (g water/g dry powder)
M_o= monolayer moisture content (g water/g dry powder)
c = constant related to the energy of bonding
f = constant which corrects the properties of the multilayer with respect to the bulk liquid
h = number of layers comprising the second sorption stage

For $h \rightarrow \infty$, H and H' $\rightarrow 1$ and the t.s.s. model simplifies to the GAB model. This model was proposed after Timmermann (1989) observed that at very high water activities some systems showed a sorption larger than that predicted by the GAB model. If the data was to conform to the GAB model, plots of $a_w/[M(1-fa_w)]$ vs a_w would be linear. In all cases Timmermann (1989) noted that up to a certain a_w ($\cong$0.90) the plots deviated downwards. This suggested that the existence of the third sorption stage.

It is noted that when applying sorption isotherm models to dairy-based powders with amorphous sugars, a model could only be used up to the crystallisation of the amorphous material. Due to this consideration, it becomes irrelevant whether the models can predict accurately to very high water activities. The use of these models can be applied however to components which do not undergo phase changes.

3.2.2.4 Peleg's Double Power Model

Peleg's (1993b) four-parameter model is a semi-empirical model that can describe a sigmoid shaped isotherm through the use of a double power expression (equation 3.12):

$$M = b_1 a_w^{n_1} + b_2 a_w^{n_2} \tag{3.12}$$

where b_1, b_2, n_1 and n_2 are constants (n_1<1 and n_2>1).

This equation is not derived from any theoretical considerations. It has however been described as a semi-empirical model due to the following concepts. Firstly, at low water activities, sorption is primarily determined by a process of a decreasing rate with respect to water activity (dM^2/d^2a_w<0), similar to a Langmuir kinetic. Secondly, at

higher water activities there is a shift towards free condensation, manifested by the isotherms' ever increasing slope. Peleg (1993b) noted that the formats of the BET and GAB models were defined on the basis of the same two mechanisms.

Peleg (1993b) compared this model with the GAB model for sorption data of agar-agar, carrageenan, gelatin, low methoxyl pectin and wheat bran to water activities of 0.85-0.95. It was found that the double power model had a comparable or slightly better fit than the GAB model. The double power model is also only applicable to a_w=0.9. Beyond a_w>0.95 it could be applied if a_w was replaced by a transform $-\ln(1-a_w)$ as with the GAB model. Lewicki (1998) compared Peleg's double power model and the GAB model with a model proposed by Lewicki. It was found that the GAB model described 35.5% of the analysed isotherms with a root mean square (RMS)≤±10%. Peleg's equation described 77.4% of the isotherms with RMS≤±10% and Lewicki's proposed model described 71.0% of the isotherms.

Peleg (1993b) found the power n_1 on all materials was of the order of 0.3-0.8, n_2 was between 6 and 15 and b was between 14-35% and 25-120% moisture on a dry mass basis for b_1 and b_2 respectively. These values provide initial guesses when solving the model. Like the GAB model, Peleg's model also predicts infinite adsorption at a_w=1. Lewicki (1998) noted that Peleg's model requires higher precision of parameters otherwise the calculated moisture content is loaded with high errors. It was also noted that the GAB equation is less susceptible to precision of parameters estimation.

3.2.2.5 FF Equation

Iglesias and Chirife (1995) put forward the FF equation developed by Ferro Fontan *et al.* (1982) as an alternative to the GAB model. It is applicable over the same range (a_w 0.1-0.9) and has only three parameters. The FF equation is given by equation 3.13:

$$\ln\left(\frac{\gamma}{a_w}\right) = \alpha(M)^{-r_f} \tag{3.13}$$

where γ is a parameter which accounts for the 'structure' of the sorbed water, α is a constant and r_f is a constant which entails net isosteric heat with moisture content.

The FF equation was compared with the GAB model on 156 isotherms. The average error for the FF equation was 3.3% which was not quite as good as that obtained from the GAB model (2.6%) [Iglesias and Chirife 1995].

3.2.2.6 Lewicki's Three Parameter Model

Lewicki (1998) presented the following equation (equation 3.14):

$$M = \frac{F_L}{(1-a_w)^{G_L}} - \frac{F_L}{1-a_w{}^{H_L}} \tag{3.14}$$

where F_L, G_L and H_L are constants with no physical significance.

Equation 3.14 assumes that there are two processes which occur in parallel. The first process prevails at high water activities, and the second plays a major role at low water activities. G_L is related to the level of adsorption. At larger values of G_L, the adsorption is stronger and this becomes evident at lower water activities. H_L influences the slope of the isotherm. Low values of H_L influence the slope at low water activities and an increase in H_L extends the effect to high water activities. F_L does not effect the shape of the isotherm, it just moves it relative to the vertical axis.

Lewicki's equation was compared with the GAB model and Peleg's double power model. Lewicki's equation gave a better approximation than the GAB model but not as good as Peleg's equation. The difference between Lewicki's model and the other two models is that the precision of the moisture content estimation is dependent on the error that the parameters are loaded with and practically independent of water activity. This is a unique property which means that the precision of the estimation at low water activities is the same as that at high water activities.

3.3 MOISTURE SORPTION ISOTHERMS FOR DAIRY POWDER COMPONENTS

This section summarises the isotherm literature on components which are likely to be present in dairy powders. Isotherms that have been measured due to inconsistency in the available data or those which are lacking from the literature are also included. Some general physical property information is also included where appropriate. The isotherms for each component given in this section are used in section 3.4 for predicting isotherms for multicomponent powders, section 4.3 for creating T_g versus a_w profiles and in chapter 7 for the model.

3.3.1 Protein

Milk proteins are divided into two general classes depending on whether they are soluble (whey proteins) or insoluble (caseins) [Otter *et al.* 1997, Kinsella 1984] . The properties of the two classes are very different and will be discussed in turn.

3.3.1.1 Whey Protein

The concentrations of whey protein and casein in milk are given in table 3.2. It is noted that the total protein does not add to 100%. The reasons for this are that the minor proteins are not included in this table and also that it is uncommon to get 100% recovery of the proteins from milk during protein measurement [Norris 2002]. Whey proteins are globular and exist as discrete molecules with varying numbers of disulphide crosslinks. Compared to caseins, these proteins are more heat sensitive, less sensitive to calcium, can engage in thiol disulfide interchange, and form disulfide-linked dimers or polymers e.g. with κ-casein [Kinsella 1984].

Table 3.2: Concentrations of protein in milk [Otter *et al.* 1997]

Protein	Concentration in milk [g/kg]	Proportion of Total Protein [approx. % w/w]
αS1CN	12-15	30.6
αS2CN	3-4	8.0
βCN	9-11	28.4
κCN	2-4	10.1
Total Casein	*24-28*	*79.5*
αLa	0.6-1.7	3.7
βLg	2-4	9.8
BSA	0.2-0.4	1.2
Ig	0.5-1.8	2.1
Protease peptone fraction	0.6-1.8	2.4
Total Whey Protein	*5-7*	*19.3*

A whey protein isolate powder (whey protein 98.0%, lactose 0.1%, fat 0.3% and ash 1.6% on a dry mass basis) supplied by the New Zealand Dairy Research Institute, Palmerston North, New Zealand was used for determining an isotherm for whey protein. The isotherm data for the whey protein isolate powder is given in figure 3.1. It can be seen that up to a water activity of about 0.6, that there is no significant temperature dependence between the 4, 20 and 37°C sets of data. The isotherm obtained at 50°C is however significantly lower as would be expected. The GAB isotherm model (equation 3.6) was fitted to the data at 4, 20 and 37°C. This gives a good approximation of the isotherm for whey protein over the temperature range 4°C to 37°C, up to a water activity of around 0.6. The coefficients for M_o, c and f are 8.358 g/100g dry powder, 9.630 and 0.774 respectively.

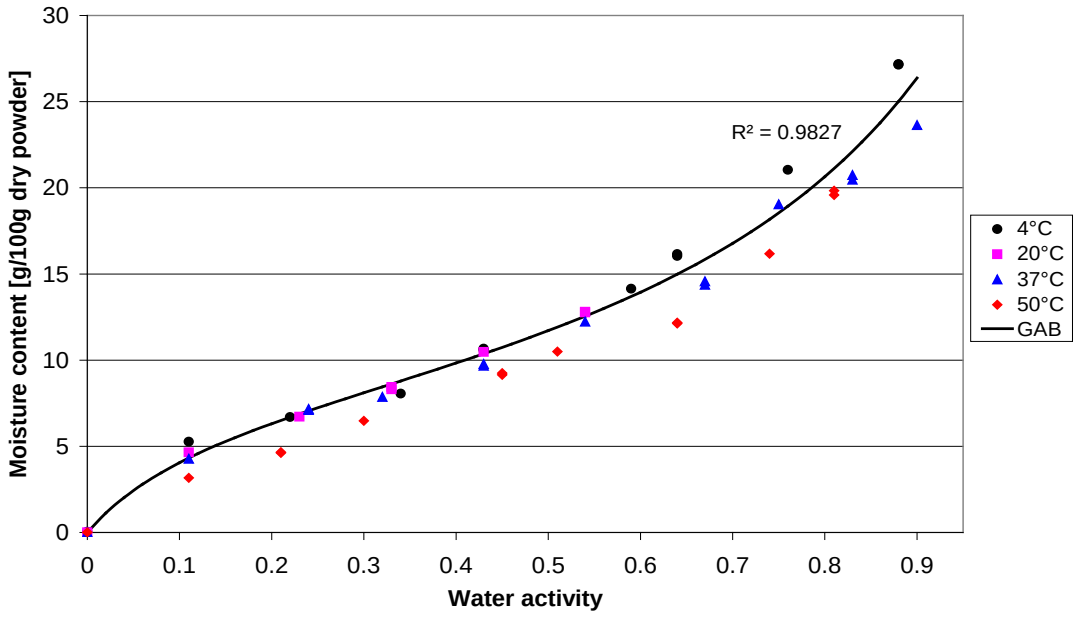

Figure 3.1: Moisture sorption isotherm for whey protein

3.3.1.2 Casein

Caseins are present in four times the concentration of whey proteins in milk (table 3.2). The major components of caseins include αs_1-casein (αs_1CN), αs_2-casein (αs_2CN), β-casein (βCN) and κ-casein (κCN) [Otter *et al.* 1997]. Caseins occur as spongy spherical micelles (average 120 nm, 10^8 daltons) held together by hydrophobic bonds and colloidal calcium phosphate [Otter *et al.* 1997, Kinsella 1984]. Caseins contain 2-3g of water per gram of protein and a charge of –18mV [Kinsella 1984]. Each micelle is made up of submicellar particles (10 to 20 nm) containing hydrophobically associated αs- and β-caseins. These are held in the micelle matrix by colloidal calcium phosphate, and the micelles are colloidally, electrostatically, and sterically stabilised by calcium cross-bridging and a coating of κ-casein [Kinsella 1984].

Some isotherm data for micellar casein was available in the literature (figure 3.14). Isotherms were also measured for a high micellar casein powder (HMC: 83.7% casein, 6.3% whey protein, 1.7% fat and 8.3% ash) and milk protein concentrate powder (MPC: 72.3% casein, 18.1% whey protein, 1.5% lactose, 1.8% fat and 7.4% ash) and is given in figure 3.2. The isotherm for casein was then predicted and a GAB model fitted. This is discussed in section 3.4.1.2 where the prediction method to obtain the isotherms for micellar casein is discussed. The isotherm for HMC was used in section 3.4.1.2 for predicting the isotherms of lactose, whey protein and micellar casein powders. The GAB model was fitted to the data measured at 20°C and the isotherm constants for M_o, c and f are 7.851, 8.360 and 0.680 respectively.

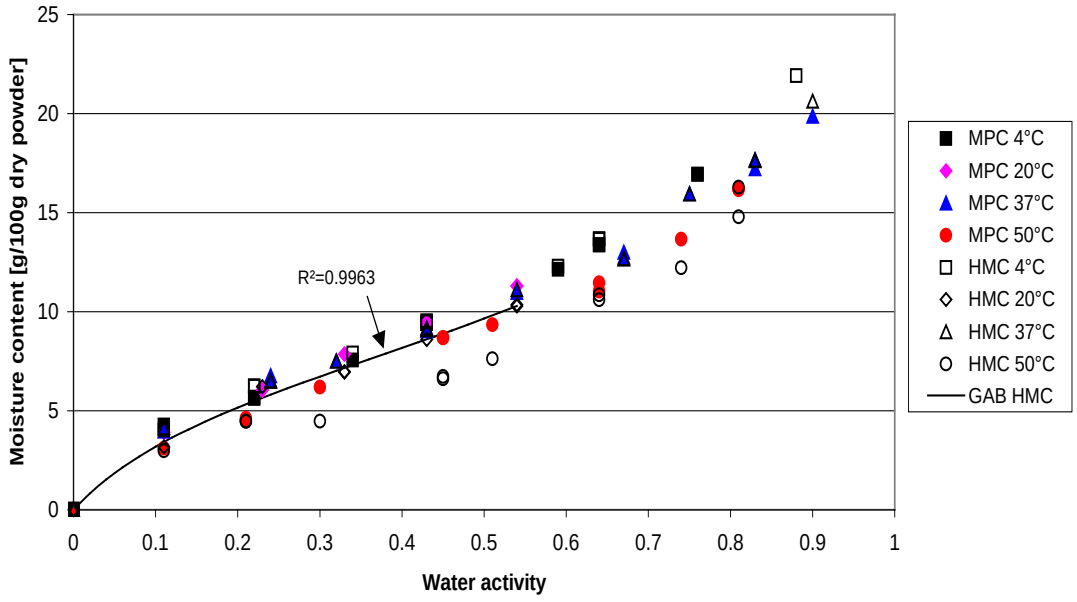

Figure 3.2: Moisture sorption isotherm for high micellar casein powders

3.3.2 Glucose

Lactose hydrolyses to the products glucose and galactose through the use of enzymes or strong mineral acids and high temperatures. Enzymatic hydrolysis prevails in the food industry for the hydrolysis of pure lactose and lactose containing products such as milk and whey [Pritzwald-Stegmann 1986]. Hydrolysis takes place at the oxygen bond between glucose and galactose and results in a solution which has different properties to lactose. The products glucose and galactose are sweeter than lactose, therefore the sweetness of the hydrolysed product can increase by a factor of three to about 0.7 (relative to sucrose which has a sweetness of 1) [Pritzwald-Stegmann 1986]. Hydrolysed lactose also shows increased solubility above lactose. The solubility of lactose is around 20g/100ml water at 20°C, this increases to up to 60g/100ml water upon hydrolysis [Pritzwald-Stegmann 1986]. The viscosity is around 380 cP at 20°C in a saturated solution of 60% (dry mass basis).

Glucose (also commonly known as dextrose, blood sugar and corn sugar), in the free or combined form (i.e. bonded with fructose in sucrose), is the most abundantly occurring sugar. In the free state it occurs in honey, fruits, starch, cellulose, blood, cerebrospinal fluid, plant juices, glycogen and urine [Schaffer 1972, Johnson 1976]. Glucose may be obtained commercially from the inversion of sucrose and from the hydrolysis and saccharification of starch [Johnson 1976]. Glucose exists in the following crystalline forms: α-D-glucose monohydrate, anhydrous α-D-glucose and anhydrous β-D-glucose. Glucose can also exist in the amorphous form, which will be the case in dairy powders where the lactose has been hydrolysed to glucose and galactose and the resulting solution spray dried.

3.3.2.1 Crystalline Glucose

α-D-glucose monohydrate ($C_6H_2O_6.H_2O$) crystallises from solutions at concentrations between 30% and 70% and at temperatures below 50°C. The melting point of α-D-glucose monohydrate is 83°C and the specific rotation at 20°C is +102° to +47° [Shallenberger and Birch 1975]. Unlike anhydrous α-D-glucose which dissolves rapidly at 25°C, the monohydrate does not. The heat of solution of glucose monohydrate is –25.2 calories/g at 25°C [Hendricks *et al.* 1934].

Anhydrous glucose is purified and crystallised D-glucose without the water of crystallisation. Anhydrous α-D-glucose is obtained by evaporating glucose solutions at above 50°C and it dissolves rapidly at 25°C to a concentration of about 62%. Anhydrous α-D-glucose will remain in that state to about 80% RH at 25°C. At 85-89% RH anhydrous α-D-glucose will convert to the α-D-glucose monohydrate and continue to adsorb moisture above 90% RH [Ditmar 1935]. Kooi and Armbruster (1967) and Donnelly *et al.* (1973) looked at the moisture sorption of anhydrous glucose. It was found to adsorb very little moisture until around 90% RH. At 90% RH, equilibrium moisture contents of 17 and 18% were reached at 24 and 30°C respectively. Donnelly *et al.* (1973) found that at 37.8°C, the moisture content reached 69% and a glucose solution formed. α-D-glucose crystals melt at 146°C and the specific rotation at 20°C is +52°.

β-D-glucose crystallises from water solutions in the anhydrous form at temperatures above 100°C. The melting point of β-D-glucose is 148-150°C and the specific rotation at 20°C is +52°. β-D-glucose is more soluble than α-D-glucose and consequently has a greater initial solubility [Shallenberger and Birch 1975]. β-D-glucose rapidly picks up moisture upon exposure to a humid atmosphere and converts to α-D-glucose in the presence of a few tenths of a percent of moisture [Kooi and Armbruster 1967]. β-D-glucose rapidly dissolves to a clear 50% solution at 25°C. The heat of solution of anhydrous glucose is –14.5 calories/g at 25°C indicating that heat is adsorbed when the sugar dissolves [Hendricks *et al.* 1934].

Glucose occurs in the α and β forms in solution. D-glucose mutarotates in water to give a mixture of about 31.1-37.4% α-D-glucopyranose and 64.0-67.9% β-D-glucopyranose. D-glucose does not occur in either the α or β-furanose form in solution [Shallenberger and Birch 1975]. D-glucose has a lower solubility in water than sucrose. Mathlouthi and Reiser (1995) prepared a table on glucose solubility from 0°C to 91°C which shows that the solubility increases from 32.3% (dry substance) to 85.0%. At 25°C the solubility is 50.8%. Pancoast and Junk (1980) have prepared tables for specific gravity, density and boiling point as a function of glucose concentration. They have also prepared tables on the effect of temperature and concentration on density, freezing point and viscosity of glucose solutions

The isotherm for crystalline glucose is required as glucose may be dry blended with dairy powders. The isotherm for α-D-glucose monohydrate will be used as this is the most common crystalline form. Figure 3.3 shows the isotherm for crystalline glucose where a GAB isotherm model has been fitted (R^2=0.9923). The values for constants M_o, c, f are 6.341g/100g dry powder, 0.151, 0.923 respectively.

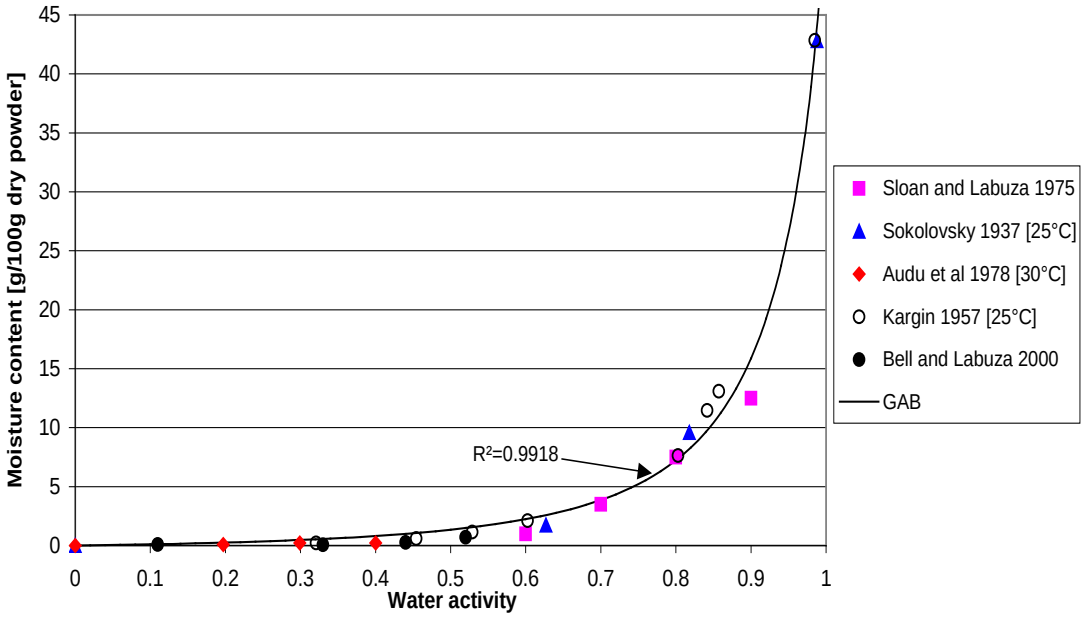

Figure 3.3: Moisture sorption isotherm for crystalline glucose

3.3.2.2 Amorphous Glucose

The sorption isotherm for amorphous glucose is given in figure 3.4 as taken from Zhang and Zografi (2000) and measured at –10, 30 and 40°C. An isotherm from Kargin (1957) has been quoted as the isotherm for amorphous glucose [Strolle *et al.* 1970]. As shown in figure 3.3, this compares with data obtained for crystalline glucose. The GAB isotherm model has been fitted to the data at –10°C and those at 30 and 40°C. It is difficult to determine whether the difference in the two isotherms (that at –10°C and that at 30/40°C) is due to a temperature effect or amorphous glucose crystallisation. When examining the T_g data for amorphous glucose (figure 4.2), the dry T_g is around 33.7°C. The isotherm data obtained at 30°C and over, has the potential for crystallisation of the amorphous glucose to occur, especially when a four week equilibration period has been used. A T_g of –10°C is not reached until a moisture content of 10g/100g dry glucose. Crystallisation is unlikely to have occurred during equilibration at –10°C. Therefore the isotherm at –10°C is likely to be the best available data for approximating an isotherm for amorphous glucose at 20°C. The difference in the isotherms between the two sets of data is more likely to be due to glucose crystallisation as opposed to a temperature effect. Kargin (1957) did state that glucose glasses tended to liquefy rather than crystallise. However, it is unclear whether Kargin (1957) was dealing with amorphous glucose or crystalline glucose when this statement was made.

The GAB constants for M_o, c and f were found to be 5.148 g/100g dry powder, 4.014 and 1.411 respectively for the data measured at –10°C. The GAB constants for M_o, c and f were found to be 9.591 g/100g dry powder, 0.441 and 1.262 respectively for the data measured at 30 and 40°C.

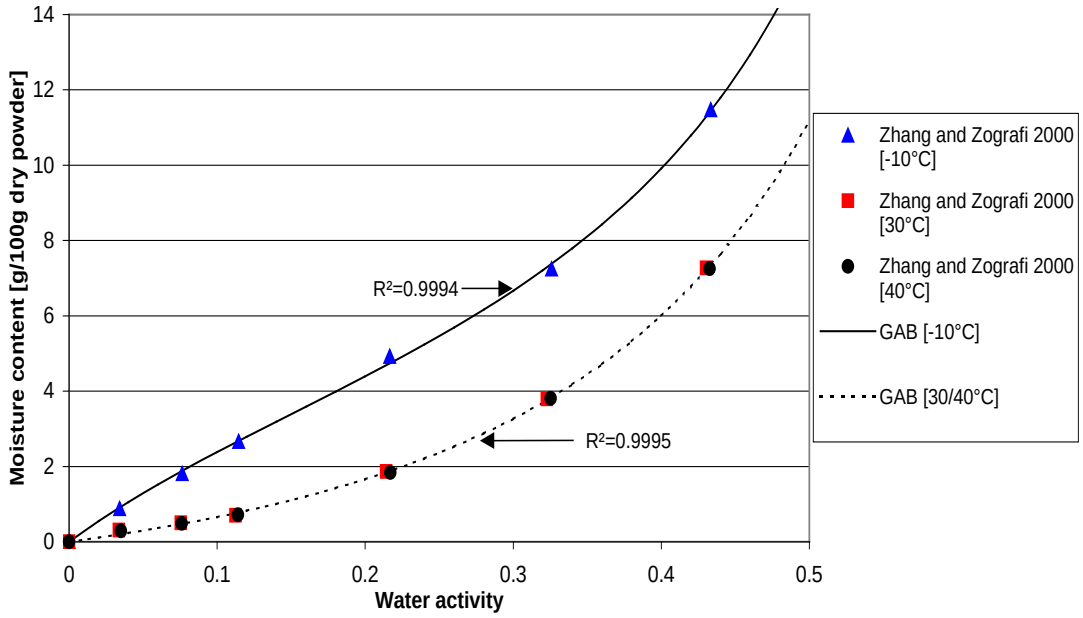

Figure 3.4: Moisture sorption isotherm for amorphous glucose

3.3.3 Galactose

The properties of galactose also need to be discussed since it is the other product of lactose hydrolysis.

3.3.3.1 Crystalline Galactose

Galactose exists in the following forms:
1. Anhydrous α-D-galactose
2. Anhydrous β-D-galactose
3. D-galactose monohydrate
4. L-galactose

Anhydrous α-D-galactose normally crystallises from water or alcohol solution at room temperature as the anhydrous pyranose form. This has a melting point of 165-167°C and a specific rotation of +80° at 20°C [Shallenberger and Birch 1975]. α-D-galactose also exists as a monohydrate, which has a melting point of 118-120°C [Shallenberger and Birch 1975].

Anhydrous β-D-galactose crystallises from an ethanol-water solution at 0°C in the pyranose form. β-D-galactose melts at 143-146°C. When it is maintained at a temperature of 140°C, it resolidifies and then melts again at 164-167°C. Apparently an equilibrium between the two pyranose anomers is established in the original melt, and as α-D-galactose crystallises it does so at the expense of the β-form. The specific rotation of β-D-galactose is +80° at 20°C [Shallenberger and Birch 1975].

In solution, the percentage distribution of the isomers of the mutarotated sugars at 20°C for D-galactose is as follows: α-pyranose 29.6-35.0%, β-pyranose 63.9-70.4%, α-furanose 1.0% and β-furanose 3.1%. This equilibrium is affected by temperature. With

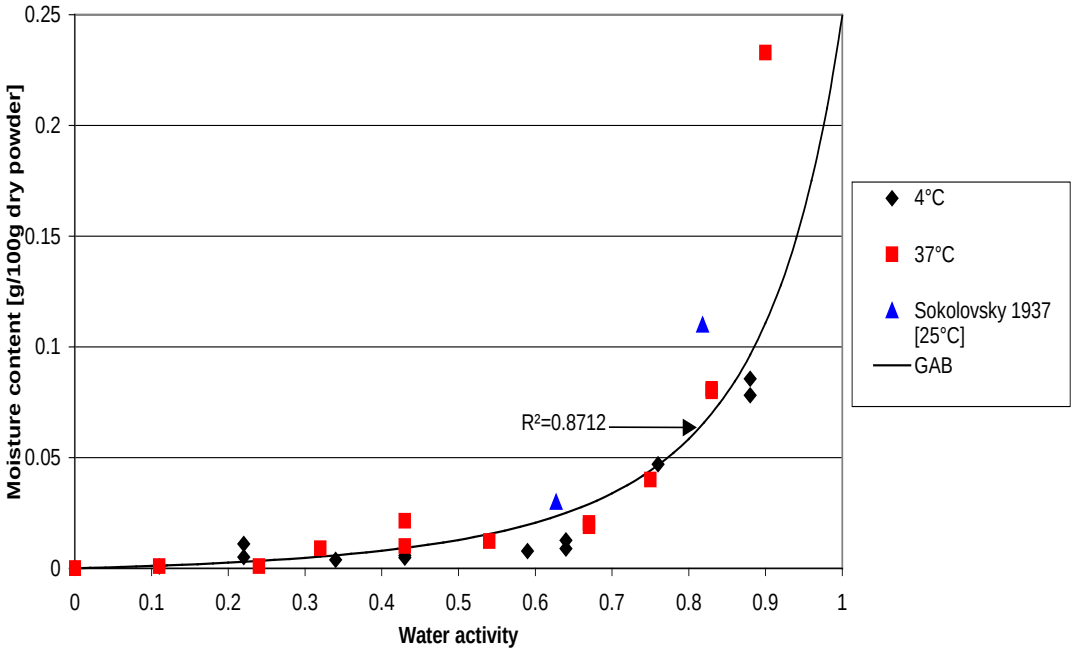

Figure 3.5: Moisture sorption isotherm for crystalline galactose

an increase in temperature, both furanose forms seem to be generated at the expense of β-D-galactopyranose [Shallenberger and Birch 1975].

An isotherm for crystalline galactose is given in figure 3.5. The GAB isotherm model has been fitted (R^2=0.8712), with the constants M_o, c and f being 0.567 g/100g dry powder, 0.0197 and 0.817 respectively.

3.3.3.2 Amorphous Galactose

No isotherm data could be found in the literature for amorphous galactose. An attempt was made to make amorphous galactose by freeze-drying. This was unsuccessful due to collapse of the matrix during drying. A further attempt was made to freeze dry lactose/galactose and maltodextrin/galactose mixtures with the theory being that the higher molecular weight component would stabilise the matrix [Roos and Karel 1991c] and could later be subtracted from the isotherm for the powder. This would leave the isotherm for amorphous galactose. By making up a number of mixtures of different proportions and subtracting off the isotherm for the other component, an isotherm for amorphous galactose could be determined (assuming that the isotherms for the two components were completely additive). This was also unsuccessful, as a totally amorphous powder could not be made. This was shown by crystals being present when the powder was examined under the polarising microscope.

Since glucose and galactose have the same molecular weight and similar structures (hydroxyl group at C-4 in axial position for galactose rather than the equatorial position as is the case for glucose), the isotherm for amorphous glucose (figure 3.4) could be used as an estimate of the isotherm for amorphous galactose. It is noted that this is used only as there is no isotherm for amorphous galactose available. Also the T_g versus moisture content profiles for amorphous glucose and galactose (figures 4.2 and 4.4 respectively) are very similar indicating that the two sugars may behave similarly with respect to moisture and the glass transition temperature.

3.3.4 Sucrose

Sucrose is a disaccharide sugar obtained from sugar cane and sugar beets. Sucrose is composed of one molecule of α-D-glucose in the pyranose form linked to one molecule of β-D-fructose in the furanose form [Shallenberger and Birch 1975]. Hydrolysis of sucrose results in the formation of equal quantities of D-glucose and D-fructose [deMan 1999].

3.3.4.1 Crystalline Sucrose

General properties of crystalline sucrose are given in table 3.3. Sucrose has a specific rotation of +66.5° [deMan 1999]. It is highly soluble, making it an excellent ingredient for syrups and other sugar containing foods [deMan 1999]. Mathlouthi and Rieser (1995) give data and relationships for the solubility, surface tension and density of sucrose solutions.

Table 3.3: General properties of crystalline sucrose [Reiser *et al.* 1995]

Properties	Crystalline Sucrose
Molecular weight [g/mol]	342.30
Melting point [°C]	186 [182 – 192]
Boiling point [°C]	Decompose at temperatures very close to the melting point
Density [kg/m³]	1588.4 at 20°C*
Specific heat [kJ/kg K]	1.235 at 20°C*

* denotes equations for property given in Reiser *et al.* (1995).

Isotherm data for crystalline sucrose were summarised by Billings (2002) and are given in figure 3.6. A GAB model was fitted (R^2= 0.9635) and the constants M_o, f and c were found to be 0.0127 g/100g dry powder, 1.091 and 14.679 respectively.

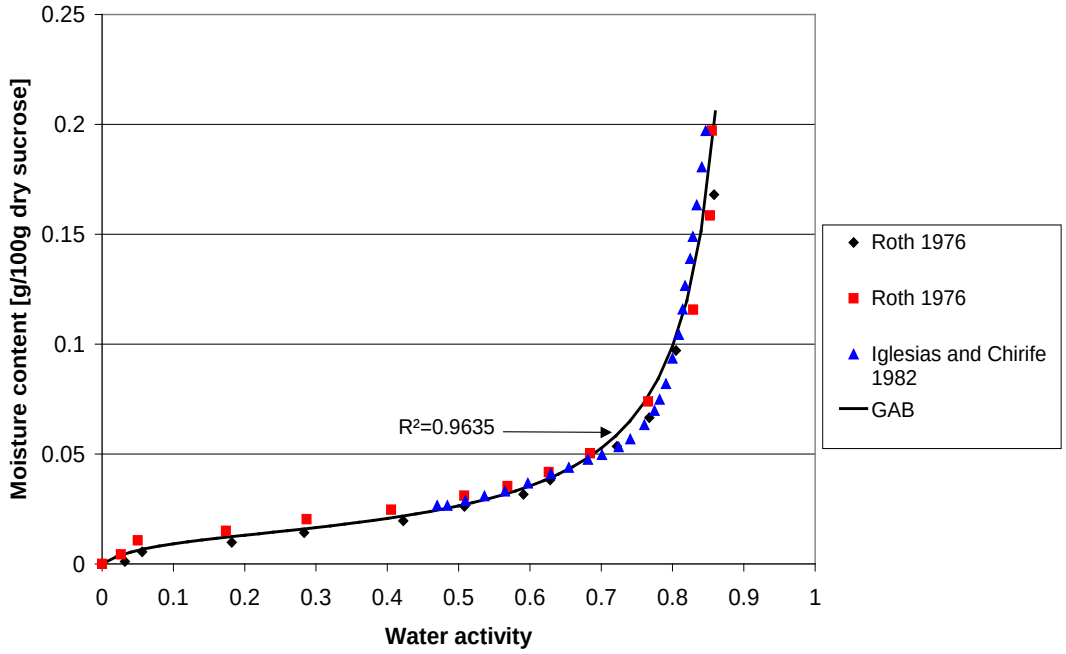

Figure 3.6: Moisture sorption isotherm for crystalline sucrose

3.3.4.2 Amorphous Sucrose

Isotherms for amorphous sucrose have been measured by a number of researchers at a range of temperatures including 25°C [Chinachoti and Steinberg 1984, Makower and Dye 1956, Roos and Karel 1990, Roos and Karel 1991a], 35°C [Iglesias *et al.* 1975] and 47°C [Iglesias *et al.* 1975]. A comparison of these isotherm data is given in figure 3.7. It can be seen that there is good agreement between all data and that there appears to be a slight temperature dependence on the isotherm for amorphous sucrose. Examination of the data up to a water activity of 0.35 highlighted that there was a slight temperature dependence between the sets of data. The isotherms measured at 35°C and 47°C are higher than those measured at 25°C. It is noted that the low data point at 0.33 a_w from Roos and Karel (1990) is likely to be due to partial crystallisation of the amorphous sucrose at 25°C. At a water activity of 0.33, amorphous sucrose has a T_g of around 17°C, therefore crystallisation is likely to occur at a temperature of 25°C as the sample is above its glass transition temperature.

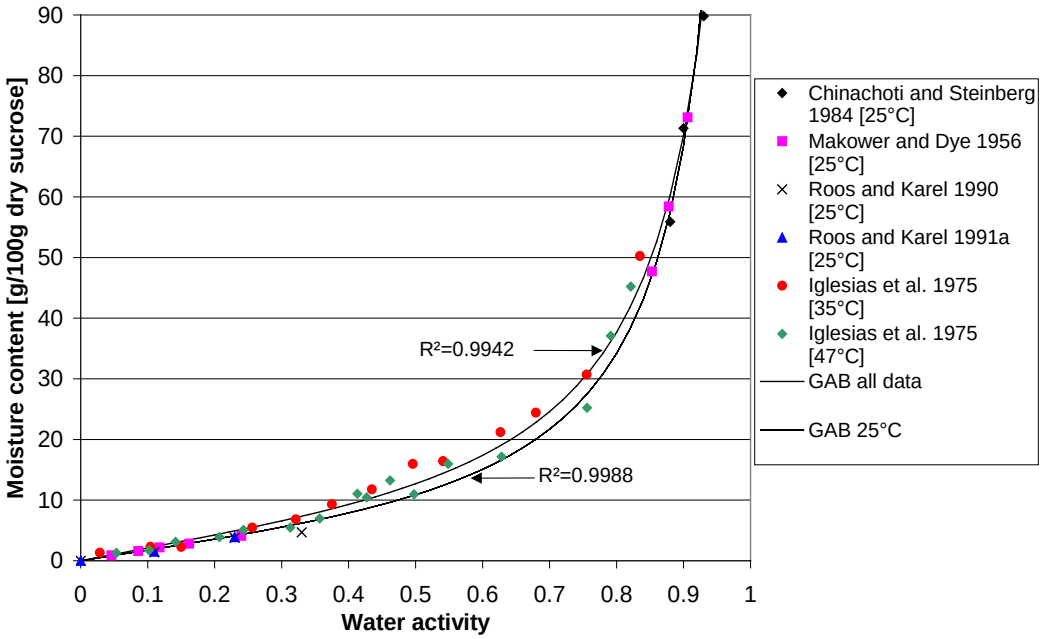

Figure 3.7: Moisture sorption isotherm for amorphous sucrose

The GAB isotherm model was fitted to the data measured at 25°C and also over all the data since there was not a very strong temperature dependence noticed. The constants M_o, f and c were found to be 8.017 g/100g dry powder, 0.988 and 2.256 with an R^2=0.9988 for the data measured at 25°C. The constants M_o, f and c were found to be 9.490 g/100g dry powder, 0.970 and 2.356 with an R^2=0.9942 for the isotherm fitted over all data. The isotherm fitted to the data at 25°C was used in the model in chapter 7 as the amorphous sucrose isotherm was being used to predict the isotherms for multicomponent powders that had been measured at 20°C. However, it is not expected that there would be much difference if the isotherm fitted over all the data was used for predictions.

3.3.5 Fructose

Fructose (also known as laevulose and fruit sugar) is the most widely occurring ketose and occurs bound to glucose in sucrose [deMan 1999]. It is usually found accompanied by sucrose in an uncombined form in fruit juices and honey [Schaffer 1972]. It is the sweetest known sugar, with a relative sweetness of 1.0-1.5, and is usually obtained from the inversion of sucrose by acids or invertase [Schaffer 1972].

3.3.5.1 Crystalline Fructose

The only known crystalline isomer of D-fructose is β-D-fructopyranose which is anhydrous [Shallenberger and Birch, 1975] and has a melting point around 102-104°C. Fructose is a very hygroscopic sugar which will easily pick up moisture from air [Pancoast and Junk 1980, Vanninen and Doty 1979]. Donnelly and Fruin (1973) studied the hygroscopicity of fructose at storage conditions of 25, 56, 75 and 90% RH

and 24, 30 and 37.8°C. Fructose adsorbed moisture at 75% RH and equilibriated between 41% and 43% moisture content as a clear solution at all three temperatures. There was a continuing rise in moisture content with RH and at 90% RH the equilibrium moisture content was 85.1% at 24°C, 78.6% at 30°C and 72.7% at 37.8°C. At these moisture contents, the fructose changed from a clear viscous syrup to a free flowing liquid. The isotherm for crystalline fructose was measured at 4, 20 and 37°C, as shown in figure 3.8. The GAB model was fitted to all the data since there was no clear temperature dependence. The constants M_o, f and c were found to be 0.0178 g/100g dry powder, 1.455 and 1.533 respectively with an R^2=0.9906.

Pancoast and Junk (1980) give the solubility data for fructose in water over a temperature range of 20°C to 50°C. The solubility of fructose in water is 78.94% and 86.94% at 20°C and 50°C respectively. In solution, D-fructose may undergo conversion to its various anomers. These include β-pyranose, β-furanose and α-pyranose. At 20°C the percentage distribution of the isomers is 68.4-76.0 for β-pyranose, 28.0-31.6 for β-furanose and 4.0 for α-pyranose [Shallenberger and Birch 1975]. Vanninem and Doty (1979) noted that the furanose form is markedly less sweet than the pyranose form and the sweetness of a fructose solution is mainly dependent on the equilibrium between these two anomers. The equilibrium between the isomers is dependent on time, pH, concentration and temperature. In order to provide maximum sweetness, fructose is preferably used in neutral or slightly sour foodstuffs of relatively low sugar content, which are consumed cold. Vanninem and Doty (1979) also noted that the change in sweetness is reversible. Pancoast and Junk (1980) present tables of viscosity as a function of temperature. They also give tables of refractive index, freezing point depression, density and specific gravity as a function of concentration.

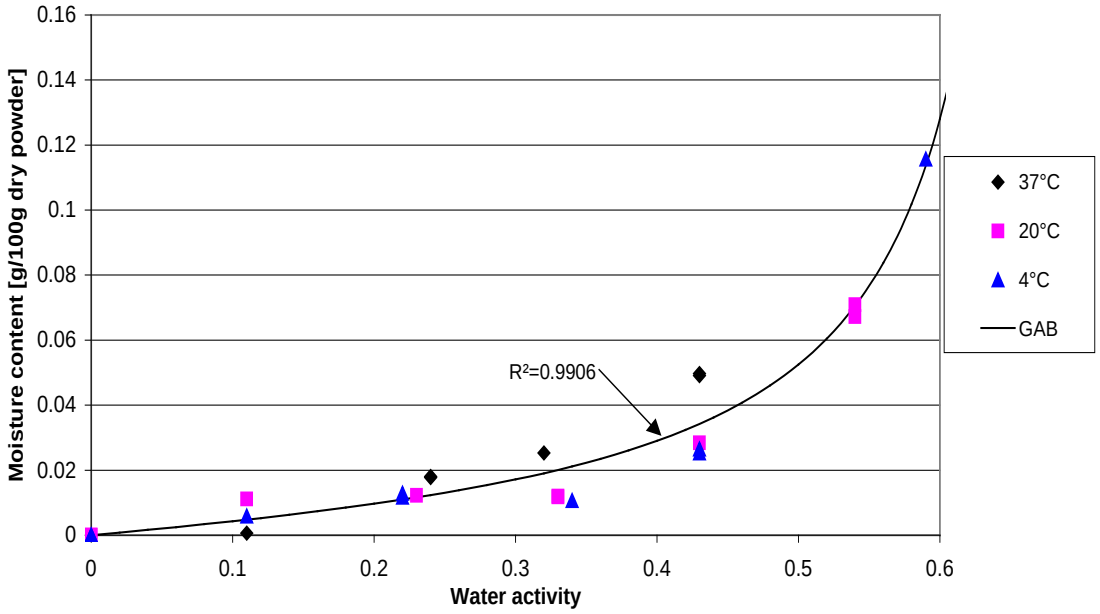

Figure 3.8: Moisture sorption isotherm for crystalline fructose

3.3.5.2 Amorphous Fructose

Isotherm data for amorphous fructose was obtained from Ditmar (1935), Sokolovsky (1937), Sloan and Labuza (1975) and Zhang and Zografi (2000) and is shown in figure 3.9. The GAB model was fitted through all of this data (R^2=0.9657) giving values for the constants M_o, f and c of 316.398 g/100g dry powder, 0.566 and 0.076 respectively. Using the above constants, the predicted isotherm did not fit the data well below $0.6a_w$. The GAB was then fitted using just the data up to a water activity of 0.6. The constants M_o, f and c were found to be 32.059 g/100g dry powder, 0.893 and 0.271 respectively, with an R^2 of 0.9655. It is suggested that the GAB constants obtained using the data up to $0.6a_w$, be used to predict the moisture content up to $0.66a_w$. Above $0.66a_w$, the GAB constants obtained over all the data would be appropriate to use.

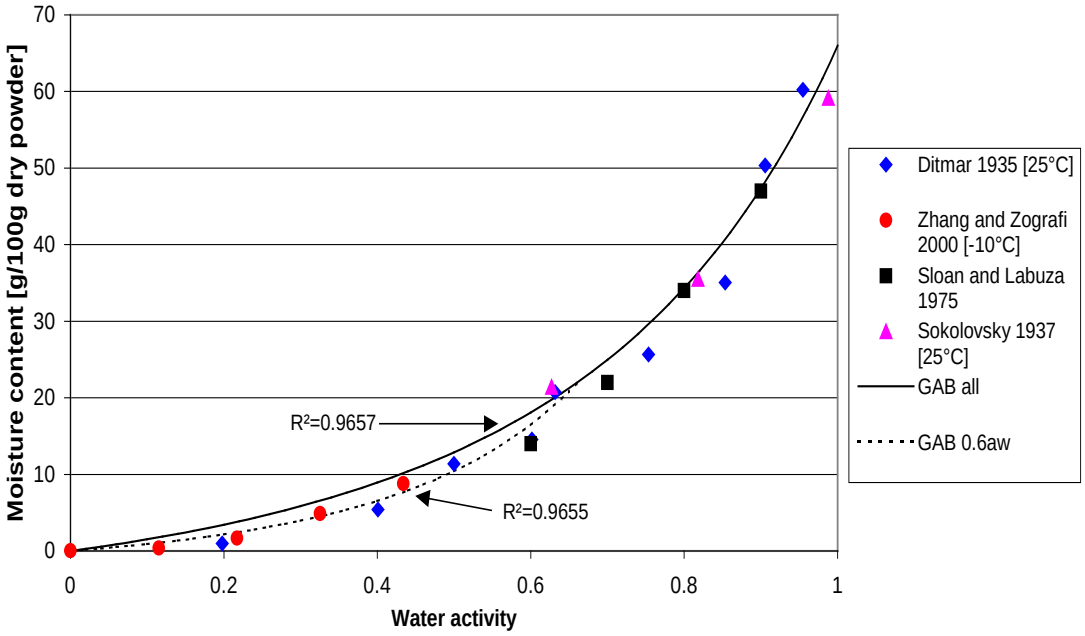

Figure 3.9: Moisture sorption isotherm for amorphous fructose

3.3.6 Maltose

Maltose (also known as malt sugar and maltobiose) is the reducing disaccharide 4-(α-D-glucosido)-D-glucose composed of two glucose units. Maltose consists of two D-glucopyranoses joined by a 1,4'-beta-glycoside bond. Maltose is commercially produced by the hydrolysis of starches using the enzyme amylase [Johnson 1976]. The enzyme diastase is also used to produce maltose from the degradation of starch [Stecher 1968]. Maltose is not currently added to dairy powders. However its physical properties and sticking and caking behaviour were investigated as maltose may be added to powders in the future.

3.3.6.1 Crystalline Maltose

Only β-D-maltose is known in the crystalline state and is obtained as a monohydrate. The melting point of β-D-maltose is 102-103°C and has an specific rotation of +111.7° to +130.4° at 20°C as reported by Hassid and Ballou (1957) and a specific rotation of +118 to +136° at 20°C as reported by Shallenberger and Birch (1975). The relative sweetness of maltose is 0.6 (relative to sucrose which is 1) [Sowden 1957]. No isotherm data was available for crystalline maltose.

In solution, the distribution of α and β-D-anomers for maltose is about the same as that for glucose and is about 32% α- and 64% β-D-anomer [Shallenberger and Birch 1975]. Maltose is soluble in water, slightly soluble in alcohol, and crystallises in fine needles [Stecher 1968]. Maltose is an easily digested sugar and may be used as a food grade disaccharide in confectionary, infant food and beverages, or may be a major component of enzymically prepared high maltose syrups. These syrups have desirable non-hygroscopic properties similar to hard candies. They are useful in controlling crystal formation in frozen dessert preparation and are also of high value in the baking and brewing industries due to the high fermentables content [Shallenberger and Birch 1975, Johnson 1976].

3.3.6.2 Amorphous Maltose

The isotherm for amorphous maltose is given in figure 3.10. It is noted that some of this data are quoted as being for crystalline maltose [Audu *et al.* 1978]. However this coincides with that obtained for amorphous maltose [Roos and Karel 1991c,d]. The GAB model was fitted to this data (R^2=0.9852), excluding some data that were thought to be outliers (due to amorphous maltose crystallisation), and the constants M_o, c and f were found to be 97.445 g/100g dry powder, 0.167 and 0.611 respectively.

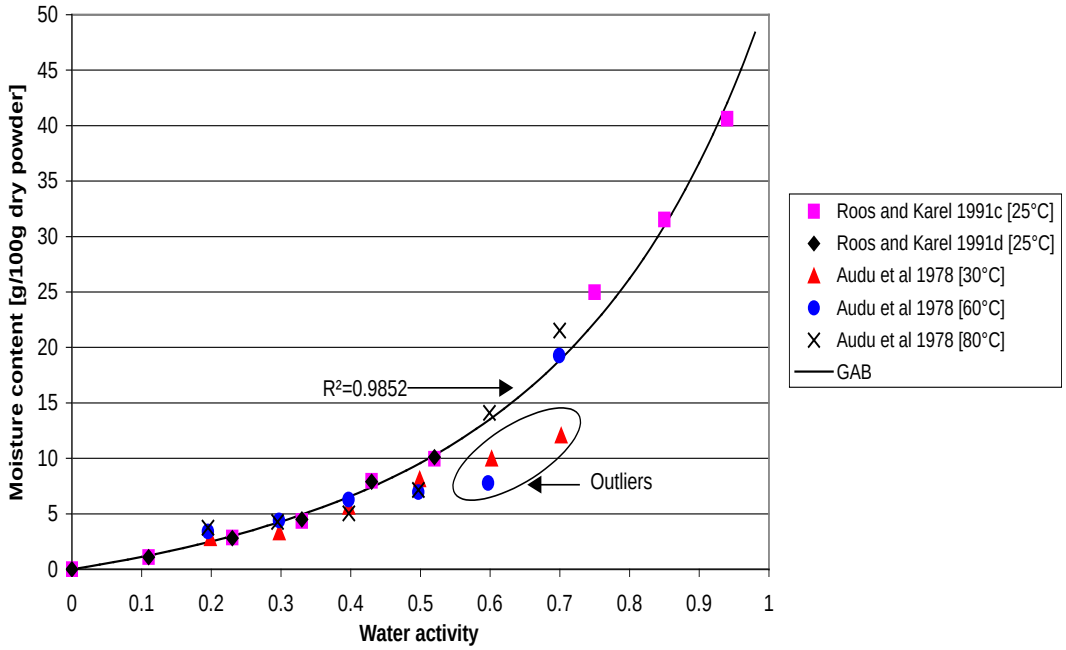

Figure 3.10: Moisture sorption isotherm for amorphous maltose

3.3.7 Maltodextrin Powders

Maltodextrins have become common carriers to use, in order to raise the T_g of powders during spray drying, due to them being neutral in colour, taste and relatively cheap. Increasing the T_g of the powder increases viscosity and retards crystallisation thereby improving drying characteristics. They also decrease stickiness and hygroscopicity of dried powders enabling more successful storage. Maltodextrins are the products of the hydrolysis of starch. The extent of hydrolysis is indicated by the dextrose equivalent (DE) value given to the maltodextrin powder, which is a measure of the reducing sugars present [Fanshawe 2001, A.E. Staley Manufacturing Company]. Technically, maltodextrins are starch hydrolysis products with a DE less than 20. Above a DE of 20 the products are called corn syrups. Properties of maltodextrins can be related to the DE and typically, as the DE increases, solubility increases and viscosity and film formation decrease [Fanshawe 2001]. Therefore in terms of sticking problems, maltodextrins with higher DE values are likely to be more sticky than those with lower DE values.

Due to the fact that the properties of the maltodextrin powder will depend on the DE, a single isotherm for maltodextrin powders is not possible. Figure 3.11 shows isotherms for maltodextrin powders with varying DE values as measured by Roos and Karel (1991d) at 25°C. These isotherms have not been included in the model (chapter 7) as more investigation is required to be able to predict an isotherm for a maltodextrin powder based on its DE value.

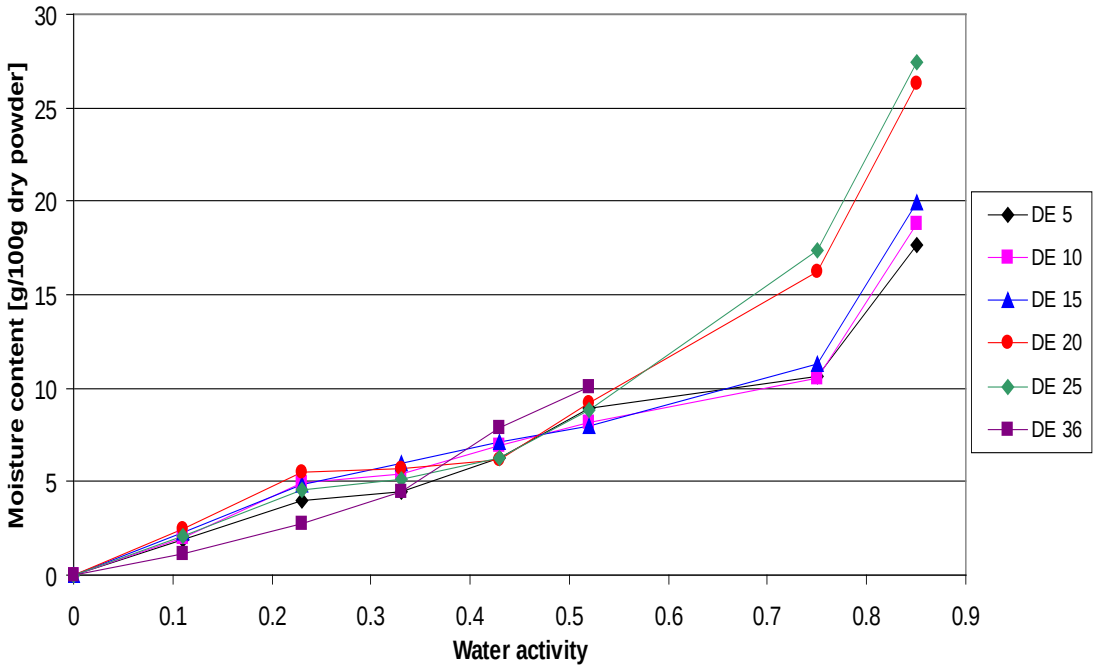

Figure 3.11: Moisture sorption isotherms for maltodextrin powders [Roos and Karel 1991d]

3.3.8 Cocoa

Cocoa powder is added to a number of powders in order to give a chocolate flavour to the powder. Some physical properties of cocoa powder are given in Meursing (1976). The density of fat free dry cocoa powder, cocoa powder with 10% fat and cocoa powder with 20% fat are 1.45, 1.40 and 1.35 g/ml respectively. The specific heat for 10% fat and 20% fat cocoa powder is 0.41 and 0.42 cal/g respectively.

Figure 3.12 shows the isotherm for a cocoa powder used in dairy powders (Dezaan cocoa powder supplied by Fonterra Research Centre, Palmerston North, New Zealand) as measured at 4, 20, 37 and 50°C. There was no temperature effect seen with data obtained at 4, 20 and 37°C and a small temperature effect seen with the data at 50°C, especially at the lower water activities. A GAB model and polynomial model were fitted to the 4, 20 and 37°C data. The polynomial model gave a better prediction of the isotherm data and more importantly fitted the data better at the lower water activities (equation 3.12). This is important as the powders are dried to generally a water activity between 0.1 and 0.2 therefore it is more important that an isotherm model fits well at the low a_w range where the predictions are going to be made.

$$M = 0.053 + 32.02a_w - 102.71a_w^{\,2} + 158.01a_w^{\,3} - 61.64a_w^{\,4} \qquad (3.12)$$

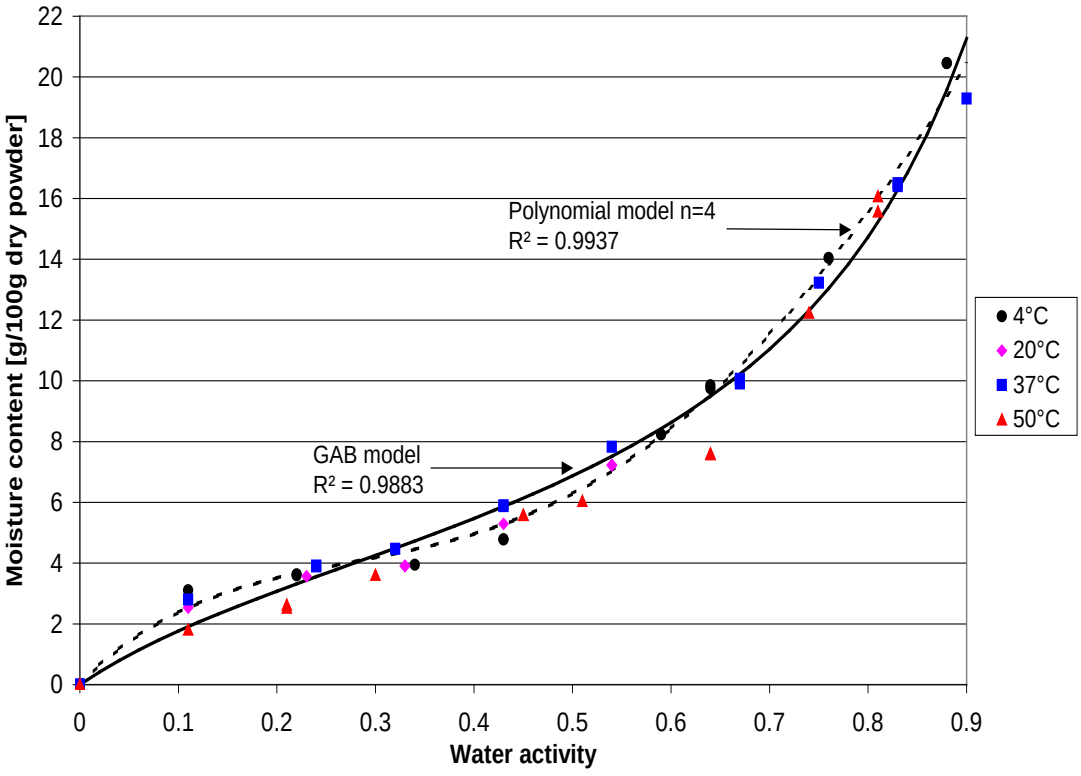

Figure 3.12: Moisture sorption isotherm for cocoa powder

3.4 PREDICTING MOISTURE SORPTION ISOTHERMS FOR MULTICOMPONENT POWDERS

Since every component has a unique isotherm, food powders will also have unique isotherms based on their composition and the states in which these components exist in the powder. As previously discussed, it would be useful to be able to predict isotherms for the following reasons:

1. They take time to measure (typically 3 weeks)
2. A powder needs to exist before it can be measured
3. Prediction allows for an understanding of the moisture relationship of a new powder during the formulation stage.

Several methods have been investigated in the literature for predicting isotherms for multicomponent powders. The most common method has been using an additive isotherm approach. Labuza (1968) suggested that it can be assumed that the amount of water sorbed at any water activity can be predicted by the mass weighted addition of the moisture that the components would sorb alone, assuming no interactions between components occur. This approach, shown by equation 3.16, has been used by a number of authors [Berlin *et al.* 1968, Palnitkar and Heldman 1971, Berlin *et al.* 1972, Iglesias *et al.* 1975, Iglesias *et al.* 1980] with satisfactory results being found in some cases [Berlin *et al.* 1968, Berlin *et al.* 1972, Iglesias *et al.* 1975].

$$M_p = \sum_{i=1}^{n} x_i M_i \tag{3.16}$$

where M_p = predicted moisture content at a given a_w (g/100g dry powder)
x_i = mass fraction of component *i* (dry basis)
M_i = moisture content for component *i* at given a_w

Berlin *et al.* (1968) compared the isotherm for milk powders with the combined isotherms for lactose, salt (anhydrous Jenness-Koops salt mixture), centrifuged casein and β-lactoglobulin. There was good agreement, with the predicted isotherm being slightly lower than the measured isotherm, up to the breakpoint in the isotherm which occurred due to lactose crystallisation. It was also stated that comparing the relative masses sorbed by the components at different water activities suggests that water vapour sorption by milk powders occurs through a sequence of sorption sites as determined by the water activity. Casein preferentially binds moisture at low water activities. When the water activity increases lactose binds water more strongly and crystallisation occurs when sufficient moisture has been adsorbed. At water activities above 0.5 the salts bind water which can allow protein destabilisation.

Palnitkar and Heldman (1971) compared the isotherm of beef products with isotherms predicted from the addition of freeze-dried beef components. There was poor agreement with the predicted isotherm being significantly lower than that obtained experimentally. The lack of agreement was attributed to two factors:

a. an interaction between the components results in increased moisture adsorption; or
b. the procedures used to fractionate components reduced the moisture adsorption of the individual components.

Berlin *et al.* (1972) constructed composite sorption isotherms for a dried milk-orange product and two dehydrated sweet whey-soy mixtures. The close agreement between the predicted and measured isotherms clearly demonstrates the additive nature of moisture sorption in the composite products. The only discrepancy occurred due to the breakpoint in the isotherm caused by lactose crystallisation.

Similar observations were noted by Iglesias *et al.* (1975) in sugar beet root. The measured isotherm was compared with that of the components (sucrose and water). Good agreement was found up to the breakpoint in the measured isotherm, which occurred at about $0.25a_w$ for isotherms measured at 35 and 47°C, due to amorphous sucrose crystallisation.

Iglesias *et al.* (1980) stated that, due to the reproducibility of equilibrium moisture content data of foods using the gravimetric method (usually within ±5% in this work), a maximum permissible error of ±10% is acceptable. Therefore predicted and measured isotherms can be considered to be within agreement if the predicted isotherm falls within ±10% of the measured isotherm. Iglesias *et al.* (1980) compared predicted and measured isotherms for starch gel products. There was good agreement with some isotherms and unacceptable differences with other isotherms. The predicted isotherms were usually higher than the measured ones, indicating that interactions between components occur resulting in a decrease in water sorption. It was stated that these interactions probably consist of polymer-polymer hydrogen bonds, which compete with polymer-water hydrogen bonds, decreasing water sorption.

Allowing a maximum permissible error of ±10%, a comparison can be made between the measured and predicted isotherms from the literature, where this simple additive approach has been reported. Figure 3.13 shows the measured moisture content versus the predicted moisture content for some data given in the literature. A line of best fit

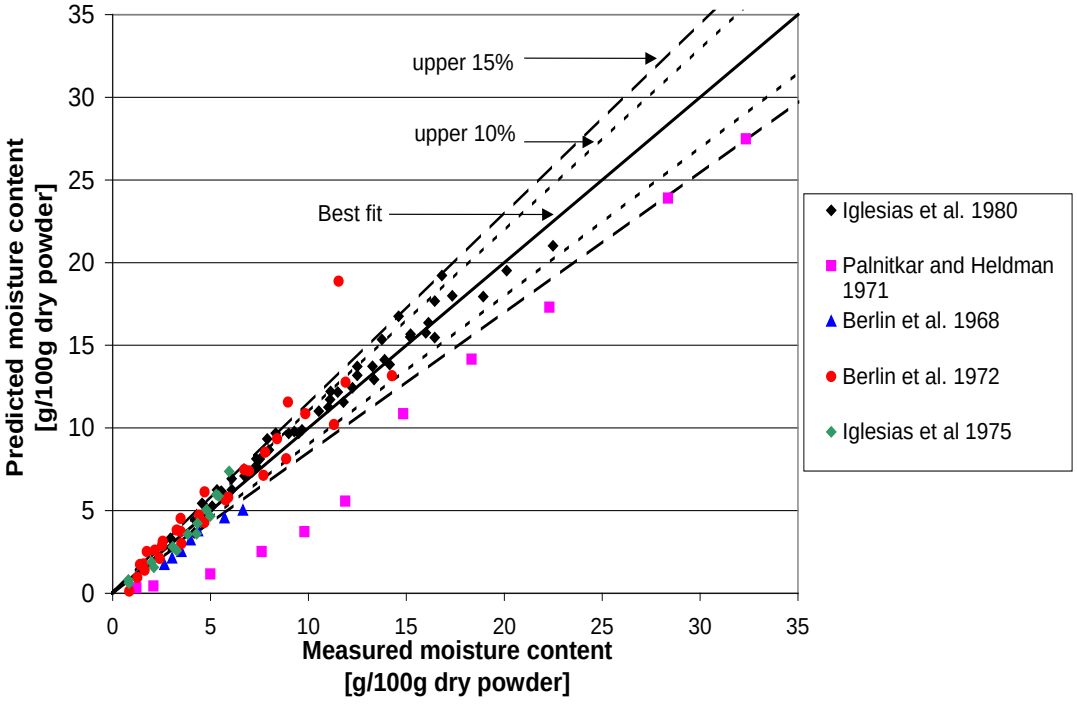

Figure 3.13: Comparison of measured versus predicted moisture contents for powders from literature

has also been drawn along with the ±10% and ±15% error bands. It can be seen that there is a considerable difference between the measured and predicted moisture contents for the data from Palnitkar and Heldman (1971), as discussed by the authors. There is good agreement with most of the data from Iglesias *et al.* (1975, 1980). Only reasonable agreement can be seen with the data from Berlin *et al.* (1968, 1972), as a considerable amount of the data is outside the ±15% error bands. In spite of this, the simple prediction method based on the weighted addition of the components isotherms appears to be a good method for predicting the isotherm for a multicomponent powder. The accuracy of the predicted isotherm is strongly affected by the accuracy of the components isotherms, hence the effort put into obtaining accurate isotherm prediction equations for the components in section 3.3.

Interactions between components were considered when predicting isotherms in the work conducted by Kamiński and Al-Bezweni (1994). This was done by introducing an interaction coefficient for each component. Good agreement was found between experimental and calculated values with relative errors no greater than 3.2%. This was tested on binary mixtures; therefore it is unclear how well this would work in multicomponent mixtures, as there may be too many interactions to easily quantify. Also, it requires that the effect of each interaction be known so that an activity coefficient can be determined. This represents a large amount of work in determining the effect of each interaction in multicomponent powders.

Sorption isotherms have been calculated based on the molar fractions and sorption isotherms of the mixture components [Chuang and Toledo 1976, van den Berg 1986]. This, however, is not a practical method, as the molecular weight of some products cannot be easily determined, and therefore the composition cannot be expressed in the form of molar fractions.

3.4.1 Experimental Validation of the Additive Isotherm Prediction Approach

Due to the inconclusive literature data available on the acceptability of the additive isotherm approach, some experimental work was done to investigate this further. The prediction of skim milk powder and cream powders from the addition of the isotherms for amorphous lactose, casein and whey protein has been investigated. The isotherm for micellar casein was also determined by subtracting off the isotherms for amorphous lactose and whey protein from the isotherms for high micellar casein powders.

3.4.1.1 Materials and Method

Powders of varying compositions of lactose, whey protein and micellar casein were made up in the proportions given in table 3.4.

α-lactose monohydrate (USP grade, The Lactose Company of New Zealand, Hawera, New Zealand), a high micellar casein isolate powder (as used in section 3.3.1.2 with composition: 83.7% casein, 6.3% whey protein, 1.7% fat and 8.3% ash) and a whey protein isolate powder (as used in section 3.3.1.1 with composition: whey protein 98.0%, lactose 0.1%, fat 0.3% and ash 1.6% on a dry mass basis) were used as the

lactose, whey protein and casein components respectively. Isotherms for skim milk powder, low fat cream powder, high fat cream powder and a dairy base powder (supplied by Fonterra Co-operative Group Limited, Auckland, New Zealand) were also measured. For comparison with milk powders, it was important to use a micellar casein powder because the structures of industrial caseins are significantly altered during processing. Due to solubility problems, micellar casein was dissolved in around 0.05 to 0.1% sodium citrate. It is unknown what effects this would have on the micelles. However, it was thought that the effects would be minimal due to the low concentration of the salt. The powders were made by freeze drying mixtures of the dissolved components using a freeze dryer (Virtis, Model 10-020) which typically operated at –58°C and a vacuum of 172 Pa (250 mTorr). Isotherms were measured at 20°C using the method stated in section 3.2.1.

Table 3.4: Composition of lactose, whey protein and micellar casein powders

Powder	Amorphous Lactose	Whey Protein Isolate	High Micellar Casein Powder
W1*	0	1	0
M1*	0	0	1
L1W1M1(a*,b)	1/3	1/3	1/3
L1W2*	1/3	2/3	0
L2W1*	2/3	1/3	0
L2M1(a,b,c)	2/3	0	1/3
W2M1	0	2/3	1/3

* denotes 3 weeks as opposed to 2 weeks equilibration time
a,b,c denotes replicates of a given powder

3.4.1.2 Results and Discussion

Using the isotherms for the high micellar casein powder and milk protein concentrate powder (figure 3.2) measured at 4, 20 and 37°C, along with their compositions given in section 3.3.1.2, the isotherms for amorphous lactose and whey protein were subtracted

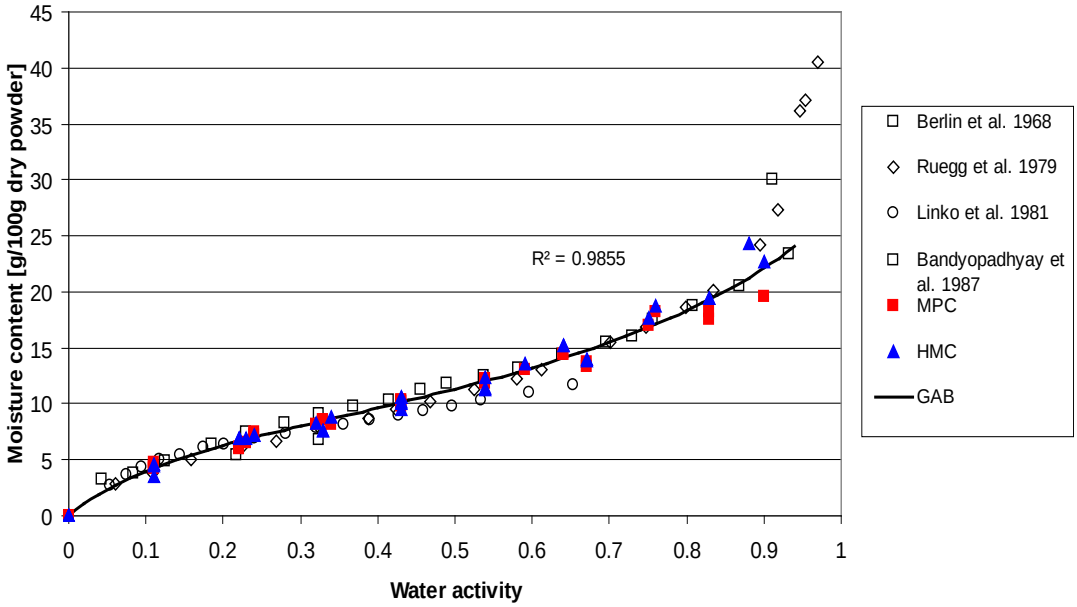

Figure 3.14: Moisture sorption isotherm for micellar casein

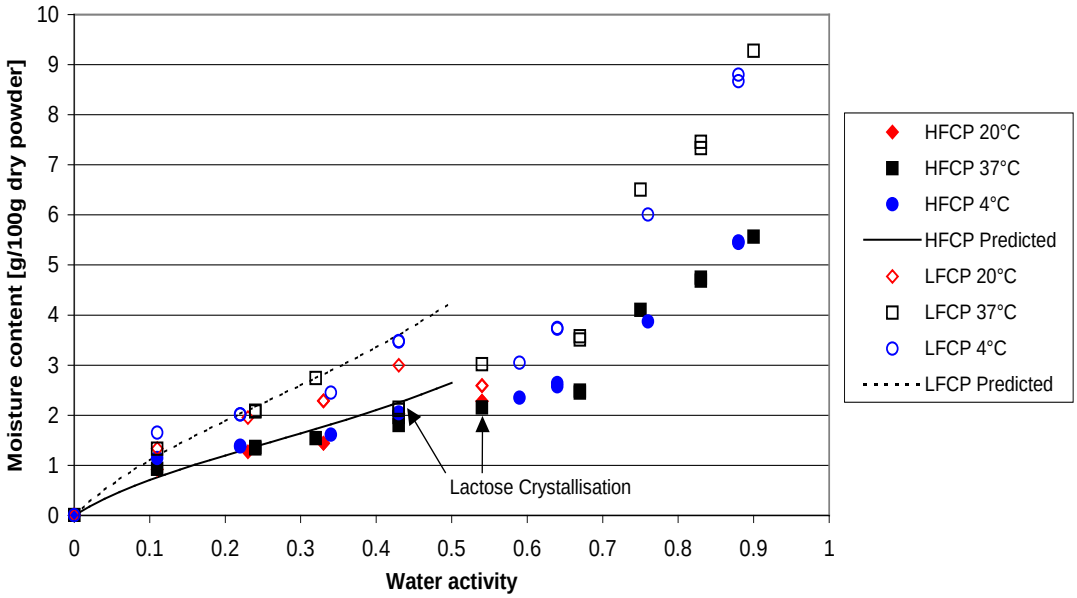

Figure 3.15: Predicted isotherms for low and high fat cream powders

(using equation 3.16) to give an approximation of the isotherm for micellar casein. The isotherms for amorphous lactose and whey protein isolate are given in figures 2.4 and 3.1 respectively. The effect of the fat was considered negligible since it was only present in very small amounts i.e. no greater than 1.7%. The resulting isotherm points for micellar casein are given in figure 3.14, where it can be seen that there is very good agreement between the data obtained from the two powders. A GAB isotherm was fitted to the data (excluding the literature data) up to $0.9a_w$ (R^2=0.9855) with the resulting GAB coefficients for M_o, c and f being 8.908 g/100g dry powder, 9.471 and 0.690 respectively. Figure 3.14 also includes the available literature data for micellar casein isotherms, for comparison with that predicted. It can be seen that there is very good agreement with the isotherm predicted and those given in literature giving confidence in the GAB isotherm model for micellar casein.

The isotherms for a low fat cream powder (LFCP) and high fat cream powder (HFCP) are given in figure 3.15. The isotherms for these powders were also predicted using the GAB isotherm models for amorphous lactose (section 2.2.2.1), whey protein isolate (section 3.3.1.1) and micellar casein given above. It can be seen that there is very good agreement between those measured and predicted, until the breakpoint in the isotherms, indicating that the milk fat does not have a significant effect on the isotherms for the powders even when it is present in a large amount. The breakpoint in the measured isotherms is due to amorphous lactose crystallisation [Berlin *et al.* 1968].

The isotherms for the powder mixtures given in table 3.4 were predicted using the isotherm for amorphous lactose (equation 2.4), whey protein (section 3.3.1.1) and high micellar casein powder (section 3.3.1.2). The α-lactose monohydrate content was also adjusted to take into consideration the water of crystallisation when determining the actual amorphous lactose content of the powder mixture. Referring to figure 3.16 it can be seen that there is good agreement between the measured and predicted isotherms except for when amorphous lactose crystallisation occurs. This can be seen for water activities above 0.43, where there is a drop in the moisture content measured. The drop in moisture content is not as significant for mixed whey protein and amorphous lactose

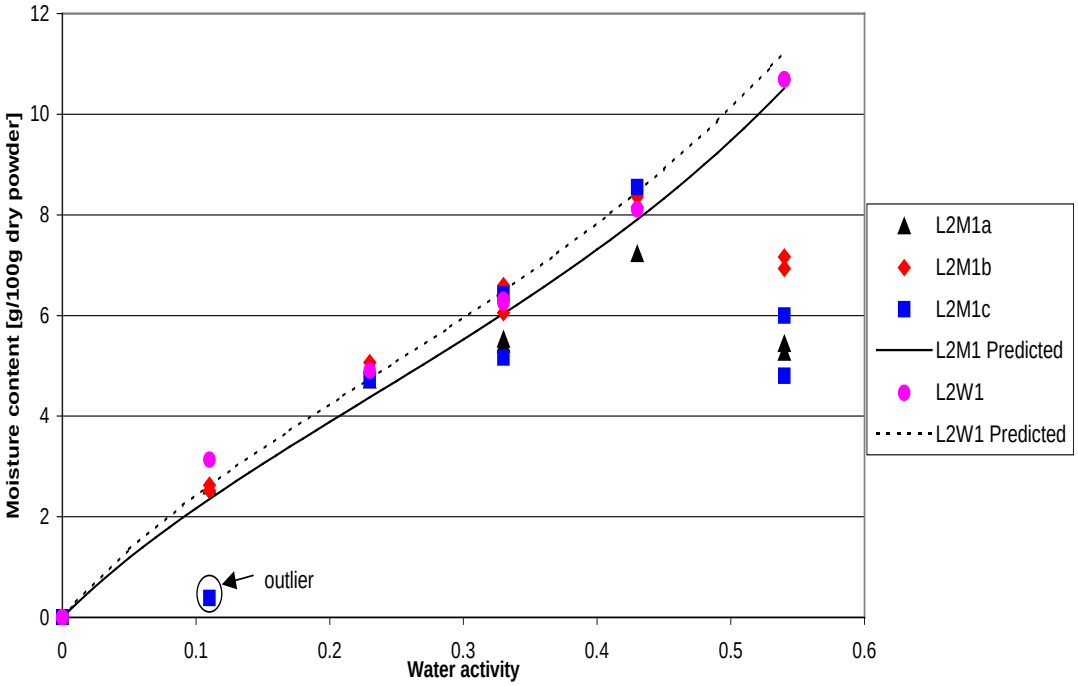

Figure 3.16: Moisture sorption isotherms showing amorphous lactose crystallisation

powders, as it is for powders without the whey protein (figure 3.16). It is probable that the amorphous lactose has crystallised in mixed whey protein and amorphous lactose powders. However, it appears that the whey protein may hinder the amorphous lactose crystallisation. Delayed crystallisation has also been noted by Berlin *et al*. (1968) in isotherms for milk and whey powders. Amorphous lactose crystallisation occurred at higher water activities, which was attributed to a lowered concentration of lactose at the surfaces of the milk powders, with the initial sorption site being some component other than lactose [Berlin *et al.* 1968]. It has also been noted that there is an overrepresentation of protein at the surface of mixed protein and lactose powders [Fäldt and Bergenståhl 1996c]. The proportion of protein relative to the other powder constituents is greater on the surfaces of the particles than in the powder in bulk. Referring to figure 3.16, the powder containing whey protein (L2W1) was equilibrated for 3 weeks and the powder containing casein (L2M1a,b,c) was equilibrated for 2 weeks. If the protein component did not effect amorphous lactose crystallisation, then it would be expected that the isotherms for both powders would show similar drops in moisture content above $0.43a_w$, since the lactose contents are similar. This is not the case, even when the powder containing the whey protein (L2W1) was equilibrated for longer, i.e. giving more time for lactose crystallisation to occur. This indicates that whey protein effects/delays the crystallisation of amorphous lactose. The implication of this is that it will require higher water activities to result in amorphous lactose crystallisation at a given temperature, when whey protein is present. When considering sticking behaviour, as discussed in section 2.2.2.3, it would require a higher $T-T_g$ for instantaneous sticking to occur.

Figure 3.17 shows an overall comparison between the measured and predicted moisture contents for the powder mixtures from table 3.4 and skim milk powder. Included are the isotherm data from Foster and Paterson (2001) and Keir (2001) which is data for dairy powders. Points which were obvious outliers or those where lactose crystallisation is likely to have occurred have been omitted from this figure. Error

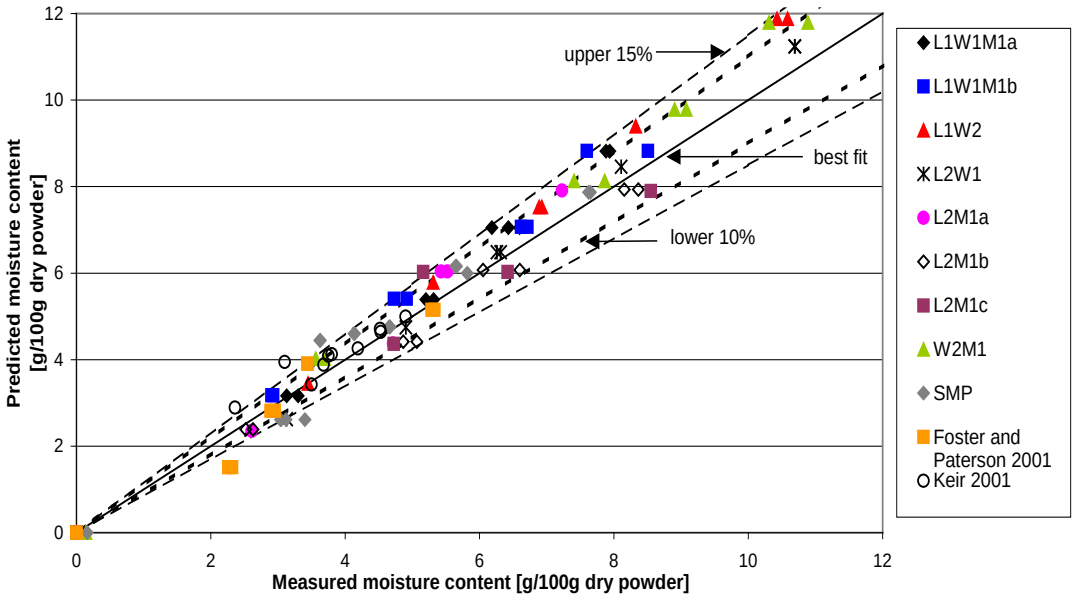

Figure 3.17: Comparison of measured versus predicted moisture contents from isotherms for lactose, whey protein, casein and milk fat containing powders

limits of ±10 and 15% have also been included. It can be seen that there is very good agreement between the measured and predicted moisture contents, with most of the data being within the ±10% error limit and almost all the data being within the ±15% error limit. In general, the predicted moisture contents are slightly greater than those measured. This indicates that there may be some interaction which decreases water sorption. As discussed previously, Iglesias *et al.* (1980) stated that the hydrogen bonding between components is likely to compete with hydrogen bonding between components and water. This would result in a decrease in water sorption. Since most of the data are within the ±10% error limits, it can be concluded that the simple additive isotherm approach is acceptable for predicting the isotherms of dairy powders.

Moisture sorption isotherms were also predicted for strawberries (fructose/sucrose/glucose) [Roos 1987] and a sucrose/fructose powder [Roos and Karel 1991a]. Figure 3.18 shows the measured and predicted isotherms for these powders. The ±10% and 15% error limits have also been included in this figure. It can be seen that there is a good fit for most of the data except for some low moisture content data. At the low moisture content, the predicted isotherm was much higher than that measured for both powders. This indicates that the predicted isotherm for either amorphous sucrose or fructose may be too high at the low water activities. Due to the inability to make completely amorphous sugar powders, further checking of the simple additive isotherm approach for amorphous sugar mixtures could not be made. However, the acceptance of fit over the water activity range of 0.33 to 0.52 for an amorphous fructose, sucrose and glucose mixture gives some confidence that this method is appropriate and acceptable. Also, sugars are only likely to be added to dairy powders in small quantities, therefore their effect on the overall isotherm will be small. Further checking of this method of isotherm prediction is done in chapter 7.

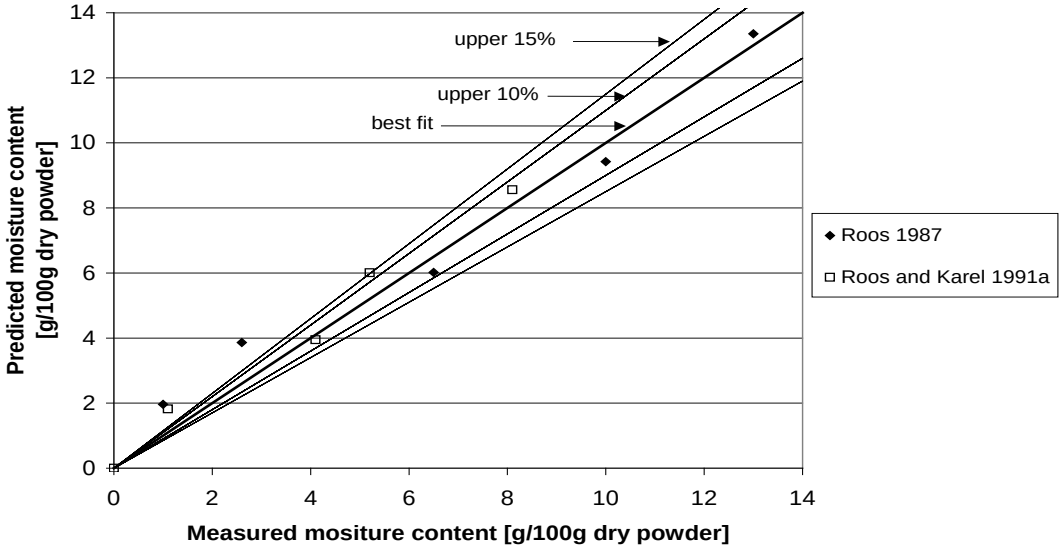

Figure 3.18: Comparison of predicted and measured moisture contents for amorphous sugar mixtures

3.5 CONCLUSIONS

Isotherms for dairy powder components have been determined and equations for their prediction given. The component isotherms were used to predict the isotherms for dairy powders and freeze-dried strawberries. A simple additive approach was used to predict the isotherms and was found to be acceptable for dairy powders. The acceptability of this approach, when dealing with mixtures of amorphous sugars, is unclear due to the lack of isotherm data available for sugar mixtures and the inability to make completely amorphous sugar powders. This method is likely to be acceptable when dealing with dairy powders that have some sugar other than lactose added, since the sugars are usually added in a small amount.

The relationship between water activity and moisture content for dairy powder components is now known. This can be used to create glass transition temperature profiles for these components, as has been done in chapter 4. The isotherms can also be used for predicting the isotherms and T_g profiles for powders, as demonstrated in chapters 4 and 7.

CHAPTER 4

PREDICTION OF THE GLASS TRANSITION TEMPERATURE

4.1 INTRODUCTION

Changes in food powders with respect to stickiness, caking, crystallisation and collapse are related to the glass transition temperature of the powder [Slade *et al.* 1993, Roos and Karel 1991a]. For this reason, it is necessary to know or be able to predict the glass transition temperature of a powder from knowledge of the composition and water activity (or moisture content) of that powder. When only one amorphous sugar is present, the T_g can be predicted directly from the water activity of the powder. Alternatively, it can be predicted by determining the moisture associated with the amorphous sugar through the use of an isotherm. When more that one amorphous sugar is present, the T_g for the powder will be related to the amounts of each amorphous sugar and the water activity or the amount of moisture associated with each sugar. Accurate T_g profiles for each amorphous sugar are therefore required so that more accurate predictions of the T_g profiles for amorphous sugar mixtures can be made. This chapter collates the T_g profile data for amorphous sugars that are likely to be present in dairy powders. A method for predicting the T_g profile for multicomponent powders is also investigated.

Being able to predict the T_g profile for a powder allows:

1. The prediction of the water activity (and hence moisture content through the use of an isotherm) that the powder should be dried to, in order to prevent caking during storage; and
2. The prediction of a window of relative humidity and temperature conditions that the dryer outlet should be operating at, in order to reduce or eliminate sticking and caking problems during processing.

4.2 GLASS TRANSITION TEMPERATURE

The glass transition temperature has been defined in section 2.2.2.2. Generally, T_g profiles are given versus water activity, moisture content or concentration (% solids). T_g data can be subject to variation due to the method of measurement and the care taken when preparing powder samples for T_g measurement. Therefore, when comparing T_g data obtained from different authors, there may be several reasons for the variations/discrepancies in such data. The following section outlines the measurement of the T_g and the potential reasons for variations in data.

4.2.1 Measurement of the Glass Transition Temperature

Glass transition is a second order transition which is characterised by a change in specific heat (c_p) [Bhandari and Howes 2000]. It results in dramatic changes in free volume, molecular mobility and physical properties of amorphous materials and can be detected by changes in mechanical, thermal and dielectric properties [Roos 1995]. The glass transition temperatures of food ingredients and products are commonly measured by thermal analysis methods such as differential scanning calorimetry (DSC) and dynamic mechanical (thermal) analysis (DMA or DMTA) [Slade *et al.* 1993]. However other methods including nuclear magnetic resonance, electron spin resonance and thermomechanical analysis have been used by a number of researchers. Slade *et al.* (1993) gives an extensive list of references to studies where methods other than DSC or DMA have been used for glass transitions.

DSC is one of the most common methods for measuring the T_g of powders where the phase change is detected by an increase in specific heat. The T_g, when measured by DSC, is subject to variation due to:

a. scanning rate used
b. location of the T_g on the DSC curve
c. enthalpy relaxation peaks

as well as the care taken during the preparation of the DSC pans (potential uptake of moisture by the powder) used for T_g measurement.

The scanning rate used is important, as the glass transition region will be overshot if the scanning rate is too high. This will result in T_g values which are significantly higher than their true value. It is fairly common to use scanning rates of 5°C/min [Chan *et al.* 1986, Roos and Karel 1990, Izzard *et al.* 1991, Roos and Karel 1991a,b,c,d,e, Roos 1993, Miller and de Pablo 2000]. However, 10°C/min has also been used by a number of researchers [Blond 1989, Orford *et al.* 1989, Orford *et al.*1990, Blond and Simatos 1991, Noel *et al.* 2000, Zhang and Zografi 2000].

There are a number of different definitions for T_g in terms of the location on the DSC curves and this can cause discrepancies and therefore make it difficult to compare T_g data obtained from different authors. Taking amorphous lactose as an example, the glass transition region can span around 10°C or more [Roos and Karel 1991a]. When comparing T_g data for amorphous lactose, it is expected that the data could differ within around a 10°C limit due to varying methods for defining T_g. The following definitions for T_g have been found in literature and are shown graphically in figure 4.1:

1. *Onset T_g ($T_{g,o}$)*: taken as the temperature where there is an initial deviation in the heat flux from the pre-transition base-line [Roos and Karel 1990, Lloyd *et al.* 1996]
2. *Endset T_g ($T_{g,e}$)*: end temperature of the glass transition region.
3. *Midpoint T_g ($T_{g,m}$)*: there are number of definitions of T_g which have been referred to as the midpoint, these include:
   i. Average – taken as the average between the onset and endset T_g values [Roos 1993].
   ii. half-step temperature – determined at the point where half the total increase in specific heat capacity (Δc_p) had occurred [Kristov and Jones 1992]
4. *Extrapolated onset T_g ($T_{g,eo}$)*: this is generally taken as the point of intersection between the line tangential to the onset T_g and the steepest slope on the rise of the endothermic step.

5. *Inflection point T_g ($T_{g,i}$)*: temperature at the inflection point on the rise of the endothermic step. Höhne *et al*. (1996) stated that this is rarely used, however, Kristov and Jones (1992) stated that this point on the DSC curve coincides with the half-step midpoint temperature.

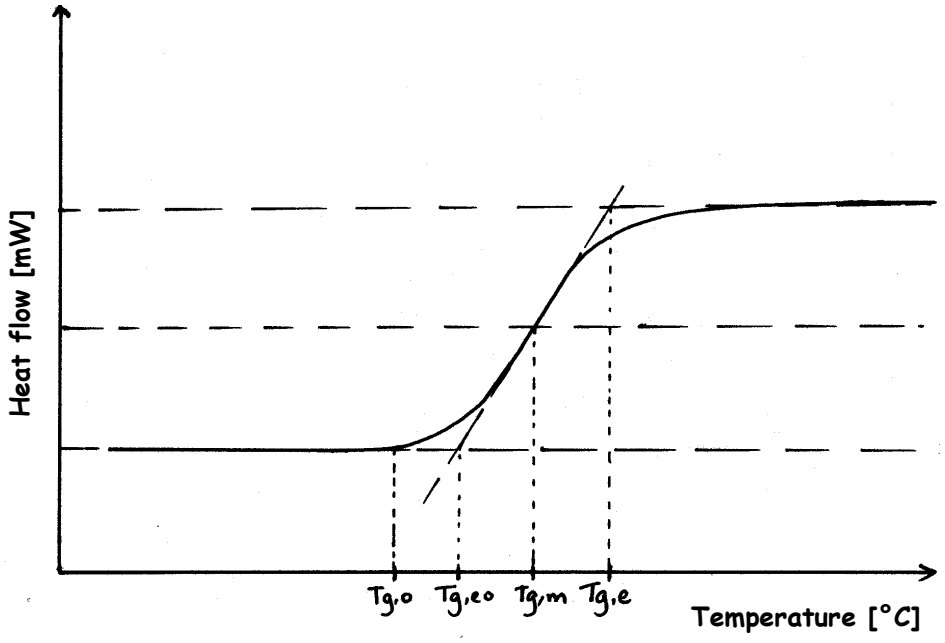

Figure 4.1: Typical DSC curve showing the glass transition

Höhne *et al.* (1996) stated that a problem with investigating the glass transition is that there may be the occurrence of "enthalpy relaxation peaks" which appear on the heating curves as endothermic events at the high temperature end of the glass transition region. These peaks can make the determination of T_g more difficult as some of the definitions for T_g ($T_{g,m}$ and $T_{g,e}$) do not make any allowances for the nonequilibrium nature of the glass transition. $T_{g,m}$ and $T_{g,e}$ are affected differently by the thermal history of the sample making them difficult to compare them from one sample to another. This relaxation peak is related to a structural relaxation of the sample during the first heat treatment and is a typical feature for glass transitions of many materials [Höhne *et al.* 1996]. In order to eliminate the hysteresis effects of these thermal relaxations when determining T_g from DSC curves, it is common practice to repeat the scan after the sample has been cooled to the start temperature [Orford *et al.* 1989, Blond 1989, Orford *et al.* 1990, Roos and Karel 1991b,c,d, Blond and Simatos 1991, Roos 1993, Miller and de Pablo 2000, Noel *et al.* 2000, Zhang and Zografi 2000]. The resulting curve shows the glass transition without the relaxation peak. The thermal history can be removed by the following procedure as given in Höhne *et al.* (1996):

1. The sample is heated to a temperature at least 15 to 30°C above T_g
2. Short (5 to 10 min) annealing at this temperature in order to establish thermodynamic equilibrium and to erase thermal history of the system
3. Rapid programmed cooling (or quenching) to a temperature at least 50°C below the glass transition
4. Immediate reheating at a constant rate.

DSC software allows the measurement of a number of T_g values. The T_g definitions and related measurements for PC series DSC7 software version 3.1 (DOS based) and

Pyris software for windows version 3.81 are given and related to the definitions that have been given above.

For version 3.1:

Onset	-	the intersection of the pre-transition baseline (the lower temperature) and the greatest slope [$T_{g,eo}$].
T_g midpoint	-	the temperature where the curve is midway between the two tangents [$T_{g,m\ –\ half\ step\ temperature}$].
J/g Deg	-	the change in specific heat at the T_g midpoint (as defined above).

For version 3.81:

Onset	-	intersection of the extrapolated tangent at the first limit and the extrapolated tangent at the inflection point [$T_{g,eo}$].
End	-	intersection of the extrapolated tangent at the second limit and the extrapolated tangent at the inflection point [$T_{g,e}$].
Inflection Point	-	point on curve where the slope changes from increasing to decreasing or vice versa [$T_{g,i}$].
Half Cp Extrapolated	-	point on curve where the specific heat change is half the change in the completed transition [$T_{g,m\ –\ half\ step\ temperature}$].
Half-Width	-	point on curve that is halfway between the onset and end points [$T_{g,m\ –\ average}$].
Fictive Temperature	-	point on enthalpy curve (taken as the integral of the specific heat over the specified temperature range) where the change of slope occurs.

It is noted that onset T_g measurements obtained from DSC software, reported in literature, are likely to be extrapolated onset temperatures [$T_{g,eo}$]. Midpoint measurements are likely to be half-step midpoint temperatures [$T_{g,m\ –\ half\ step\ temperature}$].

Further variations in the T_g data between different researchers may be due to the variations in the care taken when preparing the DSC pans with powder sample. Since amorphous sugars are hygroscopic, they pick up moisture very quickly if the DSC pans are not filled with the powder sample under dry conditions (i.e. using dry air or nitrogen). This would result in a slight increase in the moisture content of the powder, which would result in a decrease in the T_g measured. Lastly, the method used to determine the moisture content will effect the T_g profile for the amorphous sugar [Brooks 2000, Bonelli *et al.* 1997]. Brooks (2000) discussed the presence of residual moisture in freeze-dried sugars and the effect of this residual moisture on the glass transition temperature of the amorphous sugar. Freeze-dried sugars still contain a certain amount of moisture even after dehydration over a strong desiccant such as phosphorous pentoxide. Therefore, although this method of drying is meant to give a completely dry powder, there is still some moisture present, which can act as a plasticiser. Bonelli *et al.* (1997) found that freeze dried lactose, maltose and sucrose will contain a small amount of residual moisture even after desiccation over phosphorous pentoxide. Residual moisture contents were found (by vacuum oven drying at 70°C for 48 hours and by forced air oven drying at 105°C for 42 hours) in the amorphous sugar powders, which had been stored for one week over phosphorous

pentoxide at 25, 35 and 45°C. Since the powders are generally stored at around 20-25°C when being prepared for T_g measurement, only the residual moisture content data after storage at 25°C is given in table 4.1.

Table 4.1: Residual moisture content for freeze-dried sugars [Bonelli *et al.* 1997]

Sugar	Moisture content (%) [Vacuum oven at 70°C]	Moisture content (%) [Forced-air oven at 105°C]
Lactose	1.3 ± 0.5	2.0 ± 0.1
Sucrose		2.2 ± 0.4
Maltose	3.1 ± 0.9	2.8 ± 0.1

Brooks (2000) found the residual moisture content in spray dried lactose to be 1.65 g/100g dry powder and 1 g/100g dry powder after storage over phosphorous pentoxide after 1 and 3 weeks respectively. If the moisture content is measured gravimetrically, after storage over saturated salt solutions, then the residual moisture content will not be included in the moisture content stated. Moisture contents measured by oven drying or by Karl Fisher titration will include the residual moisture in the moisture content stated. The inclusion or otherwise of the residual moisture will therefore contribute to some variation between the T_g versus moisture content data obtained by different researchers. Residual moisture is also likely to be present in amorphous glucose, galactose and fructose after desiccation over phosphorous pentoxide. There was no success with freeze drying glucose, galactose or fructose solutions, and therefore residual moisture contents could not be determined for these amorphous sugars in this work.

4.2.2 Glass Transition Temperature Prediction

Carbohydrates have the largest effect in influencing the T_g of an amorphous powder. Common sugars, such as glucose, fructose and galactose, which have low molecular weights, have low T_g values. Therefore their influence is to depress the T_g in very sugar-rich foods. It has been found that the effect of fat and protein on T_g is not significant in food systems like milk powders [Jouppila and Roos 1994a,b, Shimada *et al.* 1991]. Jouppila and Roos (1994b) found that milk fat did not effect the T_g of milk powders. However, the T_g could not be determined from the DSC curve due to the dominant fat melting mechanism which occurred in the same temperature range over the RH range of 23.9 to 44.4%.

Bhandari and Howes (1999) stated that the T_g of very high molecular weight food polymers such as protein cannot be measured experimentally as they start decomposing before they reach T_g. It was suggested that the analysis could be done by looking at the plasticising effect of water and then looking at the intercept as the water content tends to zero. Imamura *et al.* (1998) looked at the effect of a bovine serum albumin protein on the phase transition of the amorphous structure in sugar. It was found that the T_g was raised by the addition of the protein except for when the water activity was low (up to about 0.1). The increase in T_g suggests that protein contributes to stabilising the amorphous structure of the sugar. However, work by Jouppila and Roos (1994b) showed no significant difference between the T_g profiles for different milk powders and amorphous lactose, indicating that the protein does not effect the T_g of the lactose.

Gordon and Taylor (1952) derived a well known empirical expression for the composition dependence of T_g from the Gibbs-DiMarzio theory of the glass transition. This empirical equation was used to calculate the T_g of a mixture of two polymers and is given as equation 4.1. The Gordon and Taylor equation was also used with satisfactory results for a binary mixture of water and a single solute [Roos 1993]. It is commonly used to calculate the plasticising effect of moisture on the glass transition temperature.

$$T_g = \frac{w_1 T_{g_1} + k w_2 T_{g_2}}{w_1 + k w_2} \tag{4.1}$$

where w_1 = mass fraction of component 1 (usually the component in the greatest concentration i.e. solute in the case of polymer/diluent blends)
w_2 = mass fraction of component 2 (usually diluent or component in smallest concentration)
T_{g1} = T_g of pure component 1
T_{g2} = T_g of pure component 2
k = constant

The problem with the Gordon and Taylor equation in its present form is that it is not applicable to tertiary or multicomponent systems. Most use of this equation has been with binary systems, i.e. fructose and glucose [Roos and Karel 1991a].

Couchman and Karasz (1978) also developed a mathematical relationship for determining the T_g of a compatible polymer mixture (equation 4.2).

$$T_g = \frac{x_1 T_{g_1} + \left(\frac{\Delta c_{p_2}}{\Delta c_{p_1}}\right) x_2 T_{g_2}}{x_1 + \left(\frac{\Delta c_{p_2}}{\Delta c_{p_1}}\right) x_2} \tag{4.2}$$

where x_1 and x_2 are the mass fractions of the two polymer components and Δc_{p1} and Δc_{p2} are changes in specific heat capacity of each component between the glassy and rubbery states.

Equation 4.2 is formally identical to the Gordon and Taylor equation, especially if it is considered that $k = \Delta c_{p2}/\Delta c_{p1}$, as was done by Couchman (1978) using the change in specific heat for pure components 1 and 2 respectively, at their glass transition temperatures. Table 4.2 gives empirical k values from literature for amorphous sugars along with changes in specific heat capacity and k values obtained from the ratio of the change in specific heat with that for water.

Brinke *et al.* (1983) used the Couchman and Karasz model to describe the T_g behaviour of polymer/diluent mixtures (where subscript 1 is for the solute and subscript 2 is for the diluent). It was found to work equally well for at least one polymer network/diluent system. With aqueous mixtures, the T_g and Δc_p for water have to be used. These values

have had much controversy. A T_g of –135°C [Johari *et al.* 1987] and Δc_p of 1.94 J/g°C [Sugisaki *et al.* 1968] are generally used [Arvanitoyannis *et al.* 1993].

Table 4.2: *k* values and change in specific heat capacity data for amorphous sugars

Reference	Sugar	*k* (empirical)	Δc_{p1} [J/g°C]	*k* [$\Delta c_{p2}/\Delta c_{p1}$]*
Parks *et al.* 1928	Glucose		0.80	2.43
Orford *et al.* 1989	Glucose		0.88	2.20
Orford *et al.* 1990	Sucrose		0.77	2.52
	Fructose		0.84	2.31
	Maltose		0.79	2.46
	Galactose		0.85	2.28
Blond and Simatos 1991	Galactose		0.75	2.59
Roos and Karel 1991b	Sucrose	4.7±0.2	0.60	3.23
Roos and Karel 1991c	Maltose	6	0.61	3.18
Roos and Karel 1991e	Glucose	4.3	0.65	2.98
	Sucrose	4.7		
	Fructose	3	0.75	2.59
	Maltose	6		
	Lactose	7		
Roos 1993	Glucose	4.52	0.63	3.10
	Sucrose	5.42	0.60	3.23
	Fructose	3.76	0.75	2.59
	Maltose	6.15	0.61	3.18
	Galactose	4.49	0.50	3.88
	Lactose	6.56		
Jouppila and Roos 1994b	Lactose	6.7		
Brooks 2000	Lactose	6.9		
Zhang and Zografi 2000	Glucose		0.54	3.59

* where Δc_{p1} is the change in specific heat capacity at the glass transition for the amorphous sugar given in the table and Δc_{p2} is the change in specific heat capacity at the glass transition for water (1.94 J/g°C)

An expansion based on equation 4.2 can be used for describing multicomponent systems (equation 4.3).

$$T_g = \frac{\sum_{i=1}^{n} w_i \Delta c_{p_i} T_{g_i}}{\sum_{i=1}^{n} w_i \Delta c_{p_i}} \tag{4.3}$$

This equation has been applied to multicomponent mixture systems such as water, glucose and fructose [Roos 1995, Arvanitoyannis *et al.* 1993]. Arvanitoyannis *et al.* (1993) compared the T_g of glucose, fructose and water systems obtained by DSC with that predicted by the above methods. It was found that the expansion of the Couchman and Karasz equation gives the best fit to experimental data at high sugar concentrations (>70% w/w) whereas at lower concentrations, the Gordon and Taylor equation can provide a better fit. In a powder, the concentration of sugar to water will be high i.e. greater than 70% (w/w) therefore, it appears that the Couchman and Karasz equation should provide a better prediction. Arvanitoyannis *et al.* (1993) showed that the Couchman and Karasz theory underestimates T_g in the case of aqueous mixtures and overestimates the T_g in the case of non-aqueous mixtures of glucose and fructose.

Matveev *et al.* (2000) stated that the Gordon and Taylor and Couchman and Karasz equations cannot approximate experimental T_g – composition dependences of many

biopolymer mixtures. Immiscible polymers retain their own T_g. Therefore biopolymer mixtures will either have two transitions or a single transition over a much broader temperature range. The latter occurs when the individual T_g values are close to each other. The additive contribution technique, as studied by van Krevelen (1990), Matveev *et al.* (1997) and Matveev *et al.* (2000) is an approach used to predict the plasticisation of biopolymers by water. The underlying idea for this technique is that the physical property of a biopolymer is determined by the sum of the increments corresponding to the structural groups in its molecule. Matveev *et al.* (2000) compared their predictions with experimental data for proteins and polysaccharides obtained by other researchers and found there to be good agreement.

Matveev *et al.* (1997) stated that foods are usually heterogeneous multicomponent systems and that the main reason for this is due to the incompatibility between proteins and polysaccharides (the food components primarily responsible for structural and physicochemical properties). Matveev *et al.* (1997) also stated that food systems can have either one or several T_g values depending on the phase state (i.e. whether there are compatible or incompatible polymers present). If two biopolymers are compatible then a single T_g, which is between that of the individual biopolymers, will result. Heterogeneous blends of incompatible polymers usually show several T_g values, which correspond to the polymers' separate T_g values. Matveev *et al.* (1997) further stated that partial miscibility or limited co-solubility of biopolymers in co-existing phases leads to shifts in the T_g for the system. The T_g will be between that of the limitedly miscible biopolymers, which shows their cosolubility. The temperature range of T_g may also broaden due to fluctuations in local composition or system microheterogeneity. Broadening of the T_g may also be seen when two incompatible materials are mixed and the T_gs of the two components are close to each other.

Studies by Kalichevsky *et al.* (1993) looked at the effect of sugars on the T_g of casein with the addition of glucose, sucrose or fructose to the casein. There was no observable change in T_g compared to the T_g of the individual sugars and casein when examined against moisture content. It is possible that the grinding/pressing technique used did not allow for interactions between the two components to occur. Kalichevsky *et al.* (1993) also looked at the effect of fructose on the T_g of sodium caseinate. Effects of the sugars on the transitions were observed with this work, where the same preparation techniques were used. This implies that the sodium caseinate interacts with the sugars and casein does not. This was confirmed by using solid state C NMR to detect any casein-sugar interactions. No evidence was found for any change in structure or conformation of casein or interaction. Also, no crystallinity was detected by X-ray diffraction indicating that there was a phase-separated system for the casein-sugar system.

The presence of fructose with sodium caseinate showed a reduction in T_g (from that for sodium caseinate). Two transitions were seen, one slightly above that for fructose and one slightly lower than that for sodium caseinate. Kalichevsky *et al.* (1993) further explained that this type of low temperature transition is frequently observed in compatible polymer-diluent mixtures which is due to the onset of short-range motions and not necessarily due to phase separation. These low temperature transitions were not noted with the casein/sugar mixtures. Therefore clear phase separation along with no evidence of interactions made it difficult to explain the lack of plasticising effect of sugars on casein. It was stated however, that it was likely that the sugars were incompatible with casein. Phase separation with amylopectin:fructose (2:1) mixture

was also noted by Blanshard (1995) where two peaks were observed on DMTA traces. One appeared to be amylopectin-rich but plasticised by both fructose and water, while the other appeared to be fructose-rich and plasticised by water but also anti plasticised by amylopectin.

Referring to the work by Jouppila and Roos (1994b), protein did not appear to have an effect on the T_g of lactose. This indicates that milk protein (casein and whey protein) is incompatible with lactose and the flow properties of the powder, in terms of sticking and caking, is limited by the lower transition relating to the lactose. The presence of protein did however increase the instantaneous crystallisation temperatures making them at least 30°C higher than that for pure lactose at some water activities. Berlin *et al.* (1968) measured the sorption isotherms for a number of milk powders and milk powder components. It was found that at 24.5°C, crystallisation (indicated by the breakpoint in the isotherm) occurred at a water activity of 0.35 for a lactose powder but did not occur until at least a water activity of 0.5 in milk and whey powder. This is in line with the delayed crystallisation noted with the work by Kalichevsky *et al.* (1993) when looking at instantaneous crystallisation temperatures.

4.3 GLASS TRANSITION TEMPERATURE PREDICTION FOR DAIRY POWDER COMPONENTS

This section summarises the T_g versus moisture content and T_g versus water activity data on amorphous glucose, galactose, fructose, sucrose, maltose and maltodextrin powders available in the literature. Equations have been fitted to these data so that predictions of the T_g for different sugars can be made. These equations are used in chapter 7 to predict the conditions for sticking and caking in dairy powders.

4.3.1 Amorphous Glucose

T_g versus moisture content data were taken from Chan *et al.* (1986), Orford *et al.* (1990), Roos and Karel (1991e), Roos (1993), Tromp *et al.* (1997), Miller and de Pablo (2000), Noel *et al.* (2000), van den Dries *et al.* (2000) and Zhang and Zografi (2000), and is given in figure 4.2. The Gordon and Taylor equation was fitted to this data, allowing both *k* and the dry T_g for amorphous glucose to vary so that the best fit possible could be obtained. The *k* value and dry T_g for amorphous glucose were found to be 4.08 and 33.7°C respectively with an R^2 value of 0.9834. The empirical *k* value obtained compares well to those given by Roos and Karel (1991e) and Roos (1993) of 4.3 and 4.52 respectively as given in table 4.2. It also compares with the *k* value (3.59) obtained from the ratio of specific heats using the change in specific heat capacity of 0.54 J/gK for amorphous glucose, as given by Zhang and Zografi (2000).

The isotherm for amorphous glucose (figure 3.4), from the data obtained at –10°C, was used to convert the data in figure 4.2 to a T_g versus water activity profile, as seen in figure 4.3. No T_g versus water activity profiles were given in the literature for amorphous glucose. The isotherm for amorphous glucose and the Gordon and Taylor equation, using the constants obtained in figure 4.2, were used to predict the T_g versus water activity data, giving an R^2 value of 0.9827. A cubic equation was also used to predict the T_g versus water activity data giving a R^2 value of 0.9836. The water activity

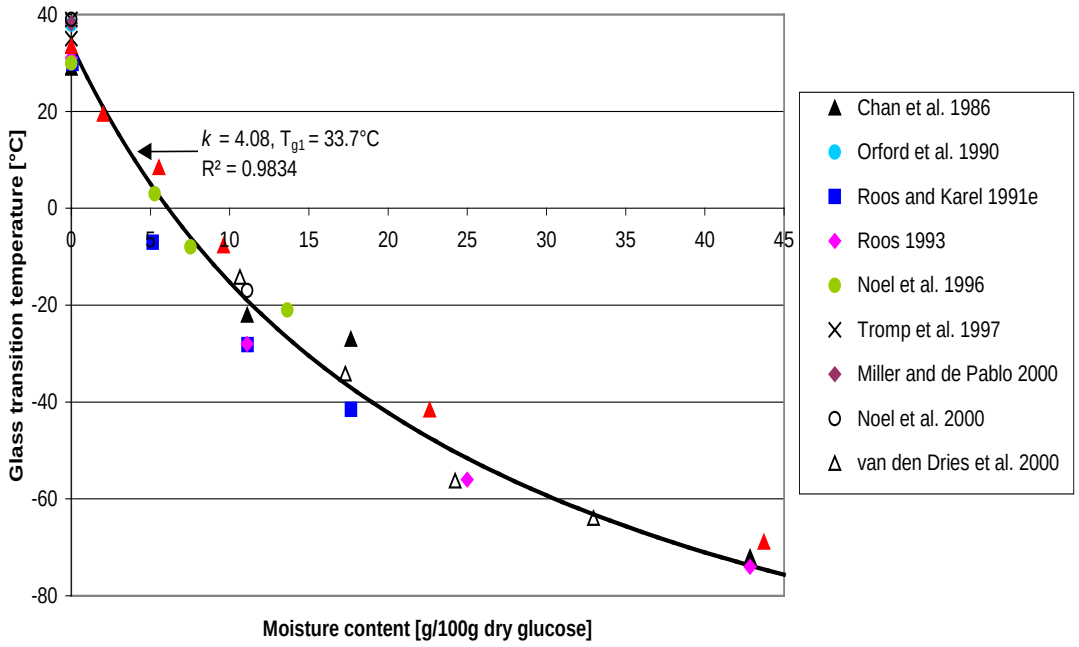

Figure 4.2 T_g versus moisture content for amorphous glucose

region of 0.04 to 0.34, over which there is a difference in fit between the two models does not contain enough experimental data to be able to tell which fit is best. It does appear that in that water activity region the cubic model probably underestimates the T_g. The combined isotherm/Gordon and Taylor equation uses two fitted parameters versus three for the cubic model and achieves the same level of fit. Considering this and the fact that the combined isotherm/Gordon and Taylor equation has a theoretical basis, it is the best model to use.

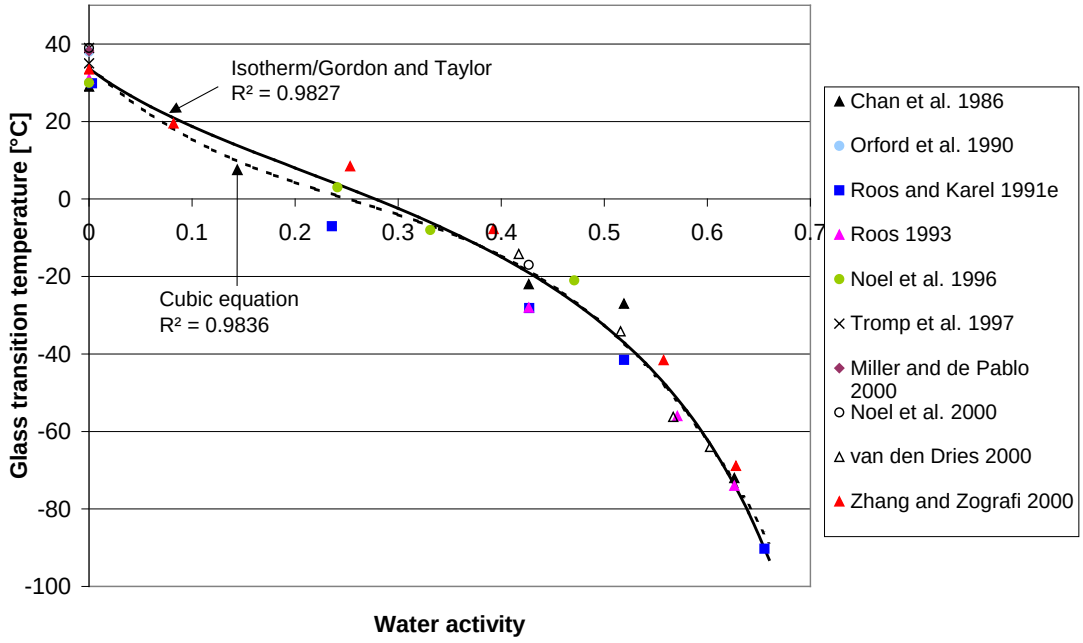

Figure 4.3: T_g versus water activity for amorphous glucose

4.3.2 Amorphous Galactose

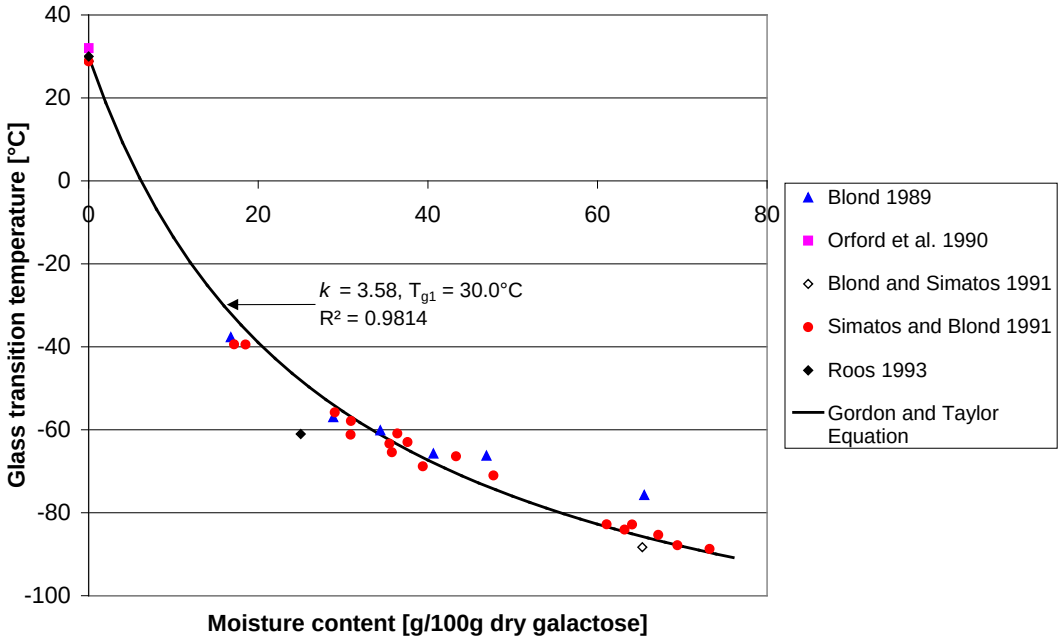

Figure 4.4: T_g versus moisture content for amorphous galactose

T_g versus moisture content data were taken from Blond (1989), Blond and Simatos (1991), Simatos and Blond (1991) and Roos (1993). Orford *et al.* (1990) also measured the dry T_g for amorphous galactose. These data are shown in figure 4.4 where the Gordon and Taylor equation has been fitted to describe the plasticisation of amorphous galactose by moisture. Setting the dry T_g to 30.0°C, *k* was found to be 3.58 giving an R^2 value of 0.9814. This differs from the *k* values found empirically (4.49) from literature in table 4.2, but it is close to the *k*=3.88 obtained using the Δc_p ratio for amorphous

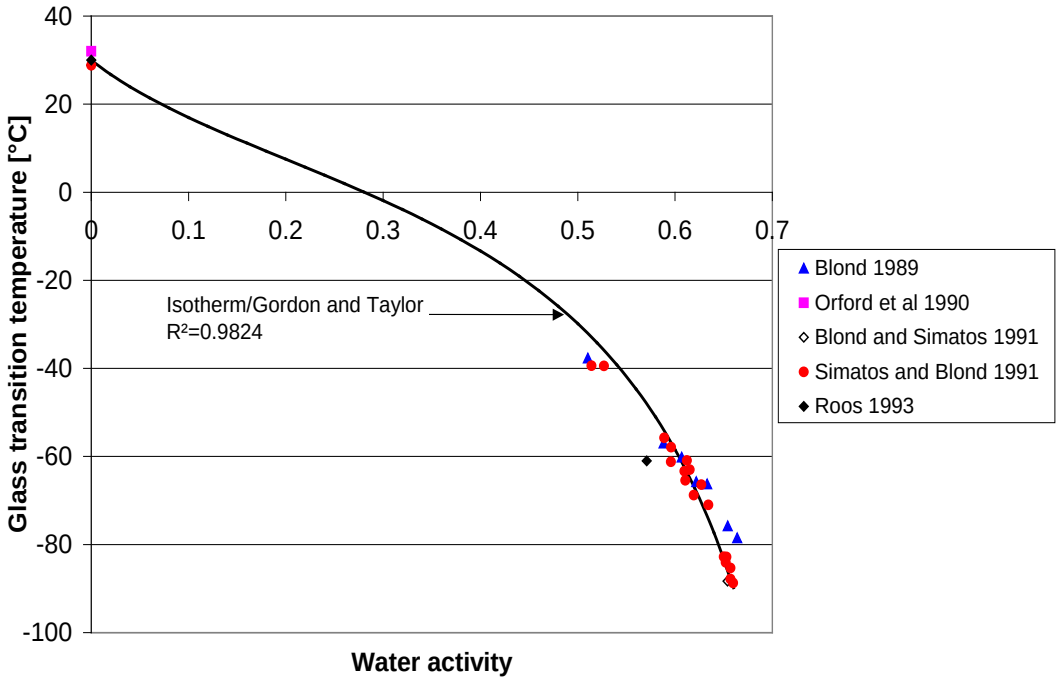

Figure 4.5: Estimated T_g versus water activity profile for amorphous galactose

galactose found by Roos (1993).

As discussed in section 3.3.3.1, there is no isotherm available in the literature for amorphous galactose. Due to the inability to make amorphous galactose powders, it could not be measured in this work. Due to similarities in the structures of glucose and galactose, the isotherm for amorphous glucose (obtained at –10°C and given in section 3.3.2.2) has been used as an estimate of the isotherm for amorphous galactose. Using this isotherm and the Gordon and Taylor equation (k=3.58, T_{gi}=30.0°C), an estimate can be made of the T_g versus water activity profile for amorphous galactose (figure 4.5). It is stressed that this T_g/a_w profile is only an estimate and is only used due to the lack of having any more accurate data available.

4.3.3 Amorphous Sucrose

T_g versus water activity and moisture content data were taken from Roos and Karel (1990) and Roos and Karel (1991a). This moisture content data do not include the residual moisture as this was measured gravimetrically with phosphorous pentoxide (P_2O_5) giving the zero moisture content. T_g versus moisture content data were taken from Izzard *et al.* (1991) and Roos (1993) and were both obtained by dissolving sucrose crystals in water and then rapidly cooling the solution in the DSC pan. The moisture content was determined by weighing the amount of water added to the crystals and therefore included the residual moisture in the moisture content stated. A completely dry amorphous sucrose T_g was obtained by melting and quenching crystalline sucrose in the DSC by Roos (1993). The data from Izzard *et al*. (1991) at a moisture content of 3.4 to 6.5 g/100g dry sucrose were obtained by personal communication (Izzard, J.M.V., Gough, A. and Kalichevsky, M.T.). No details were given about how these samples were prepared. However it is expected that they are likely to be from freeze-dried sucrose solutions, which were further dried over P_2O_5. As a result the low moisture content data from Izzard *et al.* (1991) has been considered to not include the residual moisture in the moisture content value given. Roos and Karel (1991b) left the freeze-

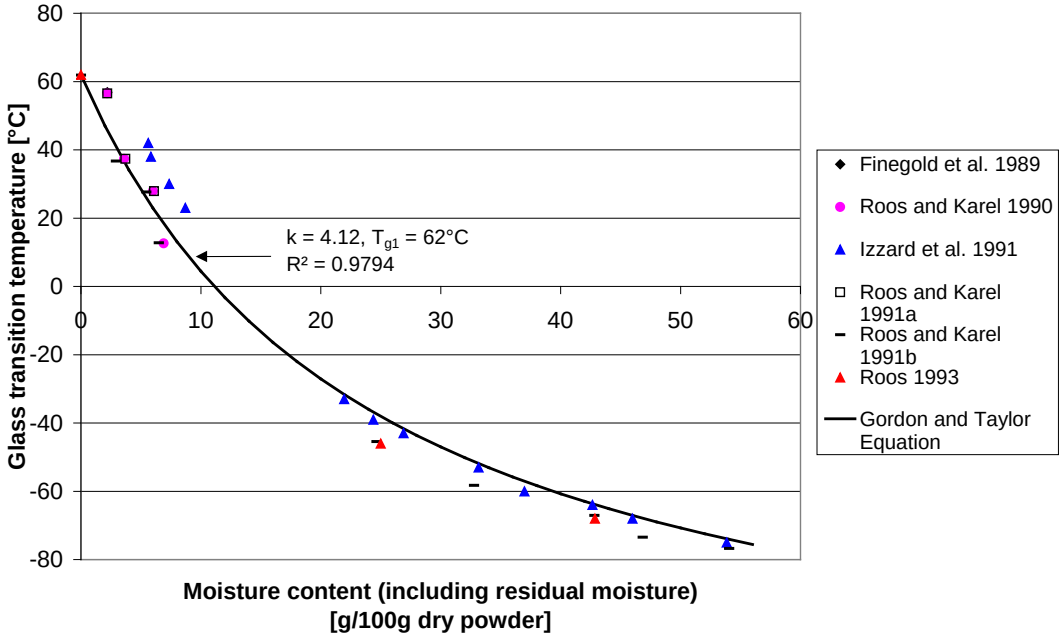

Figure 4.6: T_g versus moisture content profile for amorphous sucrose

dried amorphous sucrose over P_2O_5 for 6 months. It is likely that desiccation over P_2O_5 for such a length of time is likely to have removed the residual moisture giving a completely dry T_g. The further T_g versus moisture content data from Roos and Karel (1991b) were obtained by rehumidification over saturated salt solutions for low moisture content samples and by dissolving sucrose crystals in water for the rest. The freeze dried amorphous sucrose was dried over P_2O_5, therefore the moisture contents obtained by rehumidification over saturated salt solutions are not likely to include residual moisture but those for mixtures prepared by dissolution will. Figure 4.6 shows the T_g versus moisture content data where the moisture content includes the residual moisture. The residual moisture content of 2.2 g/100g dry powder from table 4.1 was added to the moisture content values that were measured from powders where P_2O_5 was used to give a dry powder. The Gordon and Taylor equation was fitted to these data after setting the dry T_g to 62°C, giving *k* and R^2 values of 4.12 and 0.9794 respectively. The Gordon and Taylor equation was also fitted using moisture content data that didn't include the residual moisture. A dry T_g of 56.5°c was used giving a *k* value and R^2 value of 4.51 and 0.9846 respectively.

The isotherm for amorphous sucrose, given in section 3.3.4.2, was used to convert the T_g/moisture content data to T_g/a_w data (figure 4.7). Since P_2O_5 was used to give a water activity of 0, which does not correspond to a zero moisture content, those moisture content values which included the residual moisture content were altered. The residual moisture was subtracted and then the water activity was determined using the isotherm. The combined isotherm and Gordon and Taylor equation (using T_{g1} = 56.5°C and *k* = 4.51 as found previously) was used to predict the T_g versus water activity data giving an R^2 value of 0.9930. The data by Finegold *et al.* (1989), Roos and Karel (1990) and Roos and Karel (1991a) is the original T_g/a_w data reported by the authors. Also included is the T_g/a_w data found by DSC in this work. The data by Finegold *et al.* (1989) (T_g = 56.9°C at $0.0a_w$) is difficult to see in figure 4.7. It can be seen that the T_g/a_w data agrees well with the combined isotherm/Gordon and Taylor equation. A

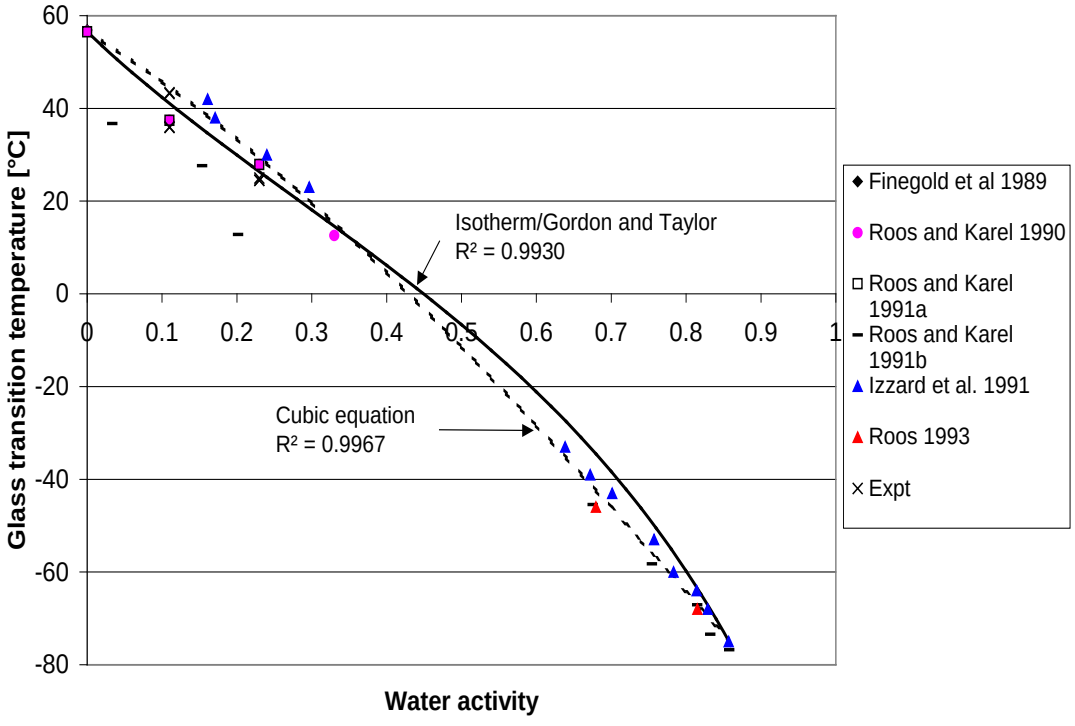

Figure 4.7: T_g versus water activity for amorphous sucrose

cubic equation was fitted to this data giving an R^2 of 0.9971. Although the cubic equation gives a better fit to the data, in terms of the R^2 values, the combined isotherm/Gordon and Taylor equation fits the data better, especially the actual T_g/a_w data, at water activities less than 0.4. Since this equation also has a theoretical basis, it is the better prediction method to use.

4.3.4 Amorphous Fructose

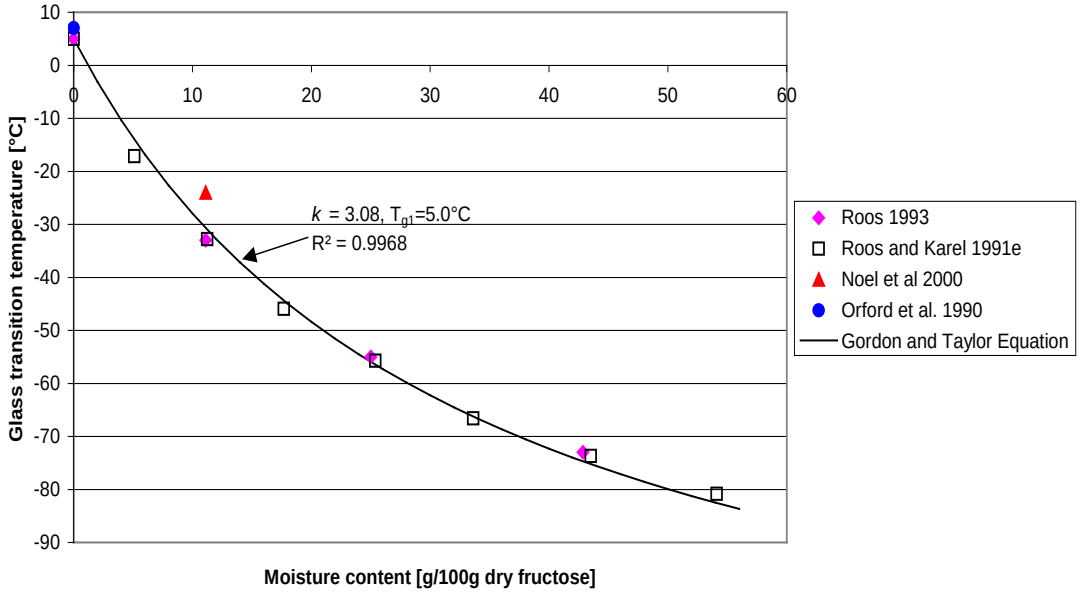

Figure 4.8: T_g versus moisture content profile for amorphous fructose

T_g versus moisture content data were taken from Orford *et al.* (1990), Roos and Karel (1991e), Roos (1993) and Noel *et al.* (2000) and are given in figure 4.8. Disagreements among these data can be explained by the scanning rates used during DSC analysis and the definition of T_g used. Roos and Karel (1991e) and Roos (1993) used a scanning rate of 5°C/min and the onset T_g, where Orford *et al.* (1990) and Noel *et al.* (2000) used a scanning rate of 10°C/min and the midpoint T_g. The data obtained at 10°C/min using the midpoint T_g is consistently above that obtained at 5°C/min using the onset T_g. The Gordon and Taylor equation was fitted to the data obtained using a scanning rate of 5°C/min and the onset T_g (5°C) giving a *k* value of 3.08 and an R^2 of 0.9968. The *k* value compares well with that obtained empirically by Roos and Karel (1991e). It does not compare as well with that obtained by Roos (1993) or those obtained using the ratio of the specific heats (table 4.2).

The isotherm for amorphous fructose, given in section 3.3.5.2, was used to convert the T_g/moisture content data to T_g/a_w data. The T_g versus water activity data are given in figure 4.9. The combined isotherm/Gordon and Taylor equation (with k = 3.08 and a dry T_g of 5.0°C found previously) was used to predict the T_g versus water activity profile (R^2=0.9970). The cubic equation was also used to predict the data, giving an R^2 of 0.9989. Since the difference in fit between the two equations is small and the combined isotherm/Gordon and Taylor equation has a theoretical basis, the combined

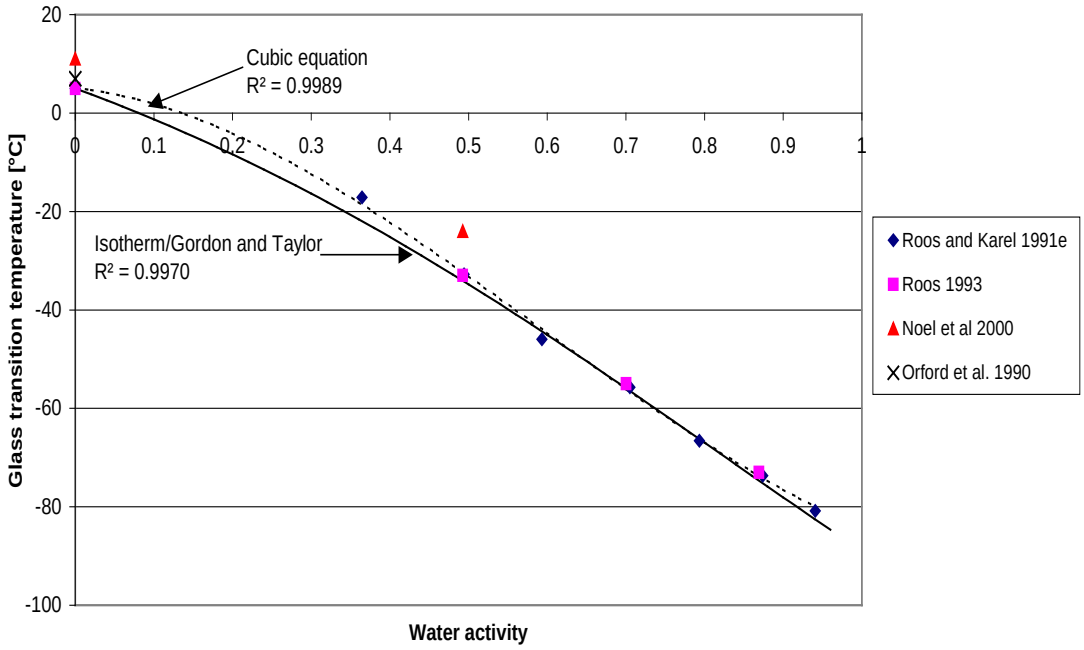

Figure 4.9: T_g versus water activity profile for amorphous fructose

isotherm/Gordon and Taylor equation is the best method for predicting the T_g of amorphous fructose from water activity.

4.3.5 Amorphous Maltose

T_g versus moisture content data were taken from Orford *et al.* (1989), Orford *et al.* (1990), Roos (1993), van den Dries *et al.* (1998) and Noel *et al.* (2000). A dry T_g for amorphous maltose was given by Miller and de Pablo (2000) and T_g/moisture content and T_g/a_w profiles were given by Roos and Karel (1991c,d). A T_g/a_w profile was also

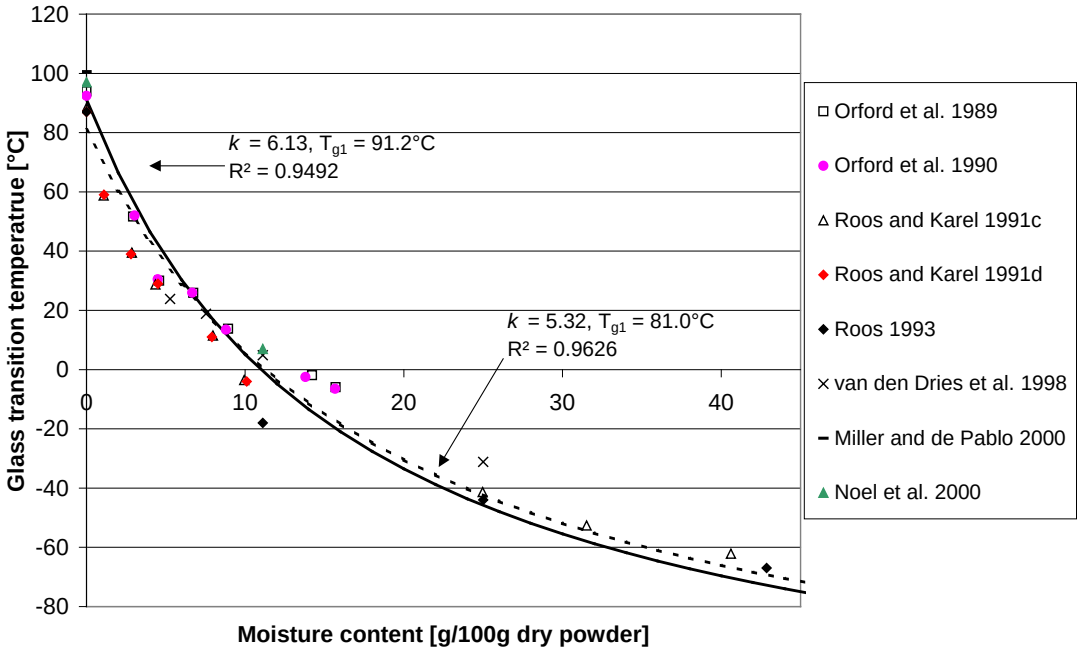

Figure 4.10: T_g versus moisture content profile for amorphous maltose

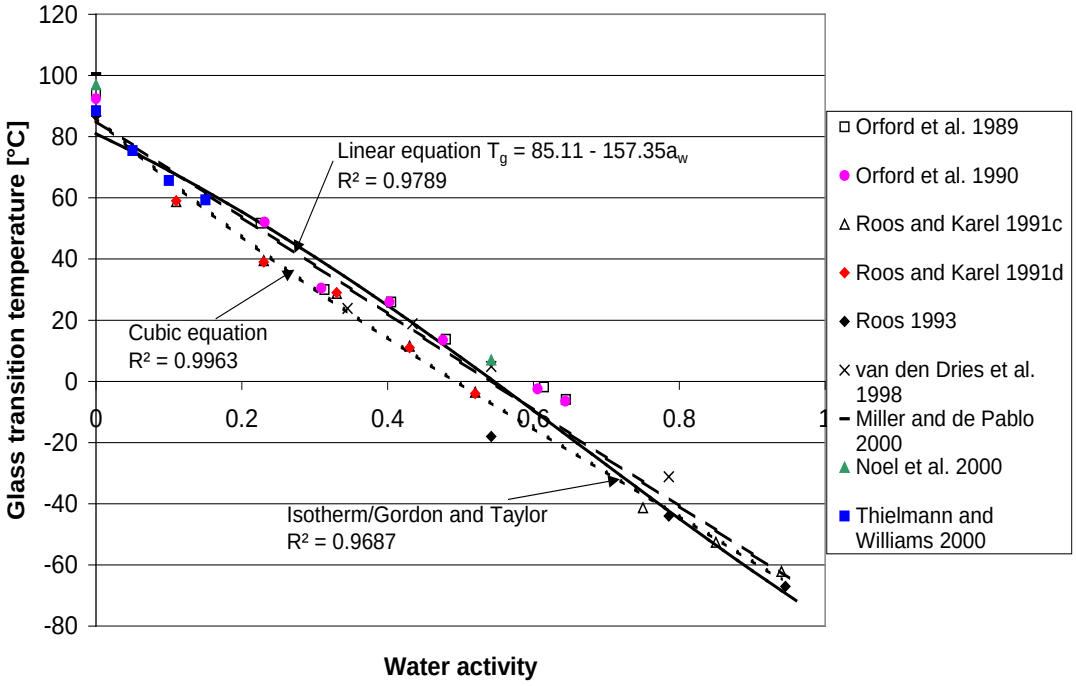

Figure 4.11: T_g versus water activity profile for amorphous maltose

given by Thielmann and Williams (2000). Figure 4.10 shows the T_g versus moisture content profile for amorphous maltose. The moisture content values were used unaltered, i.e. the residual moisture content was not included, as greater variation in the data was observed when the residual moisture was included. This indicates that the average residual moisture from table 4.1 of 2.95g/100g dry maltose may be too high. The Gordon and Taylor equation was fitted to this data. Allowing both the dry T_g and *k* value to alter gave values of 81.0°C and 5.32 for T_{g1} and *k* respectively with an R^2 of 0.9626. This dry T_g value was low compared to those from literature (88.3 to 100.6°C). The Gordon and Taylor equation was also fitted by setting T_{g1} to the average dry T_g value of 91.2°C. The *k* and R^2 value obtained was 6.13 and 0.9492 respectively. From figure 4.10 it can be seen that the Gordon and Taylor prediction where T_g was allowed to vary gives a better fit to the data. It is suggested that the Gordon and Taylor equation with *k* and T_{g1} set at 5.32 and 80.0°C respectively be used to predict the T_g versus moisture content profile for amorphous maltose. However, a dry T_g of 91.2°C should be used at zero water activity as this is the average of the dry T_g values available in literature. These *k* values obtained are comparable to those given in table 4.2.

The isotherm for amorphous maltose given in section 3.3.6.2 was used to convert the T_g/moisture content data to give a T_g versus water activity profile. The data from Roos and Karel (1991c,d) and Thielmann and Williams (2000) is the original water activity data reported by the authors. The T_g versus water activity data is given in figure 4.11. The combined isotherm/Gordon and Taylor equation was used to predict the T_g/a_w data giving an R^2 value of 0.9687. It is noted that it was not refitted to the data. A cubic equation was fitted to the original T_g/a_w data, giving an R^2 value of 0.9963 (for fit to the original data). The profile containing all the data could also be adequately described using a linear model (R^2 = 0.9789). It is noted that the cubic model, which is fitted to the original T_g/a_w data is lower than the predictions made using all the data. This implies that there may be some residual moisture present in some moisture content readings. With this in mind, the cubic equation should be used to predict the T_g/a_w

profile for amorphous maltose (equation 4.4) since it is predicted from the actual water activity.

$$T_g = 86.12 - 212.73a_w + 102.19a_w^2 - 49.66a_w^3 \quad (4.4)$$

4.3.6 Maltodextrin Powders

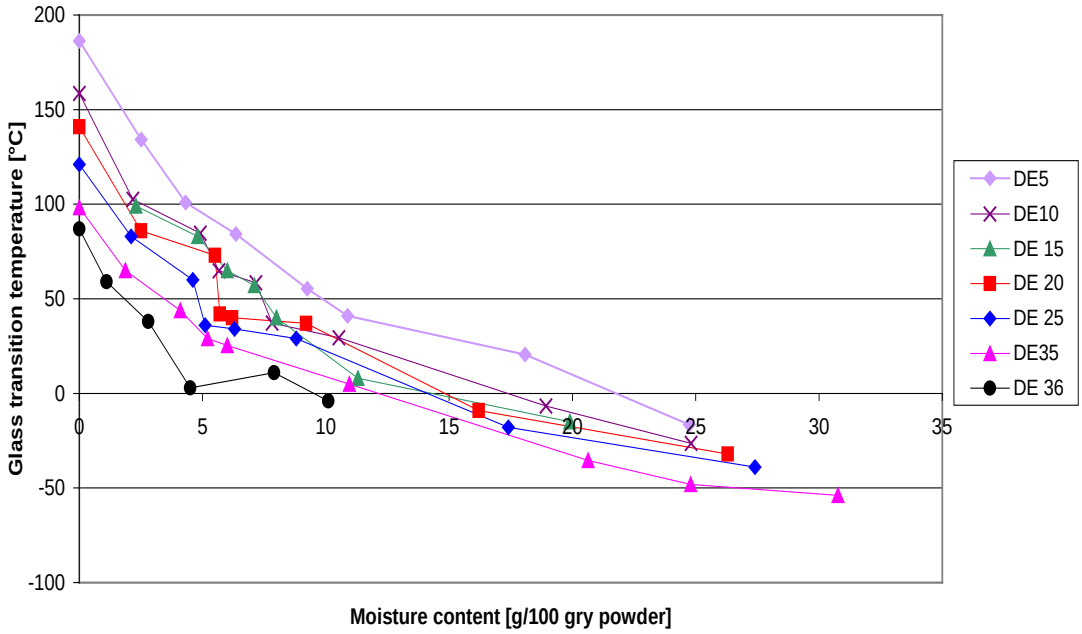

Figure 4.12: T_g versus moisture content profiles for maltodextrin powders [Roos 1991c,d]

T_g versus moisture content and T_g data have been measured by Roos and Karel (1991c,d). Figure 4.12 gives the T_g versus moisture content profile for a number of maltodextrin powders with dextrose equivalent (DE) values from 5 to 36. Figure 4.13 gives the T_g versus water activity data from Roos and Karel (1991c,d) and for two maltodextrin powders used in the New Zealand dairy industry (Star-Dri 240 and Glucidex 29 obtained from Fernz Chemicals, Auckland, New Zealand). It can be seen that the T_g profile increases as the DE decreases, at a given moisture content or water activity. An equation has not been fitted to this data as the T_g depends on the DE for the powder. Therefore any prediction equation would also have to take into account the DE of the powder. It is also unlikely that the T_g can be predicted from the moisture present and DE alone. It is likely that there would be composition differences between different maltodextrin powders, which would also effect the T_g profile.

It can be seen from figure 4.12 that there is irregular overlapping of T_g profiles for maltodextrin powders with close but different DE values. This supports the idea that a generalised prediction equation cannot be made for maltodextrin powders based on moisture and the DE, due to compositional differences between the powders. It is recommended that the T_g profile for a maltodextrin powder be measured and included into the model in chapter 7 if maltodextrin is going to be used in a powder.

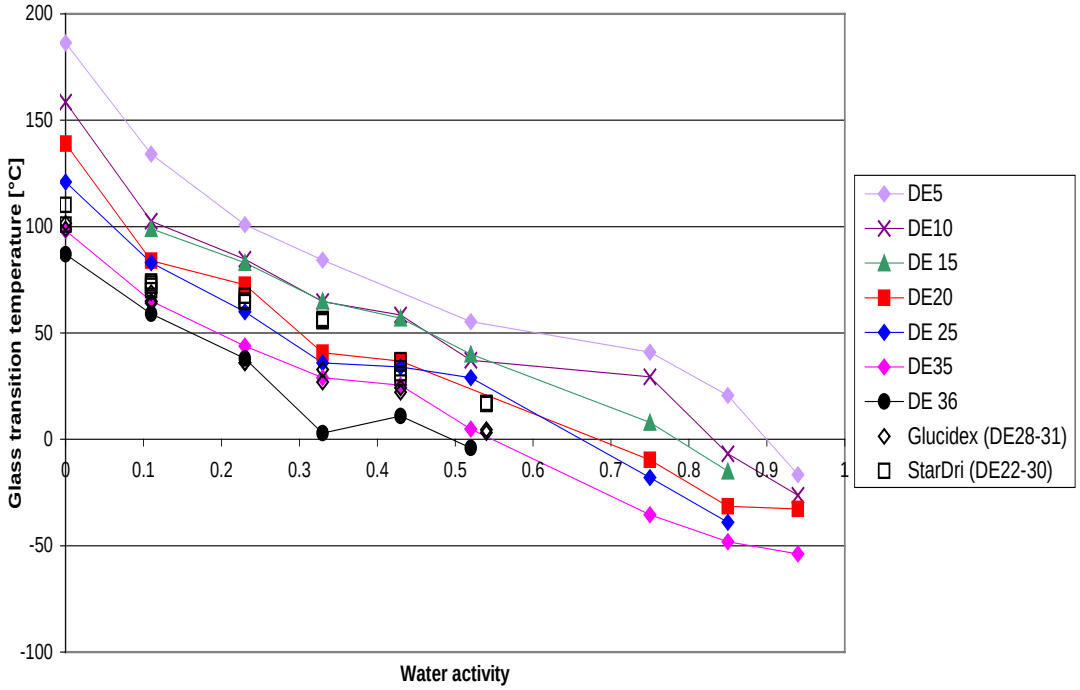

Figure 4.13: T_g versus water activity profiles for maltodextrin powders

4.3.7 Protein

As discussed by Bhandari and Howes (1999), the T_g profile for protein is difficult to measure as, at low water activities, the protein is likely to denature before it passes through its glass transition. This is not of too much concern since the T_g profile for proteins is unlikely to effect the T_g of the amorphous sugar in milk powders [Jouppila and Roos 1994a,b]. This is due to the protein and sugar being an incompatible mixture, as discussed in section 4.2.2. A T_g profile for dairy protein was not measured. A T_g profile for a hydrolysed dairy protein was measured to investigate the effect of hydrolysis on the T_g profile for the resulting powder. The T_g versus water activity profile is given in figure 4.14 for a whey protein concentrate hydrolysate (extensive hydrolysis, 20-30%) powder obtained from Fonterra Research Centre, Palmerston North, New Zealand. It is noted that an attempt was made to measure the T_g profile for the original protein that the hydrolysate was made from. However, no clear glass transitions could be seen on the DSC trace. The hydrolysis of the protein to lower molecular weight proteins dramatically lowers the T_g profile, as has also been discussed by Netto *et al*. (1998). This makes low molecular weight proteins more likely to contribute to sticking and caking problems in dairy powders than non-hydrolysed proteins. At this stage it is unclear whether the hydrolysed proteins form compatible mixtures with the amorphous sugars. This was not investigated further as there are currently no dairy powders made which have hydrolysed proteins added prior to spray drying.

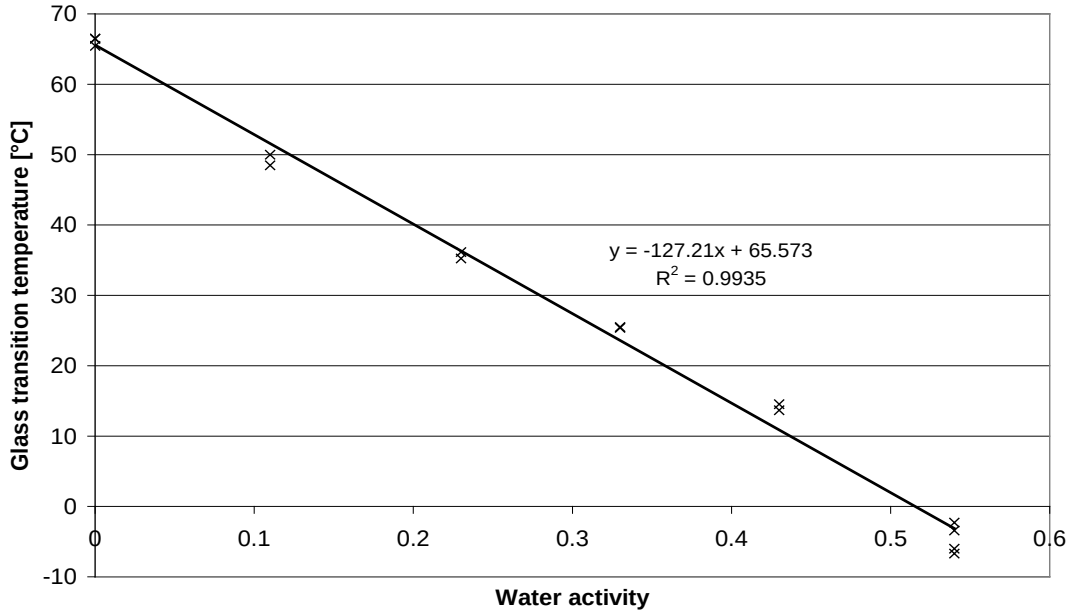

Figure 4.14: T_g versus water activity profile for a hydrolysed whey protein concentrate powder

4.4 PREDICTION OF THE GLASS TRANSITION TEMPERATURE FOR MULTICOMPONENT POWDERS

The easiest way to predict the T_g of a multicomponent powder which contains one amorphous sugar, is from the water activity of the powder and the T_g/water activity profile of the sugar. The glass transition temperature at a certain water activity is constant regardless of the amount of the amorphous sugar or other components present (so long as they do not affect, elevate or depress the T_g of the powder). Taking dairy powders as an example, the T_g at a certain water activity is fairly constant throughout all powders that contain only amorphous lactose, regardless of the amounts of milk fat and protein present. The T_g is not constant at a constant moisture content throughout dairy powders that contain different levels of lactose, protein and milk fat. When the moisture content is given, the T_g can only be estimated through use of an isotherm of the powder, so that the amount of moisture associated with the amorphous sugar can be determined and used to predict the T_g.

If two amorphous sugars are present in a powder then the T_g for the powder will be somewhere between the T_g values of the two amorphous sugars at the given water activity. It is proposed that the T_g can be predicted from the weighted addition of the T_g values of each amorphous sugar at the given water activity (equation 4.5).

$$T_g = \sum_{i=1}^{n} x_i T_{g\,i(a_w)} \tag{4.5}$$

where $T_{gi(aw)}$ = T_g of component *i* at a given water activity
x_i = mass fraction of component *i* (as a fraction of the total amorphous sugars present)

This section compares predictions made using this method (equation 4.5) with experimental data and predictions made using the modified Couchman and Karasz equation (equation 4.3). In order to use the expanded Couchman and Karasz equation, values for the dry T_g and the change in specific heat at the glass transition (Δc_p) for the amorphous sugars are required. Table 4.3 gives the dry T_g values for the amorphous sugars found in the work described in section 4.3 and the Δc_p for these sugars. The Δc_p values were taken from table 4.2. For amorphous glucose, the *k* value calculated by $\Delta c_{p2}/\Delta c_{p1}$ obtained using Δc_{p1} = 0.54 J/g°C, from Zhang and Zografi (2000), gives a *k* values (3.59) closest to that obtained empirically in section 4.3.1. Therefore, the Δc_p value from Zhang and Zografi (2000) will be used in the expanded Couchman and Karasz equation. For amorphous galactose, using the Δc_p = 0.50 J/g°C from Roos (1993), to calculate *k* (3.88), gives the closest agreement to the empirical *k* value of 3.58. The closest value for *k*, calculated from the ratios of specific heat for amorphous sucrose, is 3.23 obtained using Δc_p = 0.60 J/g°C from Roos and Karel (1991b) and Roos (1993). The empirical value was found to be 4.12 in section 4.3.3. The value of Δc_p = 0.75 J/g°C for amorphous fructose from Roos and Karel (1991e) and Roos (1993), gives a predicted *k* value (2.59) closest to the empirical *k* value (3.08) found in section 4.3.4. Therefore, this Δc_p value is to be used in the expanded Couchman and Karasz equation for amorphous fructose. Finally the *k* values predicted by $\Delta c_{p2}/\Delta c_{p1}$ for amorphous maltose (2.46 and 3.18) do not compare well with that obtained empirically (5.32). Since the Δc_p value from Roos and Karel (1991c) and Roos (1993) of 0.61 J/g°C gives the *k* value (3.18) closest to that obtained empirically, Δc_p of 0.61 J/g°C will be used in the expanded Couchman and Karasz equation.

A Δc_p value for amorphous lactose could not be found in the literature. Only empirical *k* values, as listed in table 4.2, were found. A value for Δc_{p1} can be estimated from the empirical *k* value by using the relationship $k=\Delta c_{p2}/\Delta c_{p1}$ and the Δc_p value for water. Since the work by Brooks (2000) is the most recent and also looked at the effect of residual moisture on the T_g, the *k* value obtained by Brooks (2000) was used to estimate a Δc_p value for amorphous lactose. This was calculated to be 0.28 J/g°C using the *k* value of 6.9. It is noted that this *k* value is very close to the *k* values given by Roos and Karel (1991e), Roos (1993) and Jouppila and Roos (1994b). The Δc_p value estimated for amorphous lactose also agrees well with the Δc_p values for the glass transition of amorphous lactose in skim milk powder measured in this work. The Δc_p values obtained were 0.29 and 0.34 from DSC curves for skim milk powder where there were no enthalpy relaxation peaks present.

Table 4.3: Dry T_g and the change of the specific heat at the glass transition region (Δc_p)

Component	T_g (dry) [°C]	Δc_p [J/g°C]
Lactose	101[1]	0.28[*]
Glucose	33.7	0.54[3]
Galactose	30.0	0.50[4]
Sucrose	62.0	0.60[4,5]
Fructose	5.0	0.75[4,6]
Maltose	91.2	0.61[3,7]
Water	-135[2]	1.94[8]

[1]Brooks (2000), [2]Johari *et al.* (1987), [3]Zhang and Zografi (2000), [4]Roos (1993), [5]Roos and Karel (1991b), [6]Roos and Karel (1991e), [7]Roos and Karel (1991c), [8]Sugisaki *et al.* (1968).
[*]Estimated from empirical *k* value of 6.9 from Brooks (2000).

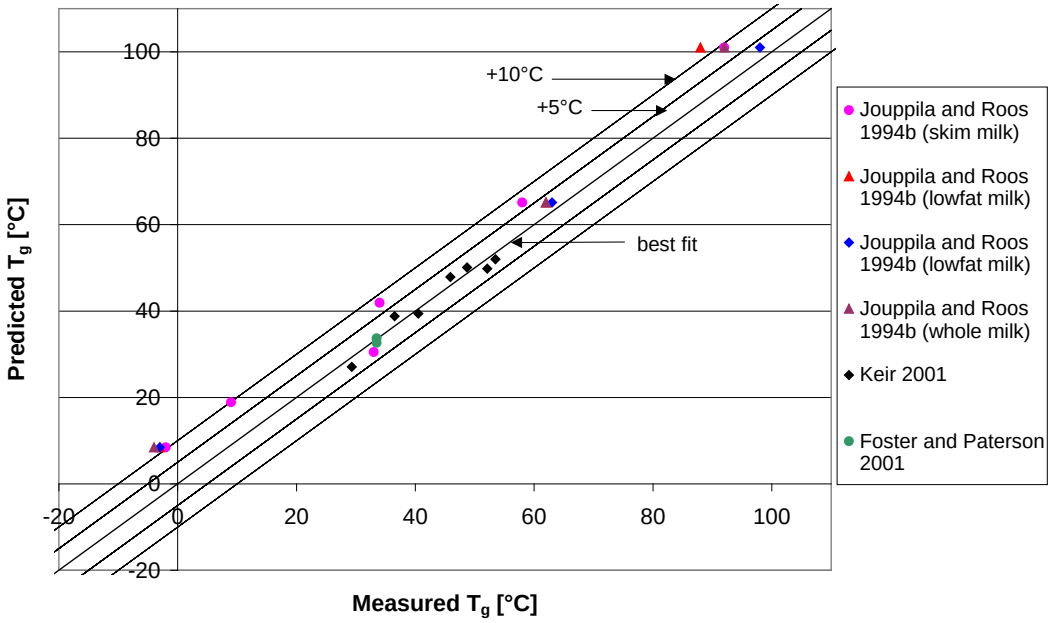

Figure 4.15: Comparison of predicted and measured T_g values for amorphous lactose, protein and fat powders using equation 4.5

Figures 4.15 and 4.16 compares measured and predicted T_g values (using equations 4.5 and 4.3 respectively) for dairy powders containing only amorphous lactose as the amorphous sugar. The data have been taken from Jouppila and Roos (1994b), Keir (2001) and Foster and Paterson (2001). It can be seen that the predicted T_g is very close to the measured T_g when using equation 4.5, especially for data measured by Keir (2001) and Foster and Paterson (2001). There is more deviation with the data from Jouppila and Roos (1994b) although the fit is still good. It is noted that the predicted T_g is higher than that measured indicating that the protein does not elevate the measured T_g of the powder. If protein did elevate the T_g, then it would be expected that the measured

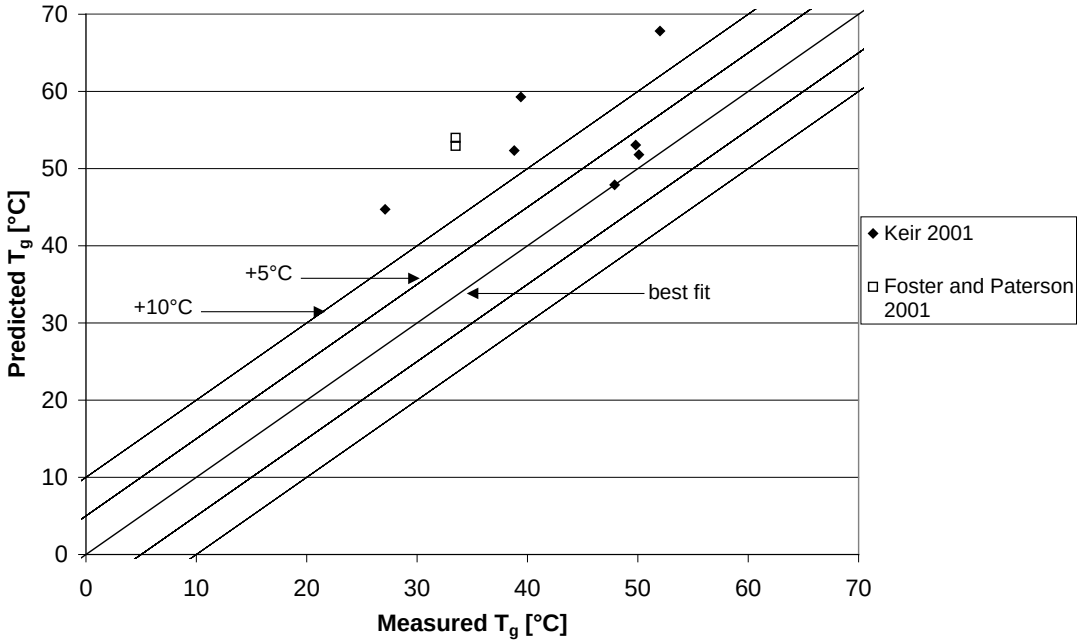

Figure 4.16: Comparison of predicted and measured Tg values for amorphous lactose, protein and fat powders using equation 4.3

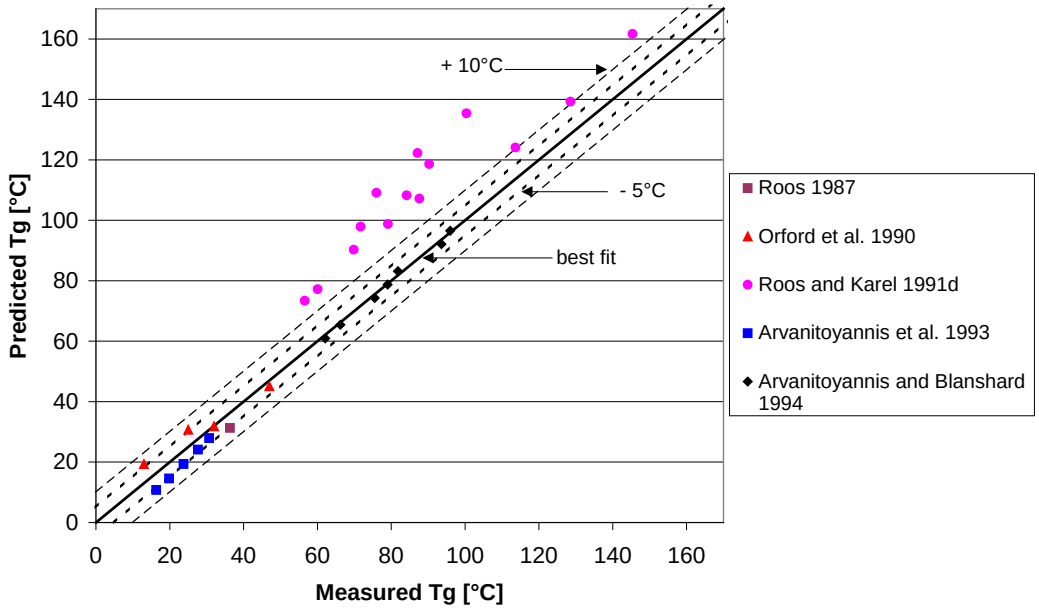

Figure 4.17: Comparison of predicted versus measured T_g values for dry amorphous sugar mixtures

T_g would be higher than that predicted. The expanded Couchman and Karasz equation was also used to predict the T_g of the dairy powders. It can be seen in figure 4.16, that the predicted T_g, using the expanded Couchman and Karasz equation is much higher than that predicted using equation 4.5 (figure 4.15) and does not give a very good fit to the measured T_g data. It is noted that the expanded Couchman and Karasz equation could not be used to predict the data of Jouppila and Roos (1994b) as the compositions of the dairy powders were not given.

Equation 4.5 was also used to predict the T_g of dry amorphous sugar mixtures. Figure 4.17 compares measured and predicted T_g values for dry amorphous mixtures of strawberries (fructose/sucrose/glucose) [Roos 1987], fructose/glucose, glucose/galactose, sucrose/glucose, sucrose/fructose [Orford *et al.* 1990], maltodextrin/sucrose [Roos and Karel 1991d], glucose/fructose [Arvanitoyannis *et al.* 1993] and sucrose/lactose [Arvanitoyannis and Blanshard 1994]. It can be seen that the simple mixing rule works well using the dry T_g values for those sugars. The data of Roos and Karel (1991d) were much lower than those predicted. It is possible that there was incomplete mixing between the maltodextrin and sucrose, meaning that the T_g profile could have been only slightly increased by the presence of the maltodextrin. It may be that the maltodextrin could have also retained its own T_g, which may or may not have been slightly depressed by the presence of the sucrose. It is thought that the later is more likely to be the cause of the lack of fit of the predictive equation (equation 4.5). Again, the T_g has been predicted using the expanded Couchman and Karasz equation and these predictions are shown in figure 4.18. Overall, equation 4.5 gives a slightly better fit than the expanded Couchman and Karasz equation, although in most cases there is little difference between the predictions using equations 4.3 and 4.5 (referring to the data by Roos (1987), Orford *et al.* (1990) and Arvanitoyannis *et al.* (1993)).

Equation 4.3 and 4.5 were further used to predict the T_g of amorphous sugar mixtures where moisture was also present. This data includes mixtures of water with glucose/fructose [Arvanitoyannis *et al.* 1993], freeze-dried strawberries composed of

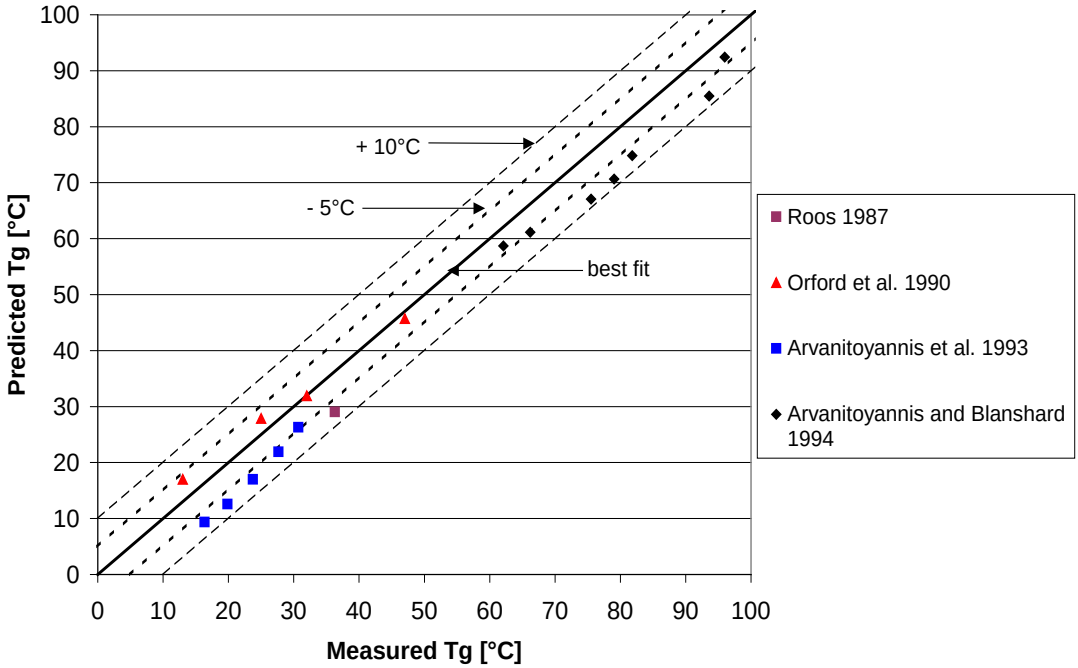

Figure 4.18: Comparison of predicted versus measured T_g values for dry amorphous sugar mixtures using equation 4.3

glucose/sucrose/fructose [Roos 1987], sucrose/fructose [Roos and Karel 1991a] and glucose/sucrose measured in this work. It is noted that the T_g data by Arvanitoyannis *et al.* (1993) was given versus the sugar content. For equation 4.5 to be used, this required that the water activity for the powder at each moisture content be predicted. The simple additive approach for predicting isotherms (equation 3.13) was used to do this by solving for the water activity so that the given moisture content was obtained. The predicted water activity was then used to predict the T_g for each sugar by using the

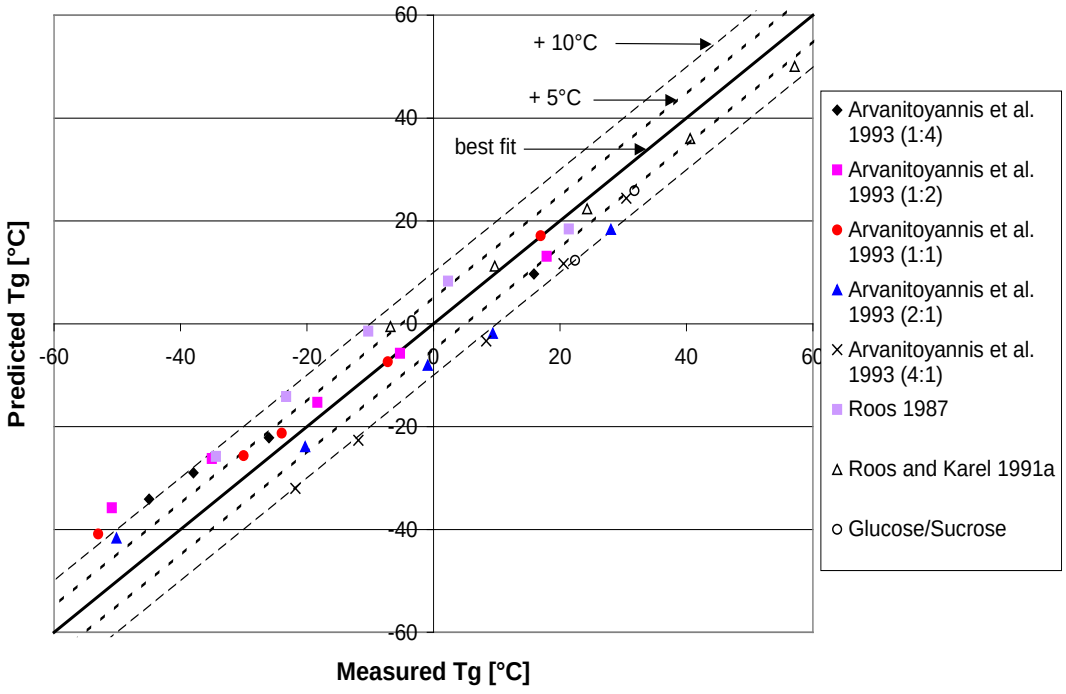

Figure 4.19: Comparison of predicted versus measured T_g values for three component powders, using equation 4.5

combined isotherm/Gordon and Taylor equations. The overall T_g for the powder was then predicted using equation 4.5, i.e. by the weighted addition of the T_g values obtained for each sugar at the predicted water activity. The expanded Couchman and Karasz equation did not require the water activity to be predicted. This prediction could simply be made using the information given. When predicting the T_g, using equation 4.5, for the powders from Roos (1987) and Roos and Karel (1991a) (where both the water activity and moisture content was given), the T_g was predicted for each sugar from the water activity by using the combined isotherm/Gordon and Taylor equation. The T_g of the mixture were then determined by the weighted addition of the components T_g values (equation 4.5).

Figure 4.19 shows the comparison of the predicted and measured T_g values using equation 4.5. Figure 4.20 shows the comparison when the expanded Couchman and Karasz equation has been used. It can be seen that there is a slightly better fit, within ±10°C, when using equation 4.5 compared to the expanded Couchman and Karasz equation. In the light of the results for predicting the T_g of amorphous sugar mixtures (figures 4.19 and 4.20) with water and the T_g profile for dairy powders (4.15 and 4.16), the equation for predicting the T_g proposed in this work (equation 4.5) gives better predictions of the T_g for multicomponent powders.

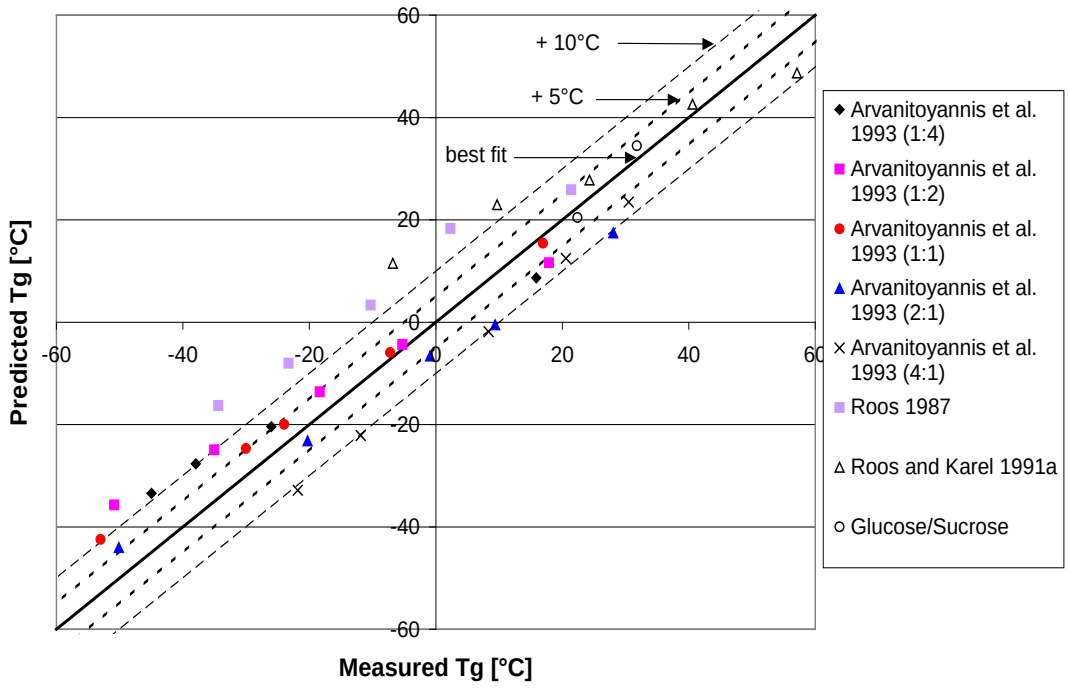

Figure 4.20: Comparison of predicted versus measured T_g values for three component powders, using the extended Couchman and Karasz equation (equation 4.3)

4.5 CLOSURE

Glass transition temperature profiles for amorphous sugars have been determined and equations for their prediction given. The T_g of an amorphous sugar, in a multicomponent powder, can be predicted from the water activity of the powder through the use of the combined isotherm/Gordon and Taylor equation (with appropriate dry T_g and *k* values). In the case of amorphous lactose and maltose, the T_g can be predicted from the water activity by a cubic relationship. The T_g is more easily predicted from the water activity rather than the moisture content of the powder, as the moisture content also includes moisture associated with proteins, which will be present in dairy powders, which do not effect the T_g of the powder. A method for predicting the T_g of a multicomponent powder was proposed, which predicts the T_g based on the weighted addition of the T_g values for the amorphous sugars present, at the powder's given water activity. This method was compared with the Couchman and Karasz equation and was found to give an overall better fit, especially for the prediction of the T_g of amorphous lactose in dairy powders. It is recommended that the proposed method be used for the prediction of T_g in multicomponent powders. The proposed T_g prediction method has been used further in chapter 7.

The T_g versus water activity profiles for some amorphous sugars have been used in chapter 5 for relating the $T\text{-}T_g$ to the rate of sticking experienced with these sugars.

CHAPTER 5

AMORPHOUS SUGAR STICKING MECHANISM

5.1 INTRODUCTION

The role of amorphous lactose in causing sticking and caking problems in dairy powders was discussed in chapter 2. This amorphous sugar sticking mechanism is not limited to amorphous lactose and is likely to occur for all amorphous sugars. Since the dairy industry has moved towards the production of speciality powders, it is now not uncommon for dairy powders to contain other sugars. If these sugars are added as a wet blend (i.e. prior to spray drying) then the sugar will be in the amorphous form in the final powder. The presence of a sugar combined with the lactose already present, will affect the T_g profile for the powder and therefore the sticking and caking characteristics of the powder, as discussed in chapter 4. Currently, sucrose is added to some powders and a number of powders have had part of the lactose component hydrolysed. This necessitates the investigation of the sticking behaviour of amorphous sucrose, glucose and galactose (the later two sugars being the products of lactose hydrolysis). Fructose is also added to a few powders but typically as a dry blend and currently maltose is not added to any powders. However, the sticking behaviour of amorphous fructose and maltose will also be studied to cover the possibility that it will become more common to add these sugars to dairy powders as a wet blend in the future.

This chapter will discuss the amorphous sugar sticking and caking mechanism in more detail and investigate the sticking characteristics of amorphous sucrose, maltose, glucose, galactose and fructose. The overall aims of this chapter are to determine:

1. Whether the rate of sticking is proportional to the $T-T_g$ of the powder
2. What $T-T_g$ is required to give a rate of sticking that would be unacceptable during spray drying

Before these matters can be investigated, the mechanism for amorphous sugar sticking needs to be described in more detail.

5.2 AMORPHOUS SUGAR STICKING MECHANISM

The mechanism for amorphous lactose sticking and caking was described in section 2.2.2.3. The mechanism for sticking and caking of other amorphous sugars is thought to be the same, therefore, the mechanism described in section 2.2.2.3 can be generalised to cover amorphous sugars rather than just amorphous lactose. Sticking and caking problems are caused by the amorphous sugar being exposed to conditions that exceed the T_g of the sugar, thereby reducing the viscosity of the amorphous sugar. This results in the formation of liquid bridges, which can later solidify, giving a caked powder. Figure 5.1 below is identical to figure 2.5, which describes amorphous lactose sticking and caking, except that it has been modified so that it covers amorphous sugars in general.

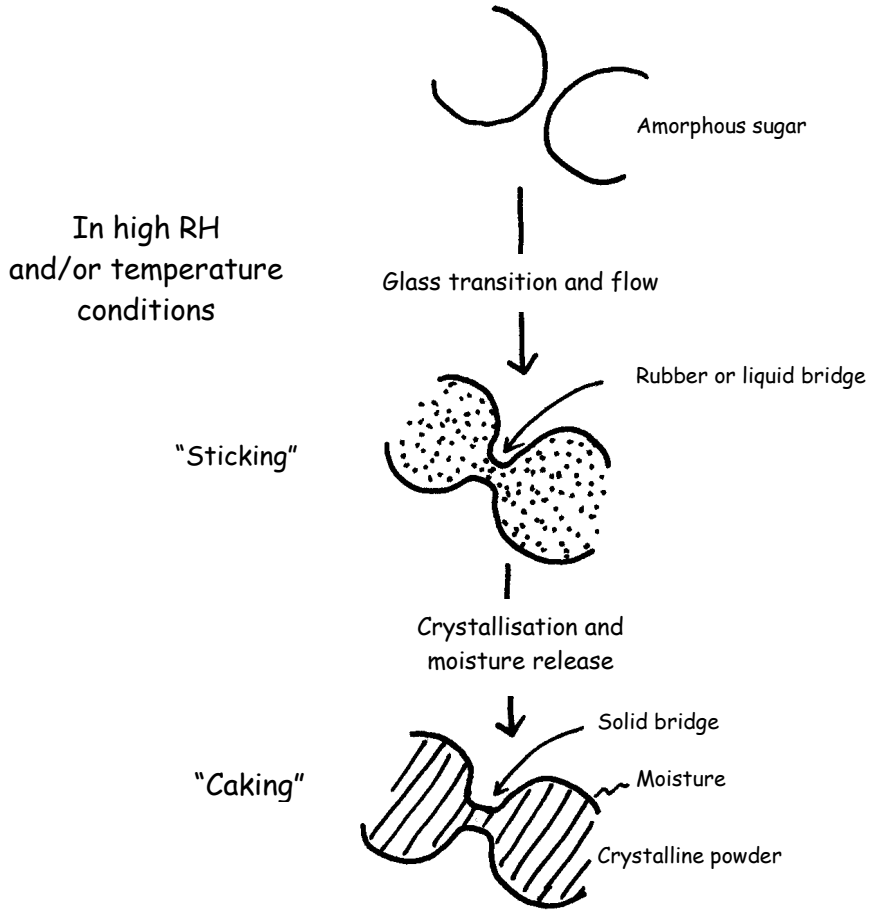

Figure 5.1: Amorphous sugar caking mechanism

A number of equations have been put forward to explain/describe liquid bridging. Liquid bridging can be considered analogous to the fusion that occurs during sintering [Downton *et al.* 1982]. Frenkel's (1945) equation has been shown to be valid for describing the fusion process of spherical polymer beads of uniform size [Rosenzweig and Narkis 1980, Rosenzweig and Narkis 1981 – both cited in Wallack and King 1988]. Frenkel's equation (5.1) relates the interparticle bridge radius with the time for coalescence of particles due to surface energy driven viscous flow.

$$r_b^{\,2} = \frac{3R_p \sigma t}{2\mu} \tag{5.1}$$

where r_b and R_p are the bridge and particle radii respectively, σ the surface tension of the bridge material, t the exposure or contact time and μ the viscosity of the bridge material.

Peleg (1993a) pointed out that the shortfalls of this model in real food powders was due to the following factors:

1. Particle size is rarely uniform
2. Particle shape is almost never spherical
3. Viscosity of bridge material cannot be expected to be always Newtonian.

However, Peleg (1993a) also stated that although Frenkel's equation may not give an accurate description of the fusion process during caking, it does show its progress and an approximation can be made of the rate, if an estimation of the surface tension and viscosity can be made.

Downton *et al.* (1982) also presented an equation to describe viscous flow driven by surface energy (equation 5.2):

$$\mu = \frac{k\sigma t}{KD} \tag{5.2}$$

where k is a dimensionless proportionality constant equal to 1, σ the surface tension, t the contact time, μ the viscosity and KD the distance over which flow must occur.

Downton *et al.* (1982) used this equation to predict the critical viscosity required for sticking to occur. The critical viscosity is the viscosity required for sticking to occur during a short contact time (e.g. 1-10s) and is predicted from equation 5.2. It was found to be in the range of 10^6-10^8 Pa.s. The sticky point test of Lazar *et al.* (1956) was used to determine the sticky point temperature over a range of moisture contents for a sucrose/fructose mixture. The viscosity at the sticky point temperature were measured and all points fell within 0.3×10^7 to 4.0×10^7 Pa.s. It was concluded that since the measured critical viscosities fell within the range predicted by the model, that the model gave a good description of the stickiness phenomenon and was based upon the correct interpretation of the stickiness mechanism.

Equation 5.2 differs from the Frenkel model by the removal of the factor 3/2 and the removal of r_b^2/R_p^2. Both equations indicate that greater surface tension or contact times increases the tendency towards sticking, while greater viscosity or greater distances over which flow must occur (KD or initial particle radius, R_p) decrease the tendency towards sticking. Wallack and King (1988) used Frenkel's model to predict the critical viscosity for sticking in a short period of time. This was for a maltodextrin/sucrose/fructose mixture and coffee powder and the critical viscosities were found to be 10^6-10^8 Pa.s and 10^5-10^7 Pa.s respectively. Using similar experiments to Downton *et al.* (1982), the critical viscosities were found to fall within the range predicted by the Frenkel model. The values for surface tension and contact time used for predicting the critical viscosity range from equations 5.1 and 5.2 were fairly similar. An estimate of the interstitial concentrate surface tension of 70 mN/m and a contact time of 1-10s was used in both equations for determining stickiness. Downton *et al.* (1982) assumed that k=1, an average particle size diameter of 7 μm and K (the fraction of the particle diameter required as bridge width, $2r_b$, for a sufficiently strong bridge) was 0.01-0.001. Wallack and King (1988) measured the particle size of the maltodextrin/sucrose/fructose mixture and coffee extract powder and used those values in the Frenkel equation.

The mechanism for sticking described depends on a decrease in the viscosity of the material. Specifically it is the decrease in the system viscosity at temperatures above the T_g that is the principle factor that makes many chemical and physical processes possible to occur in other than extremely long times [Sun 1997]. It is therefore desirable to know or be able to predict the viscosity of the amorphous sugars as a function of temperature. A typical method for measuring viscosity is the falling ball method as used by Downton *et al.* (1982) and Wallack and King (1988). Williams *et al.*

(1955) proposed the Williams-Landel-Ferry (WLF) equation (equation 5.3) to relate the relaxation time of mechanical properties to the temperature above the glass transition temperature. Viscosity is a property governed by the relaxation of an amorphous structure, therefore equation 5.3 can be used to relate the viscosity of an amorphous material to the temperature above the glass transition temperature.

$$\log \frac{\mu}{\mu_g} = \frac{-C_1\left(\mathrm{T}-\mathrm{T}_g\right)}{C_2+\left(\mathrm{T}-\mathrm{T}_g\right)} \tag{5.3}$$

Williams *et al.* (1955) reported the constants C_1 and C_2 to be applicable for many materials with values of 17.44 and 51.6K respectively. Soesanto and Williams (1981) found these constants to be adequate for describing the viscosity of fructose/sucrose solutions. Roos and Karel (1991c) found the WLF equation, with the use of the universal constants, to describe the temperature dependence of the viscosity of sucrose solutions above T_g. This was done using the viscosity data of Bellows and King (1973). Aguilera *et al.* (1993) used the WLF equation, with the universal constants, to predict the viscosity of a fish protein hydrolysate matrix at the onset of collapse. A viscosity of 10^5 to 10^7 Pa.s was obtained, which agrees well with the range for stickiness of maltodextrin/sucrose/fructose and coffee powders as predicted by Wallack and King (1988).

The use of the universal constants has been criticised and it has been suggested that they are only used if there is not sufficient data available for calculating the constants [Peleg 1992]. Peleg (1992) found C_1 and C_2 values from the literature ranging from 13.7 to 34 and 24 to 80K respectively. Angell *et al.* (1994) stated that C_1 could be a universal constant with a value of 16 but C_2 is system dependent and should be determined for the system in question. Levi and Karel (1995) used the WLF equation to predict the relaxation time for collapse in a maltodextrin powder at 2% and 5% moisture. The different moisture contents required different values for the constants C_1 and C_2. In the case of 2% moisture, the values for C_1 and C_2 were 17.23 and 50.7°C respectively. For 5% moisture they were 9.68 and 37.1°C respectively. In both cases a very good fit was obtained and the R^2 value was 0.95. The WLF equation can also be used with a temperature other than the T_g as the reference temperature. The values for C_1 and C_2 obtained using a different reference temperature can then be adjusted to give the values for C_1 and C_2 for T_g used as the reference temperature. Details of these equations are given in Ferry (1970), Peleg (1992) and Levi and Karel (1995). From the above discussion, it is clear that these "universal" constants should only be used when there is not enough information available for them to be calculated. The WLF equation should be used allowing the values for C_1 and C_2 to change.

A number of researchers have measured the sticky point of powders containing amorphous sugars. This is generally given as sticky point temperature versus moisture content curve and therefore has not been analysed with respect to the T_g of the powder. Lazar *et al.* (1956) developed a method for determining the sticky point of powders. This involves placing a test tube containing a sample at a given moisture content into a water bath. The temperature of the bath is then increased until such a temperature (sticky point temperature) that the force required to turn a stirrer, placed in the powder bed, increases sharply. This method was used to measure the sticky point of spray-dried tomato powders at different moisture contents. Downton *et al.* (1982) used this method with a heating rate of 1°C every 3 minutes to find the sticky point curve for a

sucrose/fructose (7:1) powder. Roos and Karel (1991a) measured the T_g profile for a sucrose/fructose (7:1) powder and compared it with the sticky point curve of Downton *et al.* (1982). The sticky point was very close to the end temperature of the glass transition and was between 10 and 20°C above the onset glass transition temperature. This indicates that instantaneous sticking occurs at a fairly constant $T-T_g$, which will probably be dependent on the powder. It is noted that sticking can occur at a lower $T-T_g$, but it will take longer for a given level of sticking to occur. Therefore, when considering the storage of powders, it would be unwise to store a powder above the T_g of that powder at a particular a_w/moisture content. Chuy and Labuza (1994) measured the T_g, surface caking temperature and advanced caking temperature, which is the same as the sticky point of Lazar *et al.* (1956), for a number of food powders and a maltodextrin powder. The surface caking temperature is the temperature at which the powder, which is placed in ampules, fails to separate into finite particles after shaking and tapping against a hard surface. The surface caking temperature and advanced caking temperature for the maltodextrin powder (DE 10) was found to occur at 13 to 30 and 25 to 37.5°C above the T_g respectively. Excluding one of the powders due to lack of confidence in the T_g profile measured, the surface caking and advanced caking temperatures ranged from 22 to 44°C and 22 to 41°C above T_g.

Sun (1997) used a lot of literature data and compared the temperature for structural collapse, DSC measured glass softening and sugar recrystallisation with the T_g for the sugar. Each of these physical state changes occurred at a fairly constant $T-T_g$, which also relates to a fairly constant viscosity range. The glass softening point is associated with structural deformation or collapse during freeze-drying. The glass softening point was found to occur at 16.1°C above T_g. Structural collapse was found to occur, on average, at 12.1°C above T_g. It is thought that the glass softening point and structural collapse temperatures are measuring the same thing and that the difference in temperature is just due to the different methods for determining them. Spontaneous sugar recrystallisation for lactose was found to occur at 50.3°C above T_g and for sucrose it was found to occur at 43.5°C above T_g. Using the WLF equation, the bulk viscosity at which these changes occurred was estimated. The bulk viscosity for structural collapse and glass softening were estimated to be of the order of 10^{8-11} Pa s and 10^{7-10} Pa s respectively. These agree well with the data of Bellows and King (1973). Spontaneous carbohydrate crystallisation was predicted to occur when the viscosity of the amorphous sugar was of the order of 10^{3-6} Pa s. This work has shown that these physical changes depend more on the T_g of the system and less on the type of sugar. The changes are also shown to occur instantaneously over a certain $T-T_g$ and therefore at a constant viscosity range. It is noted that this work used transition temperatures that were measured using scanning rates of 10 to 20°C/min and therefore, the actual transition temperatures are likely to be significantly less than those used. Therefore, the transition temperatures and derived viscosities cannot be taken as absolute.

5.3 AMORPHOUS SUGAR STICKING EXPERIMENTS

5.3.1 Objective

This work was carried out to determine whether the rate of sticking and caking that occurred in sugars, other than lactose, followed the $T-T_g$ for the powder and not the individual temperature and relative humidity combinations used to establish a given $T-T_g$. This work was also carried out to determine what $T-T_g$ is required for sticking and caking to occur within the time frame associated with spray drying. This information can then be used in the model to determine what $T-T_g$ it is appropriate to operate under during spray drying.

5.3.2 Materials

Edible grade sucrose (New Zealand Sugar Company Limited, Auckland, New Zealand), grade I maltose monohydrate (Sigma Chemical Company, St Louis, MO), USP grade α-lactose monohydrate (The Lactose Company of New Zealand, Hawera, New Zealand), analytical grade D(+) glucose (BDH Laboratory Supplies, England) and D(+) galactose (UNIVAR, Asia Pacific Specialty Chemicals Limited, Australia) and general purpose reagent D(-) fructose (BDH Laboratory Supplies, England) were used for all experiments. Approximately 20% solutions were made up for each powder and frozen at –18°C for at least 20 hours and then placed in a –70°C freezer overnight. The solutions were frozen at –18°C so that larger ice crystals would form which would later aid the freeze drying process. The solutions were left for around 20 hours to allow enough time for all freezable water to freeze. Placing the frozen samples into a -70°C freezer then completed any freezing that had not occurred and also reduced the temperature of the sample so that no thawing occurring when transferring the samples from the freezer to the freeze dryer. The samples were placed into the freeze dryer with a plate temperature of –10°C. The plate temperature was then increased by 10°C every 24 hours and the samples were removed from the freeze dryer once they had been at 20°C for at least 24 hours. Ramping the temperature in such a way increased the rate of drying but also prevented retrograde collapse (i.e. collapse of the freeze-dried matrix during warming [MacKenzie 1975]).

Due to collapse problems associated with freeze drying glucose, galactose and fructose, these amorphous powders were made by stabilising the lower molecular weight sugar with lactose. Solutions of lactose and the lower molecular weight sugar were made in the proportion of (lactose:other sugar) 80:20 for glucose and galactose and 90:10 for fructose. This elevated the T_g profile for the powder, therefore making it easier to freeze dry and also allowing a larger range of relative humidity and temperature conditions to be tested. The resulting powders were easier to test given the existing rig set-up where temperatures less than ambient could not be achieved. Given the dry T_g values for amorphous glucose, galactose and fructose, temperatures less than ambient conditions would need to be used for stickiness trials. The freeze-dried two component powders were then examined under polarising microscope to determine whether any crystals were present. Crystals were seen in all mixture powders (figure 5.2), therefore making these powders unusable for predicting T_g profiles, as it was unknown whether crystals of both sugars were present. X-ray diffraction was used in an attempt to

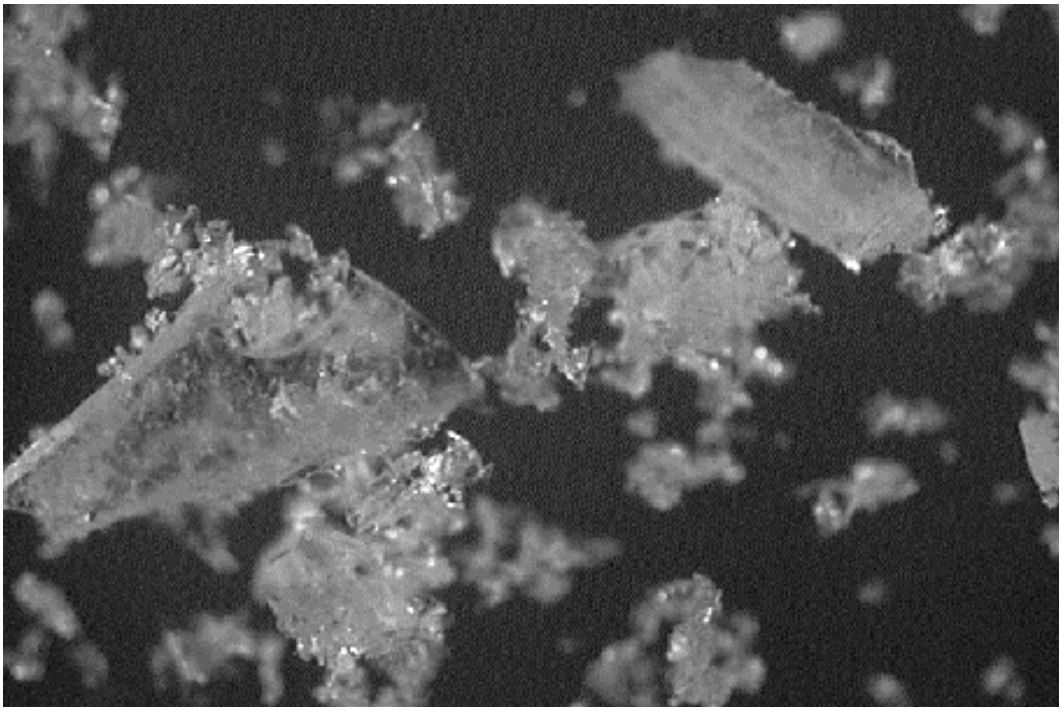

Figure 5.2: Polarising microscope image for an amorphous lactose and glucose mixture

determine what crystals were present, i.e. to answer whether it was just the lower molecular weight sugar crystallising out or whether both types of sugar crystals were present. Crystals were not noticeable when using X-ray diffraction. This does not imply that they were not present, just that the level was below the detectable limit of the X-ray diffraction apparatus (0.1-1%) or that the patterns for the crystals could not be seen as they were hidden by the curve for the amorphous material [Whitten 2002].

5.3.3 Method

The following section outlines the method used for investigating the mechanism of amorphous sugar sticking and caking. Details of the equipment used are also given since this apparatus and the method for its use have been developed at Massey University over the last 5 years and it is not currently known to be in use anywhere else. The objective of this work was to determine whether sticking of amorphous maltose, sucrose, glucose, galactose and fructose was related to the $T\text{-}T_g$ of the sugars and not the temperature and relative humidity conditions used to establish a given $T\text{-}T_g$. The overall experimental approach used was to expose the different sugars to different combinations of temperature and relative humidity, to give similar and different $T\text{-}T_g$ values, and measure the caking strength of the powder with time.

5.3.3.1 Temperature/Relative Humidity Rig

The rig used to produce an air supply at a constant relative humidity and temperature was developed by O'Donnell (1998) and modified by Brooks (2000). O'Donnell *et al.* (2002) provides a detailed description of the apparatus (schematic given in figure 5.3), which is capable of maintaining an air supply at a constant temperature (± 0.2-0.3°C)

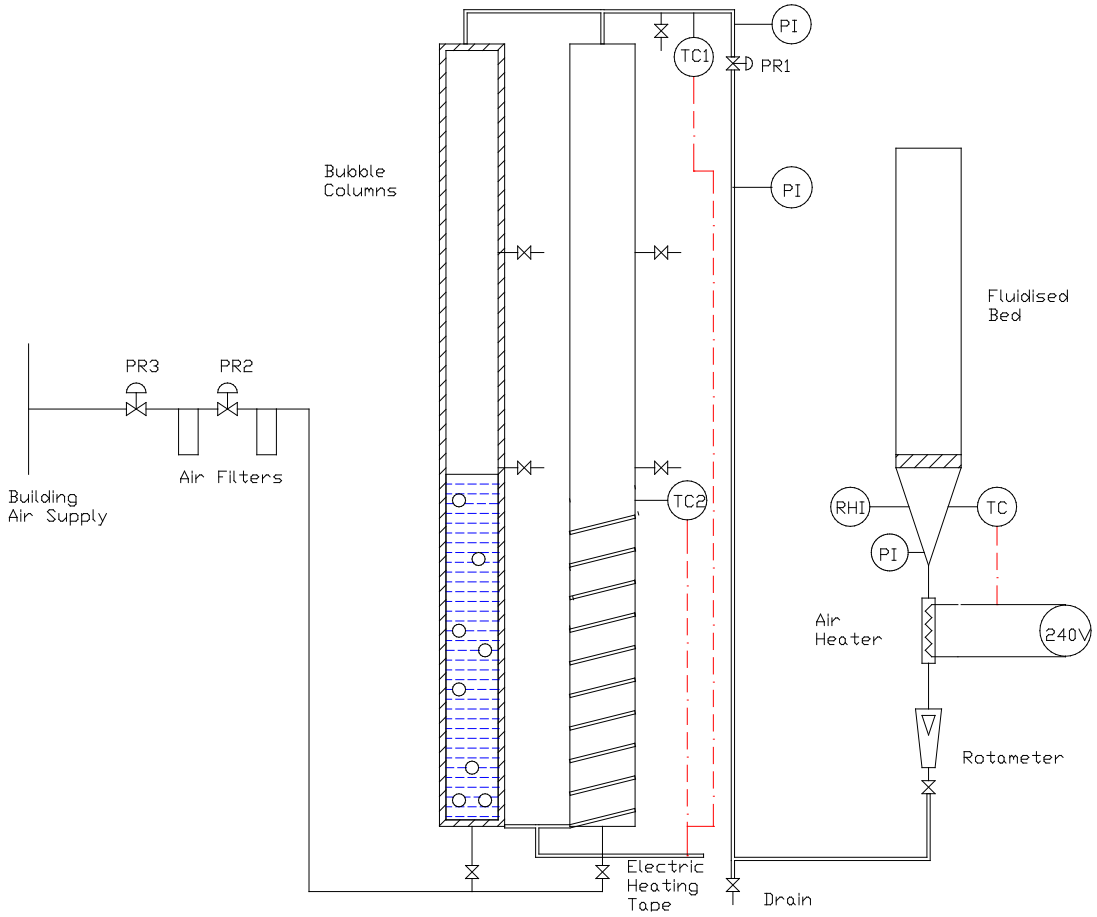

Figure 5.3: Relative humidity air supply apparatus (PR2, PR3 are pressure regulators; TC, TC1, TC2 are temperature control loops; RH1 is a relative humidity probe).

and relative humidity (± 1.2-1.8%). The rig uses a "two-pressure principle" to produce air at a constant relative humidity [Wexler and Daniels 1952]. Air is saturated with water vapour at high pressure and then passed through an expansion valve to lower pressure. The relative humidity of the low pressure air stream is equal to the ratio of the low and high pressures [O'Donnell *et al.* 2002]. The rig has two 1.8m high steel columns which can be filled up to 1.07m high with water, which can then be kept at a constant temperature through the use of heating coils which are wrapped around the columns. Air is bubbled through the columns of water at pressures of up to 6 bar and then passed through an expansion valve. The expansion valve brings the pressure close to ambient, therefore adjusting the ratio of the two pressures sets the relative humidity. The heating coil can also be used to adjust the relative humidity, as an increase in water temperature means that the air bubbling through the column heats up and therefore is saturated with more water vapour as it passes through the column. The air stream is then passed through an in-line air heater which is used to achieve a desired outlet air temperature. An extra pressure regulator to the incoming airline was added in order to eliminate pressure fluctuations from the compressor.

The original set up designed by O'Donnell (1998) was used for fluidising lactose. Brooks (2000) modified the set-up so that a hose could be attached, for the use of constant relative humidity and temperature conditions away from the rig. The current set-up for the rig allows for a fluidised bed to be attached or for the air stream to be directed away and used away from the rig. This rig was also used for providing

Figure 5.4: Testing chamber and modified blow tester

constant temperature and relative humidity conditions for the work investigating the effect of milk fat on dairy powder sticking and caking (chapter 6) and the model validation (chapter 7).

Brooks (2000) also developed an experimental set-up for using the blow test on a powder bed as discussed in section 2.2.2.3. The rig was used to give the desired relative humidity and temperature conditions in the testing chamber (figure 5.4). Full details on the modifications made to the blow tester are given in Brooks (2000). However some details are repeated here due to the extensive use of the equipment in this work. The air stream at the desired relative humidity and temperature was directed to a testing chamber that consisted of a glass enclosure, a segmented distributor plate (figure 5.5) and the blow tester (figure 5.4). Air was directed through the top of the glass enclosure and then passed through (in a reverse airflow pattern) a segmented distributor plate. The blow tester was suspended over the powder without disturbing it. A compressed airline was connected to the blow tester to use to take the caking strength/stickiness measurements when required. The blow tester could be easily turned to the desired location on the bed and a reading could be taken which would just effect the powder in a segment of the powder bed.

Figure 5.5: Segmented distributor plate

5.3.3.2 Preconditioning of Powder

The freeze dried powder was preconditioned using the rig, to the relative humidity that the sticking experiments were to be carried out at. This was done by fluidising the powder at a given relative humidity for approximately 15 hours. Care was taken to ensure that the relative humidity of the powder would be such that the powder would be stable (i.e. under its glass transition temperature) under ambient conditions so that no sticking, caking or crystallisation occurred prior to starting the sticking experiments. The powder was preconditioned to a number of water activities, so that the sticking experiments could be carried out using a variety of temperature and relative humidity conditions to achieve similar $T-T_g$ values for the powder. After preconditioning, the powder was stored in airtight plastic bags in a 4°C room until use. Each plastic bag contained enough powder to perform one experiment. This avoided the powder picking up moisture each time a bag was opened to remove a sample for testing and allowed a fresh sample to be used for each experiment.

5.3.3.3 $T-T_g$ Sticking Trials

The rig was set to the appropriate testing conditions by adjusting the incoming pressure, outlet pressure, temperature of water in the columns and the heater temperature as described in section 5.3.3.1. Once the desired relative humidity and temperature conditions were achieved in the testing chamber, the preconditioned powder was spread over the testing plate. The glass lid of the chamber was fitted and timing commenced. Conditions in the testing chamber (temperature and relative humidity), along with the caking strength, as measured using the blow tester, were measured with time. Measurement concluded when either the caking strength became constant, the caking strength exceeded the maximum reading obtainable with the equipment used, or the maximum number of readings for the set-up had been taken. The relative humidity used during testing was generally within ± 2% of the relative humidity that the powder had been preconditioned to. In this way, the powder was exposed only to a step change in temperature at the start of each experiment. A slight difference between the powder relative humidity and that being tested was not considered crucial, as the surface of the powder would equilibrate very quickly to the conditions being tested. Since sticking is a surface related phenomenon, it is only important that the surface is at the temperature and relative humidity conditions that are being tested.

5.3.3.4 T_g Profiles

T_g profiles were measured for the two-component powders, i.e. those powders which were made up with lactose in order to stabilise the lower molecular weight sugar (glucose, galactose or fructose). The T_g profiles were measured using the DSC after the powder had been humidified over saturated salt solutions. More detail on measuring the T_g profile is given in section 4.2.1. These profiles were used to determine the $T-T_g$ for each experiment performed. This was used, rather than a predicted T_g profile, in order to avoid the error involved with predicting and also because crystals were present in those powders. Since it could not be determined whether the crystals were lactose and/or the other component, it therefore could not be determined in what proportions

the amorphous sugars were present in the powder. A T_g profile therefore could not be predicted and it was more accurate to measure one for the powder.

5.3.4 Results and Discussion

The results and analyses performed on the data from the stickiness trials will be discussed using amorphous sucrose. It is noted that the same analysis was used for all amorphous sugars and the raw data and subsequent analysis for each sugar are given in appendix A2. The only exception is that the analysis of the raw data for amorphous glucose/lactose, galactose/lactose and fructose/lactose powders used the actual T_g profiles measured for the blends. The analysis for amorphous sucrose and maltose used the T_g profiles for the sugars given in the section 4.3. Using the relative humidity and temperature conditions that the powder was exposed to during the stickiness trial, the T-T_g for that trial was calculated. Figures 5.6 and 5.7 shows the collection of all the stickiness trials performed using amorphous sucrose with the RH and temperature conditions and consequent T-T_g given in the legend.

It can be seen in figure 5.7 that at low T-T_g values, i.e. a T-$T_g \approx 9°C$, the change in stickiness with time is very slow and no significant change in stickiness can be seen over a period of days. T-T_g values of 16 – 22°C give much quicker rates of sticking. In general, it can be seen that the rate of change in caking strength with time increases as the T-T_g increases. Values greater than 22°C were required for sticking to occur almost instantaneously. Figures 5.6 and 5.7 also show that trials with similar T-T_g values gave similar rates of sticking even when the RH and temperature conditions used to obtain that T-T_g differed. This can be seen more clearly in figure 5.8 which plots the rate of change in caking strength with time versus the T-T_g. This was obtained by taking the slopes of the data in figures 5.6 and 5.7 and plotting against their T-T_g values. In some cases, where the data did not have a linear relationship, the slope was taken from the initial change in caking strength. In figure 5.7, a non linear relationship can be seen for the trial done with RH and temperature conditions of 20.4% and 43.5°C giving a T-T_g

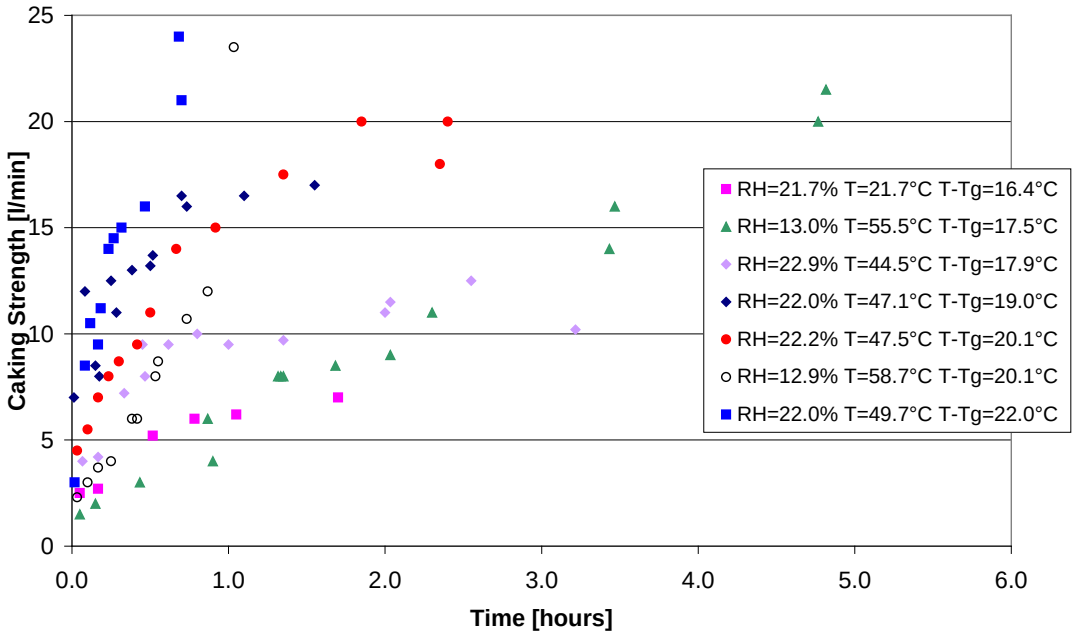

Figure 5.6: Caking strength versus time for amorphous sucrose

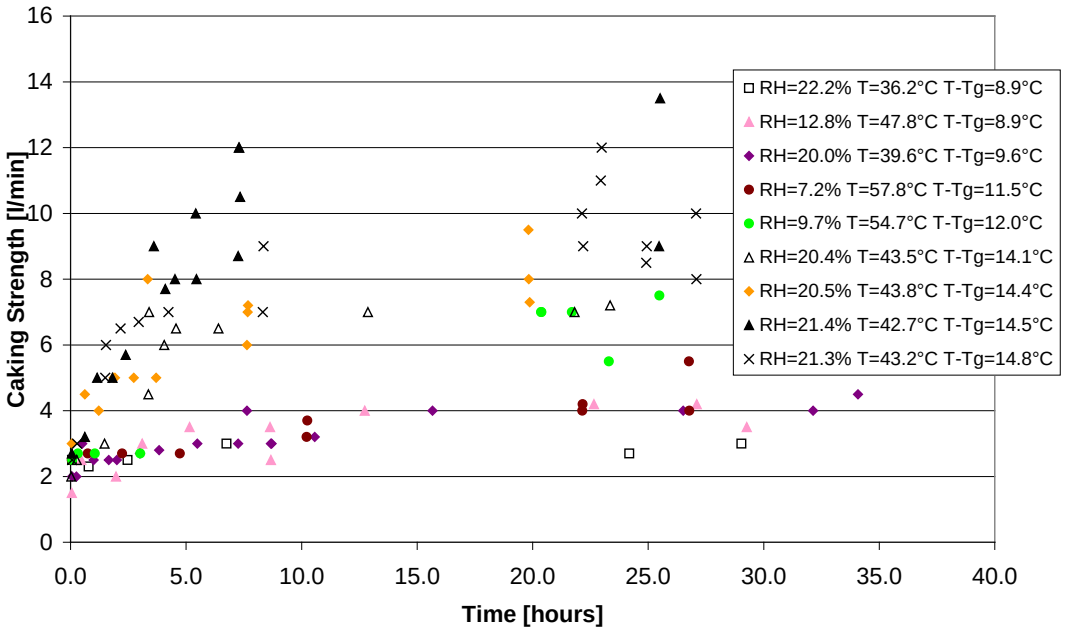

Figure 5.7: Caking strength versus time for amorphous sucrose

of 14.1°C. This data shows an initial linear change in caking strength and then the rate decreases and the curve eventually plateaus. This kind of relationship can be explained by considering the relative rates of flow and crystallisation in the powder at those conditions. Initially, flow would occur and liquid bridges would form giving the initial increase in strength of the powder. It is noted that flow would cease at some point due to one of two reasons:

1. The liquid bridges between the powder particles were the same size as the particles and essentially a continuous mass of amorphous sugar would be seen which had no distinguishable powder particles. If this occurred extensive collapse/shrinkage would be seen in the powder.
2. Crystallisation could occur at a rate greater than the rate of flow. Some flow of amorphous material may occur but it would be essentially "frozen" in place as crystallisation occurred.

If flow ceased due to the first reason, this would show as a very linear change in caking strength with time and the caking strength would eventually exceed the upper limit for the blow test once extensive collapse occurred. If the $T-T_g$ was lower and therefore, flow did not occur as quickly, then a different relationship between caking strength and time may be seen. When looking at the relative rates of flow and crystallisation, it would be expected to see an initial linear increase in caking strength with time while flow was occurring. Then at some point when there was enough molecular mobility, crystallisation would begin. As crystallisation proceeded the rubbery amorphous material that was forming the liquid bridges would begin to get fixed in place as some of the sugar molecules began to align with each other and crystallise. The change in caking strength would then occur at a different rate, which would be more proportional to the rate of crystallisation, as the formation of liquid bridges slowed down and the solidification of the liquid bridges took place. This would show up as a curved graph in figures 5.6 and 5.7. Therefore, in looking at the rate of bridge building, it is only necessary to consider the initial rate data from figures 5.6 and 5.7.

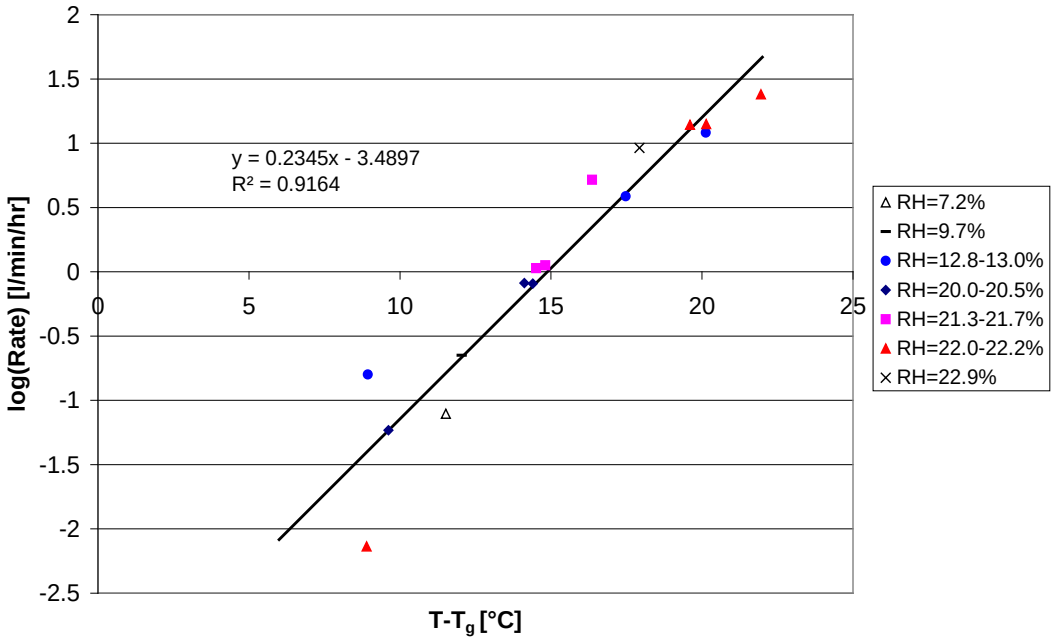

Figure 5.8: Rate of sticking versus T-T_g for amorphous sucrose

Figure 5.8 shows more clearly that the rate of sticking is related to the T-T_g of the powder and not the RH and temperature conditions used to obtain that T-T_g value. It also shows that the higher the T-T_g value, the higher the rate of sticking. The rate of sticking has been graphed on a log scale due to the large difference in rates for low and high T-T_g values. Using the log scale, a fairly linear relationship can be seen between the log of the rate of sticking and the T-T_g of the powder.

The same analysis was done for amorphous maltose and amorphous glucose/lactose, galactose/lactose and fructose/lactose mixtures. Best fit lines were fitted through the data. In the case of amorphous glucose/lactose, the very slow rates were left out from the analysis as these rates were indistinguishable from zero. It would require a certain

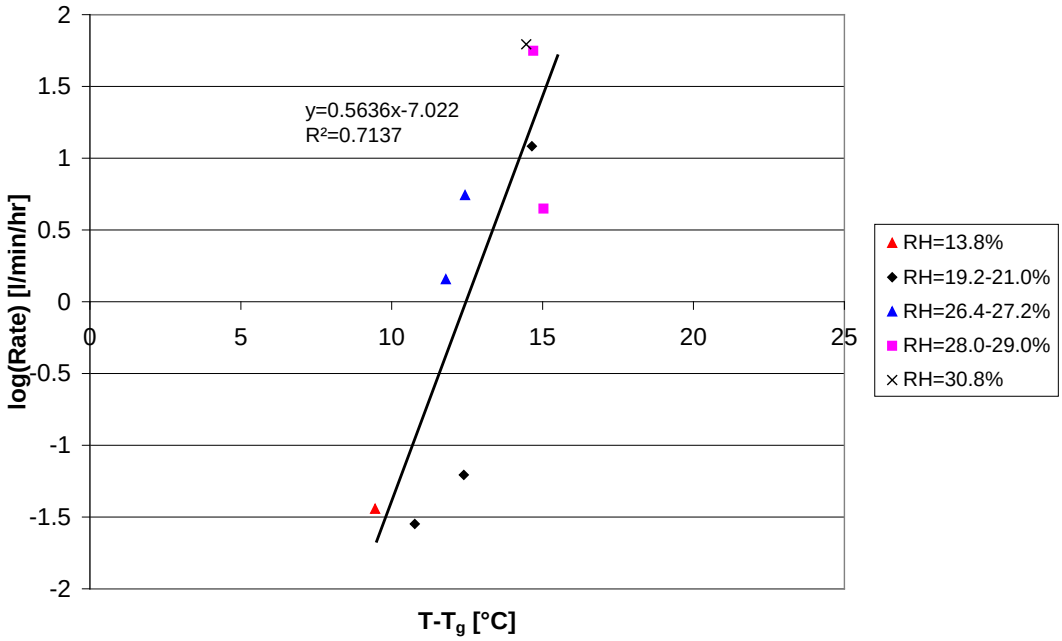

Figure 5.9: Rate of sticking versus T-T_g for amorphous maltose

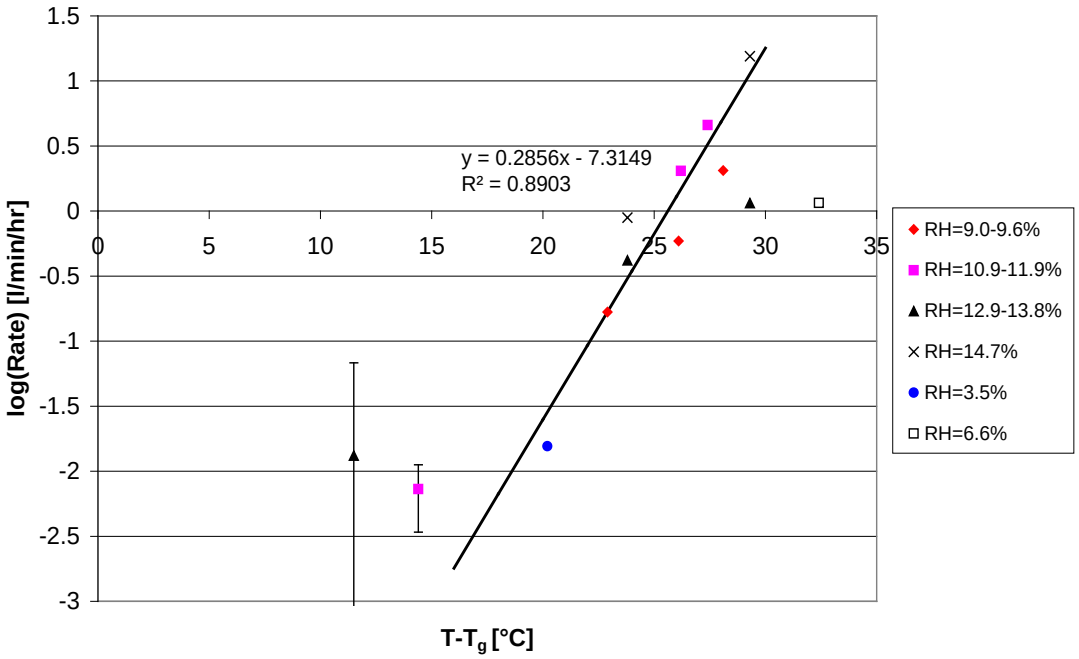

Figure 5.10: Rate of sticking versus T-T_g for amorphous glucose/lactose powder

T-T_g before the rate of sticking was indistinguishable from zero, therefore a relationship can only be fitted from that T-T_g and above. Some data at very high T-T_g was also left out from the analysis, as a lower rate of sticking was found with very high T-T_g values. It is possible that at very high T-T_g values the rate of crystallisation becomes much faster than the rate of flow and therefore only a very small amount of flow might have occurred before the rubbery material solidified through crystallisation. This would result in only very small bridges forming. If this was occurring, then taking the slope of the initial change in caking strength with time does not give the rate of sticking. It is more likely to relate to the rate of crystallisation. However, experiments were also performed at T-T_g values of 35.0 and 37.4°C and instantaneous sticking occurred i.e. the maximum caking strength value that could be achieved using the blow tester was exceeded during the time it took to reassemble the testing chamber after commencing the experiment. Collapse was also noted with these experiments. It is therefore not clear whether these low rates of sticking at high T-T_g values were due to a different mechanism (i.e. crystallisation) occurring or whether they were outliers.

Figures 5.9, 5.10, 5.11 and 5.12 show the relationship between the rate of sticking and the T-T_g for amorphous maltose, amorphous glucose/lactose, galactose/lactose and fructose/lactose respectively. Figure 5.10, 5.11 and 5.12 show that the stickiness of amorphous glucose/lactose, galactose/lactose and fructose/lactose mixtures are proportional to the T-T_g and not the conditions used to obtain the T-T_g. Since the stickiness of amorphous lactose is also proportional to the T-T_g of the powder and not the conditions used to obtain the T-T_g [Brooks 2000], then it can be concluded that the stickiness of amorphous glucose, galactose and fructose is also proportional to the T-T_g.

Table 5.1 shows the T-T_g values, resulting from the RH/temperature conditions that different experiments were operating under, that resulted in instantaneous sticking of the amorphous sugar. Instantaneous sticking occurs when conditions are such that the maximum blow test reading is exceeded in the time taken to put the testing chamber together and take the first reading (usually less than 2 minutes). The T-T_g values given

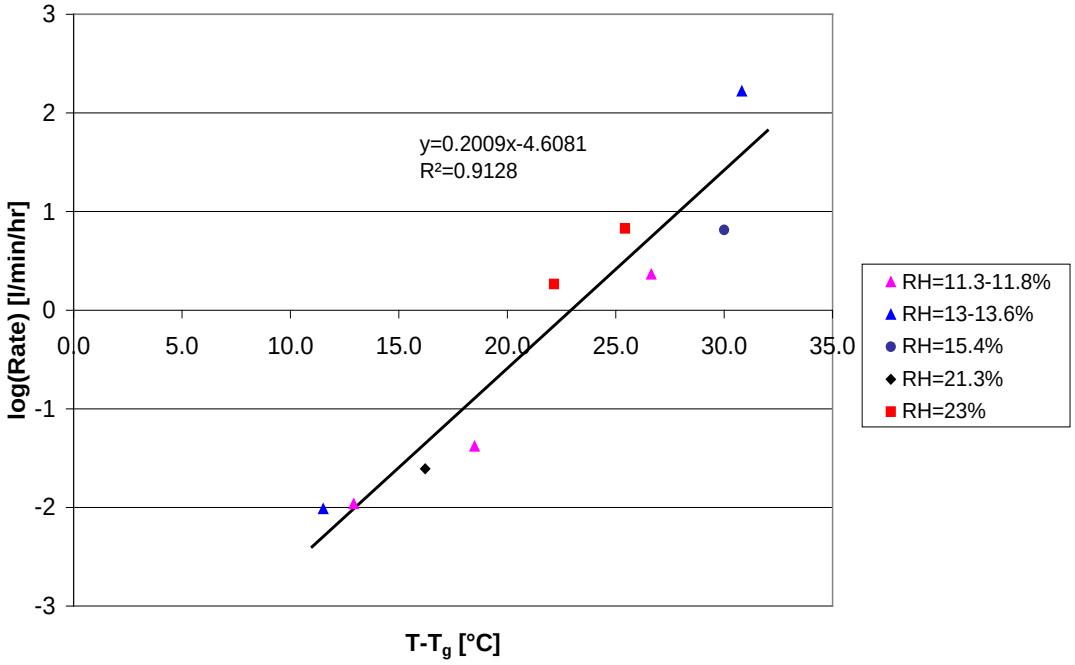

Figure 5.11: Rate of sticking versus T-T_g for amorphous galactose/lactose powder

in table 5.1 are not the instantaneous sticking points, they are just values for which instantaneous sticking did occur. It is possible that instantaneous sticking could also occur at a slightly lower T-T_g for a particular sugar. It is noted that instantaneous sticking did not occur under any of the experimental conditions used for amorphous galactose/lactose powder. However, the caking strength did exceed the maximum value for one experiment in less than 5 minutes so this T-T_g has been stated in table 5.1. It is noted that for the lower molecular weight sugars (i.e. glucose, galactose and fructose) that were made as mixtures with lactose, relatively much higher T-T_g values are required for instantaneous sticking. These freeze dried mixtures contained some crystalline material, as observed under the polarising microscope, which made it impossible to predict the mixtures' T_g profiles since the relative amounts of lactose and

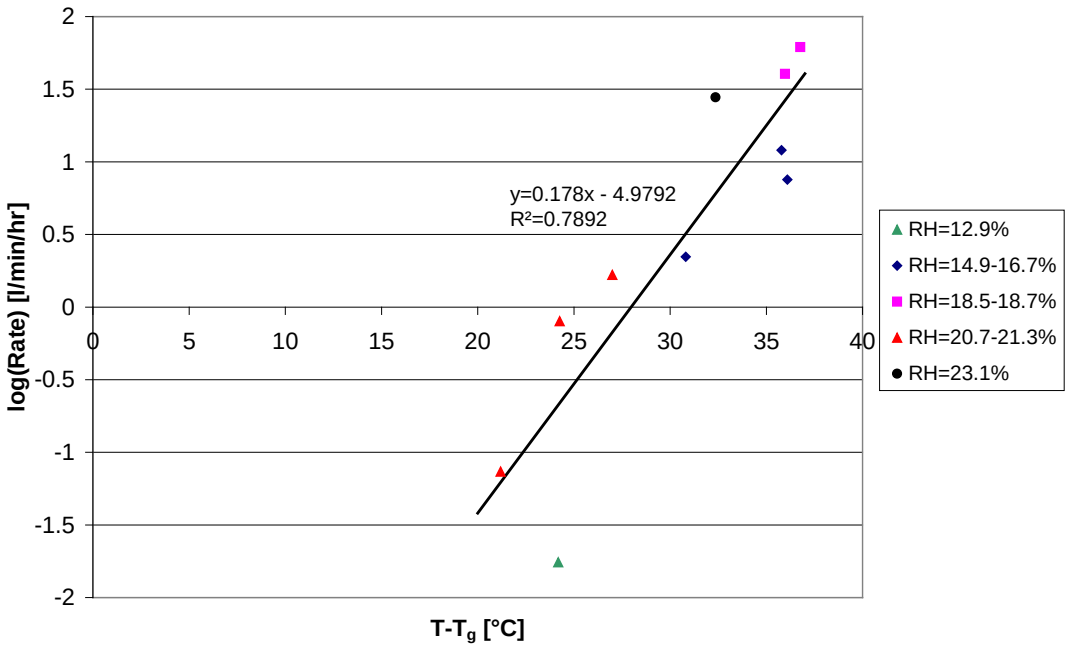

Figure 5.12: Rate of sticking versus T-T_g for amorphous fructose/lactose powder

the lower molecular weight sugar in amorphous form could not be determined. It is possible that the presence of crystalline material affects the rates of flow (through increased viscosity) and therefore sticking and caking in these powders. Having some crystalline material present means that there is less amorphous material present. Therefore it would take more time for the same level of flow and sticking to occur since there is less amorphous material available at the contact points between particles. Therefore, for the same sized amorphous bridge to form, it would require amorphous material from further away to flow to the liquid bridge. As stated in equation 5.2, an increase in the distance over which flow must occur (represented by the term *KD*) will decrease the tendency towards sticking and therefore require increased time for the same level of sticking to take place.

Table 5.1: T-T_g values for instantaneous sticking

Sugar	**T-T_g [°C]**
Lactose	25.0*
Sucrose	20.3
Maltose	19.0, 25.3, 29.0
Glucose/Lactose	35.0, 37.4
Galactose/Lactose	30.8
Fructose/Lactose	41.3

*Brooks (2000)

An alternative explanation is the effect of the viscosity and/or surface tension of the mixture. Maltini and Anese (1995) compared the viscosities of concentrated glucose, fructose and sucrose solutions with those predicted using the WLF equation. There did not appear to be any significant difference in the experimental and predicted viscosities when the universal constants, and 10^{14} cP was used as the viscosity for the glass, was used for all comparisons. Therefore there was no difference in viscosity between the different sugars when related to the T-T_g. Mathlouthi *et al.* (1996) also found there to be very little difference between the viscosities of sucrose, glucose and fructose solutions. Downton *et al.* (1982) stated that the rate at which the bridges are formed is governed by the viscosity of the material. With this in mind, there should be no difference between the rate of bridge formation with the different sugars (if surface tension is constant) since the viscosities appear to be the same when related to the T-T_g. The driving force for the formation of bridges is governed by the surface tension of the amorphous material, i.e. as the surface tension increases the tendency towards sticking increases. Comparing the surface tension of a concentrated lactose and 10% sucrose solutions (66mN/m [Bronlund 1997] and 71.5mN/m [Mathlouthi *et al.* 1996]), sucrose has a higher surface tension therefore the T-T_g at which instantaneous sticking occurs should be lower, since the driving force for bridge formation is higher. This is seen to be the case in table 5.1. The surface tension of 10% fructose and glucose solutions, as found by Mathlouthi *et al.* (1996), are 73.8 and 72.8 mN/m respectively. The surface tensions for these sugars is greater than that for sucrose. However, a decrease in the T-T_g required for instantaneous sticking was not found for these sugars when mixed with lactose. The T-T_g for instantaneous sticking was even higher than that required for amorphous lactose. This indicates that the difference in the T-T_g values for instantaneous sticking is not related to the surface tension or viscosity of the different sugars.

At this stage it is worthwhile discussing the merits of the experimental technique used for this work. Methods for measuring stickiness in the currently available literature

tend to focus on measuring a point, the sticky point temperature, at given moisture conditions. These values are therefore the conditions for instantaneous sticking, i.e. sticking that occurs instantly after a change in either temperature or relative humidity is applied. This sort of measurement is ideal for determining the conditions (temperature and relative humidity) that will cause a powder to become sticky during spray drying where the residence time in the dryer is small. It does not, however, give information for the conditions that will cause sticking when the residence time is greater, which could be the case in fluidised beds or during storage. Single sticky point measurements can also give the impression that sticking occurs at a single temperature for a given moisture content or water activity. This obviously depends on the definition for sticking used, and is true if sticking is considered to occur at a critical viscosity. In this work sticking, like caking and collapse, is considered a time-dependent phenomenon. That is, the rate that sticking will occur will depend on the driving force for sticking. As has been found in this work, the driving force for sticking is in fact the $T\text{-}T_g$ (which represents a decrease in viscosity) for the powder and not the actual temperature or relative humidity conditions being used. The experimental procedure developed by Brooks (2000) and in this work contributes to research into T_g related flowability problems as it allows continuous readings to be taken over time rather than just one point being measured. This therefore allows the observation of the time-dependent side of these sticking and caking problems to be made under constant $T\text{-}T_g$ (temperature and relative humidity) conditions.

Further analysis can be performed using the Frenkel and WLF equations (equations 5.1 and 5.3 respectively). The strength of a liquid bridge is proportional to the cross sectional area (πr_b^2) of that bridge. Therefore, when considering the Frenkel equation, strength is proportional to $\Delta r_b^2/\Delta t$. The Frenkel equation can be rearranged for r_b^2/t (equation 5.4):

$$\frac{r_b^{\,2}}{t} = \frac{3\sigma R_p}{2\mu} \tag{5.4}$$

Rearranging the WLF equation for μ and substituting into equation 5.4 and taking the log gives equation 5.5 where $k_F = 3\sigma R_p/2\mu_g$:

$$\log\left(\frac{r_b^{\,2}}{t}\right) = \log k_F + \frac{C_1\left(\mathrm{T}-\mathrm{T}_g\right)}{C_2 + \left(\mathrm{T}-\mathrm{T}_g\right)} \tag{5.5}$$

If the mechanism can be described by the above equation then plotting $\log(r_b^2/t)$ versus $(T\text{-}T_g)/(C_2 + T\text{-}T_g)$ should yield a straight line with a slope equal to C_1 and an intercept equal to $\log k_F$. If the initial rate of change in caking strength can be considered to describe the rate of sticking then the rate of sticking obtained from figures 5.6 and 5.7 and used in figure 5.8 can be used to describe $r_b^{\,2}/t$. A plot of the log(rate of sticking) shown in figure 5.8 versus $(T\text{-}T_g)/(C_2 + T\text{-}T_g)$ is shown in figure 5.13. It is noted that the values for C_1 and C_2 were allowed to vary when fitting the Frenkel/WLF equation. The values for C_1 and C_2 obtained are those which gave the best fit of the data to the Frenkel/WLF model. It can be seen that the data follows a linear relationship, indicating that the WLF and Frenkel models do apply to this system. The value for C_1 obtained was 14.8, which is close to the universal constant of 17.44 stated by Williams *et al.* (1955). C_2 was found to be 25.3, which differs from the universal constant of

51.6. A linear relationship was also fitted to the data with C_1 and C_2 set to the universal constants. This still gave a very good fit with the R^2 value (0.9079) being only slightly less than that obtained when the slope was not set (R^2=0.9256). Obtaining a strong linear fit gives confidence that the viscosity based mechanism used for the Frenkel model and the WLF model holds true for the amorphous sucrose system.

This analysis was done for all sugars and is summarised in table 5.2. It can be seen that in the case of sucrose, galactose/lactose and glucose/lactose, a good fit was found between the data and the Frenkel/WLF model, with R^2 values being over 0.9. For fructose/lactose and maltose, the linear fit was still good, with R^2 values of 0.7948 and 0.7136 respectively. It is noted that, in some cases, the constants C_1 and C_2 were limited to vary between 0 and 100. This limit was placed on the constants found for galactose/lactose, glucose/lactose and fructose/lactose as in these cases the constants tended to very large numbers or to negative values. This range limit was placed on the values of the constants after consideration of the range of values found in literature, discussed in section 5.2. This variation in the values obtained for the constants indicates that the universal constants are not applicable to all sugars. It is noted that amorphous maltose appeared to behave quite differently from the other amorphous sugars. When instantaneous sticking occurred for the other powders apart from maltose, the powder would become very glassy or transparent looking and extensive flow and collapse would take place. Generally the very rubbery material had to be washed from the distributor plate to be removed. Amorphous maltose behaved differently. The powder that became instantaneously sticky (i.e. had a caking strength reading that exceeded the maximum reading) could be tapped from the distributor plate and then be snapped and broken in the fingers to give a free flowing product. If the powder was then left in the lab, in would go glassy looking over a period of days, extensive flow would occur and then over a period of weeks, white flecks would be seen amongst the glassy looking mass, indicating that crystallisation had begun. It appears that with amorphous maltose, the same sticking mechanism applies, but the powder subsequently behaves differently from the other amorphous sugars. These observations

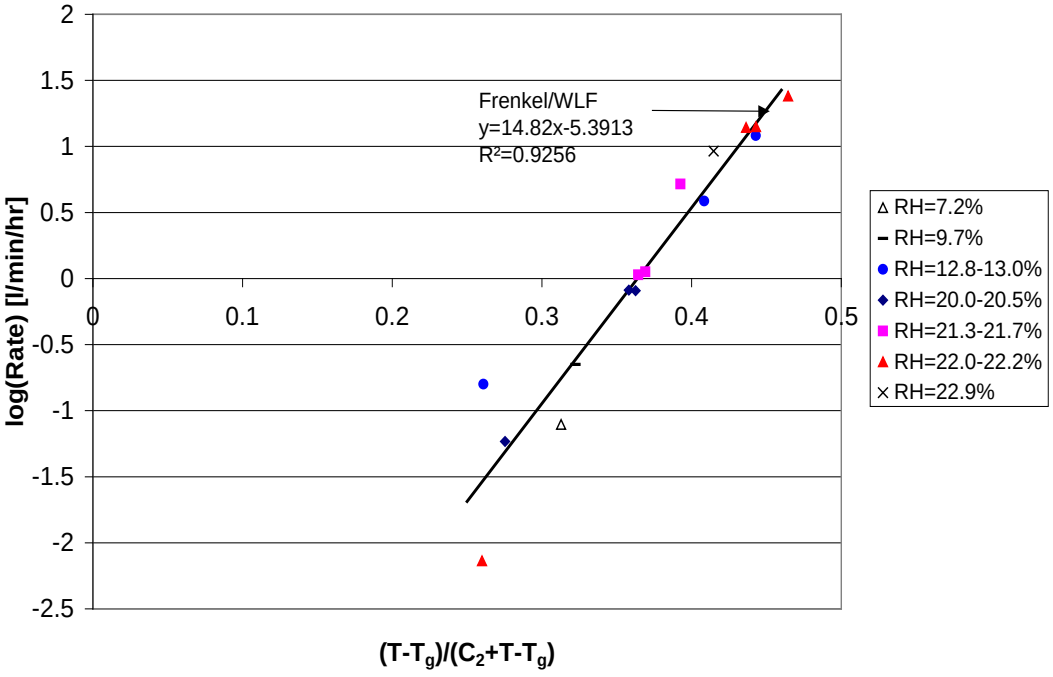

Figure 5.13: Frenkel/WLF model fitted to rate of amorphous sucrose sticking data

also show that sticking is a surface phenomena and that it takes time for the moisture to migrate into the amorphous maltose particle. The observations also show that amorphous maltose is dramatically affected by moisture i.e. there is a large lowering of the viscosity with small increases in the moisture present.

Table 5.2: Constants from fitting Frenkel/WLF model to rate of sticking data

Sugar	C_1	C_2	K_F	R^2
Lactose*	1.6	3.5	3.96×10^{-2}	0.9652
Sucrose	14.8	25.3	4.06×10^{-6}	0.9256
Maltose	71.2	100	1.33×10^{-9}	0.7136
Glucose/Lactose	100	2.0	2.47×10^{-93}	0.9040
Galactose/Lactose	29.2	100	4.09×10^{-6}	0.9059
Fructose/Lactose	21.1	22.3	2.26×10^{-12}	0.7948

*Analysing the data from Brooks (2000)

Van Krevelen (1990) put forward a basic linear growth rate equation to describe the rates of nucleation and growth during crystallisation. Equation 5.6 describes the rate of growth.

$$v = v_o \exp\left(-\frac{E_D}{R\mathrm{T}}\right)\exp\left(-\frac{W^*}{k^*\mathrm{T}}\right) \tag{5.6}$$

where v = rate of growth (m/s)
v_0 = constant fort he zero condition (m/s)
E_D = activation energy for the (diffusive) transport process at the interface (J/mol)
W^* = free energy of formation of a surface nucleus of critical size (J/mol)
k^* = Boltzmann constant (J/mol/K)
R = ideal gas constant (J/mol/K)
T = temperature (K)

An analogous equation can be written to describe sticking. The first term in the exponential is related to molecular mobility and represents the ability of molecules to join the growing crystal [Bronlund 1997]. The second term represents the surface nucleation phenomena. This term is a function of how supercooled the solution is and can therefore be neglected as it can be assumed that supersaturation or supercooling is very high and it is only mobility which is controlling the rate of sticking. The second exponential term will tend to unity, therefore it can be ignored. Van Krevelen (1990) found a correlation between temperature and viscosity corresponding to a WLF type relationship. The first exponential term can be replaced by equation 5.7 resulting in equation 5.8 which describes the rate of sticking based on Van Krevelen's equation.

$$\frac{E_D}{R\mathrm{T}} \cong \frac{C_1'}{R\left(C_2 + \mathrm{T} - \mathrm{T}_g\right)} \tag{5.7}$$

$$s = s_o \exp\left(-\frac{C_1'}{R\left(C_2 + \mathrm{T} - \mathrm{T}_g\right)}\right) \tag{5.8}$$

where s = rate of sticking
s_o = zero condition
C_1' = constant (17.2 kJ/mol)
C_2 = constant (51.6 K)

Taking the natural logarithm of equation 5.8 gives equation 5.9, which can be used to determine whether the rate of sticking is described by this molecular mobility type mechanism.

$$\ln s = \ln s_o - \frac{C_1'}{R}\left[\frac{1}{C_2 + \mathrm{T} - \mathrm{T}_g}\right] \tag{5.9}$$

Plotting lns versus $1/(C_2+T-T_g)$ should yield a straight line of slope $-C_1'/R$ and intercept equal to $\ln s_o$. This has been done for all sugars and the plot for amorphous sucrose is given in figure 5.14. A summary of the constants, C_1', C_2 and s_o, obtained from equation 5.9, for all sugars, is given in table 5.3.

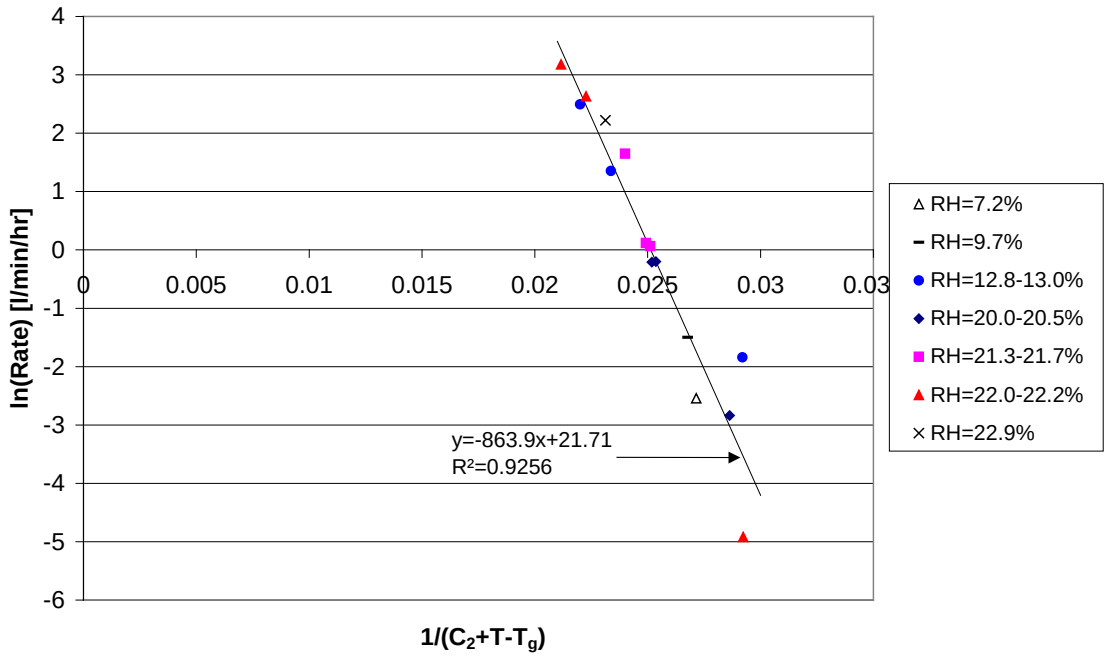

Figure 5.14: Van Krevelen model fit to rate of amorphous sucrose sticking data

Table 5.3: Constants from fitting the van Krevelen model to rate of sticking data

Sugar	C_1'	C_2	S_o	R^2
Lactose*	0.1	3.5	3.1	0.9652
Sucrose	7.2	25.3	2.69×10^{9}	0.9256
Maltose	100	83.8	1.84×10^{54}	0.7135
Glucose/Lactose	3.3	7.1×10^{-5}	6.33×10^{6}	0.9044
Galactose/Lactose	56.0	100	7.13×10^{23}	0.9059
Fructose/Lactose	9.0	22.3	2.87×10^{9}	0.7948

*Analysing the data from Brooks (2000)

Both approaches use the WLF equation and are therefore equations for the rate of sticking (taken from the initial slope of the caking strength versus time data at each T-T_g) based on viscosity. They are therefore equivalent equations, which is indicated by both approaches giving identical fits in terms of the R^2 values. It is noted that the R^2 value for amorphous glucose/lactose differ slightly. This is likely to be due to the restriction on the values for C_1, C_1' and C_2 applied when analysing that data. If both equations are equivalent then the value for C_2 will be the same using each approach and equation 5.10 will hold:

$$\frac{T - T_g}{C_2 + T - T_g} = a\frac{1}{C_2 + T - T_g} + b \qquad (5.10)$$

where a and b are the slope and intercept respectively. For this to be true, the slope must be equal to $-C_2$ and the intercept equal to 1 (see appendix A2). The C_2 values obtained for lactose, sucrose, galactose/lactose and fructose/lactose mixtures, through using the Van Krevelen equation are the same as those obtained using the Frenkel/WLF model (equation 5.5). The values for C_2 do not agree for amorphous maltose and glucose/lactose mixtures due to the restrictions placed on the values that C_1 and C_2 can take for these powders. Appendix A2 also shows that the values for C_1 and C_1' should not be the same and one can be determined if the other and C_2 are known. C_1 can also be determined from the intercepts of the Frenkel/WLF model and van Krevelen equation.

5.3.5 Conclusions

This work confirmed that rate of sticking of amorphous sugars is related to the T-T_g of the powder and not the individual temperature and relative humidity conditions used to give a specific T-T_g. Successfully fitting a Frenkel/WLF based model and the Van Krevelen model to the rate of sticking data for the amorphous sugars shows that the sticking of amorphous sugars is indeed a viscosity related mechanism.

5.4 CLOSURE

The sticking of amorphous sugars was found to be a viscosity related mechanism and the rate of sticking was found to be related to the T-T_g of the powder. Therefore, any model used to predict the sticking and caking of powders containing amorphous sugars will only need to be based on the T_g of the powder and not the temperature and relative humidity conditions used to obtain a certain T-T_g.

The fat component of dairy powders may also contribute to sticking and caking problems in dairy powders, especially when it is present in a large proportion. The role of milk fat in the sticking and caking properties of dairy powders is the subject of the following chapter.

CHAPTER 6

FAT MELTING MECHANISM

6.1 INTRODUCTION

Milk fat can be a major component in dairy powders. Therefore it is necessary to investigate the sticking and caking properties of milk fat. High fat powders, such as cream powders, have been known to have smearing problems during processing, where the powder builds up over the inside of the dryers, cyclones and fluidised beds. A high fat cream powder is particularly troublesome and as a result a free flow agent is used with this powder but the problem persists. This chapter investigates the mechanism for sticking and caking due to milk fat and will also determine how much milk fat is required before it contributes to flowability problems.

6.2 PHYSICAL PROPERTIES OF MILK FAT

Over 400 fatty acids have been identified in milk fat, although only 20 individual fatty acids account for most of the residues. These are principally present as triacylglycerides (95-98% of total lipid). The other components include diaclyglycerols, monoacylglycerols, free fatty acids, free sterols and phospholipids [Herrera *et al.* 1999]. Three major types of fine structure of milk fat can be observed according to freeze fracture microscopy [Söderberg *et al.* 1989]. These include:

1. An amorphous fine structure relating to the liquid state of milk fat;
2. Small regions within an amorphous phase showing some degree of order. These regions are layers of only a few nm thick and appear to relate more to the liquid state although this has not been fully characterised;
3. Smaller and larger regions with a high degree of molecular order. This is different to type 2 and relates to the crystalline state of milk fat.

The physico-chemical state of fat in the powder particle depends upon the manufacturing method, while the properties of the powder as influenced by fat in turn depend upon this state [King 1965]. A well dispersed and protected fat is required for powders which are designed for reconstitution. A well dispersed and protected fat results from spray drying and it is required in order to avoid greasy films on containers, fat clumps and oily patches on the surface of the reconstituted milk [King 1965]. Encapsulated fat occurs in a finely emulsified state where it is complexed with milk proteins [King 1965, Buma 1971d]. Buma (1971d) stated that fat which is not encapsulated is known as extractable fat or free fat. Free fat originates from four different sources as defined by Buma (1971d):

1. *Surface fat*, which is present as pools or patches of fat on the powder particle surface particularly in surface folds and at contact points between the particles;
2. *Outer layer fat*, consists of fat globules in the surface layer of the powder particles, which can be reached directly by fat solvents;
3. *Capillary fat*, consists of fat globules inside the powder particles which can be reached by fat solvents via capillary pores or cracks;

4. *Dissolution or 'second echelon' fat*, consists of fat globules inside the powder particles which can only be reached by fat solvents via the holes left by the dissolved fat globules in the outer particle layer or close to wide capillaries in the powder particle.

Free fat on the surface of a powder can pool causing flowability problems as discussed in section 1.2.3. Free fat which is capable of pooling occurs in a coalesced, de-emulsified state where the membranes around the fat globules have been removed or damaged [King 1965]. Figures for the amount of free fat as a percentage of the total fat produced during spray drying have been given from different researchers in King (1965). The range presented is 1 to 20% with the average being around 12%. Spray drying is much less disruptive on the fat resulting in less free fat being produced in spray drying compared to methods including roller drying and freeze drying [King 1965].

6.2.1 Melting Profile for Milk Fat

Due to its complex composition, the melting profile for milk fat extends from –40 to 40°C [Herrera *et al.* 1999]. DSC thermograms show three endothermic peaks, corresponding to three important melting ranges. A typical DSC thermogram is given in figure 6.1 which shows the three important melting ranges. This data was obtained from Boston (2000) and was measured by holding for 10 mins at 70°C, cooling to –63°C at 10°C/min, holding at –63°C for 10 min, scanning from –63 to 50°C and then holding at 50°C for 2 mins. The first melting range begins at –40°C and the amount of fat melting gradually increases to around 0°C. The second and most significant peak occurs between 0 and 20°C, with the maximum occurring at 15 to 18°C and a minor peak at around 8°C. The highest melting region is between 20 and 37°C and appears as a shoulder on the main melting peak [Sherbon 1974]. There are seasonal changes in

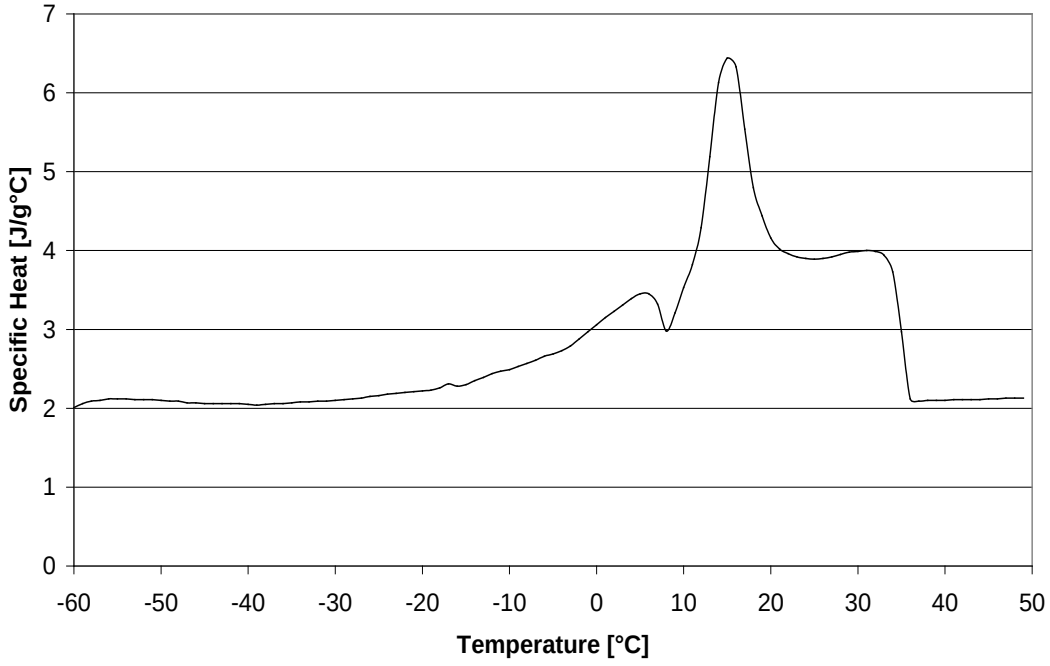

Figure 6.1: DSC thermogram for milk fat

milk fat composition which affect the melting thermograms of milk fat. Norris *et al.* (1973) stated that the amount of liquid fat present at any temperature between 0 and 22°C is at a maximum in July and at a minimum in November. The temperature at which melting is completed, however, is relatively constant, being unaffected by the seasonal changes in fat composition [Sherbon 1974]. It is noted that the resolution of the peaks in the milk fat melting DSC thermogram is affected by the rate of heating, but the temperatures at which the peaks occur remains constant [Norris *et al.* 1973]. Figure 6.2 shows the proportion of fat in the solid state at different temperatures as supplied by the New Zealand Dairy Research Institute (1998). This data was taken from the 1987/88 dairy season (September – May).

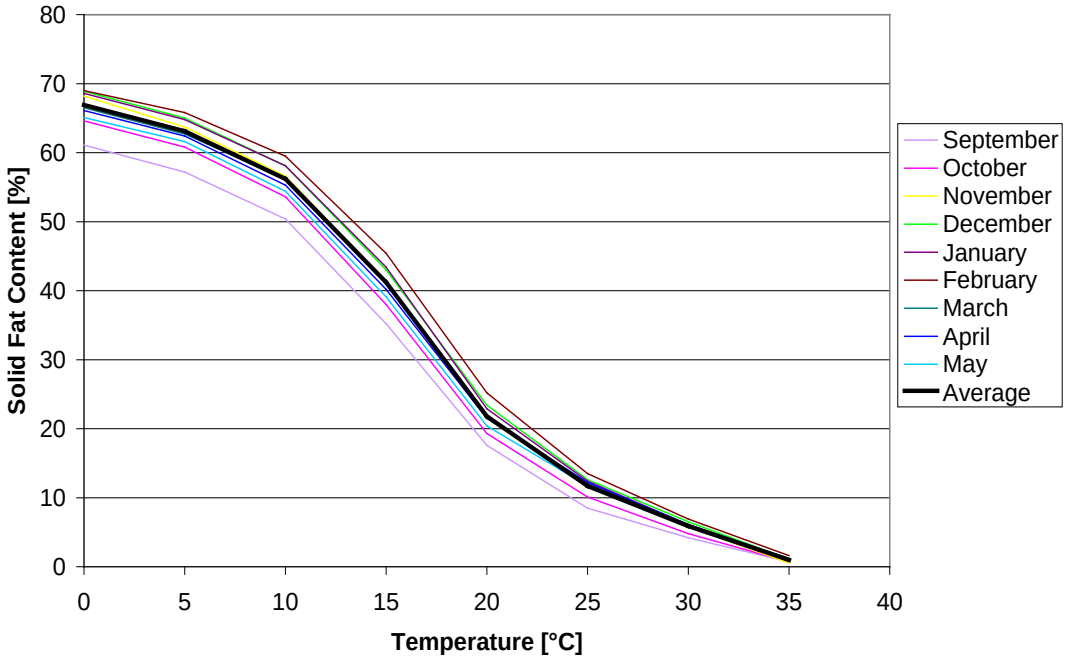

Figure 6.2: Solid fat content versus temperature for milk fat

6.2.2 Milk Fat Crystallisation

Crystallisation can be divided into two steps: nucleation and growth, and both can occur simultaneously. In general, nucleation requires supersaturation and that is the driving force for crystallisation. Nucleation of milk fat usually occurs through supercooling (the difference between the melting point of the fat and the actual solution temperature) and once formed they can grow and develop into crystals [Herrera *et al.* 1999]. Crystal growth occurs by the diffusion of the triacylglycerides from bulk solution across a boundary layer where they can become incorporated into the crystal lattice structure of an existing crystal or nucleus [Walstra 1987]. Crystallisation of milk fat is complex due to the mixture of various triacylglyerols present [Breitschuh and Windhab 1998]. The concentration of each triacylglyeride can be low, therefore requiring increased supercooling for nucleation and the wide range of triaclyglycerides present can also complicate crystal growth. Mixed crystals can easily form due to the low supersaturation of one triacylglyeride [Breitschuh and Windhab 1998]. Similar, but incompatable, triacylglycerides will either become incorporated into a mismatched lattice or diffuse back to the bulk solution. Mixed crystals are generally composed of

molecular species with similar chain length fatty acids. The growth of existing crystals is slowed down by the presence of multiple triacylglycerides [Grall and Hartel 1992].

Milk fat can solidify in three different crystal structures (α, β' and β) resulting from the magnitude of the driving force for crystallisation (degree of supercooling and/or supersaturation) [Huyghebaert and Hendrickx 1971]. α and β' are known as the metastable polymorphic modifications and are transformed to the stable β form with time. Rapid cooling gives the unstable α form, which will convert to the more stable β form upon holding. However, even after long periods of storage, both α and β' can still be present.

The following factors influence crystallisation and the properties of the final solid and liquid fat fractions and have been summarised by Grall and Hartel (1992) and Breitschuh and Windhab (1998):
- degree of supercooling/rate of cooling
- final temperature cooled to
- residence time at a particular temperature
- agitation
- source and nature of milk fat
- scale of operation

If rapid cooling is used, low melting triaclyglycerides can become trapped in a crystal lattice that has been formed by the high melting triacylglycerides. As a result, the resulting product will contain more liquid fat. Partition of solid and liquid fat fractions is promoted by slower cooling and by stepwise cooling with suitable holding times at each temperature [Dimick *et al.* 1996].

Herrera *et al.* (1999) looked at milk fat crystallisation by measuring the solid fat content (SFC) with respect to time using pulsed nuclear magnetic resonance (pNMR). The samples were heated to 80°C and held for 30 min, then the NMR tubes were filled with

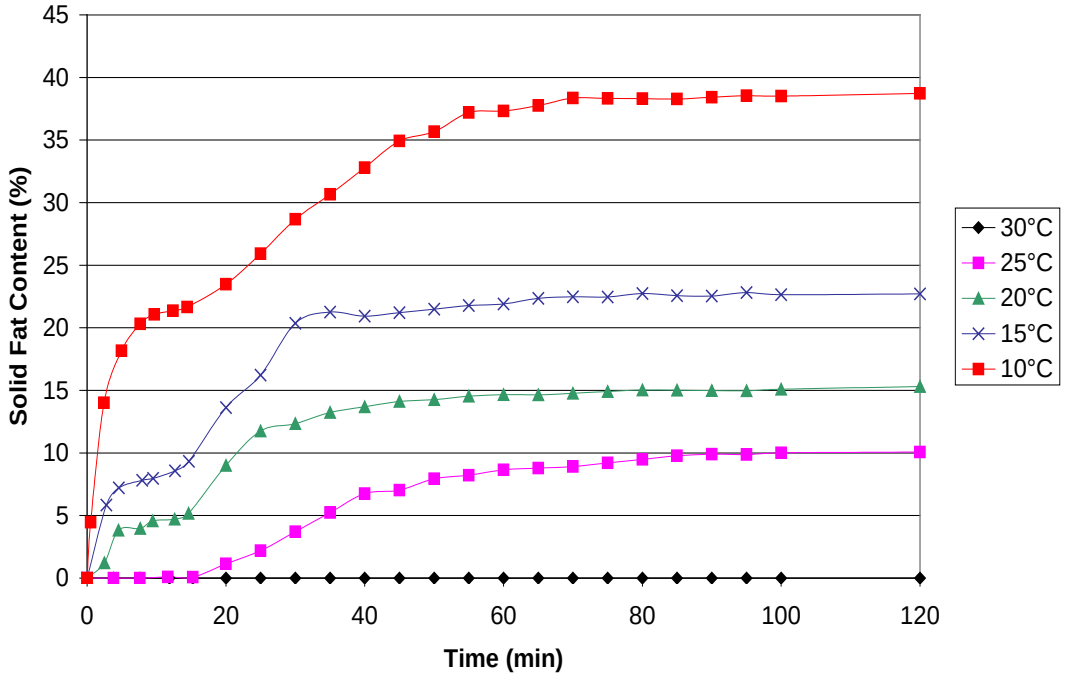

Figure 6.3: Change in solid fat content with time [Herrera *et al.* 1999]

anhydrous milk fat and kept at 80°C for a further 30 min. The NMR tubes were then put into a bath at the crystallisation temperature. SFC was measured as a function of time. Figure 6.3 is a reproduction of the results of Herrera *et al.* (1999). It is noted that the initial rise in SFC followed by the lag is also seen with the data of Breitschuh and Windhab (1996) and Breitschuh and Windhab (1998). Comparing the crystallisation curves of Breitschuh and Windhab (1998) and Herrera *et al.* (1999), the times for crystallisation are reasonably comparable in some cases. In other cases the crystallisation rate was quicker in the experiments done by Breitschuh and Windhab (1998) which would have been due to mixing. Grall and Hartel (1992) showed that agitator velocity can significantly increase the rate of crystallisation of milk fat. This was explained by the promotion of secondary nucleation during increased impellor shear. Breitschuh and Windhab's (1998) crystallisation curves were based on changes in viscosity as measured by a rheometer.

Herrera *et al.* (1999) fitted their data to the Avrami-Erofeev equation (Eq 6.1) [Ng 1975]:

$$-\ln(1-x) = (k_n t)^n \tag{6.1}$$

where t is time, k_n is the rate constant, x is the fractional extent of crystallisation at any time and n represents the index of the reaction which is an integer and should be set to 2, 3 or 4 [Herrera *et al.* 1999]. Table 6.1 lists the parameters of the Avrami-Erofeev equation as calculated by Herrera *et al.* (1999). $t_{1/2}$ is the half time of crystallisation and relates to k_n through the following relationship (Eq 6.2):

$$(t_{1/2})^n = 0.693 / k_n \tag{6.2}$$

Table 6.1: Avrami-Erofeev equation parameters (setting *n* = 3) [Herrera *et al.* 1999]

Temperature [°C]	k_n [min^{-1}]	$t_{1/2}$ [min]
30	0.001±0.000043	8.8±0.07
25	0.010±0.00045	4.1±0.04
20	0.069±0.0022	2.2±0.06
15	0.131±0.0034	1.7±0.03
10	0.140±0.0032	1.7±0.02

6.3 FAT MELTING MECHANISM

The occurrence of caking in dairy-based powders has been attributed to fat present in the following ways:

1. Surface fat melts forming liquid bridges of fatty composition, which can later solidify [Buma 1971e, Peleg 1977, Wakiyama *et al.* 1992, McKenna 1997].
2. Lactose crystallisation occurs disrupting the encapsulated fat, which is then released to the surface where it can form liquid bridges as described above [King 1965, Saito 1985, Munns 1989, Pearce 1992, Fäldt and Bergenståhl 1994,1995,1996a,b,c].

The situation arising from lactose crystallisation occurs when the amorphous lactose present is able to crystallise due to an increase in temperature or moisture, as related to the glass-rubber transition. For all other situations where the temperature and moisture content are not high enough for glass-rubber transition, it is possible that the temperature is still high enough for milk fat to melt, flow and form liquid bridges.

As shown in figure 6.2, 60% of the milk fat has a melting point of greater than 15°C and close to 100% of the milk fat is molten at 35°C. At ambient conditions around 20°C, a significant percentage (77%) of the milk fat is in a fluid-like state and is able to flow over the particle surfaces and contribute to caking if the temperature is subsequently dropped. In countries where the temperatures are around 35°C, a large percentage of the milk fat has melted and is capable of forming fat bridges. Peleg (1977) stated that viscous liquid bridges may cause flow difficulties in fat-containing powders. It was noted that if the temperature is increased during storage or processing, some fat may melt forming liquid bridges of fatty composition. If the temperature drops later on, the fat can resolidify, resulting in a lumpy product. The detergent industry has had similar problems with ingredients that have low melting points [Peleg 1977]. The mechanism for this type of caking is given in figure 6.4.

McKenna (1997) observed surface fat on whole milk powder (WMP) using confocal laser scanning microscopy (CLSM). CLSM identified the occasional presence of relatively larger regions of fat on the surface as well as fat within the powder particles. Transmission electron microscopy showed regions of coalesced fat globules within the same samples. Using CLSM, it was evident that regions of surface fat appeared to pool at the joining points of agglomerated powder particles. This observation supports the fat-melting mechanism for caking.

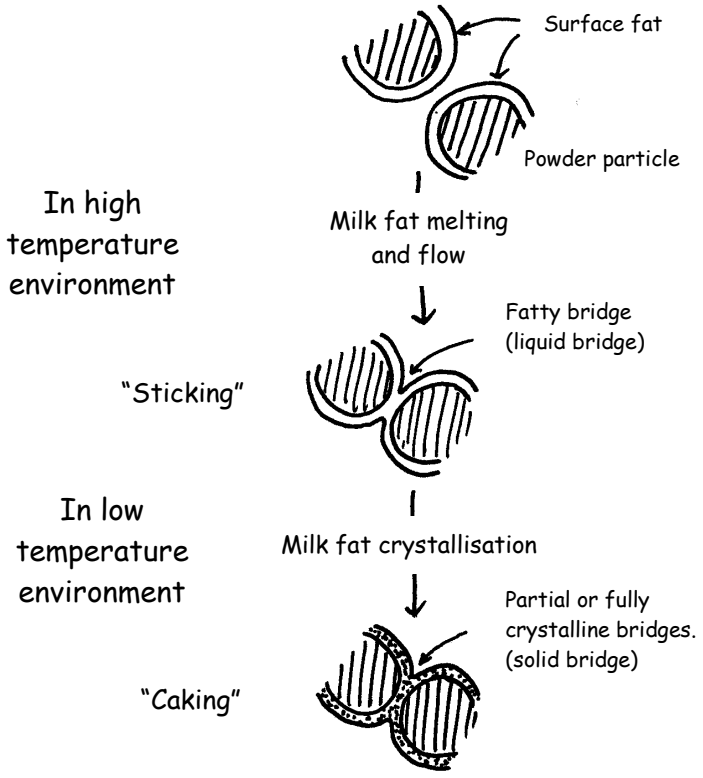

Figure 6.4: Milk fat melting mechanism

An increase in free fat in powders stored under conditions supporting lactose crystallisation has been observed by many. Saito (1985) noted that during the storage of whole milk powder in a humid atmosphere, a substance which was rather spherical in shape and had no sharp edges adhered to the surface of the powder. This deposit differed to that on the surface of skim milk powder and could be remove by washing with an organic solvent and by ashing. The deposit was proposed to be fat which had emerged from the interior of the particles. King (1965) also noted that when milk powder absorbs moisture and develops into a dry, hard and powdery texture, this coincides with the release of fat. At a critical moisture content, 8.9-9.2% fat was released for a powder with a fat content of 27-28%. Lactose crystallisation was observed during this time with a polarising microscope. The crystallisation ruptured the continuous mass of the SNF (solids not fat) and rendered the fat accessible to the solvents. Pearce (1992) stated that milk powders consist of spherical particles of amorphous lactose containing embedded casein micelles and fat globules. Under conditions where the amorphous lactose can crystallise, the protein, minerals and fat are excluded from the ordered structure of the crystals and are expelled. Faldt and Bergenstahl (1995) observed that in humid atmospheres, there is an almost complete release of encapsulated fats onto the powder surface during storage of lactose containing powders. This has previously been shown by electron spectroscopy. At a lactose/sodium caseinate ratio of 60/40, fat coverage of the powder surface is approximately 5%. After storage in a humid atmosphere, there is a release of fat and a surface coverage of 50% fat is obtained compared to an almost completely encapsulated fat phase before storage. Surface coverage of fat after storage in a humid atmosphere is 70-80% for powders with a lactose/sodium caseinate ratio of 99/1 and 95/5 (dry weight) [Fäldt and Bergenståhl 1996c].

There is general agreement that this phenomenon can be explained by the crystallisation of amorphous lactose to give crystalline lactose [King 1965, Saito 1985, Munns 1989, Pearce 1992, Fäldt and Bergenståhl 1994, Roos and Karel 1992, Fäldt and Bergenståhl 1996a,c]. The explanation is related to the glass-rubber transition where an increase in the water content, as occurs during storage in a humid atmosphere, results in a decrease in the glass transition temperature of lactose. This enables the amorphous lactose to begin crystallising and causes a phase separation between the lactose and protein. When fat is present, crystallisation of lactose causes stress on the fat globules inside the particles and forces the fat to spread to the powder surface. After lactose crystallisation has occurred, lactose crystals are not observed on the surface even when fat released onto the surface is limited [Saito 1985, Fäldt and Bergenståhl 1994, 1995, 1996a,c]. Fäldt and Bergenståhl (1996c) postulated that the presence of fat droplets inside the powder particles probably reduces the size of the lactose crystals. It has been shown that as the lactose concentration decreases, the amount of fat released after humid storage was reduced significantly and that for powders containing mass fractions of lactose of 0.05 and 0 (dry weight) there was no change in surface composition after humid storage [Fäldt and Bergenståhl 1996c]. This supports the theory given above. Fäldt and Bergenståhl (1995) also suggested that the crystallisation of lactose induces a change in the powder porosity which may contribute to the release of fat onto the powder surface. Buma (1971a) has shown there to be a correlation between free fat levels and porosity. Fat release (methyl linoleate) onto powder surfaces, due to lactose crystallisation, has also been observed in lactose/gelatin matrices after humid storage [Shimada *et al.* 1991].

Munns (1989) looked at the effect of temperature and moisture on caking of milk powders. It was found that as storage temperature increased the free fat level and the degree of caking increased considerably. An increase of 10% m/m free fat was detected when temperature increased from 30°C to 55°C. Also, an increase in moisture increased the free fat levels and the degree of caking. Under increasingly humid atmospheres (3.2 to 4.7% m/m) the free fat increased by approximately 25% m/m. It is unclear however, whether the increase in the degree of caking was due to an increase in free fat causing fat bridges or whether it was in fact due to amorphous lactose caking as described in section 2.2.2.3.

Crofskey (2000) investigated the cause of caking with spray dried cream powders. Some of this work used an air gun to fire powder particles at a wall in order to investigate particle-wall interactions. Both the amorphous lactose and fat melting mechanisms were looked at by determining the proportion of powder stuck to the wall under particular relative humidity and temperature conditions. When looking at the contribution of the fat melting mechanism towards caking with a low fat cream powder (LFCP), it was found that the effect was relatively constant up to 40°C and then increased linearly with temperature. This coincided with the surface fat content following the same trend where the surface fat content was constant from 20 to 40°C and then increased linearly with temperature above 40°C. Therefore, the percentage of powder stuck to the wall appeared to be proportional to the amount of surface fat present. Crofskey (2000) stated that this could possibly be explained by a surface tension related phenomenon involving the fat and particle surfaces. The surface tension of the fat decreases as the temperature increases. If the surface tension of the fat becomes equal to or less than the surface tension of the other particulate material, the fat is able to spread and flow over the surface of the particle. In the light of the above results, this critical surface tension point for LFCP is likely to occur around 40°C. Crofskey (2000) also stated that the flow may be accentuated by a decrease in fat viscosity as powder temperature increases. As the fat spreads, fat is able to move from the capillaries to the surface of the particle, thus increasing the total area of fat coverage.

The influence of temperature for a high fat cream powder (HFCP) was quite different. A significantly higher percentage of the powder stuck to the wall in general and the increase in the amount stuck occurred from 20 to 40°C, but remained fairly constant above 40°C. Crofskey (2000) used surface tension to explain this result. HFCP has a higher proportion of fat at the particle and capillary surface. When the critical surface tension is exceeded, as the temperature is increased above 40°C, the fat spreads over the surface. Due to the close proximity of the fat globules at the surface, a layer of fat is formed that covers the entire particle surface. Since there is a layer of fat present, increasing the temperature above 40°C does not show a further increase in sticking as the thickness of the fat layer is not likely to have an effect on the particle-wall interaction. Also, since there does not appear to be an increase in the surface fat content as the temperature is increased above 40°C, it appears that the fat does not flow from the capillaries to the particle surface. This is likely to be due to the particle surface being completely covered in fat.

The experimental work done in this chapter will look at flowability problems due to fatty liquid bridging and solidification as a result of temperature fluctuations. Increases in free fat due to lactose crystallisation will cause caking problems itself. In this case

the problem can be avoided by preventing lactose crystallisation and it is therefore irrelevant whether the increase in free fat causes further flowability problems.

6.4 CAKING EXPERIMENTS

6.4.1 Initial Work

The purpose of the initial work was to determine whether the fat played a significant role in the caking of dairy-based powders. Since the mechanism was proposed to be a fat melting and resolidifying mechanism it was necessary to expose a powder to temperature fluctuations. A low fat cream powder (LFCP), containing 55% milk fat, was used as it has been reported that there are sticking/smearing type problems with powders that contain this level of fat, especially during production. As a control, a skim milk powder (SMP) was used and exposed to the same conditions as the low fat cream powder. Samples of LFCP and SMP were placed over P_2O_5 for one week prior to experimentation and left over P_2O_5 while experiments were being conducted. Placing the samples over P_2O_5 ensured that amorphous lactose crystallisation would not occur and interfere with the results, as the T_g of amorphous lactose at the resulting water activity is 101°C [Brooks 2000].

After exposure to certain temperatures, the caking strength of the samples was measured using the blow test developed by Paterson *et al.* (2001). The samples were placed in a 4°C environment followed by exposure to 20°C. At this point half of the samples were exposed to 33°C followed by 20°C and then 4°C. The other half of the samples were exposed to 55°C followed by 20°C and then 4°C. The samples were left at each temperature overnight or longer before caking strength and free fat contents were measured. Under these conditions the free fat will be able to flow and possibly pool and

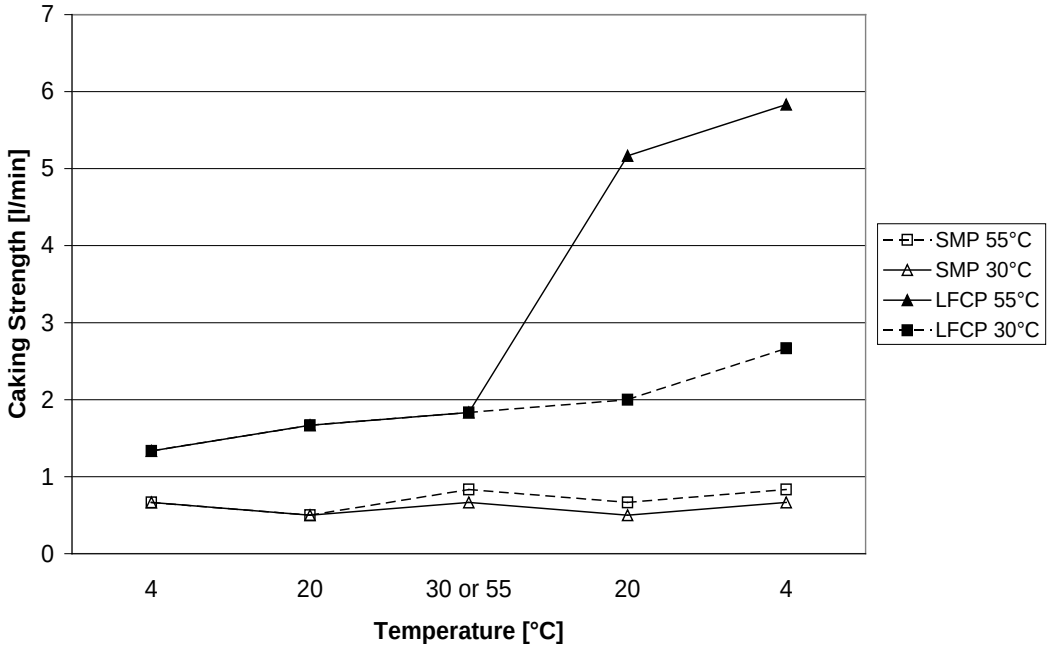

Figure 6.5: Change in caking strength with temperature for a low fat cream powder and a skim milk powder

then later crystallise when the temperature was decreased.

From figure 6.5 it can be seen that the skim milk powder shows no significant change in the caking strength with temperature fluctuations. This is expected since the powder contains around 0.8% fat and the water activity is low enough to prevent any changes originating from amorphous lactose. The low fat cream powder behaves differently. Increasing the temperature to 30 and 55°C shows a slight increase in caking strength. This is likely to be due to molten fat bridges or pooling occurring between particles. Referring to figure 6.2, since all milk fat is liquid at around 35°C, it is not surprising that no difference in caking strength was noted at these two temperatures. Dropping the temperature back to 20°C shows a further increase in the caking strength. This can be explained by crystallisation of some of the milk fat or solidification of the milk fat bridges. A further proportion of milk fat crystallises when the temperature is reduced to 4°C explaining the further increase in caking strength. At the time when performing these experiments it could not be explained why there was such a large increase in caking strength when the cream powder was cooled from 55°C compared to when it was cooled from 30°C. However, in the light of the work by Crofskey (2000), the increase in caking strength correlates to an increase in surface fat due to the surface tension and viscosity effects discussed in section 6.3. The free fat content was measured for these powders, as the method for measuring the surface fat content had not been developed. The free fat values do show that there was an increase in the readily available fat (i.e. the fat that can be extracted using petroleum spirit and a 5 min extraction time) at 55°C, compared to that measured at 30°C. This supports the theory given by Crofskey (2000). The measured free fat contents at 30 and 55°C were found to be 28.5 and 37.2g/100g dry powder respectively. It is noted however, that upon cooling to 4°C, the free fat contents for the powder after exposure to both 30 and 55 °C, were about the same (28.9g/100g dry powder).

6.4.1.1 Confocal Laser Scanning Microscopy

A confocal laser scanning microscope (CLSM) was used in order to detect whether pooling of fats had occurred particularly on the particle surfaces. Observations were made at 20°C before and after exposure to a higher temperature of 55°C. It was expected that there might be more evidence of pooling after exposure to higher storage temperatures due to more fat being present in the liquid state at these higher temperatures. McKenna (1997) investigated the applicability of several different mounting media for CLSM work. Glycerol and propylene glycol, which were investigated by McKenna (1997), were used and compared for observing fat in dairy-based powders. McKenna (1997) stated that the use of glycerol resulted in gradual dissolution of the powder and gave some background fluorescence in the presence of the dye Nile blue. Propylene glycol was a less viscous mounting media which resulted in streaming of the powder, although dissolution was slow. Nile blue was also used to stain the fat in the powders. Nile blue is non-fluorescent at the wavelengths used in confocal microscopy. However, it contains small amounts of Nile red which readily diffuse into the oil droplets allowing them to be imaged [Brooker 1995]. Fat crystals cannot be positively stained, as the dye is unable to penetrate the crystal lattice. Brooker (1995) stated that the crystals may be seen by negative contrast if there is a strong fluorescing and dominant oil phase in the background. Due to the presence of

other components such as lactose and proteins, such a technique could not be used to view the milk fat crystals.

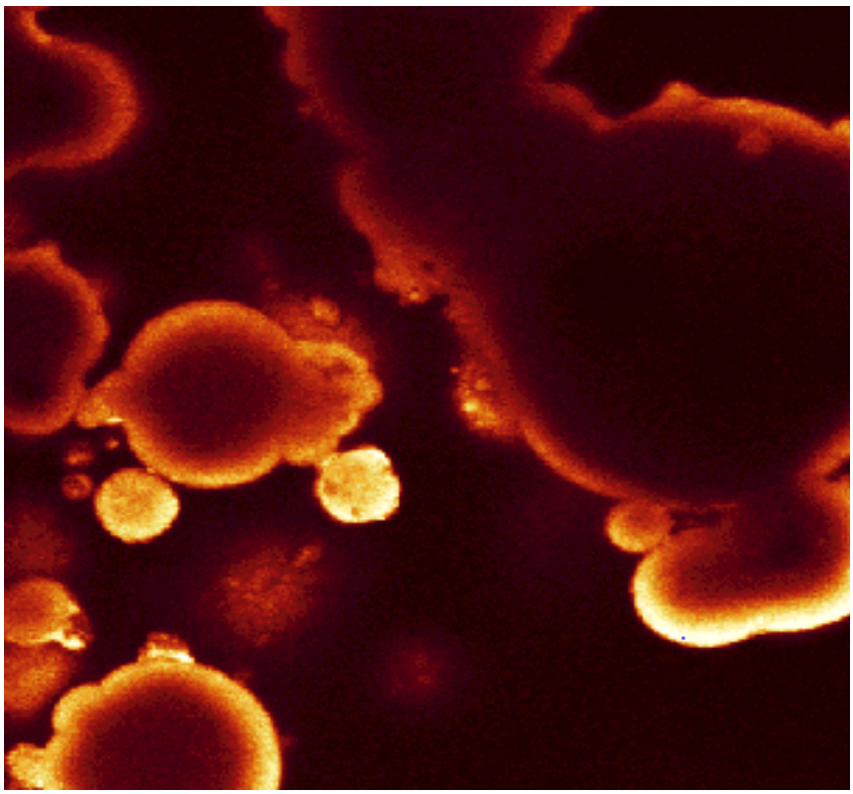

Figure 6.6: CLSM observation of fat bridging and pooling

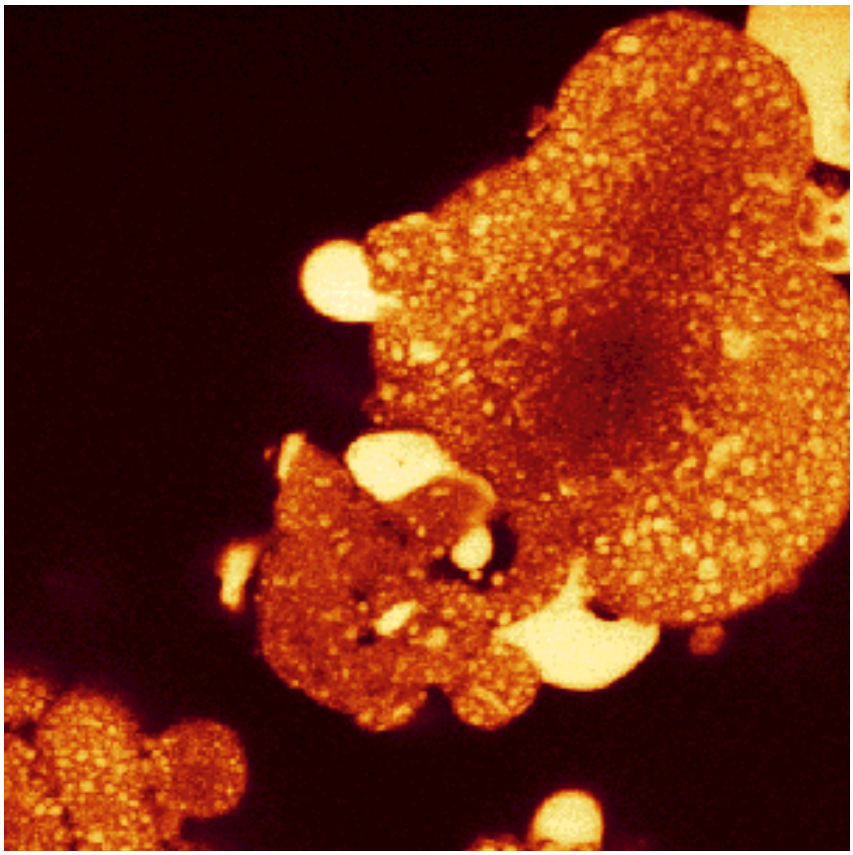

Figure 6.7: CLSM observation of fat pooling

The CLSM was used to observe pooling of fat in the low fat cream powder after it had been heated to 55°C and then stored at 20°C. Glycerol was used as the mounting media and Nile blue dye was used to stain the fat. Figures 6.6 and 6.7 show typical observations from photographing at a particular depth in the powder. Liquid fat appears as the stained yellow parts in these figures. Figure 6.6 shows some small areas of fat bridging and fat pooling and figure 6.7 shows areas of significant fat pooling in the low fat cream powder. Since the dye does not penetrate fat crystals, only liquid bridging can be seen using the CLSM. However, since around 80% of milk fat is molten at 20°C, there would be more evidence of liquid bridging than solid or partially crystalline bridging.

6.4.2 Surface Fat Measurement

Since sticking and caking problems are surface related phenomena, it is necessary to be able to measure the amount of fat at the particle surface. Although the typical method described in section 6.4.1 gives repeatable measurements of the free fat, it makes no distinction between the surface fat and free fat due to the extraction time used. Buma (1971a) found that 60-80% of the fat could be extracted in 10 minutes at room temperature. It is highly unlikely that this is all surface fat. Therefore a shorter extraction time is needed to measure the surface fat. Buma (1971d) noted that extraction times as short as 10 s or at most 1 min would be needed to measure the surface fat, but even in such a short time, it is possible that some of the fat may be represented by the outer layer and capillary fat. Buma (1971d) further stated that extraction for 10 min at room temperature probably yields free fat from the surface, outer layers and capillaries. Prolonged extractions would be needed to extract the dissolution fat. In the light of Buma's (1971b,d) results it was decided to investigate whether it was possible to make an estimation of the time needed to extract the surface fat.

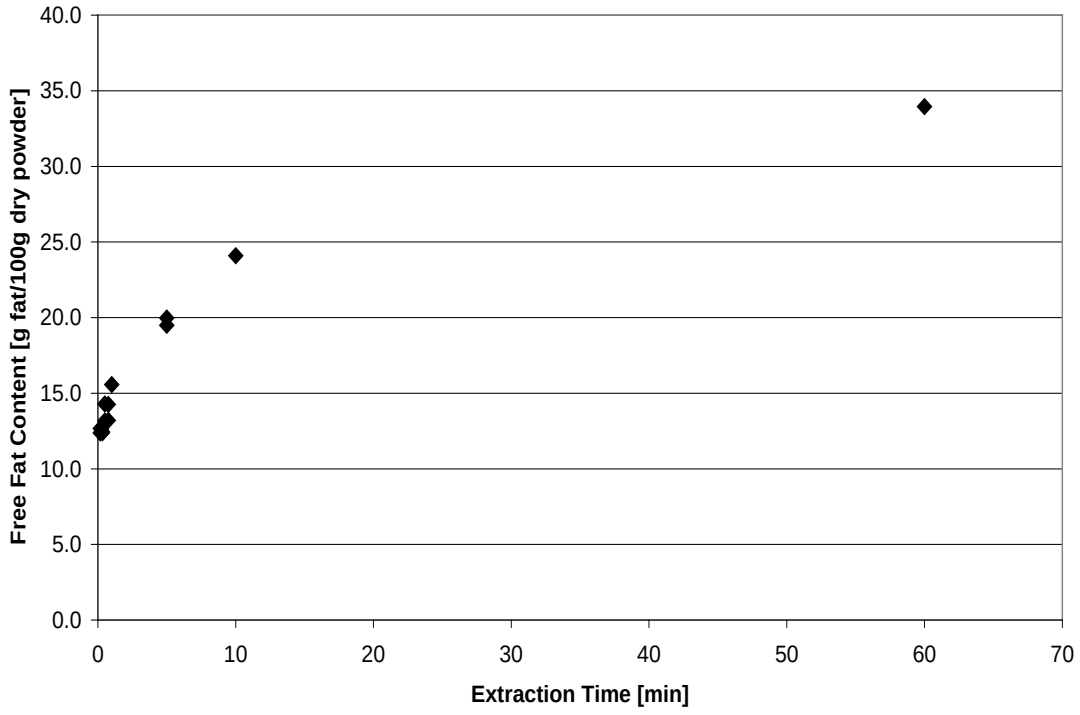

Figure 6.8: Free fat content versus extraction time for a low fat cream powder

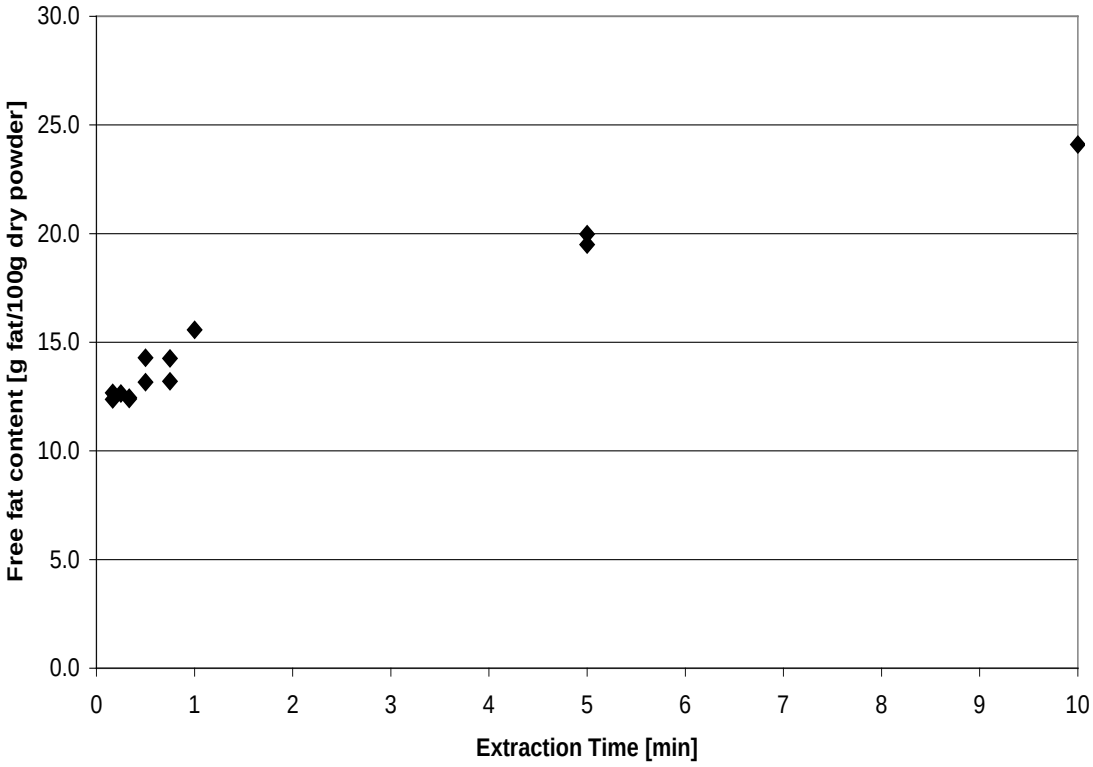

Figure 6.9: Free fat content versus extraction time (up to 10 minutes)

The free fat content of a low fat cream powder (containing around 55% total fat) was measured using a standard technique (adapted from the free fat content test given by Anchor Products (1997)) for varying extraction times. The standard method used was to wash around 8g of powder with 100 ml petroleum ether (boiling point 40 to 60°C) for the desired time. The solution was then filtered through Whatman No.1 filter paper. The filtration step took around 20 s to filter all of the solution. A quick wash of the glassware was done with 25 ml petroleum ether, which was also filtered. Filtration then continued for a further 5 minutes. The petroleum ether in the filtrate was then evaporated off using a rotary evaporator at 45°C and then further evaporated in an oven at 102°C for 2 hours or to constant weight. The free fat content was calculated as a percentage of the total mass of the powder sample. The powder used had been stored over P_2O_5 for around 3 weeks prior to testing and all extraction was done at room temperature.

Figures 6.8 and 6.9 show the free fat content measured at the different times. Figure 6.9 shows the free fat content measured with up to 10 minutes extraction time. It can be seen that the measured free fat content increases with the extraction time but is fairly constant up to an extraction time of 20s.

In the light of Buma's (1971d) recommendations and the results of this work it is clear that 10 s is an appropriate extraction time to use for approximating the amount of surface fat.

6.4.3 Relationship Between Total Fat and Surface Fat

Since fat related problems of stickiness in dairy powders is influenced only by the surface fat, a relationship between total fat and surface fat was needed in order to be able to predict the surface fat content of powders. Buma (1971d) looked at the relationship between total fat content and free fat content, as measured by a 10 minute extraction at room temperature. In particular, Buma looked at the total fat content and free fat content of homogenised and unhomogenised milk powders from cyclone and main spray dryer fractions. In homogenised cyclone and main powder fractions, the amount of free fat increased in the range of 30-60% total fat. For the main fraction, the increase began at around 45% total fat. Up until these total fat contents, the free fat content is constant and shows no change with total fat content. Buma (1971d) stated that when the fat content exceeds 40%, it is likely that the fat globules touch each other. This would have a dramatic effect on the free fat content, as measured in the traditional way, as it would be easier for solvents to reach fat in the interior of the particles via holes which have been left by dissolved fat globules which are touching in the outer layers [Buma 1971d]. The physical structure of the powder particles is formed during atomisation and subsequent drying of the milk droplets. Therefore, all process steps prior to atomization, with the exception of homogenization, as this may cause physico-chemical changes in the milk, are of minor importance when considering the amount of extractable fat in powders. [Buma 1971d].

It is expected that the relationship between total fat content and surface fat content will be similar to that between the total fat content and free fat content. In order to look at the relationship between the surface fat content and total fat content, several different powders were obtained with varying levels of fat. These powders have been made at different factories under different conditions and therefore it was expected that there will be differences in porosity related to the amount of free fat. Free fat content is also affected by particle size [Buma 1971c]. Therefore the particles size and specific surface

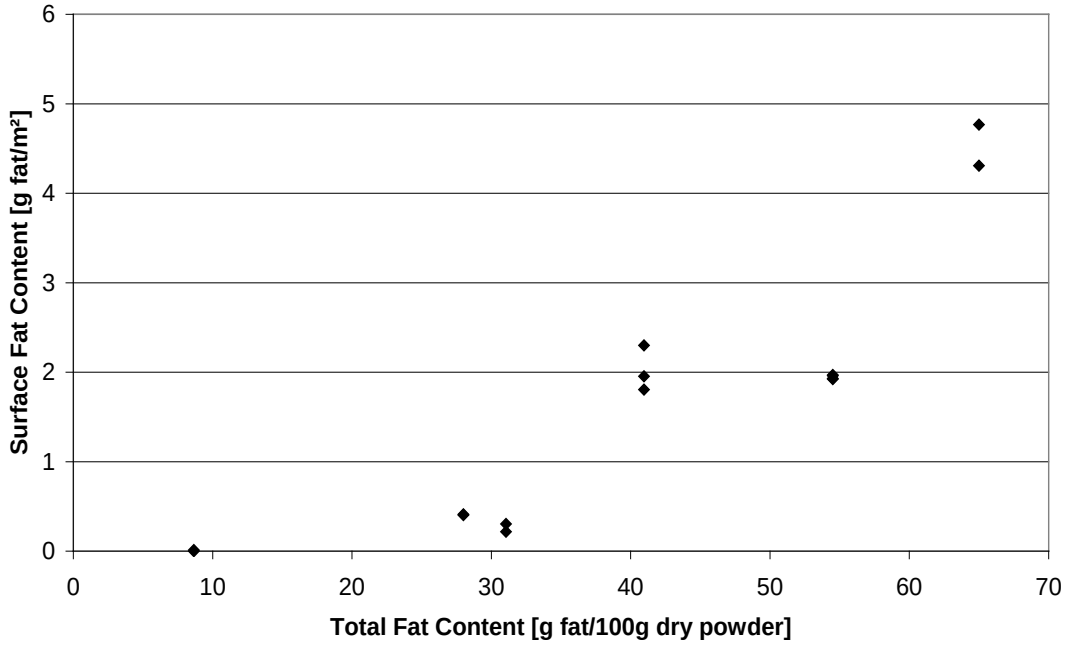

Figure 6.10: Relationship between total fat content and surface fat content expressed in terms of the specific surface area

areas of each of the powders were measured using a Malvern Mastersizer 2000 at Fonterra Research Centre (Palmerston North, New Zealand).

Table 6.2 shows the typical compositions of the powders used in this work. The powders were stored at room temperature over P_2O_5 for one month in order to prevent amorphous lactose crystallisation. The surface fat content was measured for each powder using the method described in section 6.4.2. The total fat content of each powder was measured using the Majonnier fat extraction procedure outlined in Horwitz (1980). This method involves dissolution of the powder in water and the addition of ammonium hydroxide, ethyl alcohol, diethyl ether and petroleum ether. Figure 6.10 shows the relationship between the total fat content and the surface fat content when expressed in terms of the specific surface area (particle size). It can be seen that the surface fat content only begins to increase when the total fat content is over 30%. The relationship is also fairly linear and it appears that the total fat content and specific surface area (i.e. particle size) can be used to estimate the surface fat content. It does not appear that the non-fat composition or manufacturing techniques account for very much of the relationship.

6.4.4 Caking Experiments

The objective of the following work was to determine the caking potential of the liquid fat as it flows and forms liquid bridges, and the increase in caking strength as these liquid bridges solidify.

6.4.4.1 Powder Selection

In order to use this information in a model, it needs to be applicable to all powders, therefore it was necessary to perform similar experiments on a selection of powders with differing fat contents. The following powders were selected as they had varying fat contents but contained other normal components, i.e. they do not include speciality ingredients such as sucrose or cocoa powder. Table 6.2 outlines the approximate compositions of the dairy powders as supplied by Fonterra (Auckland, New Zealand).

Table 6.2: Compositional and specific surface area data for powders used in caking experiments

	Milk fat (%)	Lactose (%)	Protein (%)	Surface Fat Content (g/g)	Specific Surface Area (m^2/g)
High fat cream powder (HFCP)	71	12	11	0.341	0.075
Low fat cream powder (LFCP)	55	23	16	0.126	0.064
Cheese powder 1 (CP1)	42	28	19	0.235	0.116
Cheese powder 2 (CP2)	32	34	20	0.041	0.158
Whole milk powder (WMP)	28	37	27	0.020	0.049
Buttermilk powder (BMP)	9	46	35	0.001	0.132
Skim milk powder (SMP)	0.8	49	39	0.000	0.072

6.4.4.2 Method

This work was performed in the reverse flow packed bed as described in Brooks (2000). The rig was operated without water in the columns and by heating air from the compressed air lines. The heated air was directed to the reverse flow bed, where the temperature and relative humidity of the incoming air were recorded. At the start of the run, the apparatus was heated to the desired temperature, which was above the final melting point of the milk fat in the powder. The powder to be tested was smoothed over the testing chamber and the apparatus put back together with the airflow off. The airflow was then redirected back through the bed at which point timing commenced. The caking strength was measured using the modified blow test as described in section 5.3.3.1. Caking strength measurements were taken with time during the high temperature stage. The bed was kept at the higher temperature for approximately two hours. It is likely that the liquid bridges formed during the first few minutes once the powder bed had reached the high temperature. After a period at a high temperature the bed was then cooled down to ambient temperatures by turning off the heating of the air stream. During this time the caking strength was measured and readings for temperature and relative humidity of the incoming air were recorded. Measurements continued to be taken until the caking strength was constant indicating that the crystallisation of the liquid milk fat bridges had concluded.

Initial trials gave a large amount of scatter and it was difficult to reproduce data. This problem was later eliminated by using a standard packing procedure when setting up the testing chamber. Packing involved pouring powder over the distributor plate, tapping five times on a table, turning the plate 90° and tapping a further five times. The powder was then smoothed over the plate with a ruler removing the excess powder. This packing procedure gave a more repeatable experimental technique, which allowed the investigation of further factors, which might have affected the results.

The following factors were also investigated in order to establish a standard testing method. The effect of the air flow rate used through the packed bed was tested by using similar temperatures and packing procedures but flow rates of 3 and 6 l/min. It was expected that the temperature the powder was heated to above the final melting temperature of the milk fat would have no effect. This was checked by heating the powder to a temperature above the final melting temperature of the milk fat in the packed bed while using a standard packing procedure and keeping the flow rate constant. To determine whether the temperature the powder was heated to affected the results, the powder was heated to various temperatures between 40 and 55°C. The caking strength was measured with time over this period. Turning off the heating of the incoming air stream allowed the temperature through the bed to decrease with time to ambient temperatures. The caking strength continued to be measured with time until constant along with temperature and relative humidity readings in the packed bed arrangement. It is noted that heating the powder to above the final melting temperature of the milk fat allows the removal of the thermal history of the fat in the powder. Also, to ensure that the location on the plate at which the readings were taken did not have any effect, the positions of the readings were randomised.

6.4.4.3 Results and Discussion

The effect of the air flow rate used and the temperature that the powder was heated to on the eventual development of fatty bridging are shown in figure 6.11. It can be seen that there was no effect from either factor. In the light of Crofskey's (2000) work it could be expected that the temperature should have had some effect. Unfortunately, this work was done well before the work by Crofskey (2000), and this factor was not considered to be of too much importance at the time, therefore no further work looked at this factor.

There was no significant increase in the caking strength found with any powder during the initial stage where the temperature of the powder bed was above the final melting point of the milk fat. An increase in the caking strength was only found when the temperature through the bed was later decreased to room temperature or lower as seen in figure 6.12. The increase in caking strength with time as the temperature through the bed was decreased can be attributed to the crystallisation of the milk fat in the liquid bridges formed during the high temperature stage, giving rise to partially solid bridges. Crystallisation of milk fat is a function of temperature and time; therefore during the cooling stage the caking strength of the powder cannot be directly related to the temperature at that particular time. The caking strength can only be related to temperature once equilibrium has been reached at a specific temperature, as has occurred at the end of each experiment.

At the end of each experiment the powder had reached an equilibrium since the bed temperature was constant and milk fat crystallisation had concluded. The final caking strength of the powder could then be related to the amount of surface fat on the powder and the temperature that the powder has decreased to, after being at a temperature above the final melting point of the milk fat. Using the solid fat content profile given in figure 6.2, an overall comparison is given in figure 6.13. Figure 6.13 shows the final caking

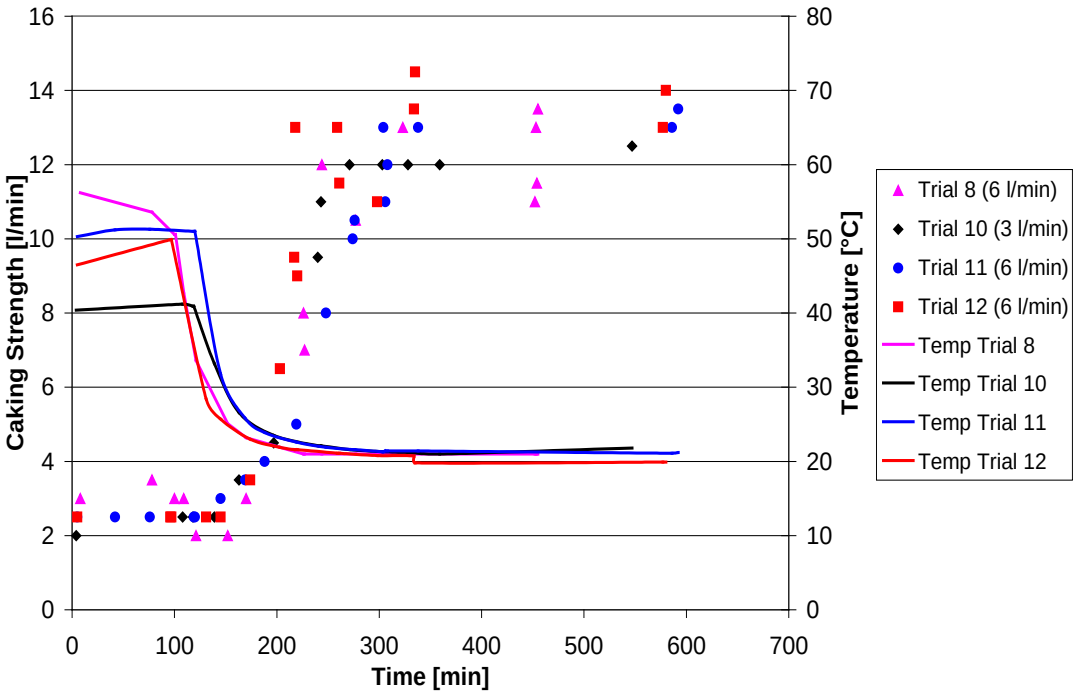

Figure 6.11: Effect of heating temperature and flow rate

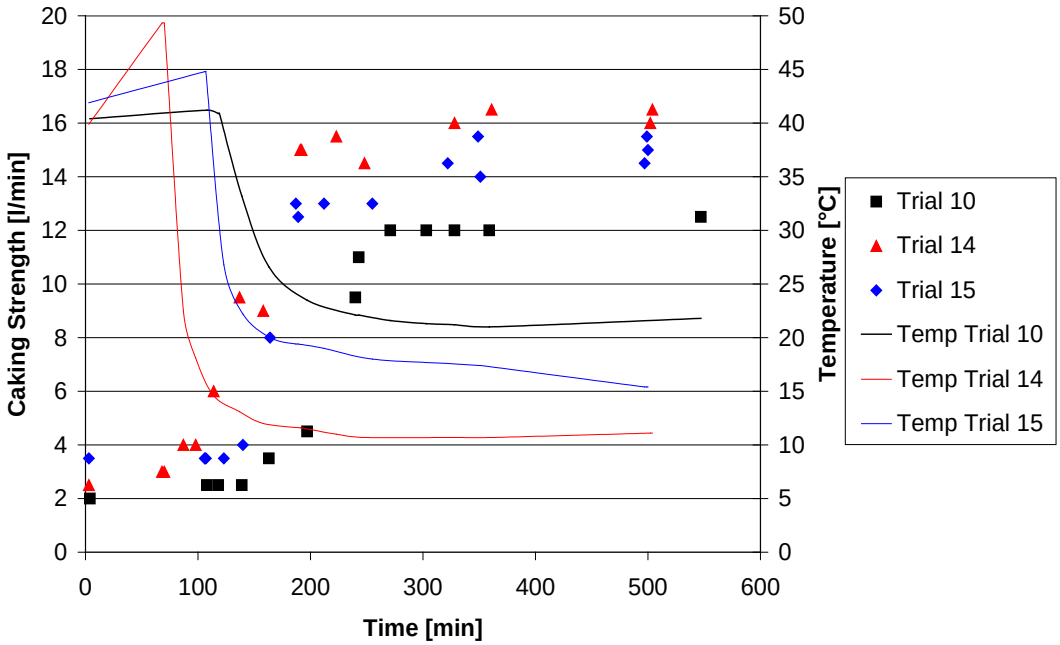

Figure 6.12: Relationship between caking strength and temperature powder cooled to for a low fat cream powder

strength of the different powders, related to the amount of surface fat and the temperature that the powder were cooled to. These two parameters are combined and presented as the amount of surface fat which had been in the liquid state (as had occurred when the powder was heated above the final melting point of the milk fat) and had then crystallised due to a decrease in powder temperature. Although the melting profile of milk fat shows seasonal variations, an approximation of the melting profile of the milk fat in the powders was made using the average solid fat content data in figure 6.2. Figure 6.13 shows that there is a strong relationship between the solidified surface

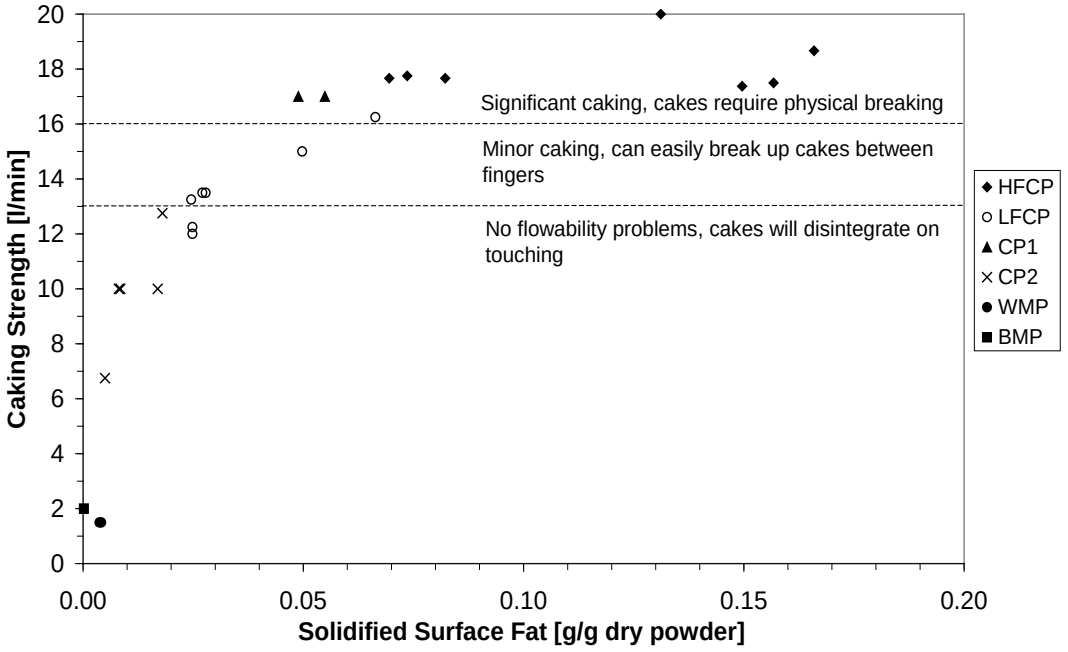

Figure 6.13: Overall comparison between solidified surface fat content and caking strength of various powders

fat content and the caking strength of the powder. Since a variety of dairy powders, manufactured at various dairy companies, were used in this work it shows that the relationship is unaffected by the non-fat compositions of the powders. Figure 6.13 also highlights the fact that it requires a high level of milk fat to be present before caking due to the milk fat is a problem. Of all the powders tested the three powders with the highest milk fat contents experienced significant caking problems. These are the high and low fat cream powders (HFCP and LFCP) and cheese powder 1 (CP1), of which there have been customer complaints with regard to caking. The total fat contents of these powders were measured to be 65.0, 54.5 and 42.0% respectively, as given in table 6.2. Considering the surface fat content as an indicator of whether a powder is going to have caking problems, a surface fat content of 1.95g fat/m² or 0.126g fat/g powder is required, as taken from table 6.2.

Using the typical solid fat content data to analyse this work requires that the surface fat composition is the same as the total fat composition. This can be determined by comparing the DSC melting profiles for both the surface fat and total fat for a given powder. Figures 6.14 and 6.15 show comparisons of the surface and total fat for CP1 and HFCP. It can be seen that the DSC thermograms for the surface and total fat contents are very similar, with both showing three melting fractions. The thermograms indicate that the compositions of the surface fat and total fat are similar. Therefore, any further analysis can use the composition of the total fat to approximate that of the fat at the surface. Using this analysis also assumes that the fat compositions for all powders are the same. This requires that no fractions of fat have been removed from the fat component of any of the ingredients for the particular powder. Discussion with Philpot (2000) gave assurance that the fat compositions in each of the powders should be the same, as no fractionation is used. This can also be checked by comparing the DSC profiles of the fat component for each powder. The DSC profiles were obtained by heating the extracted fat samples to a temperature above the final melting point (55°C), and then cooling to -50°C. The samples were then rescanned at 5°C/min and the

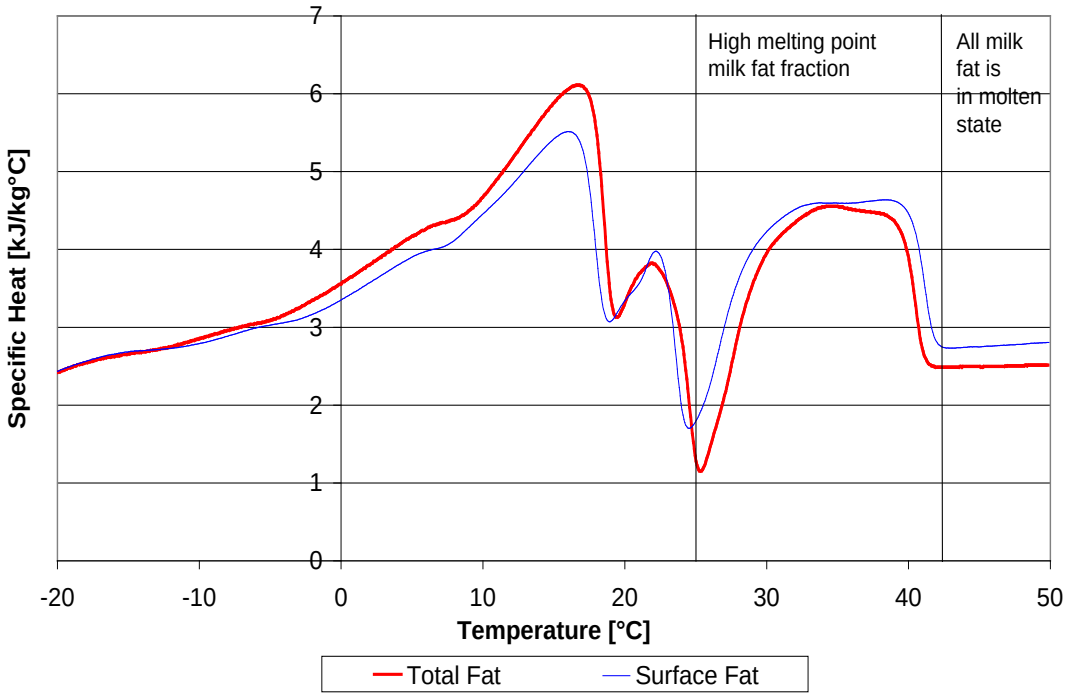

Figure 6.14: DSC profiles for fat extracted from cheese powder 1

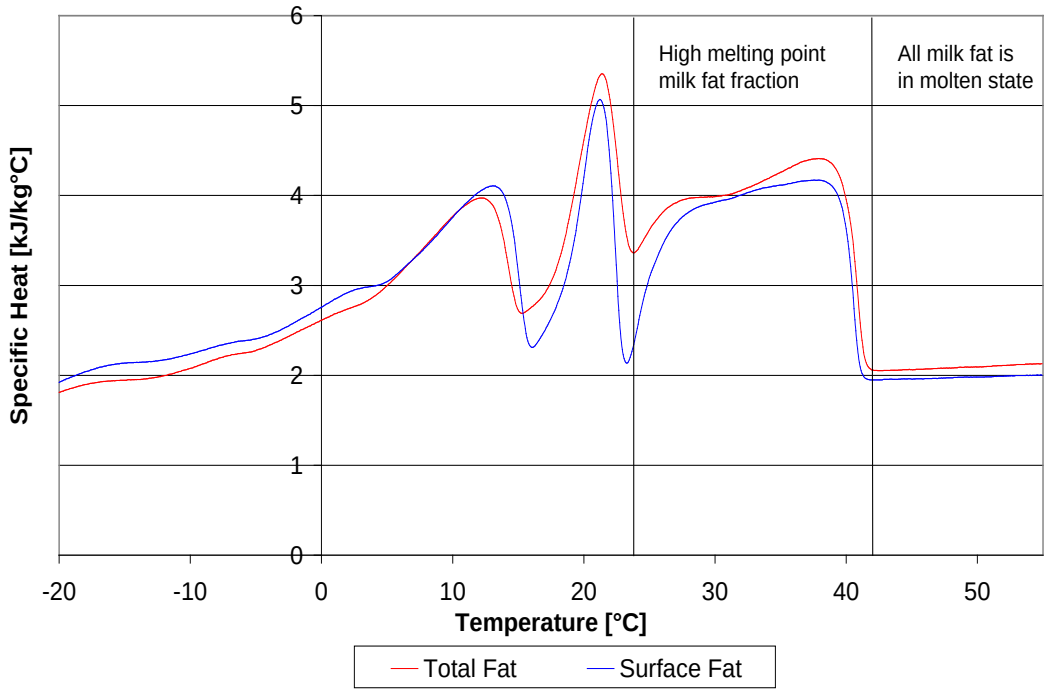

Figure 6.15: DSC profile for fat extracted from a high fat cream powder

resulting DSC curve is given in figures 6.14 and 6.15, after the data had been corrected for the sample mass and the scanning rate used. Comparing the DSC profiles for HFCP and CP1, it can be seen that there are some differences in the curves. Although the melting curves for the high temperature melting part of the milk fat are comparable, the other two melting peaks are not. This indicates that the melting profiles for the different powders may be different. It is possible that the samples were not left at the low temperature for a sufficient time to allow milk fat crystallisation to occur. It is likely that the high melting fraction would have completely crystallised, but there is less confidence that complete crystallisation would have occurred for the lower melting fractions. If this is the case, then the melting profiles for the lower melting fractions would not be as prominent as they would be if crystallisation had been complete. With this in mind, it is not correct to conclude that the milk fat compositions in the two powders are different after comparing the DSC melting profiles. Also, since no fractionation of the milk fat was done on any of the raw materials for the powders, it is reasonable to assume that the milk fat composition was the same in all powders. Furthermore, under normal storage conditions, the high melting point fraction will be the fraction that experiences the most changes in its state (i.e. solid to molten to solid fat and so forth) and this fraction is comparable between powders. It is noted that both the surface and total fat samples used in the DSC work were obtained during the surface and total fat content determinations. This requires that all of the total fat is removed from the powder during the extraction. Since the curve for the surface fat and total fat are the same, this indicates that all the fat was extracted, which gives confidence in the total fat content measurement used.

Work was done for Anchor Products, Waitoa to investigate the cause of caking in a dairy base powder [Foster and Paterson 2001]. Two different cyphers were used to investigate whether the amorphous lactose and/or fat components were contributing to caking with this powder. To determine the contribution of the fat, experiments almost identical to those described in section 6.4.4.2 were performed. The surface fat contents

and total fat contents were also measured and were found to be 1.39 and 1.06 % surface fat (total mass basis) and 36.17 and 35.70 % total fat (total mass basis) for the two cyphers respectively. This powder contained a mixture of milk fat and coconut oil (~ 1:1 mix) therefore a melting profile for the powder was needed. The melting profile, obtained using the DSC in a similar fashion to the work described above, showed that all fat was in the molten state at about 30°C. With this in mind the powder was heated to just below 40°C during the heating stage and then cooled to room temperature to allow crystallisation. After these tests the powder was found to still be very free flowing indicating that the fat did not contribute to caking with this powder. In comparison to the dairy powders used in the previous work, this dairy base powder had a very low surface fat content. When comparing the caking behaviour of this powder to the other dairy powders, it would be expected, based on the surface fat content, that caking due to the fat component would be insignificant. Based on the total fat content, it could be expected that some degree of caking would occur due to the fat, but this was not seen to be the case. From this work it is suggested that the surface fat content be used directly to determine whether the fat is likely to cause caking problems with a dairy powder.

6.5 CLOSURE

This work has shown that sticking and caking problems due to the milk fat in dairy powders during storage occurs through the fat melting mechanism. Caking problems due to the milk fat are only significant when the total fat content is high and consequently there is a high level of surface fat. Significant caking was observed only in powders with a total fat content of greater than or equal to 42% which related to a surface fat content of 0.235g fat/g powder or 1.95g/m^2 when the particle size and hence surface area is considered. A linear relationship was found between the total fat content and the surface fat content expressed in terms of the specific surface area. The surface fat content can therefore be estimated from the total fat content and the particle size (specific surface area). Also, the relationship shows that the surface fat content is not significantly affected by the non-fat components in the powder or the processing conditions, provided care is taken to ensure the amorphous lactose present cannot crystallise.

The sticking and caking behaviour of the amorphous sugars and milk fat have been investigated. The prediction of isotherms and T_g profiles for dairy powder components are given in chapters 3 and 4 along with methods for predicting isotherms and T_g profiles for multicomponent powders. The following chapter puts together the information gathered to this point in the form of a model. The use of this model and its validation is the subject of chapter 7.

CHAPTER 7

PREDICTION OF STICKING AND CAKING CONDITIONS IN DAIRY POWDERS

7.1 INTRODUCTION

This chapter combines the information gathered to this point, for use in the prediction of sticking conditions in dairy powders. Sticking is related to the T-T_g of the powder, as shown in chapter 5 for amorphous sucrose, maltose, glucose, galactose and fructose. This has also been shown previously for amorphous lactose [Brooks 2000]. Since the rate of sticking can be directly related to the T-T_g of the powder, it is important that the T_g of the powder can be accurately predicted. This was investigated in chapter 4 and a method for predicting the T_g of a multicomponent powder was discussed. This method requires accurate T_g profiles for the amorphous sugars. These profiles were determined in section 4.3 and equations for their prediction were given. The prediction of the T_g can be made from both the water activity and the moisture content. If the T_g is to be predicted from the moisture content of a multicomponent powder, then a method for predicting the moisture associated with the T_g affecting components, i.e. the amorphous sugars, is needed. A simple additive approach for predicting the isotherm and hence the moisture associated with the amorphous sugars was found to be adequate in chapter 3. Knowing the moisture associated with the amorphous sugars, from either the moisture content or the water activity, allows the T_g of the powder to be predicted. This chapter demonstrates the use of these predictive equations and investigates the accuracy of the prediction methods used. Also investigated is the sticking of a number of dairy powders. This has been done to allow an appropriate T-T_g for avoiding sticking during drying to be recommended.

7.2 STICKING PREDICTION MODEL

The model uses the isotherm equations for the components given in section 3.3 and the equations for predicting the T_g profiles for the amorphous sugars from water activity, given in section 4.3. Table 7.1 summarises the isotherm prediction information for the components where the GAB isotherm model has been used (equation 3.6). The isotherm for crystalline lactose (α-lactose monohydrate) is to be predicted by the tss equation (2.7-2.9). The parameters M_o, f, c and h are 0.025 g/100g dry lactose, 0.92, 8.8 and 30 respectively [$0 \le a_w \le 1$]. The isotherm for cocoa powder is predicted using a polynomial equation, where $M = 0.053 + 32.02\ a_w - 102.71\ a_w^2 + 158.01\ a_w^3 - 61.64\ a_w^4$ [$0 \le a_w \le 0.9$].

Table 7.2 summarises the equations for predicting the T_g for each component, from the water activity of the powder. The T_g will be predicted using either the combined isotherm/Gordon and Taylor equation or a polynomial equation ($T_g = a + b a_w + c a_w^2 + d a_w^3 \ldots$). If the combined isotherm/Gordon and Taylor equation is to be used, then the appropriate GAB constants for the amorphous sugar should be taken from table 7.1.

Table 7.1: GAB constants for components

Component	M_o (g/100g)	f	C	Range of use
Whey protein	8.358	0.774	9.630	$0 \le a_w \le 0.9$
Casein	8.908	0.690	9.471	$0 \le a_w \le 0.9$
Amorphous lactose[1]	6.27	1.01	2.81	$0 \le a_w \le 0.5$
Amorphous sucrose	8.017	0.988	2.256	$0 \le a_w \le 1$
Amorphous maltose	97.445	0.611	0.167	$0 \le a_w \le 1$
Amorphous glucose	5.148	1.411	4.014	$0 \le a_w \le 0.43$
Amorphous galactose[2]	5.148	1.411	4.014	$0 \le a_w \le 0.43$
Amorphous fructose	32.059	0.893	0.271	$0 \le a_w \le 0.66$
	316.398	0.566	0.076	$0.66 < a_w \le 1$
Crystalline sucrose	0.0127	1.097	14.679	$0 \le a_w \le 0.84$
Crystalline glucose	6.341	0.923	0.151	$0 \le a_w \le 1$
Crystalline galactose	0.567	0.817	0.0197	$0 \le a_w \le 1$
Crystalline fructose	0.0178	1.455	1.533	$0 \le a_w \le 0.59$

[1]Brooks (2000)
[2]assumed to be the same as amorphous glucose

Table 7.2: T_g prediction information for amorphous sugars (predicted from water activity)

Sugar	Prediction method	Constants	Range of use
Amorphous lactose[1]	Cubic equation (Use T_g = 101°C at a_w=0)	a = 99.458 b = -366.33 c = 652.06 d = -530.66	$0 < a_w \le 0.575$
Amorphous sucrose	Isotherm/Gordon and Taylor	T_{g1} = 56.5°C k = 4.51	$0 \le a_w \le 1$
Amorphous maltose	Cubic equation (Use T_g = 91.2°C at a_w=0)	a = 86.12 b = -212.73 c = 102.19 d = -49.66	$0 \le a_w \le 1$
Amorphous glucose	Isotherm/Gordon and Taylor	T_{g1} = 33.7°C k = 4.08	$0 \le a_w \le 0.65$
Amorphous galactose	Isotherm/Gordon and Taylor	T_{g1} = 30.0°C k = 3.58	$0 \le a_w \le 0.65$
Amorphous fructose	Isotherm/Gordon and Taylor	T_{g1} = 5.0°C k = 3.08	$0 \le a_w \le 1$

[1]Brooks (2000)

A model was developed for predicting the water activity and moisture content of a powder given the composition and the maximum storage temperature that the powder will experience during storage. This model is provided on CD at the end of the appendix. A guide for using the model is given in appendix A3. The following provides a step by step guide as to how the model works, for calculating the water activity, moisture content and T_g of a multicomponent powder. The inputs to the model are the composition and the maximum likely temperature that the powder will reach during storage.

If the T_g of a powder is required, where the composition is known (either on a dry or wet mass basis), then the T_g can be predicted directly from the water activity using the weighted addition of the T_g equations given above. If the T_g of a powder is to be predicted from the moisture content of the powder, then the isotherm needs to be

predicted so that the water activity of the powder, at the given moisture content, can be determined. Once the water activity is known, the T_g can be predicted from the weighted addition of the T_g values for each amorphous sugar in the powder. The T_g is again calculated from the water activity using the equations given in table 7.2. It is noted that most of the equations in table 7.2 use the combined isotherm/Gordon and Taylor approach. Once the water activity of the powder is known, then the isotherm for each component is used to determine the moisture that would be associated with each amorphous sugar. The moisture content calculated here is the moisture that would be associated with that amorphous sugar component if it were the only component of the powder. The actual moisture that is associated with the amorphous sugar component in the powder is the amount of moisture calculated from the isotherm multiplied by the mass fraction (dry mass basis) in which the component is present in the powder. When determining the T_g from the Gordon and Taylor equation, the moisture content for the component is used as if it was the only component of the powder. It is noted that the model has been set up in two ways, the first where the composition is entered on a total mass basis and the second where the composition is entered on a dry mass basis.

This model can also be used to predict the water activity and hence moisture content that the powder should be dried to, in order to prevent sticking and caking problems during storage. In order to do this, the model requires that the maximum likely temperature that the powder will be exposed to during storage be entered. The model will then calculate the water activity and hence moisture content of the powder so that the T_g of the powder is slightly less than the maximum storage temperature. A safety margin of 5°C has been used, so the model will calculate the T_g for the powder so that the maximum $T-T_g$ during storage is –5°C. If the powder is dried to an extent such that it will only ever experience temperature conditions that are less than the T_g of the powder, then sticking and caking problems due to the amorphous sugar sticking mechanism will not be encountered. This is provided it does not undergo extensive temperature gradients which can cause moisture to migrate through the powder [Bronlund 1997].

The model can be further used to determine combinations of temperature and relative humidity that can be used during drying. This requires that a $T-T_g$ for instantaneous sticking be entered. The model will then use a safety margin of 10°C and determine temperature and relatively humidity combinations such that the T_g of the powder is always 10°C above the temperature at the powder surface. It has been estimated that the powder surface will generally be about 10°C below the temperature of the air during drying [Buma 1970].

The concepts described above are demonstrated in the following section using a number of dairy powders. Validation of the concepts used in the model will be given for these powders. Further work has also been done to investigate the $T-T_g$ that is required for instantaneous sticking during processing.

7.3 MODEL VALIDATION

The validation of the model has been carried out in two parts, using six different dairy powders, of which most have added sugars. The first part of the model validation was for predicting the isotherms of the powders. The second involved the prediction of the T_g for the powders. Lastly, some stickiness work has been done to determine the $T\text{-}T_g$ required for instantaneous sticking, as this is required for determining temperature and relative humidity conditions that can be used during processing.

Six dairy powders were obtained from Fonterra Co-operative Group Limited (Auckland, New Zealand). These powders were made at different sites throughout New Zealand and their compositions are given in table 7.3. The dairy companies provided the protein and fat contents given from tests performed on site. The sugar composition was measured by gas chromatography at Fonterra Research Centre (Palmerston North, New Zealand). The moisture contents of the powder samples were determined gravimetrically, after desiccation over phosphorous pentoxide for three weeks. The mineral content was taken from the powder specification sheet and the cocoa content for two powders was assumed to be the remaining amount.

Table 7.3: Compositions of powders used for validation work

Component	Mass fraction (g/100g Powder)					
	Powder 1	Powder 2	Powder 3	Powder 4	Powder 5[1]	Powder 6[1]
Fat	7.4	6.3	28.2	1.1	12.3	11.9
Protein	32.2	29.7	13.4	35.6	33.0	37.5
Lactose	47.0	42.1	14.6	50.5	18.6	1.0
Sucrose		2.7[2]	32.6[3]			
Glucose					8.8	16.6
Galactose					4.9	12.0
Fructose	1.0[2]	4.2[2]				0.1
Minerals[4]	8.2	9.0	7.0	9.1	7.2	7.2
Cocoa[5]		3.3	2.8			
Moisture	2.9	2.9	1.4	2.3	1.5	1.8
Undetermined Disaccharides					5.5	6.5
Undetermined Trisaccharides					4.9	2.6
Undetermined[6]	1.4			1.3	3.4	2.9

[1]Hydrolysed lactose powders
[2]Present in crystalline form (had been dry blended in with spray dried powder)
[3]Part added to concentrate prior to spray drying (44%) and remainder is milled sucrose, which is added into the vibrating fluid bed or external fluid bed (56%).
[4]Taken from specification sheets
[5]Determined as being the remaining part of the powder
[6]Undetermined fraction, not accounted for by composition information given

The powders were analysed for the sugars lactose, sucrose, maltose, glucose, galactose and fructose. The total disaccharides, total trisaccharides and total sugar contents were determined using gas chromatography. It is noted that in some cases, there were large discrepancies between the individual sugar contents given and the total disaccharide, tisaccharide and sugar contents determined. This was found for powders 5 and 6. These powders have had part or most of the lactose hydrolysed to glucose and galactose. It appears that during the hydrolysis of lactose, a significant amount of other

sugars also formed, hence the undetermined disaccharide and trisaccharide contents. There is no way of knowing, without further analysis, what these other components are likely to be. When predicting the isotherms, the mass fraction of each component was given on a dry mass basis where the undetermined disaccharide and trisaccharide content was ignored, i.e. it was assumed that the powder was only made up of the components that had been quantified. When predicting the T_g profiles, the mass fraction of each amorphous sugar was used on a dry mass basis. Again, the undetermined components were ignored.

7.3.1 Prediction of Isotherms

Isotherms for each powder were measured by placing over saturated salt solutions for three weeks (powders 3 to 6) or 6 weeks (powders 1 and 2) and measuring the change in weight, as discussed in section 3.2.1. The isotherms were measured up to a water activity of 0.54. Above this water activity it was expected that amorphous lactose crystallisation would have occurred [Bronlund 1997], therefore making moisture content measurements above this water activity of no use. Also, the prediction equation for the isotherm for amorphous lactose is only valid up to $0.5a_w$. When other sugars are present in the amorphous form, it is expected that crystallisation would occur at a lower water activity as a result of the lower T_g profile for the powder.

The isotherms were predicted for each powder using equation 3.13 and the information given in table 7.1. The mass fraction of each component, on a dry mass basis, was used in equation 3.13. Figure 7.1 shows the predicted and measured isotherms for powder 3, with 10% error bars on the measured isotherm data. As shown in table 7.3, powder 3 comprises sucrose and a dairy powder. Some of the sucrose is added to the concentrate prior to drying and the rest is milled sucrose, which is added to the fluid beds. The fraction that was added to the concentrate would have been present in the amorphous form in the final powder. The remaining fraction would have been present in the

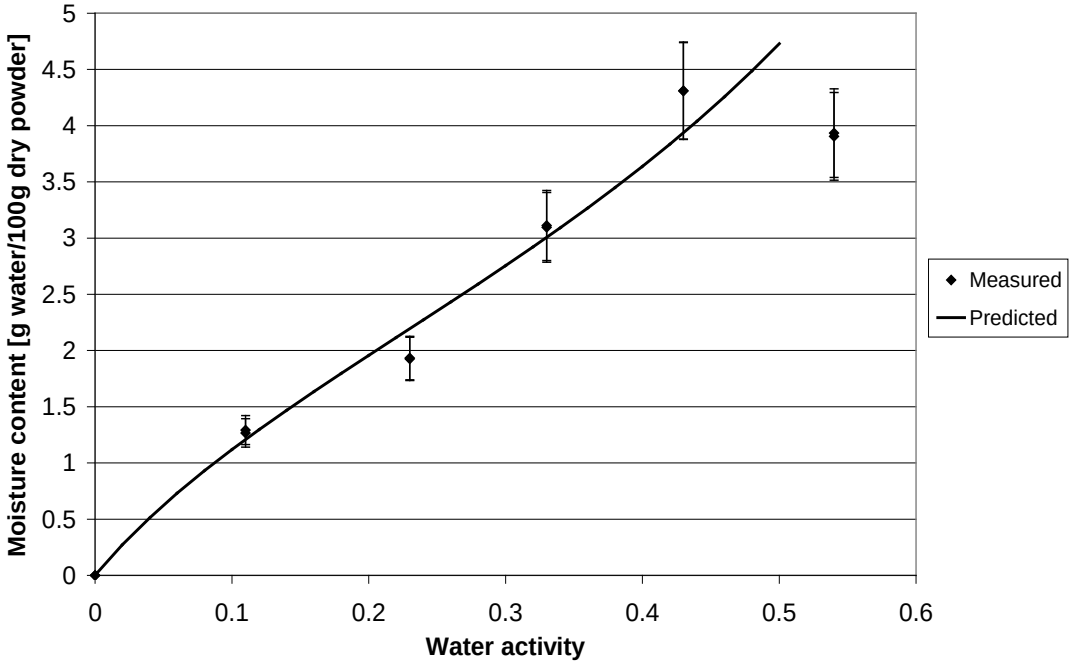

Figure 7.1: Comparison of predicted and measured isotherms for powder 3

crystalline form although it is possible that there may have been a small amount of amorphous sucrose in the milled sucrose. This is due to the high temperatures experienced at the point where the powder particles break during milling [Roth 1976]. This temperature melts the sugar at the breaking point. Rapid cooling of the sugar melt can then results in the formation of an amorphous sugar. This has not been accounted for as it is unknown what the milled amorphous sucrose content may be. It is also possible that the milled sucrose had been conditioned prior to being bagged. This would have resulted in the crystallisation of any amorphous sucrose at the surface, therefore there would be no amorphous sucrose in the sugar added to the fluid beds. It can be seen that there is good agreement between the measured and predicted isotherms, within 10% error, except for the moisture content taken at $0.23a_w$. This moisture content is lower than that predicted by the model. The moisture content measured at $0.23a_w$ is also substantially lower than the predicted moisture content for powders 4, 5 and 6 also. This may indicate that equilibrium had not been reach for these powders at $0.23a_w$. The powders were stored over the salt solutions for 3 weeks for the isotherm as recommended by Bell and Labuza (2000). T_g data on powders that had been stored for 6 weeks and longer show that equilibration had been reached by the longer storage times.

Figure 7.1 also shows a drop in the isotherm at $0.54a_w$, which is due to the crystallisation of the amorphous sugars (lactose and sucrose). Amorphous sugar crystallisation can also be seen for powders 1, 2 and 4, as shown in appendix A3. Crystallisation occurs at a lower water activity for powders 1 and 2 ($0.43a_w$ as opposed to $0.54a_w$ for powders 3 and 4), which is likely to be due to the longer equilibration times used for these powders. Crystallisation is a time dependent phenomenon, therefore a time frame of three weeks may not have been a long enough equilibration time to observe crystallisation at $0.43a_w$. However, with a longer equilibration time 6 weeks, crystallisation had occurred and could be seen from the isotherms. It is noted that a breakpoint in the isotherms for the hydrolysed powders (powders 5 and 6) was not

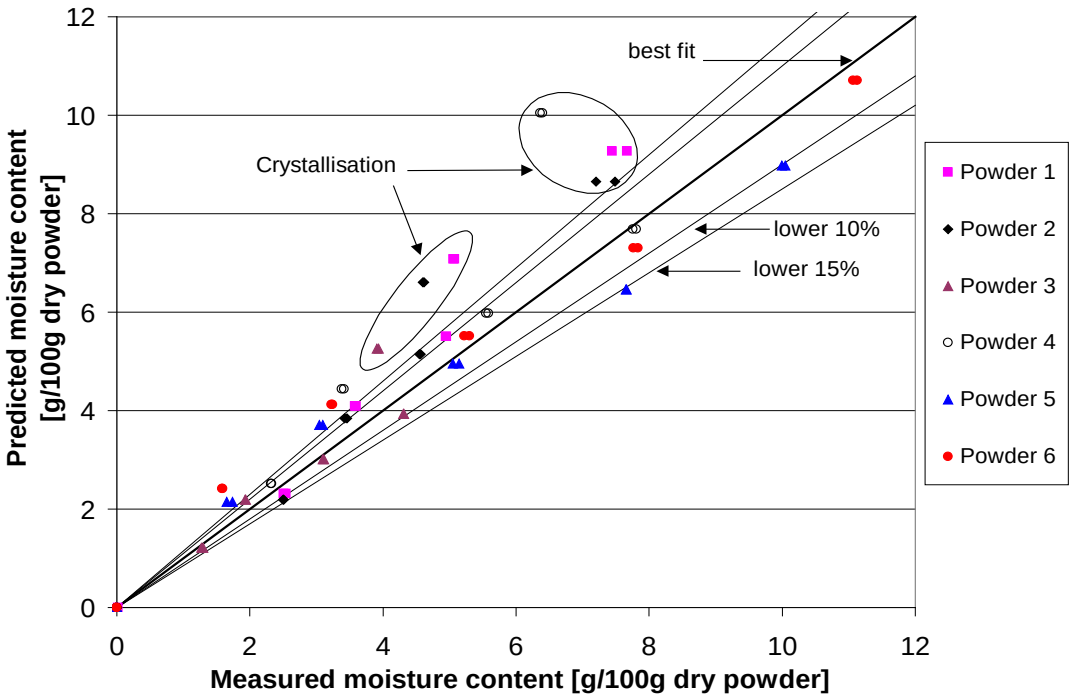

Figure 7.2: Measured versus predicted moisture content for dairy powders

observed over the three week equilibration period, even though the T_g at 0.43 and $0.54a_w$ would have been well below room temperature (around 20°C). This indicates that viscosity related changes, such as crystallisation, occur at a slower rate for amorphous glucose and galactose, or require a higher $T\text{-}T_g$ to observe the same changes as powders containing only amorphous lactose and/or sucrose. Referring to table 5.1 for the T-Tg values for instantaneous sticking for different amorphous sugars, the glucose/lactose and galactose/lactose powders required a much higher T-Tg value for instantaneous sticking compared to amorphous lactose and sucrose. This indicates that these viscosity related changes are slower for amorphous glucose and galactose than for amorphous lactose and sucrose.

Figure 7.2 gives an overall comparison of the measured and predicted isotherms by plotting the measured and predicted moisture contents at each water activity. It can be seen that most of the data agrees within ±15% of the predicted moisture contents. This is an acceptable agreement considering the sensitivity of this method to the composition and the slight discrepancies in the composition data obtained. The data where amorphous sugar crystallisation has occurred have been highlighted. These points cannot be compared to the predicted isotherm due to the change in the system which has occurred. Most lack of fit is seen at the lower moisture contents, which corresponds to water activities of 0.11 and 0.23, with most being at 0.23 a_w. It is possible that these powders had not reached equilibrium when the moisture contents were measured as lack of fit at these lower water activities was not seen for the powders 1 and 2, where longer equilibration times were used.

This work has shown that the weighted addition method for predicting isotherms is adequate and an agreement within ±15% can be expected, if not ±10%. This method is sensitive to the accuracy of the assumed/measured composition, including the state of the sugars present i.e. whether they are in the amorphous or crystalline state. It is recommended that the slight lack of agreement seen at the lower water activities be investigated further to check that there is not a inadequacy in one of the component isotherms or that there is not a significant interaction that occurs at these lower water activities.

7.3.2 Prediction of Glass Transition Temperature Profiles

The T_g profiles for the powders were measured using differential scanning calorimetry (Perkin Elmer DSC-7). The DSC was calibrated using the melting points of indium (156.6°C) and deionised water (0°C). Sealed 20µl aluminium pans were used for measurements; an empty pan was used as the reference. The powders that were placed in desiccators over saturated salt solutions and used for isotherm measurement, were used for measuring the T_g. The pans were filled with powder samples under nitrogen, in order to avoid the absorption of moisture during preparation. A scanning rate of 5°C/min was used and the extrapolated onset T_g was measured. The extrapolated onset T_g was used rather than the onset temperature as this is the T_g that is most often quoted in literature (the midpoint T_g being the alternative) and therefore many of the profiles for the amorphous sugars are from the extrapolated onset T_g. The onset T_g can be more than 5°C lower, so it would be difficult to draw conclusions from comparisons with predictions when higher T_g values for the components are given.

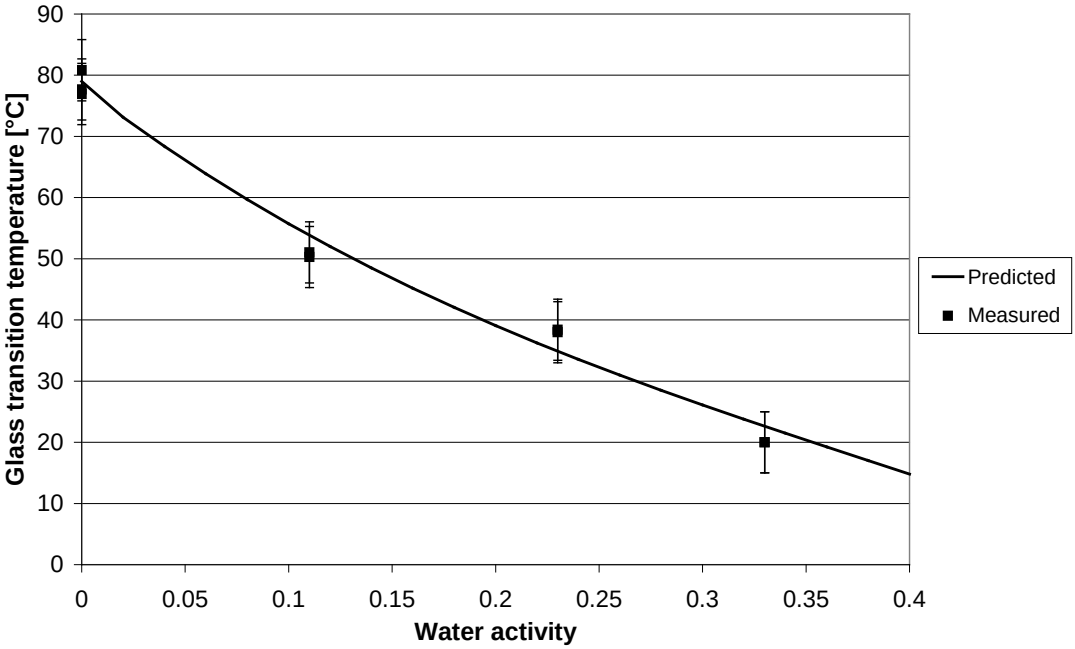

Figure 7.3: Comparison of predicted and measured T_g profiles for powder 3

The T_g profiles for the powders were predicted using equation 4.5 and the information given in table 7.2. Figure 7.3 compares the predicted and measured T_g profiles for powder 3, with ±5°C error bars included. It can be seen that there is very good agreement between the measured and predicted T_g values.

As discussed in section 4.2.1, the measurement of the T_g for powders is subject to variation due to a number of reasons. One source of variation and error occurs during the preparation of the DSC pans. This needs to be done in a dry environment and in this work it was carried out under nitrogen. It was found however, that the powders would

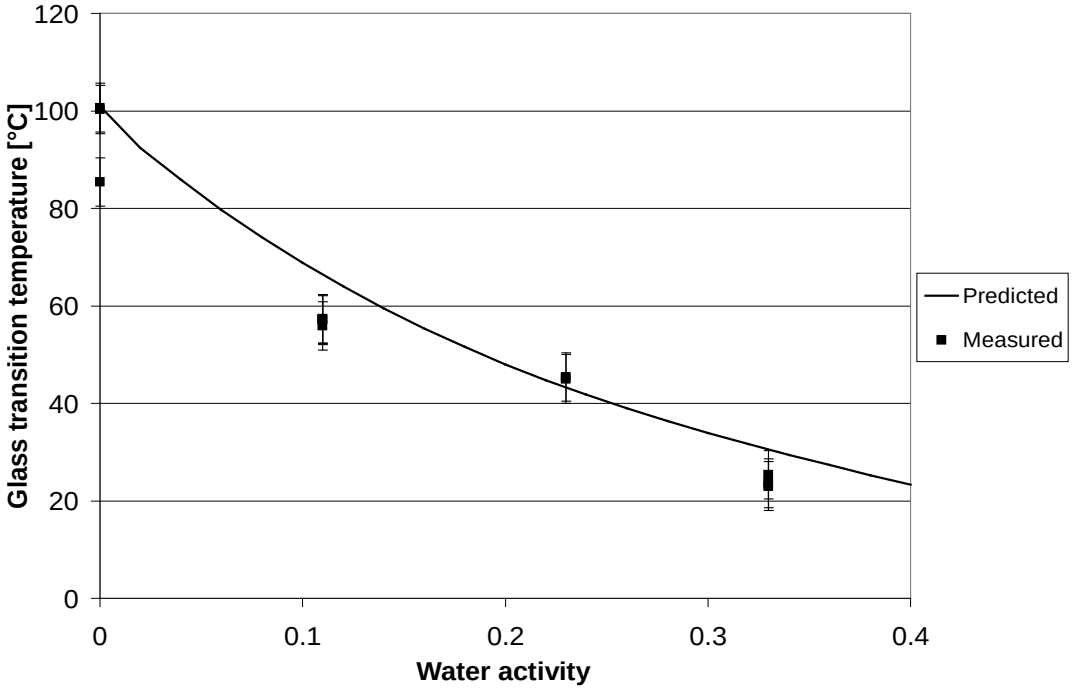

Figure 7.4: Glass transition temperature profile for powder 1

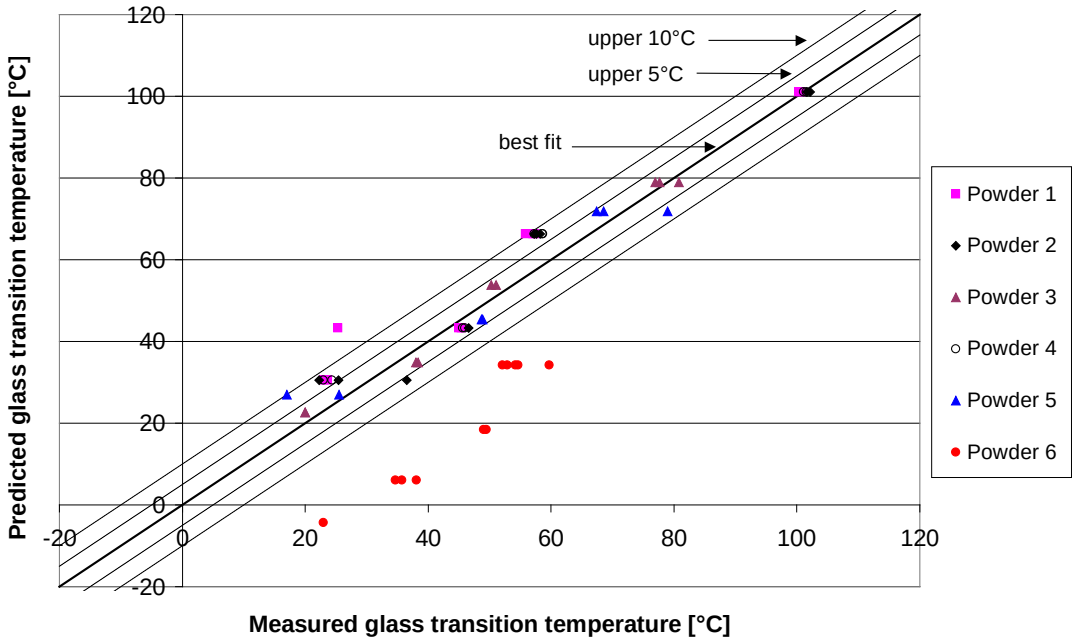

Figure 7.5: Comparison between measured and predicted T_g values for dairy powders

still pick up some moisture, especially for the low water activities, and this dramatically effected the T_g value measured. In some cases it was found that the T_g was measured to be 15°C below its actual value due to moisture pick up during preparation. This problem was overcome for $0.0a_w$ by piercing a hole in the top of the DSC pan just prior to testing. When the pan was heated to over 100°C during the first scan, the absorbed moisture was driven off and the T_g value found after rescanning was much higher. Figure 7.4 shows this clearly for powder 1. The dry T_g found without piercing a hole in the lid was 85.4°C, as opposed to a dry T_g of 100.6°C when the moisture was able to be driven off. The difference in these T_g values illustrates how much moisture adsorption occurred during the preparation of the DSC pans. Referring to the isotherm for powder 1, this corresponds to an uptake of 1g water/100g dry power during sample preparation.

The lack of agreement to ±5°C at $0.11a_w$ is likely to be due to moisture uptake during preparation. At higher water activities, there is less driving force for sorption, since the water activity of the sample is approaching the relative humidity of the environment, when nitrogen is not used. At the higher water activities there is better agreement between the measured and predicted T_g values, than at $0.11a_w$. This is shown in figure 7.5 where a comparison between the measured and predicted T_g values for all the powders tested is given. It can be seen that most of the data agrees within the ±5°C error limit and almost all the data agrees within the ±10°C error limit, excluding the data for powder 6.

Powder 6 is a hydrolysed dairy powder and the predicted T_g profile was a lot lower than that measured. This implies that there is more amorphous lactose and possibly less amorphous glucose and galactose present than found using gas chromatography. Figure 7.6 shows the predicted and measured T_g profiles for powder 6. Two prediction lines have been used, the first using the composition given in table 7.3, excluding the undetermined sugar amounts. The second prediction includes the undetermined disaccharide content by assuming that it is amorphous lactose (0.21% lactose). Including this in the prediction elevated the T_g profile but it is still significantly lower than that measured. This indicates that there are inadequacies in the composition

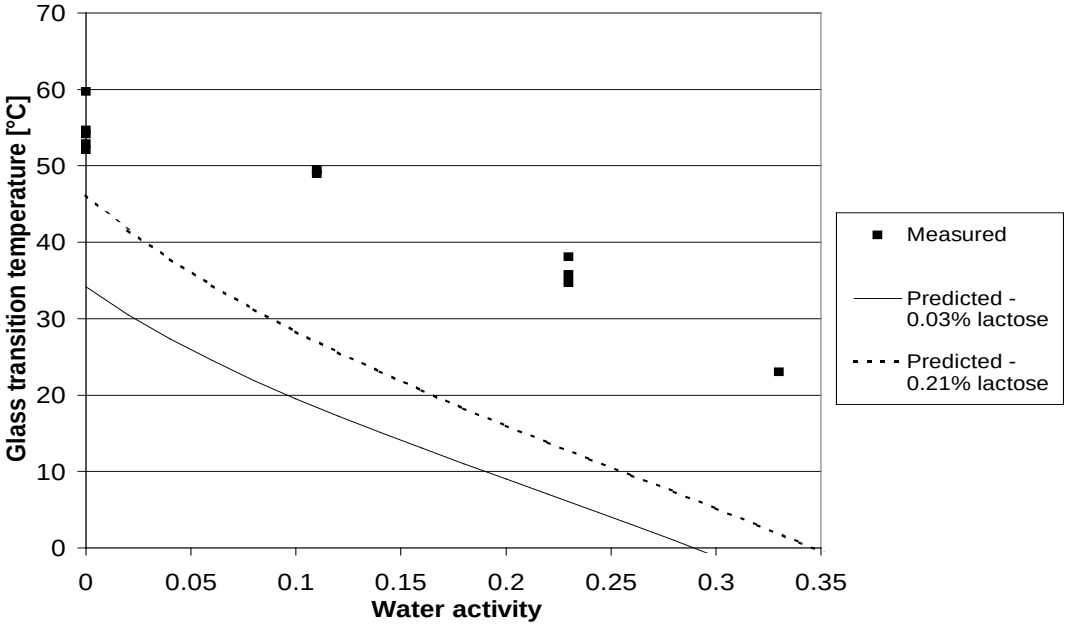

Figure 7.6: Comparison of predicted and measured T_g profiles for powder 6

determined, in particular, the sugar analysis. Further breakdown of the sugar content needs to be performed before any conclusions can be drawn from this set of data. The measured T_g profile indicates that there was a greater proportion of higher molecular weight sugars present than was accounted for with the analysis that was used. Due to the significant lack of fit of the T_g profile for powder 6, a comparison between the measured and predicted isotherms for powder 6 was not made. Excluding the data for powder 6, it can be concluded that the method proposed for predicting the T_g profile for multicomponent powders is acceptable.

It is noted that at $0.23a_w$ the measured T_g values agreed well with those predicted. This indicates that the powders at $0.23a_w$ were at equilibrium, although it appeared from some for the isotherms that they were not at equilibrium. It is noted that as the T_g profiles for the powders were measured some time after the isotherms were measured (a total time of over 6 weeks) the powders would have come to equilibrium over that time.

7.3.3 Stickiness Trials

The last part of this work investigated the development of stickiness in the dairy powders. This was done using the method given in section 5.3.3 for investigating the change in caking strength with time for amorphous sugars. Figure 7.7 shows the change in caking strength with time, for powder 3, when various relative humidity and temperature conditions are used. The different relative humidity and temperature conditions used correspond to $T\text{-}T_g$ values for powder 3 similar to one another ($T\text{-}T_g$ = 30.7 to 34.4°C). It can be seen that the rate of change in caking strength with time is similar when using different temperature and relative humidity conditions to achieve the same $T\text{-}T_g$. This demonstrates that the $T\text{-}T_g$ concept applies in dairy powders where components other than amorphous sugars are also present. Figure 7.7 also shows that a $T\text{-}T_g$ greater than 34.4°C is required for instantaneous sticking to occur.

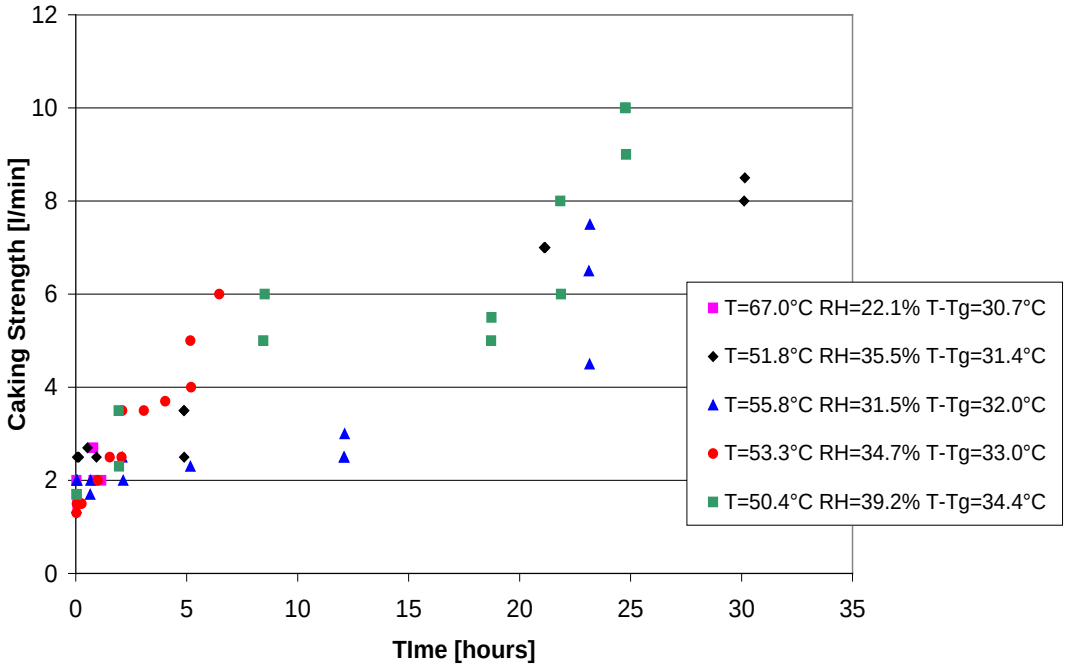

Figure 7.7: Caking strength versus time at constant T-T_g for powder 3

The caking strength versus time was also investigated for powders 4 and 5. Figure 7.8 shows the change in caking strength with time for powder 5. Various temperature and relative humidity conditions were used to give T-T_g values from 28.5 to 41.9°C. It can be seen that the rate of change in caking strength with time increases as the T-T_g increases and the rate of change in caking strength approaches zero as the T-T_g approaches zero. Figure 7.8 also shows that the rate of change in caking strength with time is dependent only on the T-T_g and not the temperature and relative humidity conditions used to achieve this. The two stickiness trials with T-T_g values of 40.7 and 41.9°C, obtained using different temperature and relative humidity conditions, show

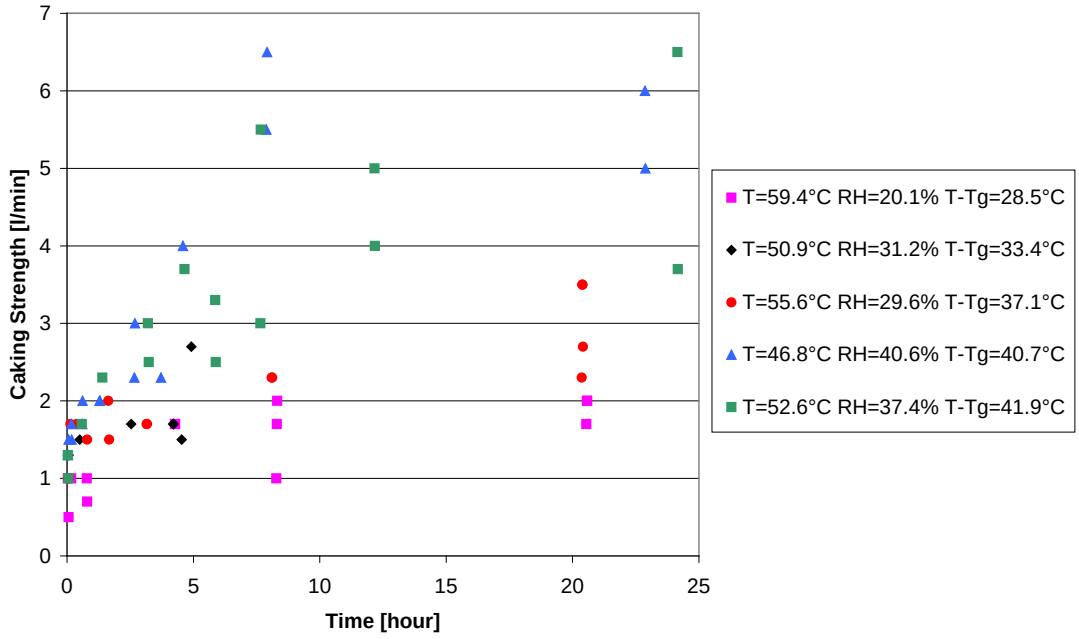

Figure 7.8: Caking strength versus time at different T-T_g values for powder 5

very similar rates of change in caking strength with time. Figure 7.8 further shows that T-T_g values greater than 41.9°C are required to achieve instantaneous sticking in this powder.

Figure 7.9 shows the change in caking strength with time for powder 4. It can be seen that quicker rates of sticking with time are attained with this powder when lower T-T_g values are used, compared to those in figures 7.7 and 7.8. Although instantaneous sticking was not achieved, sticking did develop much quicker than seen in figures 7.7 and 7.8 using T-T_g values of between 18.4 and 22.3°C. This indicates that the T-T_g required for instantaneous sticking is dependent on the composition of the powder and probably most importantly, the composition of the amorphous sugars present. The amorphous sugars present in powders 3, 4 and 5 are lactose/sucrose, lactose and lactose/glucose/galactose respectively. The rate of sticking was highest in powder 4 where only amorphous lactose was present and the T-T_g value required for instantaneous sticking appears to be the lowest in this powder. The T-T_g required for instantaneous sticking was greater in powder 3 where sucrose was also present. The T-T_g required for instantaneous sticking was much greater in powder 5 where some of the lactose had been hydrolysed to glucose and galactose. These results are in line with the T-T_g values required for instantaneous sticking given in table 5.1, where the value for glucose and galactose containing powders is much greater than that for pure lactose or sucrose powders. Table 5.1 shows that similar T-T_g values for instantaneous sticking are needed for amorphous lactose and sucrose powders. This was not shown in these sticking trials. However powder 3 also contained a large amount of crystalline sucrose. Further examination of table 7.3 shows that the rate of sticking and hence the T-T_g for instantaneous sticking may be related simply to the amorphous sugar content of the powder. The amorphous sugar content was greatest for powder 4 and the least for powder 5, which also corresponds to powder 4 requiring the smallest T-T_g and powder 5 requiring the highest T-T_g for instantaneous sticking to occur. This work highlights the fact that the T-T_g for instantaneous sticking differs between powders depending on the composition. Therefore, the T-T_g cannot be set in the model and must be changed for

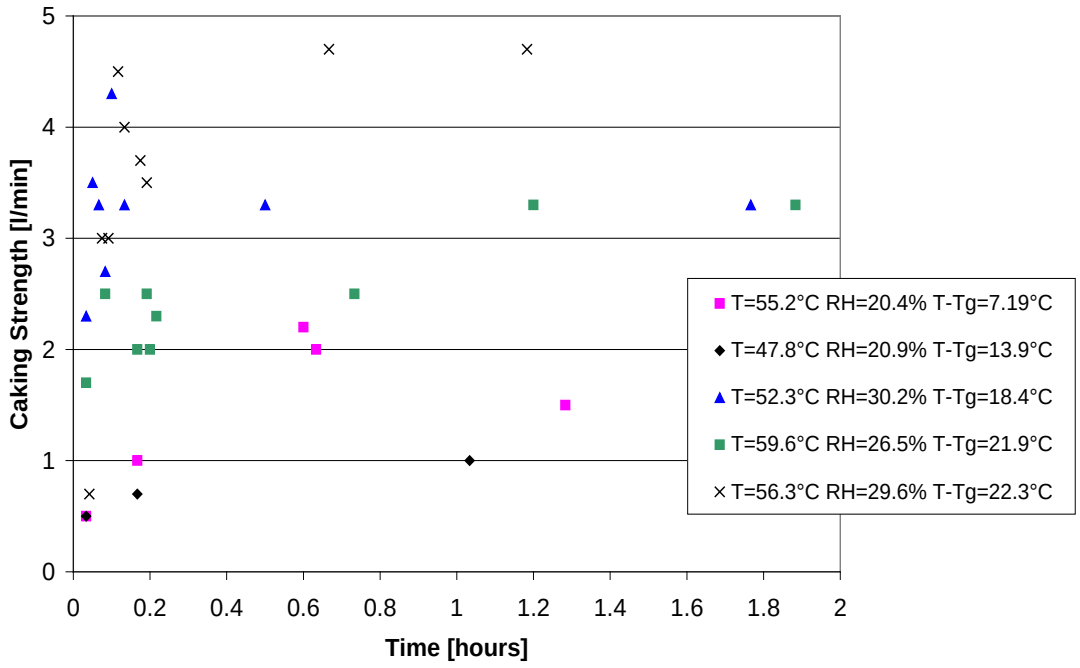

Figure 7.9: Caking strength versus time for powder 4

each powder. Further work is required to relate the $T-T_g$ value required for instantaneous sticking to the composition of the powder so that this $T-T_g$ can be predicted, for use in the model, from the composition of the powder.

Figure 7.9 also shows that the rate of sticking with time becomes very slow as the $T-T_g$ for the powder approaches zero. Therefore, in order to prevent sticking and caking problems during storage, the powder should be dried to a water activity and hence moisture content such that the T_g of the powder is never exceeded during storage. The sticking of amorphous sugars was shown to be viscosity related and therefore if the T_g is never exceeded, then the viscosity is always too high for flow and the formation of liquid bridges to occur.

7.4 SENSITIVITY ANALYSIS

Predictions made using the stickiness model are sensitive to the composition of the powder. Although specifications are given for dairy powders, the actual composition of a particular batch of powder can differ from that stated in the powder's specification. Pearce (2002) stated that the actual fraction of each component in a particular powder could vary by up to 20%. This section looks at the sensitivity of the prediction model to such changes in the composition. Powders 3 and 4 were used for this analysis. The composition of these powders and the range that each component can be present in if 20% variation is applied is given in table 7.4 on a dry mass basis.

Table 7.4: Potential variation in the composition of powders 3 and 4

Component	Mass fraction (g/100g dry powder)	
	Powder 3	Powder 4
Fat	28.6 (22.9 – 34.3)	1.2 (0.9 – 1.4)
Protein	13.6 (10.9 – 16.3)	37.0 (29.6 – 44.4)
Amorphous lactose	14.8 (11.8 – 17.7)	52.4 (41.9 – 62.9)
Amorphous sucrose	14.5 (11.6 – 17.4)	
Crystalline sucrose	18.6 (14.9 – 22.3)	
Cocoa	2.9 (2.3 – 3.4)	
Minerals	7.1 (5.7 – 8.5)	9.4 (7.6 – 11.3)

Given the variation that the composition can have, two questions are relevant:

1. How much does the moisture content and T_g vary if the powder is dried to a given water activity?
2. How much does the water activity and T_g vary if the powder is dried to a given moisture content?

Table 7.5: Sensitivity of water activity, moisture content and T_g to a 20% variation in composition

Powder	Water activity	Moisture content (% dry mass basis)	T_g (°C)
3	0.15*	1.5 (1.1 – 1.8)	47 (45 – 49)
3	0.15 (0.10 – 0.20)	1.4*	48 (40 – 55)
4	0.10*	2.3 (2.1 – 2.6)	69
4	0.11 (0.10 – 0.13)	2.6*	66 (62 – 69)

* denotes that the powder is being dried to a constant water activity or moisture content

Table 7.5 summarises the variation in water activity, moisture content and T_g that may be experienced given a 20% variation in composition. Powder 4 only contains lactose as the amorphous sugar component. Therefore, if powder 4 is dried to a constant water activity then the resulting T_g will be the same regardless of the variations in the amount of each component present. This highlights the usefulness in drying to a particular water activity rather than moisture content. Given a 20% variation in the powder composition the moisture content can vary by around 13% when drying to a given water activity. If powder 4 is dried to a particular moisture content then the actual water activity of the powder can vary by about $0.02a_w$ depending on the changes to the compositions. Subsequently the T_g can vary by around 4°C. If powder 3 is dried to a particular water activity then the moisture content can change by around 23% given a 20% variation in the powder composition. The T_g will subsequently vary by around 2°C. If powder 3 is dried to a particular moisture content then the resulting water activity can vary by $0.05a_w$ and the T_g can vary by around 8°C. Given the variations that can occur in the powder composition, it therefore cannot be expected that isotherm predictions can agree better then ±15% and that T_g predictions can agree better than ±5°C.

7.5 CLOSURE

This chapter has shown that the methods used for predicting isotherms and the T_g profiles for multicomponent powders are applicable to dairy powders. Moisture sorption isotherms can be predicted from the weighted addition of the components' isotherms. The T_g profile can be predicted from the T_g values of the components at a given water activity. A model was developed that can be used to predict the conditions required to avoid sticking and caking problems during processing and storage. To avoid sticking and caking problems during storage, the powder should be dried to a water activity and hence moisture content such that the T_g of the powder is never exceeded. In order to avoid sticking and caking problems during drying, the powder should never exceed a particular $T\text{-}T_g$ value, which is dependent on the powder being dried. Further work is required to understand the relationship between this $T\text{-}T_g$ value and the composition of the powder.

CHAPTER 8

CONCLUSIONS AND SUGGESTIONS FOR FUTURE WORK

8.1 CONCLUSIONS

This work has identified the mechanisms for sticking and caking in dairy powders and the conditions under which these phenomena occur. Two main mechanisms for sticking and caking in dairy powders were identified. Milk fat was found to contribute to sticking and caking problems when present in high amounts, that is, greater than 42% total fat. This mechanism was found to be related to the surface fat content of the powder and hence sticking and caking problems were present in powders where the surface fat content was greater than 1.95g/m^2. When a high fat powder is exposed to conditions of high temperature, the surface fat becomes completely molten and liquid bridges between particles form. These fatty liquid bridges can later partially solidify, due to the crystallisation of the milk fat, if the temperature of the powder is reduced to some temperature below the final melting point of the milk fat. The liquid bridging stage did not cause any increase in the caking strength of the powder, but the caking strength did increase when the temperature was reduced and the bridges solidified. The amount of surface fat that solidified/crystallised after being in a molten state was directly related to the caking strength of the powder. In order to prevent sticking and caking problems in dairy powders due to the milk fat during storage, it is recommended that temperature fluctuations be avoided.

The second mechanism responsible for sticking and caking problems in dairy powders was found to be due to the amorphous sugars present in the powders. This mechanism is related to the glass transition temperature (T_g) of the powder. If the powder is exposed to conditions where the T_g is exceeded, the amorphous glass becomes a rubber and flow of the amorphous material between particles can occur. The liquid bridges that form give the powder some strength and with time crystallisation of the amorphous sugar will proceed and the bridges will solidify, causing the powder to cake. Once caking has occurred, the powder can only revert back to a free flowing state by breaking the bridges between the particles. The rate of sticking of amorphous sugars with time was found to be related to the $T-T_g$ of the powder. Therefore, it is only important what the $T-T_g$ of the powder is and not the temperature and relative humidity conditions used to achieve the particular $T-T_g$. The sticking of amorphous sugars was found to be a viscosity related mechanism. This was found to hold for amorphous glucose, galactose, sucrose, fructose and maltose.

In order to predict conditions for sticking and caking in dairy powders, the isotherm and T_g profile for the powder are needed. This work also investigated methods for predicting isotherms and T_g profiles for powders of a known composition. It was found that the isotherm could be successfully predicted by the weighted addition of the amounts that each component would sorb alone. That is, the isotherm for a powder can be predicted from the weighted addition of the isotherms for each component. A new method for predicting the T_g profile for a powder was proposed and validated. This method involves the weighted addition of the T_g versus water activity profiles for the

amorphous sugar components. Methods currently in literature use the weighted addition of the dry T_g values for each component and then apply a plasticisation by the moisture effect related to the amorphous sugars. The proposed method was found to be more accurate than traditional methods given in the literature for predicting the T_g of multicomponent powders. In order to predict the T_g profile for a powder, it is necessary to determine the water activity of the powder and hence the amount of moisture that is associated with the amorphous sugars in the powder. The methods for predicting the isotherm and T_g profile require that accurate isotherms and T_g profiles for each components be used. Isotherms and T_g profiles for the components were determined, either experimentally or from available literature, and equations for the prediction of the isotherm and T_g profile for each component are determined.

Finally the prediction methods used in this work, that is, that the isotherm and T_g profiles for a multicomponent powder can be predicted from the weighted addition of the isotherms and T_g profiles of the components, were combined in a model and validated. The validation was done using a number of dairy powders of different compositions. A comparison was made between the measured and predicted isotherms and T_g profiles for these powders. It was found that the isotherms and T_g profiles could be adequately predicted using the methods used. In general, the agreement was within ±10% for the isotherms and ±5°C for the T_g profiles. The model can be used to determine the water activity and hence moisture content that a powder should be dried to in order to avoid sticking and caking problems during storage. It can also be used to determine temperature and relative humidity combinations during drying so that the powder can be dried under conditions that do not exceed a particular $T\text{-}T_g$. The $T\text{-}T_g$ required for instantaneous sticking during drying was not found. It is thought that the $T\text{-}T_g$ for instantaneous sticking will depend on the amount of amorphous sugar and the composition of the amorphous sugars present.

8.2 SUGGESTED FUTURE WORK

This work has highlighted several areas that require further research before the model can be accurately applied in the dairy industry. These are listed below:

1. Investigation of the rate of sticking in dairy powders as related to the $T\text{-}T_g$ and the amount and composition of amorphous sugars present. It is proposed that the $T\text{-}T_g$ required for sticking during processing depends on the amount of amorphous sugar present.
2. Further investigation into the validity of the methods used in isotherm and T_g prediction, particularly for dairy powders with a number of amorphous sugars present.
3. Development of a standard method for measuring the moisture content of a powder so that accurate predictions of the water activity and hence T_g can be made. The moisture content determined on site should not remove the bound moisture or residual moisture as this is not included in the isotherms and therefore predictions using the isotherms cannot be made. Alternatively, the bound and residual moisture for each component could be determined so that a correction could be made to the moisture content.

REFERENCES

A.E. Staley Manufacturing Company. Star-Dri maltodextrins & corn syrup solids from Staley. Starch & Specialty Products Group, Decatur, IL.

Aguilera, J. M., Levi, G., & Karel, M. (1993). Effect of water content on the glass transition and caking or fish protein hydrolyzates. Biotechnology Progress, 9, 651-654.

Aguilera, J. M., del Valle, J. M., & Karel, M. (1995). Caking phenomena in amorphous food powders. Trends in Food Science and Technology, 6, 149-155.

Anchor Products. (1997). Analytical methods manual - chemistry (AMM 01/07). Hamilton: Eastern Region, Anchor Products.

Anderson, R. B. (1946). Modifications of the Brunauer, Emmett and Teller Equation. Journal of the American Chemical Society, 68, 686-691.

Angell, C. A., Bressel, R. D., Green, J. L., Kanno, H., Oguni, M., & Sare, E. J. (1994). Liquid fragility and the glass transition in water and aqueous solutions. Journal of Food Engineering, 22, 115-142.

Arvanitoyannis, I., & Blanshard, J. M. V. (1994). Rates of crystallization of dried lactose-sucrose mixtures. Journal of Food Science, 59, 197-205.

Arvanitoyannis, I., Blanshard, J. M. V., Ablett, S., Izzard, M. J., & Lillford, P. J. (1993). Calorimetric study of the glass transition occurring in aqueous glucose:fructose solutions. Journal of the Science of Food and Agriculture, 63, 177-188.

Audu, T. O. K., Loncin, M., & Weisser, H. (1978). Sorption isotherms of sugars. Lebensm. Wiss. u Technol, 11 , 31-34.

Bagster, D. F. (1970). Cause, prevention and measurement of the caking of refined sugar - a review. Part 1. International Sugar Journal, 72(861), 263-267.

Bandyopadhyay, P., Das, H., & Sharma, G. P., (1987). Moisture adsorption characteristics of casein, lactose, skim milk and chhana powder. Journal of Food Science and Technology, 24(1), 6-11.

Bell, L. N., & Labuza, T. P. (2000). Moisture sorption: practical aspects of isotherm measurement and use. St Paul, MN: American Association of Cereal Chemists.

Bellows, R. J., & King, C. J. (1973). Product collapse during freeze-drying of liquid foods. AICHE Symposium Series, 69(132), 33-41.

Berlin, E., Anderson, B. A., & Pallansch, M. J. (1968). Comparison of water vapor sorption by milk powder components. Journal of Dairy Science, 51, 1912-1915.

Berlin, E., Anderson, B. A., & Pallansch, M. J. (1970). Effect of temperature on water vapor sorption by dried milk powders. Journal of Dairy Science, 53(2), 146-149.

Berlin, E., Anderson, B. A., & Pallansch, M. J. (1972). Water sorption by dried dairy products stablized with carboxymethyl cellulose. Journal of Dairy Science, 56(6), 685-689.

Bhandari, B. R., Datta, N., & Howes, T. (1997). Problems associated with spray drying of sugar-rich foods. Drying Technology, 15(2), 671-684.

Bhandari, B. R., & Howes, T. (1999). Implication of glass transition for the drying and stability of dried foods. Journal of Food Engineering, 40, 71-79.

Bhandari, B. R., & Howes, T. (2000). Glass transition in processing and stability of food. Food Australia, 52(12), 579-585.

Billings, S. W. (2002). The mathematical modelling of caking in bulk sucrose. Masterate thesis, Massey University, Palmerston North.

Blanshard, J. M. V. (1995). The glass transition, its nature and significance in food processing. In: Physico-Chemical Aspects of Food Processing, (Blackie Academic and Professional).

Blond, G. (1989). Water-galactose system: Supplemented state diagram and unfrozen water. Cryo-Letters, 10, 299-308.

Blond, G., & Simatos, D. (1991). Glass transitions of the amorphous phase in frozen aqueous systems. Thermochimica Acta, 175, 239-247.

Bonelli, P., Schebor, C., Cukierman, A. L., Buera, M. P., & Chirife, J. (1997). Residual moisture content as related to collapse of freeze-dried sugar matrices. Journal of Food Science, 62 (4), 693-695.

Boquet, R., Chirife, J., & Iglesias, H. A. (1979). Equations for fitting water sorption isotherms for foods. III. Evaluation of various three-parameter models. Journal of Food Technology, 14, 527-534.

Boston, G. (2000). Personal communication. Fonterra Research Centre, Palmerston North, New Zealand.

Breitschuh, B., & Windhab, E. J. (1996). Direct measurement of thermal fat crystal properties for milk-fat fractionation. The Journal of the American Oil Chemists' Society, 73(11), 1603-1610.

Breitschuh, B., & Windhab, E. J. (1998). Parameters influencing cocrystallization and polymorphism in milk fat. The Journal of the American Oil Chemists' Society, 75(8), 897-904.

Brinke ten, G., Karasz, F. E., & Ellis, T. S. (1983). Depression of glass transition temperature of polymer networks by diluents. Macromolecules, 16, 244-249.

Bronlund, J. (1997). The modelling of caking in bulk lactose. PhD thesis, Massey University, Palmerston North.

Brooker, B. E. (1995). Imaging food systems by confocal laser scanning microscopy. In E. Dickinson (Ed), New physico-chemical techniques for the characterization of complex food systems (pp. 53-68). Glasgow: Blackie Academic & Professional.

Brooks, G. F. (2000). The Sticking and Crystallisation of Amorphous Lactose. Masterate thesis, Massey University, Palmerston North.

Brunauer, S. (1945). The Adsorption of Gases and Vapours. Oxford: Clarendon Press.

Brunauer, S., Emmett, P. H., & Teller, E. (1938). Adsorption of Gases in Multimolecular Layers. J. Am. Chem. Soc., 60, 309-319.

Buma, T. J. (1965). The true density of spray milk powders and of certain constituents. The Netherlands Milk and Dairy Journal, 19(4), 249-265.

Buma, T. J. (1970). Determination of crystalline lactose in spray-dried milk products. Netherlands Milk Dairy Journal, 24, 129-132.

Buma, T. J. (1971a). Free fat in spray-dried whole milk. 8. The relation between free-fat content and particle porosity of spray-dried whole milk. Netherlands Milk and Dairy Journal, 25, 123-140.

Buma, T. J. (1971b). Free fat in spray-dried whole milk. 2. An evaulation of methods for the determination of free-fat content. Netherlands Milk and Dairy Journal, 25, 42-52.

Buma, T. J. (1971c). Free fat in spray-dried whole milk. 3. Particle size. Its estimation, influence of processing parameters and its relation to free-fat content. Netherlands Milk and Dairy Journal, 25, 53-72.

Buma, T. J. (1971d). Free fat in spray-dried whole milk. 10. A final report with a physical model for free fat in spray-dried milk. Netherlands Milk and Dairy Journal, 25, 159-174.

Buma, T. J. (1971e). Free fat in spray-dried whole milk. 5. Cohesion; determination, influence of particle size, moisture content and free-fat content. Netherlands Milk and Dairy Journal, 25, 107-122.

Burr, R. (1999). An Investigation into Cheese Powder Caking - Caking Review. Diploma in Dairy Science and Technology Dissertation, Massey University, Palmerston North, 10-36.

Butler, B. (1998). Modelling Industrial Lactose Crystallisation. PhD thesis, University of Queensland, Queensland, Australia.

Chan, R. K., Pathmanathan, K., & Johari, G. P. (1986). Dielectric relaxations in the liquid and glassy states of glucose and its water mixtures. Journal of Physical Chemistry, 90, 6358-6362.

Chinachoti, P., & Steinberg, M. P. (1984). Interaction of sucrose with starch during dehydration as shown by water sorption. Journal of Food Science, 49, 1604-1608.

Chirife, J., Timmermann, E. O., Iglesias, H. A., & Boquet, R. (1992). Some features of the parameter *k* of the GAB equation as applied to sorption isotherms of selected food materials. Journal of Food Engineering, 15, 75-82.

Chuang, L., & Toledo, R. T. (1976). Predicting the water activity of multicomponent systems from water sorption isotherms of individual components. Journal of Food Science, 41, 922-927.

Chuy, L. E., & Labuza, T. P. (1994). Caking and stickiness of dairy-based food powders as related to glass transition. Journal of Food Science, 59(1).

Couchman, P. R. (1978). Compositional variation of glass transition temperatures. 2. Application of thermodynamic theory to compatible polymer blends. Macromolecules, 11, 1156-1161.

Couchman, P. R., & Karasz, F. E. (1978). A classical thermodynamic discussion of the effect of composition on glass-transition temperatures. Macromolecules, 11(1), 117-119.

Crofskey, C. M. (2000). Investigation into the Caking Problems Associated with Spray Dried Cream Powders 55 and 70. Massey University, Palmerston North.

De Boer, J. H. (1953). The Dynamical Character of Adsorption. Oxford: Carendon Press.

deMan, J. M. (1999). Principles of Food Chemistry, Third Edition. Gaithersburg, Maryland: Aspen Publishers, Inc.

Dimick, P. S., Reddy, S. Y., & Ziegler, G. R. (1996). Chemical and thermal characteristics of milk-fat fractions isolated by a melt crystallization. The Journal of the American Oil Chemists' Society, 73(12), 1647-1652.

Ditmar, J. H. (1935). Hygroscopicity of sugars and sugar mixtures. Ind. Eng. Chem., 27, 333.

Donnelly, B. J., & Fruin, J. C. S. B. L. (1973). Reactions of oligosaccharides. III. hygroscopic properties. Am. Ass. of Cereal Chemists, July-August, 513-519.

Downton, G. E., Flores-Luna, J. L., & King, C. J. (1982). Mechanism of stickiness in hygroscopic, amorphous powders. Ind. Eng. Chem. Fundam., 21, 447-451.

Fäldt, P., & Bergenståhl, B. (1994). The surface-composition of spray-dried protein lactose powders. Colloid Surface A, 90(2-3), 183-190.

Fäldt, P., & Bergenståhl, B. (1995). Fat encapsulation in spray-dried food powders. JAOCS, 72(2), 171-176.

Fäldt, P., & Bergenståhl, B. (1996a). Spray-dried whey protein/lactose/soybean oil emulsions. 1. Surface composition and particle structure. Food Hydrocolloids, 10(4), 421-429.

Fäldt, P., & Bergenståhl, B. (1996b). Spray-dried whey protein/lactose/soybean oil emulsions. 2. Redispersability, wettability and particle structure. Food Hydrocolloids, 10(4), 431-439.

Fäldt, P., & Bergenståhl, B. (1996c). Changes in surface composition of spray-dried food powders due to lactose crystallization. Lebensm.-Wiss. U.-Technol, 29, 438-446.

Fanshawe, R. (2001). Powder Stickiness. An assessment of a modified sticky point apparatus and determination of stickiness curves for three maltodextrins. The Netherlands: Carlisle Friesland CRO.

Ferro Fontan, C., Chirife, J., Sancho, E., & Iglesias, H. A. (1982). Analysis of a model for water sorption phenomena in foods. Journal of Food Science, 47, 1590-1594.

Ferry, J. D. (1970). Viscoelastic properties of polymers. New York: John Wiley & Sons, Inc.

Finegold, L., Franks, F. & Hatley, H.M.(1989). Glass/rubber transitions and heat capacities of binary sugar blends. J Chem Soc. Faraday Trans. I. 85, 2945-2951.

Foster, K., & Paterson, T. (2001). Caking in Enfamil Base Powder. Institute of Technology and Engineering, Massey University, Palmerston North.

Foster, K. D. (1998). Acid-Base Catalysis of Lactose Mutarotation. Institute of Technology and Engineering, Massey University, Palmerston North.

Frenkel, J. (1945). J. Phys. (USSR), 9(5), 385.

Gordon, M., & Taylor, J. S. (1952). Ideal copolymers and the second-order transitions of synthetic rubbers. I. Non-crystalline copolymers. Journal of Applied Chemistry, 2, 493-500.

Grall, D. S., & Hartel, R. W. (1992). Kinetics of butterfat crystallization. The Journal of the American Oil Chemists' Society, 69(8), 741-747.

Greenspan, L. (1977). Humidity fixed points of binary saturated aqueous solutions. Journal of Research of the National Bureau of Standards - A, 81A(1), 89-96.

Guggenheim, E. A. (1966). Applications of Statistical Mechanics. Oxford: Claredon Press.

Haase, G., & Nickerson, T. A. (1966). Kinetic reactions of alpha and beta lactose. 1. Mutarotation. Journal of Dairy Science, 49, 127-132.

Hamano, M., & Sugimoto, H. (1978). Water sorption, reduction of caking and improvement of free flowingness of powdered soya sauce and miso. Food Processing and Preservation, 2, 197-203.

Hargreaves, J. (1995). Characterisation of lactose in the liquid and solid state using nuclear magnetic resonance and other methods. PhD thesis, Massey University, Palmerston North.

Harper, W. J. (1992). Lactose and lactose derivatives. In J. G. Zadow (Editor), Whey and Lactose Processing (pp. 317-360). Essex, England: Elsevier Applied Science.

Hassid, W. Z., & Ballou, C. E. (1957). Oligosaccharides. In W. Pigman (Ed), The Carbohydrates. Chemistry, Biochemistry, Physiology (p. 498). New York: Academic Press Inc.

Heldman, D. R., Hall, C. W., & Hedrick, T. I. (1965). Vapor equilibrium relationships of dry milk. Journal of Dairy Science, 48, 845.

Hendricks, B. C., Steinbach, W. H. J., Leroy, R. H., & Moseley, A. G. J. (1934). Heats of solution of sugars in water. Journal of the American Chemical Society, 56, 99-101.

Hermansson, A. M. (1977). Functional properties of proteins for foods - water vapour sorption. Journal of Food Technology, 12, 177.

Herrera, M. L., de León Gatti, M., & Hartel, R. W. (1999). A kinetic analysis of crystallization of a milk fat model system. Food Research International, 32, 289-298.

Herrington, B. L. (1934). Some physico-chemical properties of lactose. I. The spontaneous crystallization of super-saturated solutions of lactose. Journal of Dairy Science, 17, 501-518.

Hohne, G., Hemminger, W., & Flammersheim, H.-J. (1996). Differential Scanning Calorimetry: An Introduction for Practitioners. New York: Springer - Verlag Berlin Heidelberg .

Holsinger, V. H. (1988). Physical and chemical properties of lactose. In P. F. Fox (Editor), Advanced Dairy Chemistry Volume 3 - Lactose, Water, Salts and Vitamins . London: Chapman and Hall.

Horwitz, W. (1980). Official methods of analysis of the Association of Official Analytical Chemists. 13th Edition. Washington, DC: The Association. Section 16059.

Huyghebaert, A., & Hendrickx, H. (1971). Polymorphism of cocoa butter shown by differential scanning calorimetry. Lebensm. Wiss. u Technol., 4, 59-63.

Iglesias, H. A., & Chirife, J. (1982). Handbook of Food Isotherms. Water Sorption Parameters for Food and Food Components. New York: Academic Press.

Iglesias, H. A., & Chirife, J. (1995). An Alternative to the Guggenheim, Anderson and De Boaer model for the mathematical description of moisture sorption isotherms of food. Food Research International, 28(3), 317-321.

Iglesias, H. A., Chirife, J., & Boquet, R. (1980). Prediction of water sorption isotherms of food models from knowledge of components sorption behaviour. Journal of Food Science, 45, 450-457.

Iglesias, H. A., Chirife, J., & Lombardi, J. L. (1975). Comparison of water vapour sorption by sugar beet root components. Journal of Food Technology, 10, 385-391.

Imamura, K., Suzuki, T., Kirii, S., Takayuki, T., & Okazaki, M. (1998). Influence of protein on phase transition of amorphous sugar. Journal of Chemical Engineering of Japan, 31(3), 325-329.

Isbel, H. S., & Pigman, W. (1969). Mutarotation of sugars in solution: Part II. Advances in Carbohydrate Chemistry and Biochemistry, 24, 13.

Izzard, M. J., Ablett, S., & Lillford, P. J. (1991). Calorimetric study of the glass transition occurring in sucrose solutions. In E. Dickinson (Ed.), Food Polymers, Gels and Colloids (pp. 289-300). Cambridge: The Royal Society of Chemistry.

Jaya, S., Sudhagar, M., & Das, H. (2002). Stickiness of food powders and related physico-chemical properties of food components. Journal of Food Science and Technology, 39(1), 1-7.

Johari, G. P., Hallbruker, A., & Mayer, E. (1987). The glass liquid transition of hyperquenched water. Nature, 330, 552-553.

Johnson, J. C. (1976). Specialized Sugars for the Food Industry. New Jersey, USA: Noyes Data Corporation.

Jouppila, K., Kansikas, J., & Roos, Y. H. (1997). Glass transition, water plasticization, and lactose crystallization in skim milk powder. Journal of Dairy Science, 80, 3152-3160.

Jouppila, K., & Roos, Y. H. (1994a). Water sorption and time-dependent phenomena of milk powders. Journal of Dairy Science, 77, 1798-1808.

Jouppila, K., & Roos, Y. H. (1994b). Glass transitions and crystallisation in milk powders. Journal of Dairy Science, 77(10), 2907-2915.

Kalichevsky, M. T., Blanshard, J. M. V., & Tokarczuk, P. F. (1993). Effect of water content and sugars on the glass transition of casein and sodium caseinate. International Journal of Food Science and Technology, 28, 139-151.

Kamiński, W., & Al-Bezweni, A. (1994). Calculation of water sorption isotherms for multicomponent protein-containing mixtures. International Journal of Food Science and Technology, 29, 129-136.

Karel, M. (1975). Water activity and food preservation. In M. Karel, O. R. Fennema, & D. B. Lund (Editors), Principles of Food Science. Part II (p. 237). New York: Marcel Dekker.

Kargin, V. A. (1957). Sorptive properties of glasslike polymers. Journal of Polymer Science, 23, 47-55.

Keir, T. (2001). Milk powder stickiness: a preliminary study. Diploma in Dairy Science and Technology Dissertation, New Zealand Dairy Research Institute, Palmerston North.

King, N. (1965). The physical structure of dried milk. Dairy Science Abstracts, 27(3), 91-104.

Kinsella, J. E. (1984). Milk proteins: Physicochemical and functional properties. CRC Critical Review in Food Science and Nutrition, 21(3), 197-262.

Kooi, E. R., & Armbruster, F. C. (1967). Production and use of dextrose. In R. L. Whistler, & E. F. Paschall (Editors), Starch: Chemistry and Technology . New York: Academic Press.

Kristov, J. U., & Jones, S. A. (1992). Crystallisation Studies of Confectionery Sugar Glasses. In Research Reports (Vol. No. 699). The British Food Manufacturing Industries Research Association.

Labuza, T. P. (1968). Sorption phenomena in foods. Food Technology, 22, 263-272.

Labuza, T. P. (1975). Interpretation of sorption data in relation to the state of constituent water. In R. B. Duckworth (Editor), Water Relations of Foods (pp. 155-172). London: Academic Press Inc.

Labuza, T. P. (1984). Moisture Sorption: Practical Aspects of Isotherm Measurement and Use. St. Paul, M.N.: AACC.

Lazar, M. E., Brown, A. H., Smith, G. S., Wong, F. F., & Lindquist, F. E. (1956). Experimental production of tomato powder by spray drying. Food Technology, 10, 129-137.

Levi, G., & Karel, M. (1995). Volumetric shrinkage (collapse) in freeze-dried carbohydrates above their glass transition temperature. Food Research International, 28(2), 145-151.

Levine, H., & Slade, L. (1986). A polymer physicochemical approach to the study of commercial starch hydrolysis products (SHP's). Carbohydr. Polym., 6, 213-244.

Levine, H., & Slade, L. (1988). Principles of "cryostabilization" technology from structural/property relationships of carbohydrate/water systems - a review. Cryo-Letters, 9, 21.

Lewicki, P. P. (1997). The applicability of the GAB model to food water sorption isotherms. International Journal of Food Science and Technology, 32, 553-557.

Lewicki, P. P. (1998). A three parameter equation for food moisture sorption isotherms. Journal of Food Process Engineering, 21, 127-144.

Linko, P., Pollari, T., Harju, M., & Heikonen, M. (1981). Water sorption properties and the effect of moisture on structure of dried milk products. Lebensm. Wiss. U. Technol., 15, 26-30.

Liu, W. R., Langer, R., & Klibanov, A. M. (1991). Moisture-induced aggregation of lyophilized proteins in the solid state. Biotechnology and Bioengineering, 37, 177-184.

Lloyd, R. J., Chen, X. D., & Hargreaves, J. B. (1996). Glass transition and caking of spray-dried lactose. International Journal of Food Science and Technology, 31, 305-311.

Lomauro, C. J., Bakshi, A. S., & Labuza, T. P. (1985). Evaluation of food moisture sorption isotherm equations Part I: Fruit, vegetable and meat products. Lebensm. Wiss. u Technol., 18, 111-117.

Loncin, M., Bimbenet, J. J., & Lenges, L. (1968). Influence of the activity of water on the spoilage of foodstuffs. Journal of Food Technology, 3, 131.

Lowe, E. K. (1993). The dissolution of alpha lactose monohydrate: a mathematical model for predicting dissolution times. PhD thesis, Massey University, Palmerston North.

Ludlow, D. K., & Aukland, N. R. (1990). Caking and flowability problems of sugar in a cold environment. Powder Handling and Processing, 2(1), 21-24.

MacKenzie, A. P. (1975). Collapse during freeze drying - qualitative and quantitative aspects. In S. A. Goldblith, L. Rey, & W. W. Rothmayr (Editors), Freeze Drying and Advanced Food Technology (pp. 377-307). London: Academic Press Inc. Ltd.

Makower, B., & Dye, W. B. (1956). Equilibrium moisture content and crystallization of amorphous sucrose and glucose. Agricultural and Food Chemistry, 4(1), 72-77.

Maltini, E. & Anese, M. (1995) Evaluation of viscosities of amorphous phases in partially frozen systems by WLF kinetics and glass transition temperatures. Food Research International, 28(4), 367-372.

Mathlouthi, M., Hutleau, F. and Angiboust, J.F. (1996) Physical properties and vibrational spectra of small carbohydrates in aqueous solution and the role of water in their sweetness. Food Chemistry, 56(3), 215-221.

Mathlouthi, M., & Reiser, P. (1995). Sucrose Properties and Applications. London: Blackie Academic & Professional.

Matveev, Y. I., Grinberg, V. Y., Sochava, I. V., & Tolstoguzov, V. B. (1997). Glass transition temperature of proteins. Calculation based on the additive contribution method and experimental data. Food Hydrocolloids, 11(2), 125-133.

Matveev, Y. I., Grinberg, V. Y., & Tolstoguzov, V. B. (2000). The plasticizing effect of water on proteins, polysaccharides and their mixtures. Glassy state of biopolymers, food and seeds. Food Hydrocolloids, 14, 425-437.

McClellan, A. L., & Hansberger, H. F. (1967). Cross-sectional areas of molecules adsorbed on solid surfaces. J. Colloid Interface Sci., 23, 577-599.

McKenna, A. B. (1997). Examination of whole milk powder by confocal laser scanning microscopy. Journal of Dairy Research, 64, 423-432.

Meursing, E. H. (1976). Cocoa Powders for Industrial Processing. Koog aan de zaan, Holland: Cacaofabriek De Zaan B.V.

Miller, D. P., & de Pablo, J. J. (2000). Calorimetric solution properties of simple saccharides and their significance for the stabilization of biological structure and function. Journal of Physical Chemistry B, 104, 8876-8883.

Munns, R. J. (1989). Optimising milk powders for consumer use. Food Australia, 41(9), 938-939.

Netto, F. M., Desobry, S. A., & Labuza, T. P. (1998). Effect of water content on the glass transition, caking and stickiness of protein hydrolysates. International Journal of Food Properties, 1(2), 141-161.

New Zealand Dairy Research Institute. (1988). Milkfat Products Section. (Report No. Seasonal Survey BD 394). Palmerston North: New Zealand Dairy Research Institute.

Ng, W. L. (1975). Thermal decomposition in the solid state. Australian Journal of Chemistry, 28, 1169-1178.

Nickerson, T. A. (1974). Lactose. Webb, Johnson, & Alford (Editor), Fundamentals of dairy chemistry (2 ed.,). Connecticut: AVI Publishing.

Noel, T. R., Parker, R., & Ring, S. G. (2000). Effect of molecular structure and water content on the dielectric relaxation behaviour of amorphous low molecular weight carbohydrates above and below their glass transition. Carbohydrate Research, 329, 839-845.

Noel, T. R., Ring, S. G., & Whittam, M. A. (1991). Kinetic aspects of the glass-transition behaviour of maltose-water mixtures. Carbohydrate Research, 212, 109-117.

Norris, C. S. (2002). Personal communication. Fonterra Research Centre, Palmerston North, 18 September 2002.

Norris, G. E., Gray, I. K., & Dolby, R. M. (1973). Seasonal variations in the composition and thermal properties of New Zealand milk fat II. Thermal properties of milk fat and their relation to composition. Journal of Dairy Research, 40, 311-321.

O'Donnell, A. M. (1998). Conditioning of lactose. Masterate thesis, Massey University, Palmerston North, New Zealand.

O'Donnell, A. M., Bronlund, J. E., Brooks, G. F., & Paterson, A. H. J. (2002). A constant humidity air supply system for pilot scale applications. International Journal of Food Science and Technology, 37, 369-374.

Orford, P. D., Parker, R., & Ring, S. G. (1990). Aspects of the glass transition behaviour of mixtures of carbohydrates of low molecular weight. Carbohydrate Research, 196, 11-18.

Orford, P. D., Parker, R., Ring, S. G., & Smith, A. C. (1989). Effect of water as a diluent on the glass transition behaviour of malto-oligosaccharides, amylose and amylopectin. Int. J. Biol. Macromol., 11, 91-96.

Otter, D. E., Norris, C. S., Tsao, M., & Haggarty, N. W. (1997). Quantification of milk proteins in milk powders. In Milk Powders for the Future III. Symposium on Milk Powder Research . Palmerston North: New Zealand Dairy Research Institute.

Palnitkar, M. P., & Heldman, D. R. (1971). Equilibrium moisture characteristics of freeze-dried beef components. Journal of Food Science, 36, 1015-1018.

Pancoast, H. M., & Junk, W. R. (1980). Handbook of Sugars, Second Edition. Westport, Connecticut: AVI Publishing Company, Inc.

Paterson, A. H. J., & Bronlund, J. E. (1997). Interactions of Anlene and water vapour. In Milk Powders for the Future III (pp. 269-276). Palmerston North: New Zealand Dairy Research Institute.

Paterson, A. H. J., Brooks, G. F., & Bronlund, J. E. (2001). The Blow Test for measuring the stickiness of powders. Conference of Food Engineering 2001, AICHE conference November 4-9, 2001, Reno, Nevada.

Pearce, D. L. (2002). Personal communication. Fonterra Research Centre, Palmerston North, 17 September 2002.

Pearce, K. N. (1992). Lactose in powder technology. New Zealand Dairy Research Institute, Palmerston North.

Peleg, M. (1977). Flowability of food powders and methods for its evaluation - A review. Journal of Food Process Engineering, 1, 303-328.

Peleg, M. (1992). On the use of the WLF model in polymers and foods. Critical Reviews in Food Science and Nutrition, 32, 59-66.

Peleg, M. (1993a). Glass transitions and the physical stability of food powders. In J. Blanshard, & P. Lillford (Editors), The glassy state in foods (pp. 435-451). Leicestershire: Nottingham University Press.

Peleg, M. (1993b). Assessment of a semi-empirical four parameter general model for sigmoid moisture sorption isotherms. Journal of Food Process Engineering, 16, 21-37.

Peleg, M., & Mannheim, C. H. (1977). The mechanism of caking of powdered onion. Journal of Food Processing and Preservation, 1, 3-11.

Philpot, B. (2000). Personal communication. New Zealand Dairy Research Institute, Palmerston North, 24 July 2000.

Pritzwald-Stegmann, B. F. (1986). Lactose and some of its derivatives. Journal of the Society of Dairy Technology, 39(3), 91-97.

Reiser, P., Birch, G. G., & Mathlouthi, M. (1995). Physical properties. In M. Mathlouthi, & P. Reiser (Ed), Sucrose Properties and Applications (pp. 186-222). Glasgow: Blackie Academic and Professional.

Richardson, G. M., & Malthus, R. S. (1955). Salts for static control relative humidity at relatively low levels. J. Appl. Chem., 5, 557-567.

Rockland, L. B. (1960). Saturated salt solutions for static control of relative humidity between 5 and 40 degrees celcius. Analytical Chemistry, 32, 1375-1376.

Roetman, K., & Buma, T. J. (1974). Temperature dependence of the equilibrium β/α ratio of lactose in aqueous solution. Netherlands Milk and Dairy Journal, 28, 155-165.

Roos, Y. H. (1987). Effect of moisture on the thermal behaviour of strawberries studied using differential scanning calorimetry. Journal of Food Science, 52(1), 146-149.

Roos, Y. (1993). Melting and glass transitions of low molecular weight carbohydrates. Carbohydrate Research, 238, 39-48.

Roos, Y. H. (1995). Glass transition-related physicochemical changes in foods. Food Technology, October, 97-102.

Roos, Y., & Karel, M. (1990). Differential scanning calorimetry study of phase transitions affecting the quality of dehydrated materials. Biotechnol. Prog., 6, 159-163.

Roos, Y., & Karel, M. (1991a). Plasticizing effect of water on thermal behaviour and crystallization of amorphous food models. Journal of Food Science, 56(1), 38-43.

Roos, Y., & Karel, M. (1991b). Amorphous state and delayed ice formation in sucrose solutions. International Journal of Food Science and Technology, 26, 553-566.

Roos, Y., & Karel, M. (1991c). Water and molecular weight effects on glass transitions in amorphous carbohydrates and carbohydrate solutions. Journal of Food Science, 56(6), 1676-1681.

Roos, Y. H., & Karel, M. (1991d). Phase transitions of mixtures of amorphous polysaccharides and sugars. Biotechnol. Prog., 7, 49-53.

Roos, Y., & Karel, M. (1991e). Nonequilibrium ice formation in carbohydrate solutions. Cryo-Letters, 12, 367-376.

Roos, Y., & Karel, M. (1992). Crystallization of amorphous lactose. Journal of Food Science, 57(3), 775-777.

Rosenzweig, N., & Narkis, M. (1980). Polymer, 21, 988.

Rosenzweig, N., & Narkis, M. (1981). Polym. Eng. Sci., 21, 1167.

Roth, D. (1976). Amorphous icing sugar produced during crushing and recrystallisation as the cause of agglomeration and procedures for its avoidance. PhD thesis, University of Karlsruhe, Offenberg.

Rüegg, M., Blanc, B., & Lüscher, M. (1979). Hydration of casein micelles: kinetics and isotherms of water sorption of micellar casein isolated from fresh and heat-treated milk. Journal of Dairy Research, 46, 325-328.

Rutland, D. W. (1991). Fertilizer caking: mechanisms, influential factors, and methods of prevention. Fertilizer Research, 30, 99-114.

Saito, Z. (1985). Particle structure in spray-dried whole milk and in instant skim milk powder as related to lactose crystallization. Food Microstructure, 4, 333-340.

Schaffer, R. (1972). Naturally Occurring Monosaccharides. In W. Pigman, & D. Horton (Editors), The Carbohydrates. Chemistry and Biochemistry. (2nd ed., Vol. IA). New York: Academic Press.

Schar, W., & Ruegg, M. (1985). The evaluation of GAB constants from water sorption data. Lebensm. Wiss. u Technol., 18, 225-229.

Schuchmann, H., Roy, I., & Peleg, M. (1990). Empirical models for moisture sorption isotherms at very high water activities. Journal of Food Science, 55(3), 759-762.

Sebhatu, T., Ahlneck, C., & Alderborn, G. (1997). The effect of moisture content on the compression and bond-formation properties of amorphous lactose particles. International Journal of Pharmaceutics, 146, 101-114.

Shallenberger, R. H., & Birch, G. G. (1975). Sugar Chemistry. Westport, Connecticut: The AVI Publishing Company, Inc.

Sherbon, J. W. (1974). Crystallization and fractionation of milk fat. The Journal of the American Oil Chemists' Society, 51(2), 22-25.

Shimada, Y., Roos, Y., & Karel, M. (1991). Oxidation of methyl linoleate encapsulated in amorphous lactose-based food model. Journal Agricultural and Food Chemistry, 39, 637-641.

Simatos, D., & Blond, G. (1991). DSC studies and stability of frozen foods. In H. Levine, & L. Slade (Ed.), Water Relationships in Food (pp. 139-155). New York: Plenum Press.

Singh, P. C., & Singh, R. K. (1996). Application of GAB model for water sorption isotherms of food products. Journal of Food Processing and Preservation, 20, 203-220.

Slade, L., Levine, H., Ievolella, J., & Wang, M. (1993). The glassy state phenomenon in applications for the food industry: Application of food polymer science approach to structure-function relationships of sucrose in cookie and cracker systems. J. Sci. Food Agric., 63, 133-176.

Sloan A.E., & Labuza, T. P. (1975). Investigating alternative humectants for use in foods. Food Product Development, 9(9), 75-88.

Söderberg, I., Hernqvist, L., & Buchheim, W. (1989). Milk fat crystallization in natural milk fat globules. Milchwissenschaft, 44(7), 403-406.

Soesanto, T., & Williams, M. C. (1981). Volumetric interpretation of viscosity for concentrated and dilute sugar solutions. Journal of Physical Chemistry, 85, 3338-3341.

Sokolovsky, A. (1937) Effect of humidity on hygroscopic properties of sugars and caramel. Industrial and Engineering Chemistry, 29(12), 1422-1423.

Sowden, J. C. (1957). Monosaccharides: Occurence, Properties, Synthesis. In W. Pigman (Ed), The Carbohydrates. Chemistry, Biochemistry, Physiology . New York: Academic Press Inc.

Stecher, P. G. (1968). The Merck Index: an encyclopedia of chemicals and drugs. New Jersey: Merck and Co. Inc.

Strolle, E. O., Cording, J. Jr., McDowell, P. E., & Eskew, R. K. (1970). Effect of sucrose on crispiness of explosion-puffed apple pieces exposed to high humidities. Journal of Food Science, 35, 338-342.

Sugisaki, M., Suga, H., & Seki, S. (1968). Calorimetric study of the glassy state IV Heat capacities of glassy water and cubic ice. Bulletin of the Chemical Society of Japan , 41, 2591-2599.

Sun, W. D. (1997). Temperature and viscosity for structural collapse and crystallisation of amorphous carbohydrate solutions. Cryo-Letters, 18, 99-106.

Thielmann, F., & Williams, D. (2000). Bestimmung der glasubergangstemperatur von maltose in abhangigkeit von der relativen feuchtigkeit mittels inverser gaschromatographie. Deutsche Lebensmittel-Rundschau, 96, 255-257.

Timmermann, E. O. (1989). A B.E.T.-like three sorption stage isotherm. J. Chem. Soc., Faraday Trans. 1, 85(7), 1631-1645.

Timmermann, E. O., & Chirife, J. (1991). The physical state of water sorbed at high activities in starch in terms of the GAB sorption equation. Journal of Food Engineering, 13, 171-179.

Townsend, M. W., & DeLuca, P. R. (1991). Nature of aggregates formed during storage of freeze-dried ribonuclease A. Journal of Pharmaceutical Sciences, 30(1), 63-66.

Tromp, R. H., Parker, R., & Ring, S. G. (1997). A neutron scattering study of the structure of amorphous glucose. Journal of Chemical Physics, 107(16), 6038-6049.

Troy, C., & Sharp, P. F. (1930). α and β lactose in some milk products. Journal of Dairy Science, 13, 140-157.

Tsourouflis, S., Flink, J. M., & Karel, M. (1976). Loss of structure in freeze-dried carbohydrate solutions: effect of temperature, moisture content and composition. Journal of the Science of Food and Agriculture, 27, 509-519.

van den Berg, C. (1985). Development of BET like models for sorption of water on foods, theory and relevance. In D. Simatos, & J. L. Multon (Editors), Properties of Water in Foods: in relation to quality and stability (pp. 119-131). Dordrecht: Martinus Nijhoff Publ.

van den Berg, C. (1986). Water activity. In D. MacCarthy (Editor), Concentration and Drying of Foods (pp. 11-36). New York: Elsevier Applied Science Publication.

van den Dries, I. J., Besseling, N. A. M., van Dusschoten, D., Hemminga, M. A., & van der Linden, E. (2000). Relation between a transition in molecular mobility and collapse phenomena in glucose-water systems. Journal of Physical Chemistry B, 104, 9260-9266.

van den Dries, I. J., van Dusschoten, D., & Hemminga, M. A. (1998). Mobility in maltose-water glasses studied with 1H NMR. Journal of Physical Chemistry B, 102, 10483-10489.

van Krevelen, D. W. (1990). Properties of polymers. Their correlation with chemical structure; their numerical estimation and prediction from additive group contributions. 3rd ed. Amsterdam: Elsevier.

Vanninen, E., & Doty, T. (1979). Paper 13. The properties, manufacture and use of fructose as an industrial raw material. In G. G. Birch, & K. J. Parker (Editors), Sugar: Science and Technology (pp. 311-324). London: Applied Science Publishers Ltd.

Visser, R. A. (1982). Supersaturation of α–lactose in aqueous solutions in mutarotation equilibrium. Netherlands Milk and Dairy Journal, 36, 89-101.

Wakiyama, N., Kusai, A., & Nishimura, K. (1992). Mechanism of caking of granules containing oily materials. International Journal of Pharmaceutics, 78, 95-102.

Wallack, D. A., & King C. J. (1988). Sticking and agglomeration of hygroscopic, amorphous carbohydrate and food powders. Biotechnology Progress, 4(1), 31-35.

Walstra, P. (1987). Fat crystallization. In J. M. V. Blanshard, & P. Lillford (Editors), Food Structure and Behaviour . London: Academic Press, Inc.

Wexler, A., & Daniels, R. D. (1952). Pressure-Humidity Apparatus. Journal of Research of the National Bureau of Standards, 48(4), 269-274.

White, G. W., & Cakebread, S. H. (1966). The glassy state in certain sugar-containing food products. Journal of Food Technology, 1, 73-82.

Whitten, J. (2002) Personal communication. Massey University, Palmerston North.

Williams, M. L., Landel, R. F., & Ferry, J. D. (1955). The temperature dependence of relaxation mechanisms in amorphous polymers and other glass-forming liquids. Journal of the American Chemical Society, 77, 3701-3707.

Zhang, J., & Zografi, G. (2000). The relationship between "BET"- and "Free Volume"-derived parameters for water vapor absorption into amorphous solids. Journal of Pharmaceutical Sciences, 89(9), 1063-1072.

APPENDIX A1

NOMENCLATURE

a	Slope for equation 5.10	
a_w, a_{w1}, a_{w2}	Water activity	
b	Intercept for equation 5.10	
b_1	Constant in Peleg's double power model	
b_2	Constant in Peleg's double power model	
c	BET constant	
C	GAB constant related to temperature	
C_L	Lactose concentration	g/100g water
c_o	Adjusted GAB constant for temperature effect	
$\Delta c_{p1,2,i}$	Change in specific heat capacity at glass transition	J/molK, J/gK
C_s	Lactose solubility	g/100g water
$C_{\alpha s}$	α-lactose solubility	g/100g water
$C_{\beta s}$	β-lactose solubility	g/100g water
C_1	Dimensionless constant for WLF equation	
C_1'	Constant for van Krevelen equation	kJ/mol
C_2	Constant for WLF equation	K
D	Particle diameter	m
E_D	Activation energy	J/mol
$E_1, E_{2\rightarrow 9}, E_L$	Molar latent heat	J/mol
f	GAB constant	
F	Depression effect of disaccharides on lactose solubility	
f_o	Adjusted GAB constant for temperature effect	
F_L	Constant in Lewicki's isotherm model	
F_T	GAB constant related to temperature	
G_L	Constant in Lewicki's isotherm model	
h	Third stage sorption isotherm constant	
H	Third stage sorption isotherm intermediate	
H'	Third stage sorption isotherm constant	
H_L	Constant in Lewicki's isotherm model	
H_m	Heat of sorption of the monolayer water	J/mol
H_n	Heat of sorption of the multilayer water	J/mol
H_1	Heat of condensation of water vapour	J/mol
k	Dimensionless proportionality constant	
K	Fraction of particle diameter required as bridge width for a sufficiently strong interparticle bond	
k^*	Boltzmann constant	J/K
k_F	Constant for Frenkel/WLF equation	
K_L	Equilibrium constant	
k_n	Avrami-Erofeev rate constant	min^{-1}
k_1	Rate constant of α- to β-lactose	min^{-1}
k_2	Rate constant of β- to α-lactose	min^{-1}

M	Moisture content	g water/100g dry powder
M_f	Moisture content excluding residual moisture	g water/100g dry powder
M_i	Moisture content of component *i*	g water/100g dry powder
	(except in eq 3.3: initial moisture content	g water/g dry powder)
M_m	Monolayer moisture content related to temperature	g water/100g dry powder
M_{mo}	Adjusted monolayer moisture content for temperature effect	g water/100g dry powder
M_o	BET monolayer moisture content	g water/100g dry powder
M_p	Predicted moisture content	g water/100g dry powder
n	Index of the reaction for Avrami-Erofeev equation	
n_1	Constant in Peleg's double power model	
n_2	Constant in Peleg's double power model	
p	Water vapour exerted by the food material	Pa
p_o	Vapour pressure of pure water	Pa
Q_s	Net isosteric heat of sorption	kJ/mol
R	Ideal gas constant	J/K/mol
r_b	Bridge radius	m
r_f	Constant in FF equation	
R_p	Particle radius	m
s	Rate of sticking	
s_o	Zero condition for rate of sticking	
t	Time	s, min or hours
T,T_1,T_2	Temperature	°C or K
T_e	Equilibrium temperature	°C
T_g,T_{g1},T_{g2}	Glass transition temperature	°C or K
$T_{gi},T_{gi(aw)}$	Glass transition temperature of component *i*	°C or K
$t_{1/2}$	Half time of crystallisation	min
v	Rate of growth or nucleation	m/s
v_o	Constant for Van Krevelen equation	m/s
ΔW	Final – initial mass of sample	g water
W^*	Free energy of formation	J/mol
W_i	Initial mass of sample	g powder
w_i,w_1,w_2	Mass fraction of components	g/g powder
x	Fractional extent of crystallisation at any time	
x_i	Mass fraction of component *i*	g/g dry basis
x_1,x_2	Mole fraction of components (equation 4.2)	mol/mol

Greek Letters:

γ	Parameter which accounts for structure of sorbed water in FF equation	
μ	Viscosity	Pa.s
μ_g	Viscosity at glass transition temperature	Pa.s
σ	Surface tension (except in section 3.2.2.5 where it is a constant in the FF equation)	N/m

APPENDIX A2

AMORPHOUS SUGAR STICKING

A2.1 CAKING STRENGTH VERSUS TIME GRAPHS FOR AMORPHOUS SUGARS

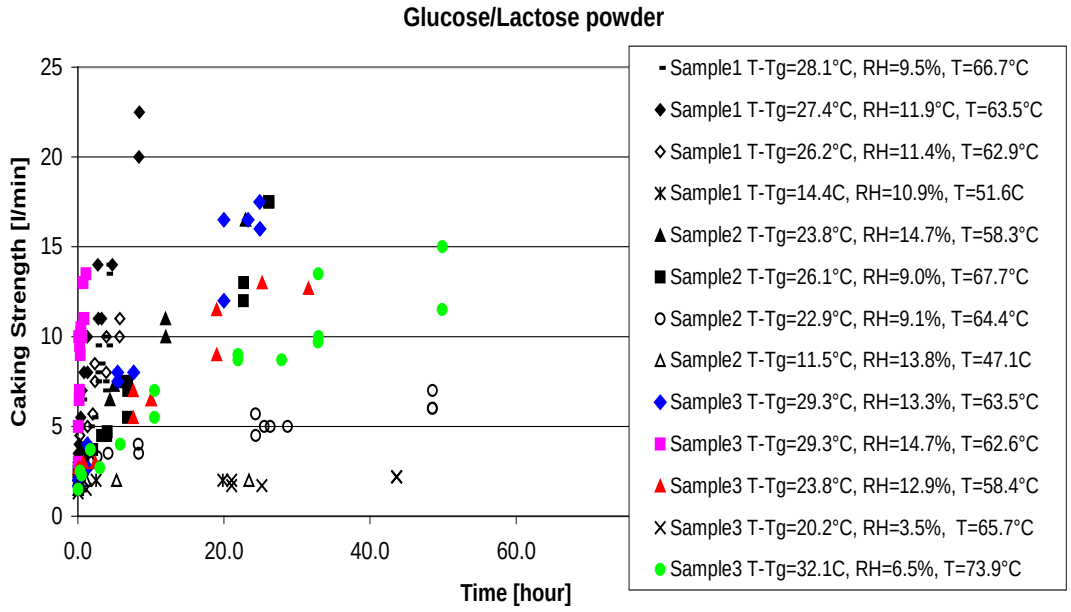

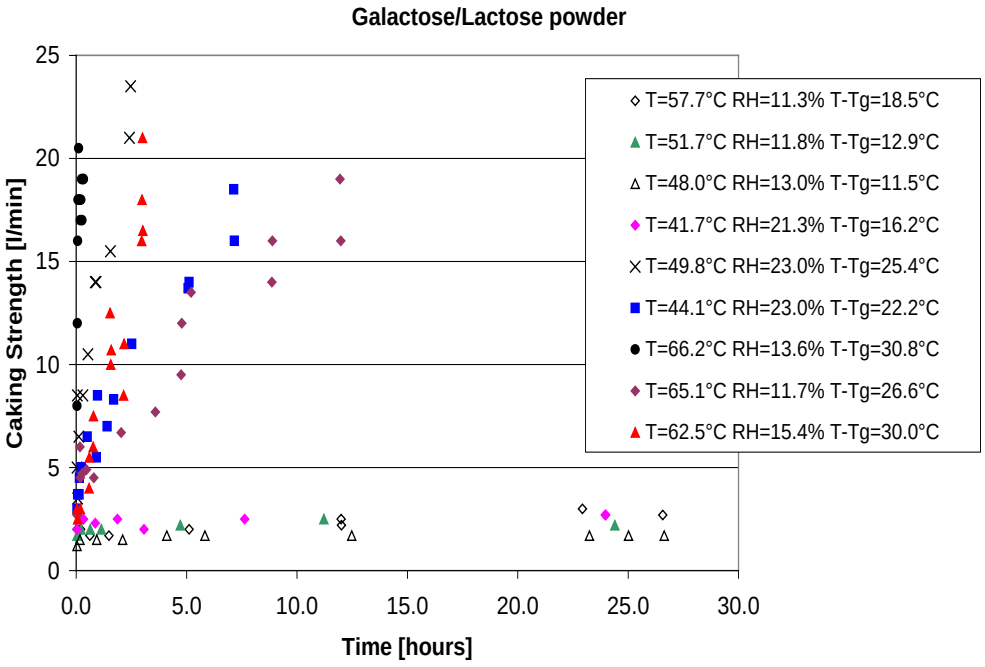

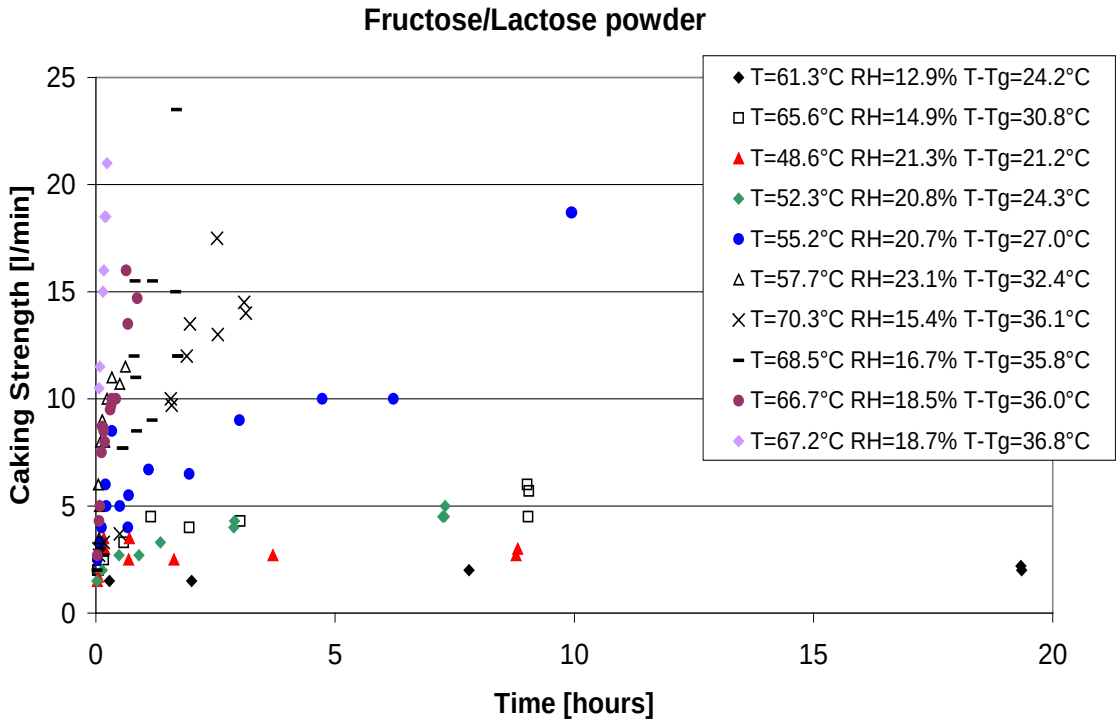
Fructose/Lactose powder
Caking Strength [l/min]
Time [hours]
0
5
10
15
20
25
T=61.3°C RH=12.9% T-Tg=24.2°C
T=65.6°C RH=14.9% T-Tg=30.8°C
T=48.6°C RH=21.3% T-Tg=21.2°C
T=52.3°C RH=20.8% T-Tg=24.3°C
T=55.2°C RH=20.7% T-Tg=27.0°C
T=57.7°C RH=23.1% T-Tg=32.4°C
T=70.3°C RH=15.4% T-Tg=36.1°C
T=68.5°C RH=16.7% T-Tg=35.8°C
T=66.7°C RH=18.5% T-Tg=36.0°C
T=67.2°C RH=18.7% T-Tg=36.8°C

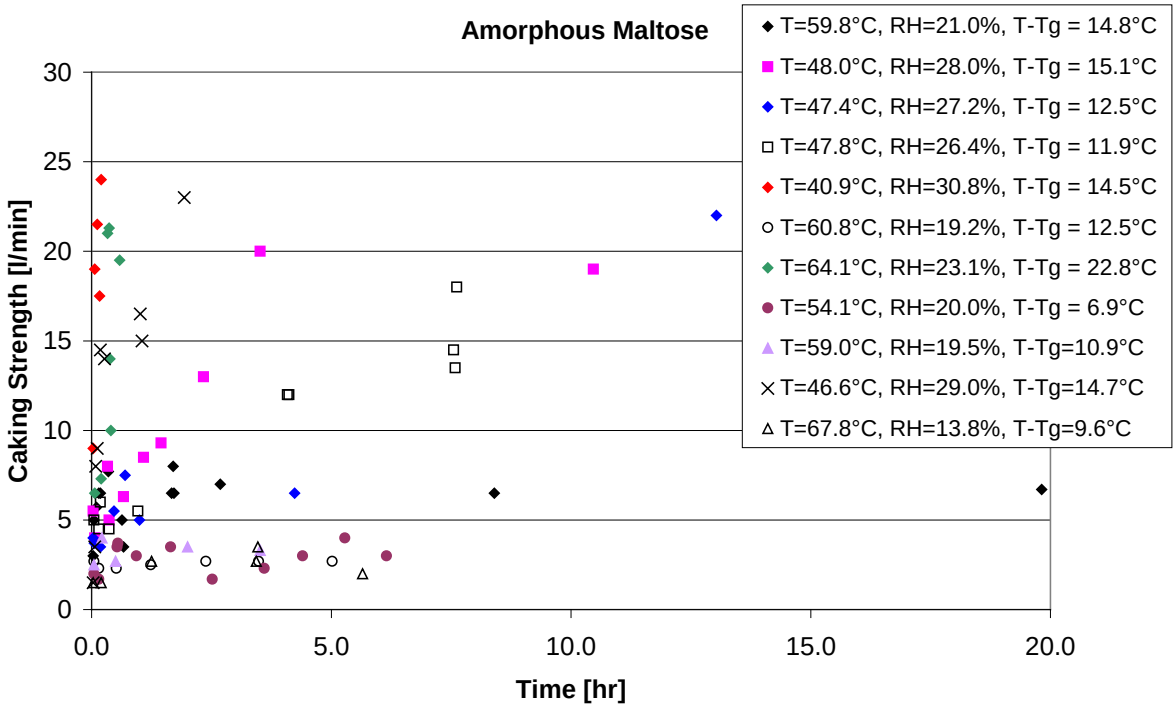
Amorphous Maltose
Caking Strength [l/min]
Time [hr]
0
5
10
15
20
25
30
0.0
5.0
10.0
15.0
20.0
T=59.8°C, RH=21.0%, T-Tg = 14.8°C
T=48.0°C, RH=28.0%, T-Tg = 15.1°C
T=47.4°C, RH=27.2%, T-Tg = 12.5°C
T=47.8°C, RH=26.4%, T-Tg = 11.9°C
T=40.9°C, RH=30.8%, T-Tg = 14.5°C
T=60.8°C, RH=19.2%, T-Tg = 12.5°C
T=64.1°C, RH=23.1%, T-Tg = 22.8°C
T=54.1°C, RH=20.0%, T-Tg = 6.9°C
T=59.0°C, RH=19.5%, T-Tg=10.9°C
T=46.6°C, RH=29.0%, T-Tg=14.7°C
T=67.8°C, RH=13.8%, T-Tg=9.6°C

A2.2 FRENKEL/WLF GRAPHS

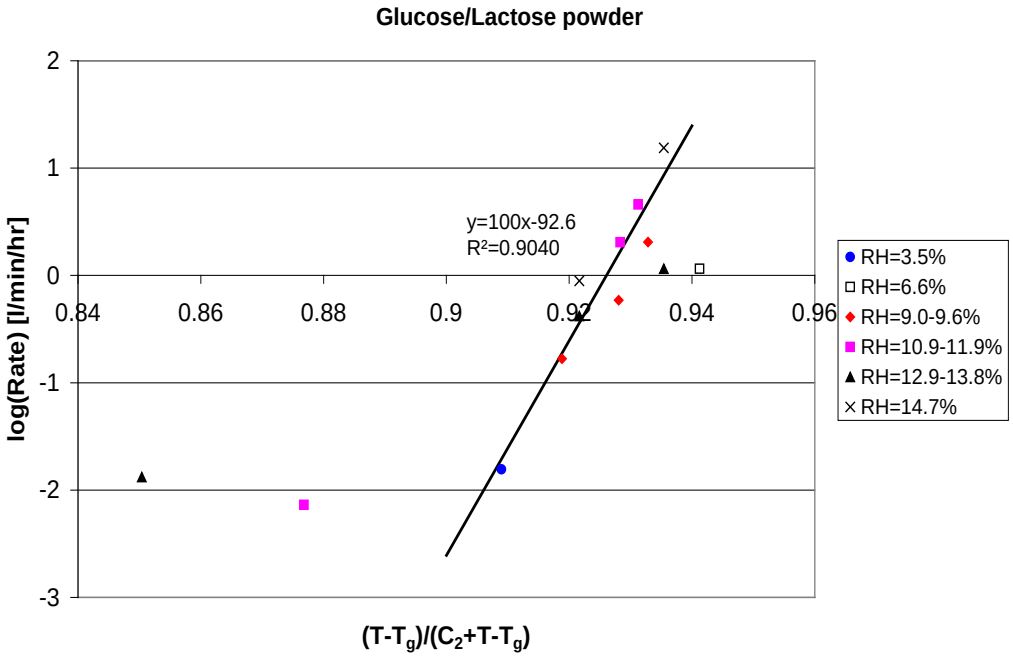

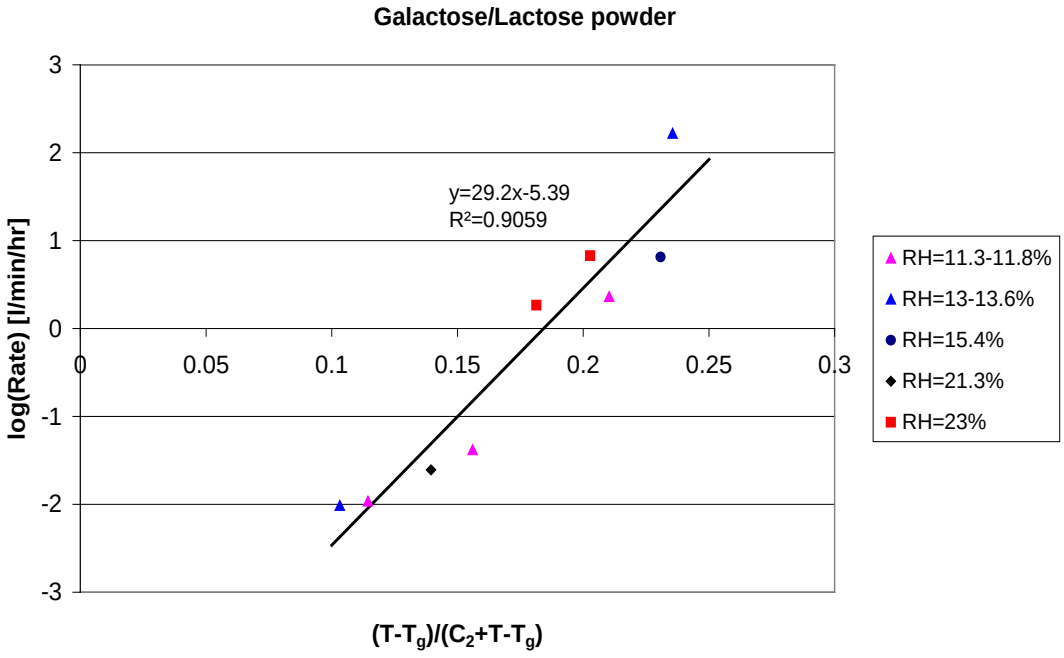

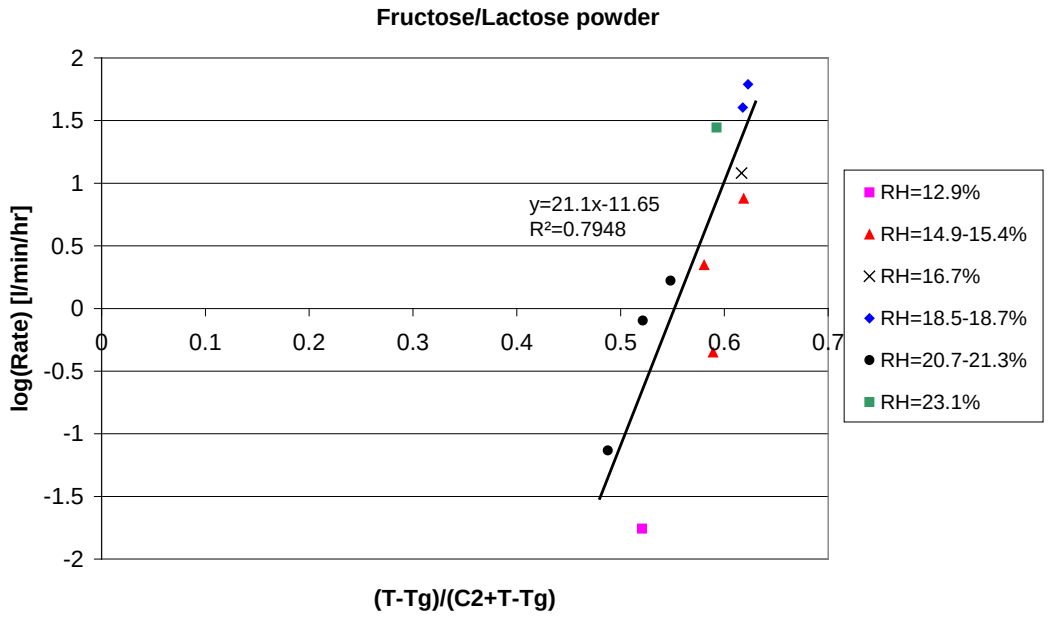
Fructose/Lactose powder
log(Rate) [l/min/hr]
(T-Tg)/(C2+T-Tg)
y=21.1x-11.65
R²=0.7948
RH=12.9%
RH=14.9-15.4%
RH=16.7%
RH=18.5-18.7%
RH=20.7-21.3%
RH=23.1%

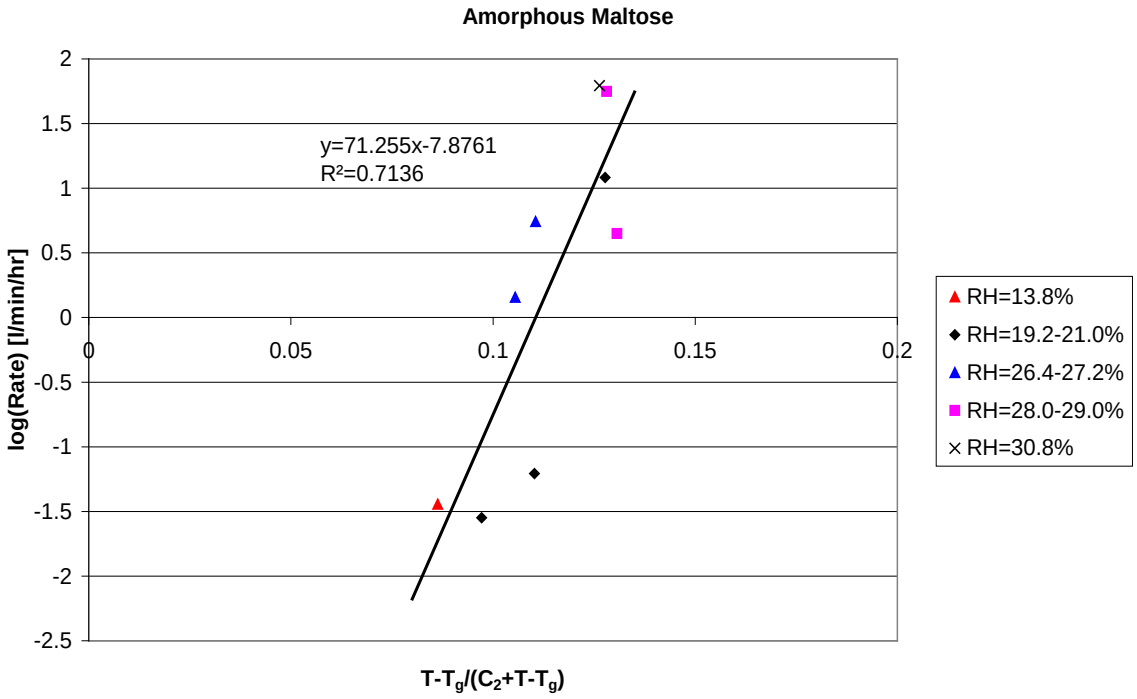
Amorphous Maltose
log(Rate) [l/min/hr]
T-Tg/(C2+T-Tg)
y=71.255x-7.8761
R²=0.7136
RH=13.8%
RH=19.2-21.0%
RH=26.4-27.2%
RH=28.0-29.0%
RH=30.8%

A2.3 VAN KREVELEN GRAPHS

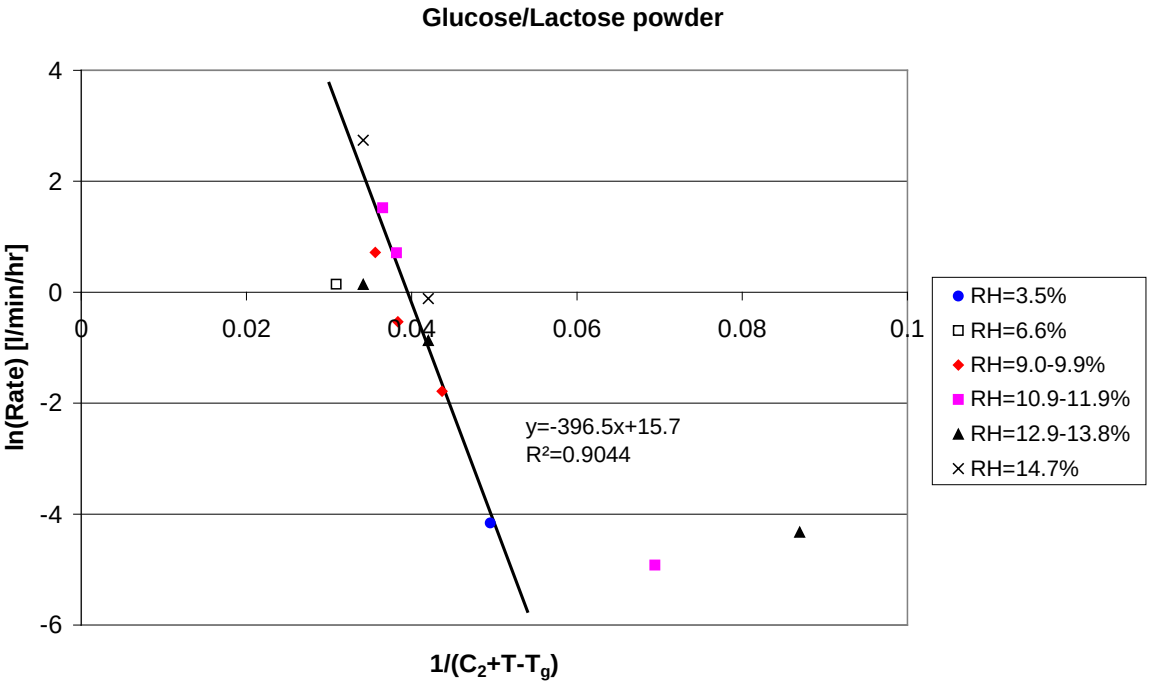

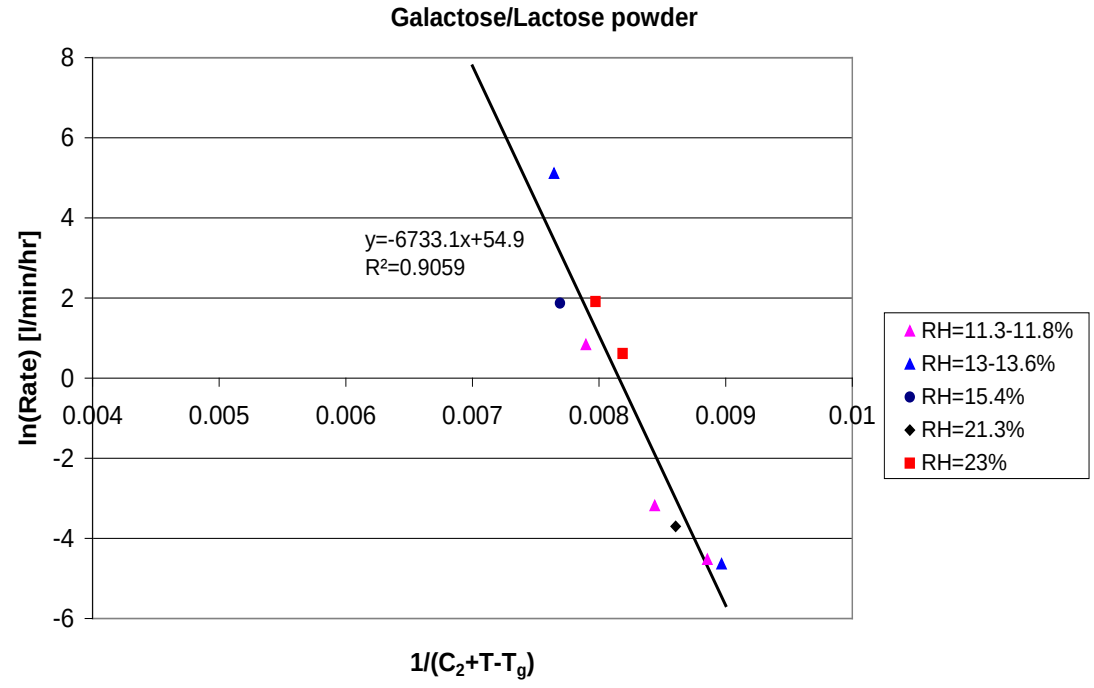

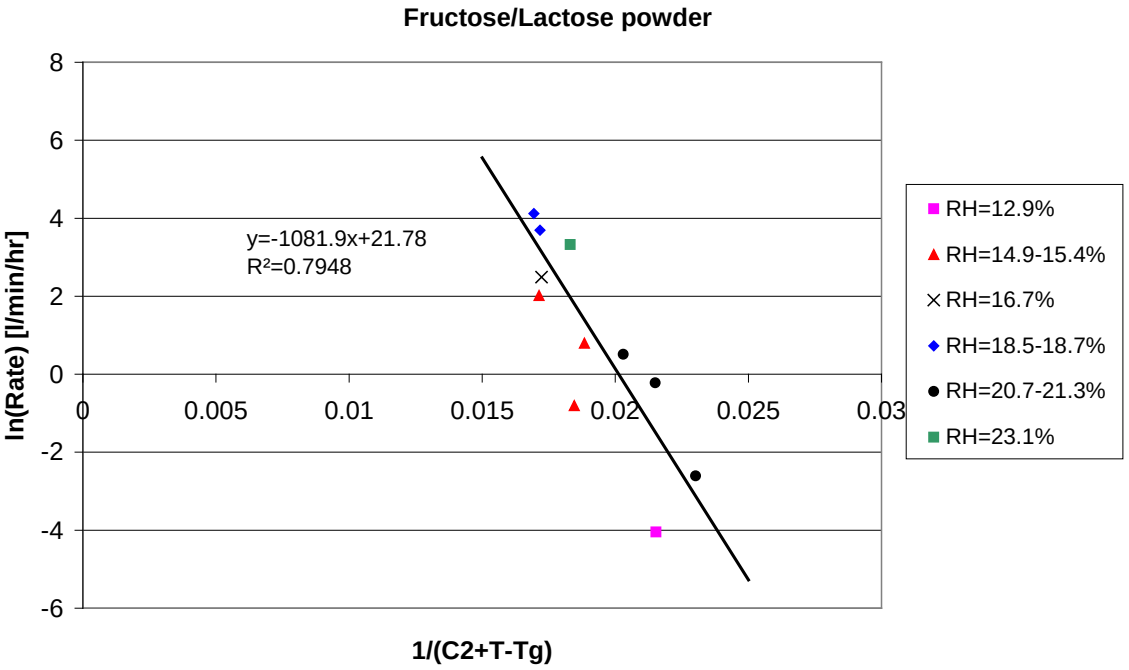
Fructose/Lactose powder
y=-1081.9x+21.78
R²=0.7948
ln(Rate) [l/min/hr]
1/(C2+T-Tg)
RH=12.9%
RH=14.9-15.4%
RH=16.7%
RH=18.5-18.7%
RH=20.7-21.3%
RH=23.1%

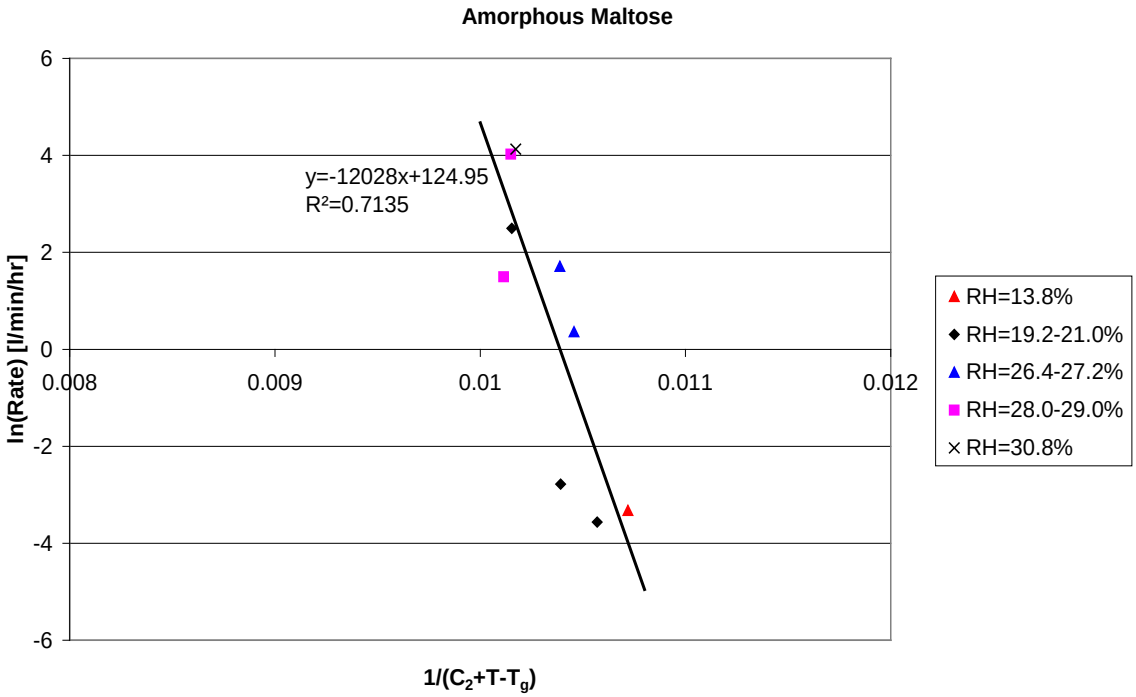
Amorphous Maltose
y=-12028x+124.95
R²=0.7135
ln(Rate) [l/min/hr]
1/(C2+T-Tg)
RH=13.8%
RH=19.2-21.0%
RH=26.4-27.2%
RH=28.0-29.0%
RH=30.8%

A2.4 COMPARISON OF WLF/FRENKEL AND VAN KREVELEN EQUATIONS

Equation 5.10:
y = *a*.x + *b*

$$\frac{T - T_g}{C_2 + T - T_g} = a\frac{1}{C_2 + T - T_g} + b$$

If $T-T_g = 0$, then $a/C_2 = -b$

If $T-T_g = C_2$, then $b=1/2 - a/2C_2$

Solving simultaneously for *a* and *b*: $a = -C_2$ and $b = 1 = (C_2 + T-T_g)/(C_2 + T-T_g)$

Therefore:

$$\frac{T - T_g}{C_2 + T - T_g} = -C_2\frac{1}{C_2 + T - T_g} + 1$$

This explains why the same C_2 and R^2 values are obtained when either the WLF/Frenkel equation or the Van Krevelen equation are used.

The following shows that the same values for C_1 and C_1' should not be obtained, however one can be found if the other is known.

Frenkel/WLF model:

$$\log\left(\frac{r_b^{\,2}}{t}\right) = \log k_F + \frac{C_1(T - T_g)}{C_2 + (T - T_g)}$$

Therefore

$$y_1 = b_1 + a_1 x_1$$

where

$$y_1 = \log\left(\frac{r_b^{\,2}}{t}\right)$$

$$x_1 = \frac{T - T_g}{C_2 + T - T_g}$$

$$a_1 = C_1$$

$$b_1 = \log k_F$$

Van Krevelen equation:

$$\ln s = \ln s_o - \frac{C_1'}{R}\left[\frac{1}{C_2 + \mathrm{T} - \mathrm{T}_g}\right]$$

Therefore

$$y_2 = b_2 + a_2 x_2$$

where

$$y_2 = \ln s$$

$$x_2 = \frac{1}{C_2 + \mathrm{T} - \mathrm{T}_g}$$

$$a_2 = -\frac{C_1'}{R}$$

$$b_2 = \ln s_o$$

Relating x_1 and x_2:

$$\frac{\mathrm{T} - \mathrm{T}_g}{C_2 + \mathrm{T} - \mathrm{T}_g} = -C_2 \frac{1}{C_2 + \mathrm{T} - \mathrm{T}_g} + 1$$

$$x_1 = -C_2 x_2 + 1$$

substituting into the Frenkel/WLF equation:

$$y_1 = b_1 - a_1 C_2 x_2 + a_1$$

substituting $y_1 = y_2/2.3$ to convert from log to ln:

$$y_2 = 2.3(b_1 + a_1) - 2.3 a_1 C_2 x_2$$

comparing with

$$y_2 = b_2 + a_2 x_2$$

then

$$b_2 = 2.3(b_1 + a_1)$$

$$\ln s_o = 2.3(\log k_F + C_1)$$

and

$$a_2 = -2.3 a_1 C_2$$

$$-\frac{C_1'}{R} = -2.3 C_1 C_2$$

Therefore:

$$C_1 = \frac{\ln s_o}{2.3} - \log k_F$$

$$C_1' = 2.3 R C_1 C_2$$

The above shows that C_1 and C_1' are not equal but are related to one another and C_2.

APPENDIX A3

MODEL VALIDATION

A3.1 ISOTHERMS FOR DAIRY POWDERS

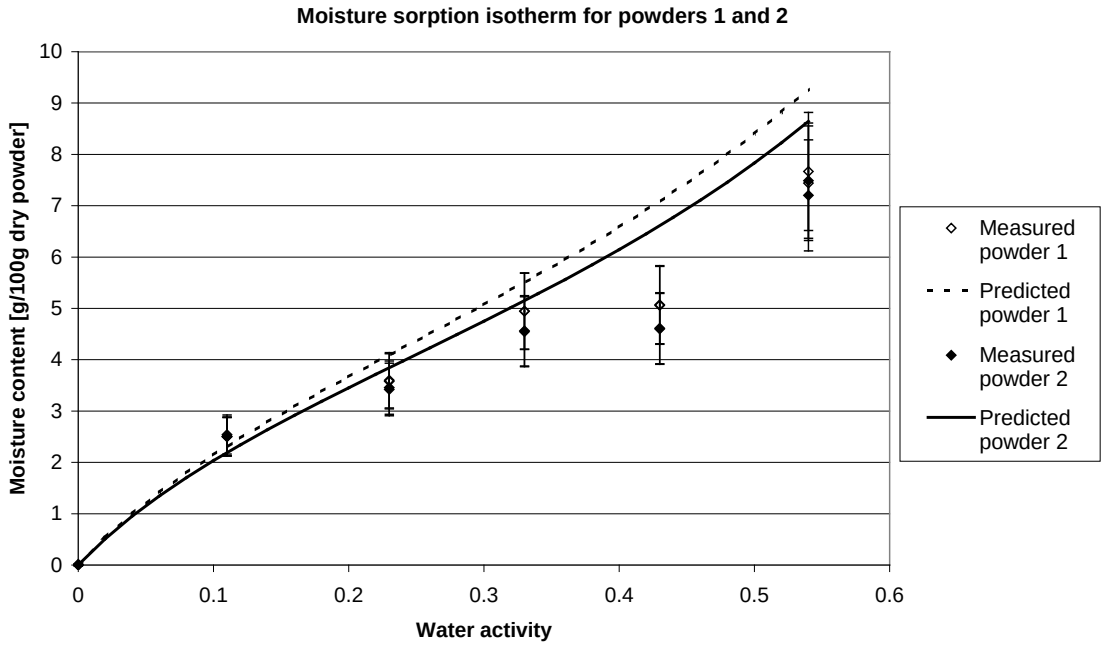

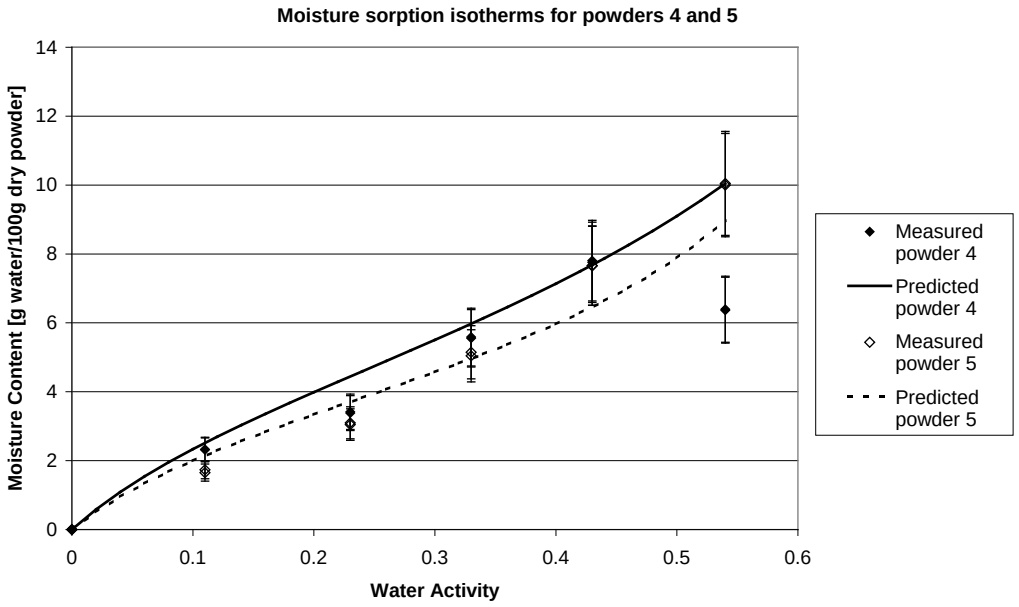

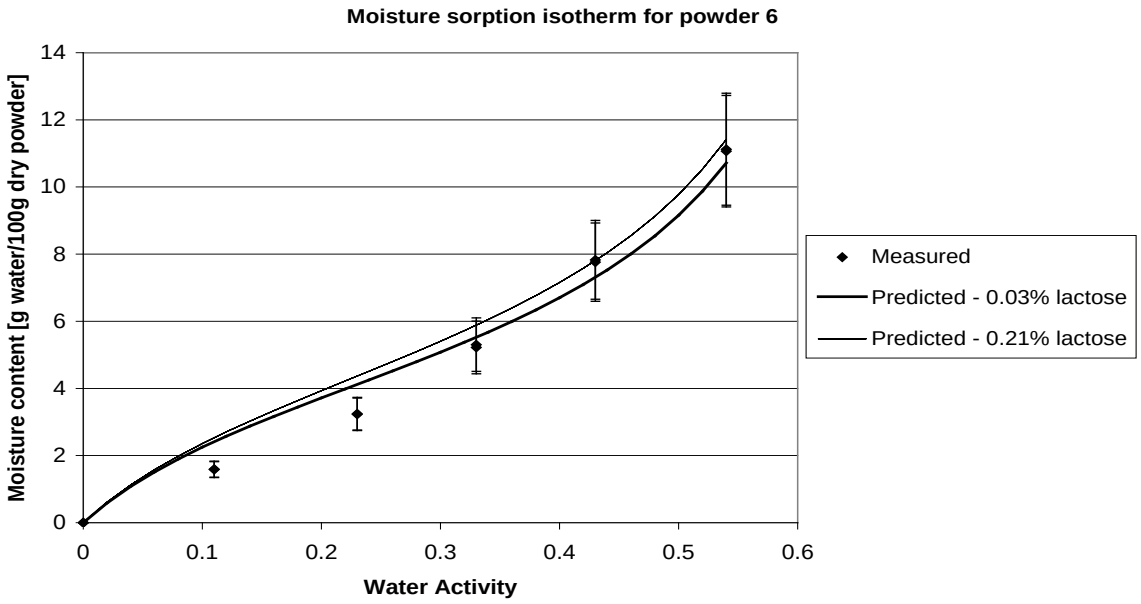

A3.2 T_G PROFILES FOR DAIRY POWDERS

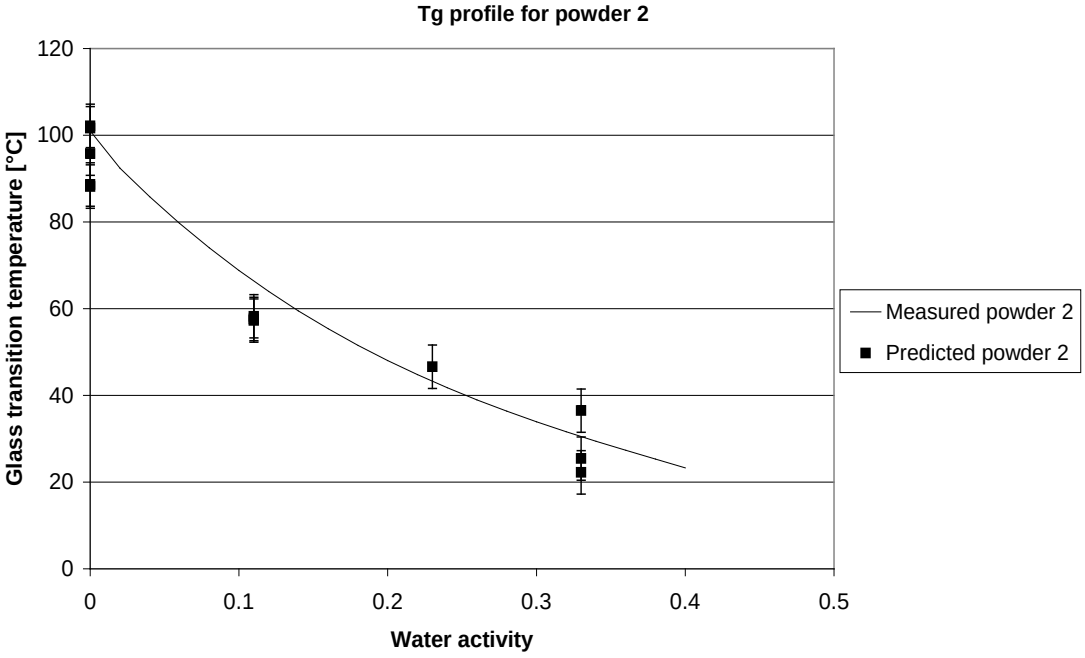

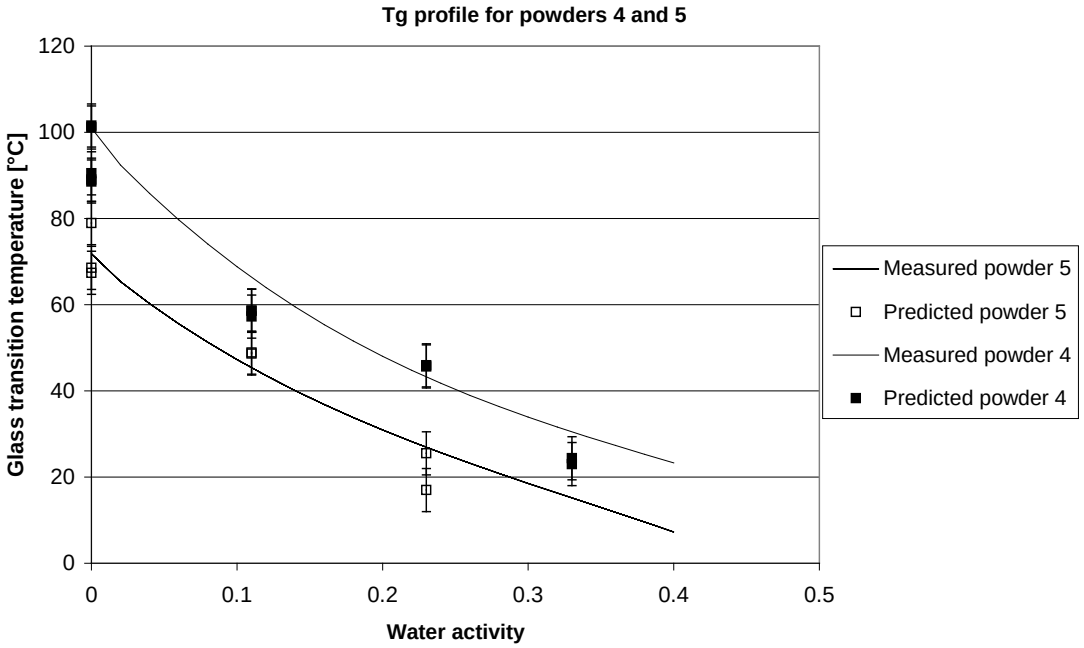

A3.3 MODEL DESCRIPTION

The following is to provide a description on how to use the model (on attached CD) for predicting the sticking and caking conditions in dairy powders. The composition of the powder can be entered on a dry mass basis or a wet mass basis. If it is entered on a dry mass basis then the model (for entry of composition on a dry mass basis) can be used to find the isotherm and T_g profile for the powder by changing the water activity. The water activity and hence moisture content that the powder should be dried to is calculated based on the maximum likely temperature that the powder will be exposed to during storage. The button storage should be used to calculate this. Similarly, the corresponding relative humidity condition for a particular dryer temperature can be calculated by pushing the drying button.

If the composition is entered on a total mass basis then the water activity and hence T_g for the powder can be calculated by pushing the moisture button. The water activity button can be used to find the moisture content for a given water activity. As with the above model, the model based on the total composition of the powder can be used to calculate the final water activity/moisture content for a powder so that sticking and caking does not occur during storage. Similarly, the temperature and relative humidity combinations for drying can be predicted. The prediction of the relative humidity of the dryer is based on the dryer outlet temperature and the $T\text{-}T_g$ for instantaneous sticking for that powder. The $T\text{-}T_g$ has been set in the model but should be changed when a method for predicting this $T\text{-}T_g$ is developed or if the $T\text{-}T_g$ for instantaneous sticking, for the particular powder, is known.

The model requires the following information to be entered:
1. powder composition (either on a dry or total mass basis)
2. maximum temperature that powder will be exposed to during storage
3. outlet dryer temperatures, to determine corresponding relative humidity.